Radioactive Measurements with Nuclear Emulsions

Radioactive Measurements with Nuclear Emulsions

by

HERMAN YAGODA
Senior Physical Chemist
National Institutes of Health

1949
NEW YORK · JOHN WILEY & SONS, INC.
LONDON · CHAPMAN & HALL, LIMITED

Preface

The photographic emulsion is one of many means for investigating radioactive radiations by the ionization produced in their traversal through matter. As is well known, radioactivity owes its discovery to the somewhat serendipical use of the photographic plate in the study of luminous phenomena. Until the development of electrical counting instruments, the emulsion played an important role in the early progress of the science. Although subsequently overshadowed by the rapid advancement of electronic devices, it again became an important tool in radioactive measurements as the result of later improvements in emulsion preparation.

The thick-layered, fine-grained emulsion is in many respects equivalent to a Wilson cloud chamber in its ability to distinguish between the tracks of densely ionizing particles. It permits the differentiation of the tracks produced by mesons, protons, tritons, deuterons, alpha particles, and fission fragments. The simple measurement of track length provides an accurate measure of particle energy. These properties render the emulsion invaluable in the study of the mechanism of nuclear reactions and warrant its designation as a "nuclear emulsion."

In the study of isotopes that decay by alpha-particle emission, simple microscopic examination of the nuclear emulsion provides the chemist, metallurgist, biologist, and petrographer with a quantitative counting tool. Each plate is virtually an independent alpha-pulse counter. Unlike the cloud chamber, which requires a separate photographic recording for each expansion, the emulsion records continuously and presents an integrated picture of the incident radiation. This property is of great importance in the study of rare radioactive events, such as low levels of alpha-particle contamination, and in the recording of the densely ionizing components of the cosmic radiation.

In the view of the increasing importance of radioactive isotopes as tracers it is worth while to describe, coordinate, and define the limitations of this simple method of instrumentation. The preparation of this work is a difficult task in view of the diverse appli-

cations of the emulsion. Essentially the same medium is employed in the study of individual tracks and in the autoradiography of minerals, metals, crystals, and plant and animal tissues containing tracer atoms. In each of these diversified applications the final interpretation of the pattern produced by the radioactive radiations is dependent on an understanding of the registration mechanism and its interferences.

The sharp distinction made between alpha- and beta-ray methods of autoradiography is somewhat artificial but is necessitated by the recording properties of these radiations. The minute range of alpha particles in solids permits the attainment of exceptionally high resolution, and the counting of individual alpha-particle tracks provides a quantitative measure of activity. The ionizing properties of the beta particle preclude these desirable effects. While the recording of alpha radiation is of importance in the study of radioactive ores and systems containing isotopes of the heavy metals, such as uranium and plutonium, by far the greater number of useful tracer isotopes decay with the emission of beta particles. Considerable effort has been expended in securing beta-ray autoradiographs exhibiting increased resolution, and these contributions are described in separate chapters.

Modern pedagogic thought advocates the coordination of the viewpoints and methodology of the different branches of science. In practice, however, each subdivision of the physical sciences is rapidly becoming more highly specialized, and it is increasingly difficult to write authoritatively in fields foreign to one's specialty. In this description of the applications of nuclear emulsions a common meeting ground is provided for physicist, chemist, and investigators in the fields of mineralogy, crystallography, biology, and metallurgy. An expert in any one of these fields will doubtless feel that his particular specialty has been presented in a most elementary fashion, and that the applications in the other fields are much too complex for ready comprehension.

The physicist who, in seeking information on cosmic radiation, simply exposes a closed package of plates on some lofty mountain peak may well question the necessity for a chapter on laboratory techniques, whereas the biologist haunted by fears of pseudophotographic effects and spurious chemical and luminescent reactions will lament the brevity of that particular section.

Although this work has been designed primarily as a guide on the use of emulsions in radioactive measurements, sufficient theoretical material has been incorporated to permit the comprehension of the basic mechanisms underlying the working methods. The procedures are representative of the efforts of different investigators whose contributions to the subject were necessarily limited by the particular problems of importance to them. In coordinating their work many gaps become evident, and fields for further investigation are thus suggested. Though an attempt has been made to make a comprehensive survey of the several fields of application, it is probable that many important contributions, developed in recent years, have escaped inclusion owing to their intimate association with the development of atomic energy.

Scientific instrumentation, like styles in women's apparel, has a tendency to run in cycles. After the discovery of spontaneous radioactive decay it was fashionable to make radioactive measurements with simple devices like photographic plates or scintillation screens. During an era of elaborate electronic recording mechanisms, these primitive detectors were looked down on as old-fashioned. However, their basic utility is again recognized in the latest-model crystal and scintillation counters.

It is noteworthy that each fundamental advancement, like Becquerel's discovery of the radioactive radiations and Rutherford's detection of the protons arising in transmutation processes, was made with simple detectors such as the photographic plate and the scintillation screen. Again, the first insight on intranuclear forces has been gained with the aid of emulsions as recording media for the heavy and light mesons associated with nuclear evaporations induced by cosmic radiation. It is gratifying that the first artificially created mesons recorded their characteristic tracks in a cleverly contrived mixture of silver bromide dispersed in an extract of cowhide.

It is a pleasure to acknowledge the aid of Nathan Kaplan in the preparation of photomicrographs of representative alpha-ray patterns and track structures. I am indebted to Dr. Eugene Gardner of the University of California Radiation Laboratory for data on the track characteristics of high-energy alpha particles and deuterons. Likewise, acknowledgment is made of spe-

cial information on betra-ray autoradiography received from Dr. S. R. Pelc of the Medical Research Council, London, and Dr. K. M. Endicott of the National Institutes of Health, prior to the publication of their methods.

HERMAN YAGODA

February, 1949

Contents

Chapter 1 · PHOTOGRAPHIC DETECTION OF NUCLEAR PARTICLES

Like an astronomer photographing stars too faint for his telescope to disclose, he has only to expose the plate for a sufficiently long time and the star reveals itself on development. So, in the case of radioactive minerals or precipitates, if no action is apparent at the end of an hour, one may be shown after twenty-four hours. If a day's exposure will show nothing, try a week's.

—Sir William Crookes, 1900

HISTORICAL INTRODUCTION

Shortly after the introduction of the silver halide emulsion as a recording medium for optical images, several curious investigators placed diverse materials in contact with the plates to determine whether an image could be produced without the action of light. In 1842 Moser [M32] observed that many nonmetallic substances, including chalk, marble, cotton, and feathers, would affect silver halide emulsions in the dark with the production of a developable image. In a continuation of these studies, Niepce de Saint-Victor [N3] noted that the nitrate and tartrate of uranium produced fog on silver chloride and iodide emulsions. In reporting this effect Niepce states that the blackening was also produced when the uranium salts were separated from the emulsion by thin sheets of paper of different colors! By attributing the blackening to luminescence phenomena the discovery of radioactivity was possibly delayed by about 30 years.

In 1896 Henri Becquerel [B10] had occasion to repeat Niepce's experiments to test an hypothesis concerning the reversibility of the fluorescent mechanism. Becquerel reasoned that, if x-rays make a fluorescent substance shine in the dark, the process may be reversible, and, during its subsequent luminescence, the phosphor may also emit invisible penetrating rays capable of photographic detection. Fortuitously, Becquerel selected uranyl sulfate for this experiment. He found that the sunlight-activated

salt emitted penetrating radiations which passed through two sheets of thick black paper and rendered enclosed Lumière gelatin-silver bromide plates developable after 24 hours' exposure.

Had Becquerel selected a non-uraniferous phosphor as the test substance, the basic phenomena of radioactivity would probably again have escaped discovery. The connecting link between Becquerel's observations and the experiments which led to the discovery of the true significance of the radiations is obscure. Different versions exist which, like Newton's falling apple and Archimedes' buoyant bath, have become part of the folklore of science. According to Soddy,[S32] one cloudy day, the sun being obscured, Becquerel placed the wrapped plate and the non-activated preparation in a drawer for several weeks, and, "wishing to see if any darkening had occurred without the sunlight," developed the plate, and found that the blackening had proceeded even though the uranyl sulfate had not received prior activation. Further studies showed that the penetrating radiation was a function of the uranium content of the compound, entirely unrelated to its fluorescing properties, and that the radiations were also capable of discharging an electroscope.

These sensational properties stimulated widespread interest in the phenomenon. It led to the discovery of polonium and radium in pitchblende by the Curies in 1898 and to the formation of the concept of nuclear instability by Rutherford and Soddy in 1902. S. Curie [C34] and, independently, Schmidt [S6] discovered that thorium compounds were also radioactive and that the invisible radiations emitted by them could be detected photographically. Campbell and Wood [C1] discovered that potassium compounds were feebly radioactive and that they caused blackening of fast emulsions.

The electroscope had been available to experimental physicists since the early part of the eighteenth century. As it was known that frictionized amber and glass would charge an electroscope, it seems in retrospect somewhat surprising that, in all the intervening years, no one had tried to determine whether substances occurred in nature which would accelerate the discharge of the instrument. With Becquerel's discovery, the photographic emulsion became a useful tool in investigating the radioactive properties of minerals and the oxide fractions isolated from them. Sir William Crookes [C26] was among the first to publish a list of

minerals that activated the photographic plate. He concluded, "After going through every mineral in my cabinet, a somewhat extensive collection, numbering many fine specimens," that only uranium- and thorium-bearing species produced the blackening. Similar studies were made by Pisani,[P24] Bardet,[B5] Ulrich,[U1] von Born,[V5] and Wherry,[W12] who noted the relative degree of blackening produced by different minerals and attempted a correlation with their uranium and thorium contents.

Placing a polished surface of the mineral or rock in contact with the emulsion restricted the blackening to the immediate vicinity of the radioactive inclusions, and the imprint was termed an "autoradiograph" of the section. By injecting radioactive compounds into animals and exposing the paraffin tissue blocks Lacassagne [L1] was able to demonstrate from the resulting "autohistoradiographs" the distribution of the radioelements in the different organs.

The first intimation that the radiographic image might be of a particulate character was obtained in 1909 by Mügge.[M33] While studying the activities of various minerals, he sprinkled some tiny crystals of uraniferous zircon on the surface of a moistened photographic plate. After 25 days' exposure microscopic examination of the developed plate revealed rows of black dots emerging from the mineral grains. He correctly attributed these markings to the feeble radioactivity of the mineral but failed to identify the series of silver grains as a tracing of the alpha-particle trajectory. Likewise, Kinoshita,[K10] working in Rutherford's laboratory in 1910 on the blackening produced by alpha radiation in emulsions, failed to observe the formation of individual tracks owing to his particular experimental arrangement wherein the particles were incident upon the plate at small angles with the normal. Under this condition the microscopic view of the track is essentially that of a distorted point.

That the passage of an alpha particle, at glancing incidence with the emulsion, produces on development a row of silver grains outlining the trajectory of the particle was first noted by Reinganum [R3] in 1911, about the same time that C. T. R. Wilson produced pictures of the paths of single alpha particles in his cloud chamber. This discovery was confirmed by numerous workers, and Makower [M3] succeeded in making photomicrographs of the fine track structures. Michl [M26] showed that the

track length and the number of silver grains per track were linear functions of the residual air-ranges of the alpha particles incident on the emulsion.

Kinoshita and Ikeuti [K11] introduced traces of Ra(C + C′) into an emulsion by touching it momentarily with a needle coated with the active deposit of radon. After exposure and develop-
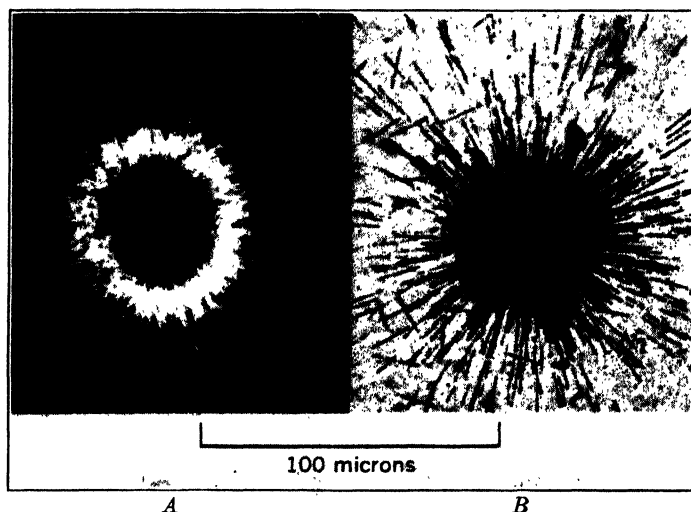
FIG. 1. Radioactive infection centers, showing annulus of radiating tracks produced by touching an emulsion with a needle point coated with polonium.

A. Heavy contact (dark-field illumination).
B. Light contact (bright-field illumination).

ment the microscopic examination of the infected areas revealed black spots with a halo of alpha-ray tracks emerging radially from the point of contact. The tracks originating from the point source generate an approximate sphere whose radius is equal to the range of the alpha particles in the emulsion. Microscopic views of radioactive infection centers in a modern-type fine-grained emulsion are reproduced in Fig. 1.

Using the needle-point technique Sahni [S1] investigated the photographic effect of beta rays. These patterns did not show the approximate spherical symmetry characteristic of alpha particles, but were irregular and nebulous, and microscopic examination failed to indicate the presence of straight tracks. Similar

experiments with gamma-ray sources yielded feebly blackened spots attributed to the production of secondary beta particles by the primary gamma radiation.

That protons produce tracks in photographic emulsions was demonstrated by Blau.[B18,19] The average distance between silver grains in proton tracks is greater than that in the tracks produced by alpha particles. Wilkins and St. Helens[W17] likewise found that deuterons produced tracks in emulsions and that alpha, proton, and deuteron tracks can be differentiated by careful microscopic determination of the relative grain densities.

Recoil atoms undoubtedly activate the emulsion, but, owing to their extremely short range in solids, the tracks produced by them are not microscopically resolvable. The massive energetic fragments resulting from the neutron-induced fission of uranium produce short heavy tracks, and special emulsions have been devised for their selective registration.

Non-ionizing nuclear particles, such as the neutron, do not produce tracks. They can be detected photographically, however, by the tracks of secondary particles produced in nuclear reactions with certain atoms in the emulsion. Slow neutrons can be captured by the nitrogen of the gelatin, the event becoming manifest by the formation of a proton track originating from the $N^{14}(n, p)C^{14}$ reaction. The emulsion can also be loaded with boron compounds, thereby providing nuclei for the $B^{10}(n, He^4)Li^7$ reaction, the event becoming manifest by the registration of a track by the alpha particle and the recoiling Li^7 nucleus.[T8] Fast neutrons striking component hydrogen atoms may cause their acceleration within the emulsion layer with the registration of a proton track.

This brief historical outline indicates that the photographic emulsion is an invaluable tool for the detection and differentiation of nuclear particles which has the unique ability to integrate the successive impacts into a discernible localized image. Cosmic-ray studies[P18] indicate that the meson, an elusive short-lived nuclear particle having a mass about 200 times that of an electron, produces a characteristic track in silver halide emulsions. This summary touches only on the more important applications of the nuclear-emulsion technique. The work of the early investigators is recorded in St. Meyer and von Schweidler's classic textbook[M25] *Radioaktivität*. An excellent summary of the more

modern work in the field of cosmic radiation is available in a review by Shapiro.[S22]

The early studies on the action of radioactive radiations on emulsions were made on the commonly available commercial plates intended for optical photography. More recently thick, fine-grained emulsions of exceptionally high silver bromide content designed primarily as recording media for densely ionizing radiations have become commercially available. The Eastman Nuclear Track (NTA) plate and the Ilford Nuclear Research plates are examples of these modern developments. These emulsions, intended for the registration of alpha-particle, proton, and fission-fragment tracks, are conveniently referred to as *Nuclear Emulsions* for purposes of differentiation from plates intended for optical or x-ray photography. The latter are also employed in radioactive studies chiefly as recording media for beta and gamma radiations. The optical-type emulsions are also rendered developable by densely ionizing radiations, but they do not record individually resolvable tracks.

PHOTOCHEMICAL AND IONIC REACTIONS OF EMULSIONS

Before embarking on a detailed exposition of autoradiography it is well to keep in mind that for years the silver halide emulsion was designed primarily as a medium for recording an image by electromagnetic radiations in the visual range and that these optical emulsions have a variable response to ultraviolet and infrared radiations, pseudophotographic agents, pressure, and chemical reactions which are likely to interfere with the specificity of the blackening produced by radioactive radiations. The reduction of light-activated silver bromide grains to metallic silver by suitable developing solutions has formed the basis of numerous analytical applications, whereby under controlled conditions the emulsion can be utilized as a recording medium for the products of diverse chemical reactions. When a complex biological or mineral surface containing radioactive constituents is brought into contact with the emulsion, molecular side reactions may also be recorded by the silver salts. It is essential that the mechanism of these potential interferences be understood in

order to evaluate properly the specificity of the radiographic image.

Chemical Reactions with Emulsions. Hydrogen sulfide gas or solutions of metallic sulfides will react with the silver compounds to form a brown stain of silver sulfide which is insoluble in the fixing bath. This molecular reaction described by Baumann [B8] is the basis of the well-known sulfur print method employed in metallurgy for the detection of iron and manganese sulfide inclusions in steels. The requisite conditions of acidity for this interfering reaction will rarely be encountered in properly prepared dry polished surfaces. In metallographic studies, however, it is common practice to etch the polished surface with acids in order to enhance surface structures. If any cracks or fissures are present they will retain some acid which will slowly liberate traces of hydrogen sulfide from adjacent metallic sulfide inclusions. If etched specimens are to be studied radiographically they should be rinsed in dilute ammonium hydroxide, washed, and dried thoroughly before making contact with the emulsion. The potential interference of elementary sulfur and metallic sulfide minerals in the detection of radioactive inclusions has been studied by Yagoda.[Y10] After 30 days' exposure on a Fine-Grain Alpha-Particle emulsion, polished surfaces of common sulfide minerals produced no evidence of chemical reaction.

It is noteworthy that, if polished sections of pitchblende are etched with dilute nitric acid, inclusions of metallic silver, which are frequently found associated with the mineral, produce a blackening on the radiograph of greater intensity than that of the pitchblende proper. During the etching process polonium is brought into solution and is deposited electrochemically on the silver. The same activation of the silver may take place in the mineral deposit, as suggested by Spence,[S33] as a result of alteration processes in the pitchblende vein.

Among other chemical reactions with the emulsion may be mentioned the work of Boruttau [B33] on the localization of hydroquinone in animal organs. The emulsion is exposed to light, moistened with sodium carbonate, and contacted with a tissue section. Reduction to silver takes place in regions containing hydroquinone. Likewise, alkaline constituents in the polished surface can be demonstrated in the method described by

Briscoe.[B40] In this modification of the basic reaction, the exposed emulsion is moistened with a developing solution devoid of alkali, and reduction to silver takes place only at areas in the section which can furnish the essential hydroxyl ions. Chloride ions can be localized electrographically in tissues, utilizing a silver chromate emulsion [Y5] and final reduction of replaced silver chloride to metallic silver. The converse process of detecting silver compounds [Y9] in polished section is readily effected by contacting the surface with pure-gelatin-coated paper moistened with dilute nitric acid and potassium bromide solutions. After washing, the residual silver bromide is rendered visible by photographic reduction.

Luminescent Interferences. Numerous non-opaque solids transform incident electromagnetic radiations into light of lower frequency. When the wavelength of the emitted radiation falls within the range of normal vision the phenomenon is termed fluorescence; when the radiations reside below the purple threshold of vision it is called photoluminescence. On the removal of the source of excitation certain crystalline solids continue to emit light for varying periods, the phosphorescent radiations residing either in the visible, the near ultraviolet, or both. The persistent phosphorescent light is often emitted with a wavelength of about 4000 A, and, though difficult to detect visually, the radiation will produce a marked blackening when brought in direct contact with blue-sensitive photographic emulsions. Polished sections of minerals are often examined under 2537 A ultraviolet light for the localization of fluorescent inclusions.[Y12] Particular components of the section may thus be activated to phosphorescence. If an autoradiograph is made shortly afterwards, blackening may be produced by luminescent as well as radioactive components.

A number of mineral phosphors are rendered photoluminescent by exposure to sunlight and will produce blackening on prolonged contact with light-sensitive emulsions. Mineral varieties of zinc sulfide, like wurtzite, and calcium fluoride, like chlorophane and antozonite, are activated by the ultraviolet components of sunlight, and their luminescent reaction with the photographic plate has been mistaken for an indication of radioactivity.[P24, H26] The photoluminescence of minerals has been studied extensively by Brown [B45] and Iimori.[I1] The phenomenon has been utilized in

the localization of certain components of polished sections by contact photography, and the imprint has been designated an autoluminograph.[Y7,12]

The persistent phosphorescence of matter by sunlight activation caused considerable confusion in the early investigations of radioactivity with hypersensitive emulsions.[L29] The current widespread interest in the distribution of ingested radioactive isotopes in plant and animal tissues warrants a word of caution, as these complex bodies may contain organic compounds of a photoluminescent nature. The investigations of Penn[P9] show that most polynuclear hydrocarbons, both carcinogenic and non-carcinogenic, produce fluorescent light with bands in the region of 4000–4400 A.

The phosphorescent radiations are readily absorbed by thin opaque filters, like black paper or suitably dyed sheets of plastic. The insertion of a filter between the source and the emulsion causes a loss of definition in the radiographic image. It also necessitates an increased exposure, as the greater part of the alpha radiation is absorbed by the filter. The nuclear-type silver bromide emulsions are weakly sensitive to light. Investigations of their properties[Y10,12] show that they are not blackened by photoluminescent mineral specimens even when the exposure is made immediately after their excitation by strong sources of ultraviolet light.

Emulsions that are sensitive to beta particles are also activated by light. These media must be employed in conjunction with an opaque filter when persistently phosphorescent material is present in the section. Their absence can be established by exposing a trial section to the unfiltered radiations from a 4-watt mercury-vapor lamp for about 1 min and contacting the irradiated specimen for 5 min. Because an exposure of several days is usually necessary for the production of a radiographic image from moderately strong sources of beta radiation, the development of an image on the briefly exposed trial plate may often be indicative of the presence of photoluminescent inclusions. If the test is negative, the complete absence of phosphorescent bodies cannot be assumed with certainty, as phosphors may be present which decay too slowly to reveal their presence during the brief exposure period.

Pseudophotographic Effects. As noted earlier, Moser and Niepce observed that many solids produced a latent image by direct contact with the emulsion in the complete absence of light.

Colson [C10] observed that metallic zinc, cadmium, and magnesium also activated the photographic plate. Extensive studies of this phenomenon were made by Russell,[R16] who found that the interposition of a thin glass plate between the test substance and the emulsion prevented the formation of a developable image, whereas sheets of porous materials like Celluloid, gelatin, or paper weakened but did not eliminate the image. After numerous experiments Russell concluded that the agent responsible for the photographic activity was hydrogen peroxide. This conclusion has been verified in more recent investigations by Keenan [K5] and Churchill,[C15] who ascribe the formation of hydrogen peroxide to oxidation processes of freshly abraded metals or to the tendency of certain organic compounds related to the terpene series, such as Canada balsam, wood, linseed oil, and shellac, to form peroxy compounds in the presence of moist air.

Sheppard and Wightman [S24] have shown that the actinic action of hydrogen peroxide is very similar to that of light. In general, emulsions that are most sensitive to light are readily activated by traces of this compound. In fast emulsions only a trace of hydrogen peroxide vapor is necessary for the activation. Comparative experiments [Y10] show that the Eastman Process plates develop a black image after a 10-min exposure 5 cm above a 3 per cent solution of hydrogen peroxide. Under the same conditions the fine-grained Eastman nuclear-type emulsions show no evidence of visual fog even after several hours' exposure to the vapor.* Russell's experiments indicate that about 10^{-9} g of H_2O_2 will produce a moderate blackening on certain light-sensitive emulsions.

Pseudophotographic effects are a serious interference with the specificity of the autoradiographic mechanism, particularly in the study of feeble sources of beta radiation, which necessitate long periods of exposure against fast emulsions. The activating vapors permeate the black papers employed as a protection

* The different behavior of coarse- and fine-grained emulsions towards hydrogen peroxide is even greater than indicated by these gross observations. In fine-grained emulsions the peroxide causes destruction of the latent image produced by densely ionizing radiations. The very same reagent which causes fogging of light-sensitive emulsions can be employed advantageously in the eradication of background alpha tracks as described in Chapter 4.

against luminous effects. Some measure of protection is afforded by impregnating the paper with paraffin. This non-permeable filter stops the passage of the peroxide, but its presence causes a decided loss in resolving power.

The potential formation of traces of hydrogen peroxide must be guarded against in the choice of materials employed in mounting the specimen and in the construction of the camera. Canada balsam, sealing wax, and rosins cannot be employed as mounting media for thin sections. Paraffin, montan wax, and plastics, such as Lucite and Bakelite, are satisfactory embedding media.[Y10] It is also desirable to employ plastics in place of wood as supports and housing during the exposure.

Fogging by wooden supports has been noted in investigations of feeble beta-ray activities like those of potassium and rubidium. Strong[S44] states: "In several instances the photographic plates were supported by pine or oak blocks. In every case it was found that these blackened the plate and this darkening spread out as a cloud for several millimeters from the parts of the block touching the plate." In studies of the imprints made by polished mineral surfaces against photographic plates Ansheles[A2] found that after 5 to 10 months' contact images were invariably produced on development. Aside from radioactive and luminescent effects from certain inclusions, Ansheles attributes the print of the rock structure to the action of air and moisture, as fissure-free areas, in perfect contact with the emulsion, did not produce blackening.

The pseudophotographic action of certain metals and alloys is of particular importance in conjunction with the use of beta-active radioisotopes as tracers in metallurgical studies. The investigations of Churchill[C15] demonstrate conclusively that the fogging action is caused by hydrogen peroxide produced in the reoxidation of the surface of the freshly abraded metal. The intensity of the photographic action varies with the time elapsed after abrasion and is most pronounced on a freshly filed surface. If the stabilized oxide film is scratched the freshly exposed metallic surface becomes active, and a print of the abrasion marks is readily produced by contact photography.

The specificity of autoradiographs of freshly polished metallic surfaces containing radioactive components will be impaired if the alloy system contains certain oxidizable metals. Thus,

Stephens [S40] found that an alloy of aluminum and silicon rendered radioactive by neutron bombardment produced, after exposure to x-ray film, a composite pattern in which the distribution of the radio aluminum was non-homogeneous and the segregates did not always correlate with grain boundaries owing to diffuse pseudophotographic effects from the freshly polished specimens.

TABLE 1. PHOTOGRAPHIC ACTION OF ABRADED METALS

Alloy Composition	Photographic Action
Pure aluminum	Strong image
Wrought aluminum alloys	Strong image
46Al + 54Cu ($CuAl_2$)	Strong image
Zinc	Strong image
Cadmium	Strong image
Magnesium	Strong image
Zinc amalgam	Strong image
Tin	Faint or none
Mercury	None
Lead	None
Copper	None
Brass	None
Iron	None
Stainless steel	None

Metals and alloys exhibiting the pseudophotographic effect are listed in Table I. Fast emulsions like x-ray and Commercial Ortho film are particularly sensitive to traces of hydrogen peroxide. Experiments with freshly abraded metals contacted with these emulsions for 120 hours show that aluminum, cadmium, bismuth, and beryllium produce images with photographic densities ranging between 0.13 and 0.10. Other metals, such as copper, silver, iron, nickel, cobalt, and arsenic, placed on the same film, did not activate the emulsion.[Y18]

Churchill found that coating a freshly abraded surface with a very thin layer of a substance that prevented access of air, like petroleum jelly, effectively stopped the fogging action by the metal. This protective measure is of doubtful utility when dealing with beta-active alloys, as petroleum products are rendered luminescent by electron impact. A thin airtight coating of a non-luminous lacquer on the thoroughly dried surface should overcome this difficulty.

Hydrogen peroxide, though the most common fog-producing agent encountered in autoradiography, is not the only chemical reagent which simulates light in producing developable sensitivity centers in silver halide emulsions. Among the other chemical fogging agents are hypophosphites, arsenites, and stannous salts. Clark [C17] investigated the fogging action of sodium arsenite in considerable detail, using special single-layer plates coated with an emulsion in which the grains were flat tablets of very nearly identical shape and size. Clark obtained a blackening curve with 10 per cent sodium arsenite identical in contour with one obtained by exposure to light. Reducing agents of this sort might conceivably be present in tissue containing radioactive and normal isotopes of arsenic or phosphorus

Oxidizing agents have an opposite effect on emulsions and tend to destroy the latent image produced either by light or incident alpha particles. As early as 1905 Joly [J6] had shown that the addition of uranyl nitrate to the emulsion reduced its sensitivity to light. More recently, Green and Livesey [G21] found that when nuclear-type emulsions are loaded with uranium salts they become desensitized to protons, and the alpha-particle tracks recorded from the decay of the uranium isotopes are weakened. By increasing the concentration of uranyl nitrate the alpha-particle sensitivity can be further diminished until a point is reached where only the more densely ionizing fragments ejected in the fission of uranium record tracks in the emulsion.

Chromic acid also desensitizes emulsions, as recognized by Lüppo-Cramer [L44] and studied in detail by Sheppard [S24] and Mees.[M23] The latter have shown that, after exposure to light, immersion in $N/50$ chromic acid greatly reduced both the photographic gamma and the speed of the plate. Copper sulfate and mercuric chloride have also been reported as causing desensitization of light-activated emulsions. Dilute solutions of chromic acid have been employed by Perfilov,[P13] prior to experimental exposure, to destroy the latent image of alpha-ray tracks which accumulate in plates as a result of the decay of traces of internal radioactive impurities. These factors, which are of great importance in the study of extremely low levels of nuclear disintegrations, are presented in greater detail in Chapters 4 and 12.

The behavior of chemical reagents on the silver bromide emulsion is not invariably analogous for both electromagnetic and radioactive radiations. Thus, Blau [B21] and Wambacher [W2] in their pioneering work on nuclear-type emulsions discovered that pinakryptol yellow sensitizes common photographic emulsions

to energetic protons and permits registration of their complete trajectories through the recording medium. As is well known, the very same dye is an effective desensitizer to light-activated plates. Likewise, mercury vapor, which increases the sensitivity of panchromatic emulsions to light, causes partial destruction of the latent alpha-ray image.[Y10]

The behavior of photographic media towards fogging agents and sensitizing dyes varies markedly with the ratio of silver halide to gelatin and the grain size of the emulsion. The fine-grained, concentrated, nuclear-type emulsions are not fogged by hydrogen peroxide vapor. The investigations of Demers[D9] likewise show that pinakryptol yellow has little effect on the grain density of proton tracks recorded in emulsions containing over 80 per cent silver bromide. *The action of various chemicals on photographic media must therefore be considered separately for each particular emulsion studied.* Generalizations must not be drawn from observations on a single type.

PRESSURE EFFECTS

That the application of pressure alone renders certain emulsions developable has been known since the early work of Warnerke (1881) and has been confirmed by numerous subsequent investigators. The intensity of the image produced by normal development varies with the pressure but is very nearly independent of the duration of its application. Studies by Bäckström[B1] on the development of a latent image by pressure on ordinary silver halide emulsions and ones sensitized towards red light show that pressures of about 1000 kg per cm² must be employed to produce a measurable effect. When a polished surface is placed in contact with the emulsion the weight of the specimen is uniformly distributed, and the pressure at any given point of contact is low even when the specimen is clamped to the plate or film to prevent displacement during exposure. Under normal experimental conditions, using plane surfaces, there is little danger of interference by pressure effects.

The nuclear-type emulsions are sensitive to abrasion and mechanical shock. By scratching the emulsion with a steel point the lines cut into the gelatin blacken during development. In cutting plates into smaller

sized sections spurious lines may develop for 2–3 mm on each side of the break which tend to run parallel with the original diamond scratch mark made on the glass backing. These lines are very fine and can be observed only under high magnification. Taylor [T9] notes that simply drawing a soft hair brush across the gelatin layer before its development produces a large number of markings simulating tracks. These abrasions are distinguished from the tracks of ionizing particles by residing entirely on the emulsion surface, whereas the trajectories of nuclear particles usually exhibit some inclination. Also, grains developed by scratches or mechanical shock have a random grain spacing. In the long tracks produced by protons the grains are far apart at the beginning of the track and are close together towards the end of the trajectory. Altering the illumination by manipulation of the mirror and condenser will show up a scratch by the furrow lines. The particle of abrasive causing the scratch is often seen embedded at the scratch termination.

The effect of simultaneous application of pressure and irradiation with light of different wavelength has been investigated by Tsi-Zé and Ta-Yuan.[T23] When the emulsion is illuminated with yellow-green light a pressure of 100 kg per cm^2 produces a marked change in density. To produce a comparable change with light of 3131 A the pressure must be augmented to over 1000 kg per cm^2. The investigations of Lu [L42] show that, when the photographic films are exposed to visible or ultraviolet light, application of pressure reduces the sensitivity. When gamma radiation is employed, the action is reversed, and photographic sensitivity is enhanced by the simultaneous application of pressure.

Ritchie and Thom [R7] observed that, on exposure of an emulsion to blue light under conditions of variable air pressure, the photographic density increased with diminution of air pressure as follows:

Air pressure in mm of Hg	758	250	51	9
Photographic density	1.08	1.30	1.53	1.64

They attribute the increase in sensitivity to the removal of bromine molecules from the grain surroundings by the air-pressure reduction. The effect of diminished pressure on the recording of tracks by densely ionizing particles has not been studied. The phenomenon may enter as a factor in experiments on nuclear scattering where the emulsion is exposed under conditions of very low pressure.

NATURE OF THE LATENT IMAGE

Detailed studies on the nature of the latent image produced by charged nuclear particles are not available. It may be assumed as a tentative working hypothesis that the general concepts of the formation of a light-activated image also apply to the fine-grained emulsions activated by densely ionizing particles. Fast optical emulsions consist of a suspension of silver halide crystals ranging in size from 1 to about 3.5 microns. The crystals are essentially silver bromide but may have admixed iodide ions within the lattice. The introduction of the iodide usually increases the sensitivity of the emulsion towards light. The nuclear-type emulsions consist of dispersions of silver bromide in gelatin, the grain size ranging between 0.1 and 0.6 micron. The substitution of silver iodide for the bromide causes a marked loss in sensitivity for densely ionizing particles. In an experimental emulsion in which the grains were composed entirely of silver iodide, Demers [D9] found that even fission fragments failed to produce a developable image. In an emulsion of fixed composition a group of large grains is more sensitive than a cluster of small grains. This is equally true in regard to the sensitivity of the emulsion towards light and radioactive radiations.

The gelatin provides a water-permeable medium for the mechanical suspension of the halide crystals. This property permits ready access of the diverse components of the developing solution to the grains without altering appreciably their initial orientation in the dry state. Land [L11] indicates that the gelatin, as a protective colloid, promotes the action of the developer on the more highly exposed grains. The traces of sulfur compounds in the gelatin also play a fundamental role in providing active centers, or sensitivity specks, which are believed to consist of minute aggregates of silver sulfide. The gelatin also serves in the absorption and probable chemical combination of the free bromine atoms released from the silver halide crystals during exposure.

For optimum sensitivity the emulsion grains must carry a limited but sufficient number of silver sulfide sensitivity specks. During development the sensitivity specks at the surface of the grain are the ones that initiate the reduction to silver. In the

quantum-mechanics description of the process, the light photon impinges on the area of a grain and, when absorbed, liberates photoelectrons in the silver halide. These high-energy electrons diffuse into the sensitivity specks which thus become negatively charged. The silver halide always contains a number of free, positively charged silver ions in the crystal lattice. These migrate to the silver sulfide and neutralize its charge by precipitation as metallic silver. This superficial deposit of silver on the light-activated grain serves as a nucleus in the subsequent reduction of the entire grain by the developing solution. When a densely ionizing particle strikes a silver bromide grain the same mechanism is presumably in operation, but the electrons originate as a result of direct ionization through collision in the crystal rather than by photoelectric effect.

The marked light sensitivity of argentite and other native silver sulfide minerals is well known in petrography and is occasionally utilized to detect these species in the microscopic examination of polished ore sections.[W14, M22] If an intense beam of light is focused on the section, the silver sulfide minerals decompose with the formation of filamentary extrusions on the surface and a sublimate of sulfur condenses on the objective. That this effect is actinic and independent of accompanying thermal effects has been demonstrated by Stephens,[S39] who absorbed the heat rays from the carbon arc light source by means of suitable filters. These observations on light-sensitive minerals lend evidence in support of the silver sulfide sensitivity speck mechanism for the formation of a latent image.*

THE AUTORADIOGRAPHIC MECHANISM

In the decay of radioactive elements three major types of radiations are emitted, all of which are capable of activating photographic emulsions in varying degrees. The alpha, beta, and gamma rays activate particular emulsions, but, owing to differences in the properties of the optimum recording media, it is

* More detailed information on the formation and development of the optical latent image is available in the comprehensive works of Neblette[N1] and Mees.[M23] The factors controlling the rate of fading of the latent alpha-ray image on delayed development are discussed in Chapter 4.

difficult to make quantitative comparisons of their individual effects. An alpha particle of 5.3 Mev energy has a range in gelatin-silver bromide of about 23 microns and dissipates 0.23 Mev per micron of average path. A beta particle of maximum energy 2.32 Mev, as emitted in the decay of UX_2, has an effective range of about 2800 microns, and it has an energy loss of only 0.00083 Mev per micron. On this basis, the alpha particle is about 300 times more effective in producing localized ionization and chemical action than the beta particle.

For a thin layer of a radium compound Rutherford [R20] found the relative ionization and penetrating power to be as tabulated.

Radiation	Relative Ionization	Penetrating Power
Alpha particles	10,000	1
Beta particles	100	100
Gamma radiation	1	1,000 to 10,000

Kinoshita [K10] has demonstrated that in the homogeneous alpha particles emitted from RaC′ each particle produces a detectable photographic effect. The gamma radiations are the most penetrating of all but have an appreciable photographic action only on fast, coarse-grained emulsions (see page 248).

The photographic action of the three radiations is exhibited graphically in Fig. 2. This depicts a cross section of a homogeneous radioactive mineral whose polished surface is in direct contact with a recording emulsion sensitive to all three radiations, such as fast x-ray film. The radiations are emitted in all directions, and each minute grain whose atoms are undergoing radioactive decomposition may be visualized as the center of a series of concentric spheres of radii equal to the range of the several radiations in the medium. Wherever these spheres intersect the plane of the emulsion and sufficient energy is absorbed the halide grains are rendered developable. Points located on the polished surface will form a sharply defined image of a diameter equal to twice the range of the most penetrating alpha particle, accompanied by a diffuse image from the more penetrating, but less active, beta and gamma rays. Radioactive nuclei slightly beyond the maximum range of the alpha particle in the mineral, as points *B* to *C*, will contribute only to the fogging of the primary pattern, and a diffuse image will be recorded on some

emulsions by the gamma radiation from the most remote nuclei, such as point *D*.

It is evident from these considerations that the autoradiographic print produced on an emulsion sensitive to all three radiations is not a true representation of the radioactive components of the polished surface. In experimental practice it is often
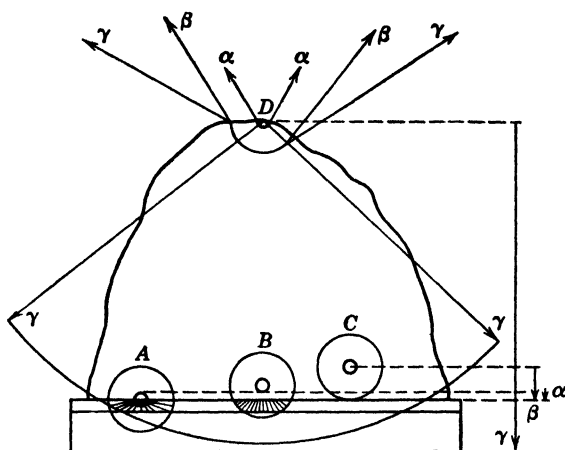
FIG. 2. Photographic action of radiations on optical emulsion. The smallest circles represent the relative range of the alpha rays. The large circles about points *A*, *B*, and *C* represent the active range of the beta radiation. The gamma rays originate from all parts of the specimen but are depicted only for the remote point *D*. In this idealized model it is assumed that the source and the emulsion have identical stopping powers.

necessary to interpose a sheet of black paper between the specimen and the plate in order to avoid autoluminescent and pseudophotographic interferences from other inclusions in the section. The black paper absorbs the greater part of the energy of the short-ranged alpha particles, and the resultant diffuse image is essentially a measure of the blackening produced by the penetrating beta and gamma radiations.

To obtain a radiographic imprint which is a true representation of the distribution of the radioactive components near the surface, it is necessary to arrange experimental conditions so that only the alpha rays activate the emulsion. This is entirely feasible through the use of the specially developed nuclear-type emulsions. Their low level of sensitivity to beta, gamma, and

electromagnetic radiations and their insensitivity to pseudophotographic effects permit the recording of a sharply defined alpha-ray pattern of the surface. Under these conditions the photographic density is a quantitative measure of the rate of alpha-particle emission from the test surface. The selective alpha-particle-emission pattern effects an elegant solution to many problems involving the spatial orientation of radioactive components in plane surfaces.

Of the synthetic radioactive isotopes only those of the trans-uranium elements emit alpha particles. The elements of chief interest as biological tracers, C^{14}, S^{35}, P^{32}, and I^{131}, decay with the emission of beta particles or gamma radiation. When members of this important class of radioisotopes are employed in tracer studies their autoradiographic localization can be effected by selecting photographic emulsions sensitive to the energies of the respective beta particles. The resolving power is in general poor, owing to scattering and to the fact that moderately coarse-grained emulsions must be employed. Better definition is secured from the use of very thin sections, which, though reducing geometric diffuseness, necessitate the use of prolonged exposures or highly active preparations. These factors are considered in greater detail in Chapter 10.

Radiography of Weak Sources. The optical photographic emulsions are serviceable in delineating a radiographic image of surfaces containing feebly radioactive segregates. On nuclear-type emulsions, sensitive only to alpha particles, about 10^6 tracks per cm^2 are necessary for the production of an image that is just discernible from the background. For convenience in subsequent observation a greater density is desirable, setting the practical limit at about 10^7 tracks. When the sample contains about 50 per cent uranium the total alpha-particle flux is obtained after an exposure of 24 hours. The exposure increases as the activity diminishes. With feebly radioactive material containing less than 1 per cent uranium in solid solution the exposure must be extended for about 2 months. This period can be reduced, at the expense of resolving power, by employing coarse-grained emulsions. These produce a greater blackening per alpha particle and also respond to the beta radiation originating from the interior of the inclusions.

In the determination of the suitability of allanite specimens as indicators of geological age, Marble[M6] employed Eastman Process plates which are exposed against the polished specimen for at least 3 weeks. Plates are preferable to film, as the weight of the specimen is less likely to cause pressure effects on a plate, and film often curls slightly in this length of time. A 35-day exposure period on an allanite specimen containing 1.07 per cent thorium and 0.069 per cent uranium yielded an autoradiograph of sufficient density for subsequent reproduction.[M8] A specimen from another locality, carrying 0.715 per cent thorium and 0.033 per cent uranium, furnished an exceedingly faint radiograph after 23 days' exposure but proved of sufficient density to demonstrate the uniform distribution of these elements in the mineral.[M7]

The distribution of the traces of thorium and uranium in rocks presents one of the most difficult problems in autoradiography. According to the measurements of Evans and Goodman[E12] the acid igneous rocks contain 3×10^{-6} g of U per gram of rock and 13×10^{-6} g of Th. Difficulties in obtaining duplicate check analyses are attributed to inhomogeneous distribution of radium, and hence of its parent element, uranium. This inhomogeneity, according to Evans, is usual rather than exceptional in rocks and introduces a sampling probable error which may greatly exceed the analytical uncertainty. A pictorial representation of the radioactive segregates would serve as an indicator of the suitability of the sample for radiometric measurement.

An approach to the solution of this problem has been attempted by Kirsch[K12] using very fast emulsions in conjunction with exposures of several weeks' duration. The extremely faint autoradiographic image is then intensified by means of mercuric chloride as in processing underexposed optical emulsions.[H23] The resultant pattern is compared with an image produced by a section of pitchblende of known uranium content which is exposed for only 5 min. Samples of granite, hornblende, gabbro, and lepidolite studied by Kirsch exhibited an essentially uniform distribution of the radioactive components. In prolonged exposures on hypersensitive emulsions precautions must be taken to avoid pseudophotographic and autoluminous reactions with the recording medium.

Microscopic examination of the alpha-ray image recorded on a nuclear-type emulsion yields reliable information on the statistical distribution of the individual tracks when their population exceeds 1000 per cm^2. In rocks of low uranium and thorium

content an ample number of tracks will be recorded after an exposure of about a month. Although track-distribution studies are not as convenient as a visually discernible radiographic image, the method permits the microscopic recognition of radioactive segregates of dimensions comparable to those of radiocolloids. The method is also extraordinarily selective, as the distinctive appearance of the alpha-particle tracks avoids confusion with the structureless images produced by fogging agents. The details of this quantitative method are described in Chapter 7.

Measurement of Photographic Density. The quantity of silver deposited in the gelatin as a result of radioactive exposure and development is determined, as in the case of an optical image, by measurement of the photographic density, D. This quantity is defined as $D = -\log_{10}(I_t/I_i)$, in which I_t and I_i are the intensities of the light transmitted by the silver deposit and that incident upon it, respectively. The photographic density of the autoradiographic image can be measured either by visual comparison against standards or, preferably, by means of automatic recording instruments. The individual images of highly segregated material may be very small, and the densitometer should be provided with slits of comparable dimensions. The instruments designed for measuring very small areas, as of motion-picture film described by Capstaff,[C2] or the Hartmann [H15] microdensitometer employed extensively in astronomical photometry, are readily adapted to autoradiographic density measurements. The more common instruments designed for the measurement of the density of spectrum lines can also be employed in measuring the density produced by segregates whose dimensions exceed the slit height.

The interpretation of the photographic density of a beta- or gamma-ray image is identical with that of an optical image. The alpha particle, however, registers an oriented track, and the density of the image is dependent on the angle of incidence as well as on the number and energy of the particles. Alpha particles collimated at right angles to the emulsion register as distorted points, whereas those entering the emulsion at glancing incidence are recorded in their full length and produce maximum opacity. The measurements of Bothe [B37] show that the photo-

graphic density is proportional to the cosine of the angle of incidence of the rays.

Using alpha particles collimated at right angles to the plane of the emulsion, Kinoshita [K10] found that the relationship between the photographic density and the number of incident particles, N, is expressed by:

$$D = D_m(1 - e^{-cN}) \tag{1}$$

where D_m is the maximum density obtainable with the particular grain emulsion and processing, and c is a constant. Wilkins and Wolfe [W16] confirmed the general applicability of this equation for several commercial emulsions and found that c is independent of emulsion thickness and that its value is proportional to the probability of an alpha particle hitting a particular surface grain. When an alpha particle penetrates to a depth d, the number of grains, k, rendered developable is equal to $(\pi r^2 d) \times (G_0/d)$, where πr^2 is the probability of one of the N alpha particles hitting a particular surface grain, and G_0 is the number of grains per square centimeter of emulsion surface. Hence c in equation 1 is equal to k/G_0.

Further investigations by Sheppard,[S25] using non-collimated alpha-ray sources held close to the film, show that the probability constant c does not stay constant but decreases with progressive increase in density. In exposures where the alpha particles strike the emulsion at all possible angles, equation 1 is no longer applicable and must be replaced by:

$$D = 1.57D_m(1 - e^{G/G_m}) \tag{2}$$

In this expression G is the number of grains activated by alpha particles and G_m is the number of grains accessible to the radiation as defined by their range in the gelatin-silver bromide medium. The number of activated grains is formulated by:

$$G = G_m[1 - e^{-k(N/G_m)}] \tag{3}$$

in which k is the average number of grains per track. Experimental data on Eastman Process film are in close agreement with these derived expressions as shown in Fig. 3. It will be observed that for process film the photographic density is very nearly a linear function of N up to 2×10^8 alpha particles per

cm^2 and that this covers the useful range of most autoradiographic exposures.

For a given emulsion and exposure the photographic density will increase with increasing energy of the alpha particle. The factors governing the grain density in single tracks are discussed in Chapter 12. According to Wilkins [W24] the photographic density is also dependent on the temperature of the exposure. At exceedingly low temperatures (−185° C) the value of c fell to about one-third of its value at 20° C. Wilkins attributes this not to a difference in range of the alpha particles but to a variation in the number of grains per track. Sheppard [S25] suggests that at very low temperatures the bromine set free by the exposure is immobile and partly recombines with the silver whereas at room temperature it is immediately absorbed by the gelatin.

FIG. 3. Relationship between density and number of alpha particles. Reconstructed from the data of Wilkins [W24] using Process emulsions having the following characteristics: $D_m = 5.0$, $G_m = 2.71 \times 10^9$ per cm^2, $k = 10$ at 20° C and 3.6 at −185° C, $\pi r^2 = 0.366\mu^2$.

The temperature during exposure enters as a significant factor in emulsions exposed to cosmic radiation in the stratosphere where both abnormally low and high temperatures are encountered depending on the position of the plates relative to the sun's rays. A predominating low temperature will cause the tracks to

develop with a lower grain density. Experiments by Salant[853] show that the developed grain density in the tracks of recoil protons traversing the emulsion at −60° C is about one-third less than in control plates kept at 20° C during the fast neutron bombardment.

Svedberg and Anderson[846] have studied the sensitivity of photographic emulsions towards alpha particles as a function of grain size in the emulsion. They find that the percentage of grains rendered developable P is dependent on the alpha-particle flux f striking unit area of the emulsion per second, the average cross-sectional area of the silver halide grains A, and the time of exposure t. They conclude that each grain hit by an alpha particle is made developable and that the sensitivity of the emulsion is expressed by:

$$P = 100(1 - e^{-Aft}) \tag{4}$$

Experiments with polonium sources emitting alpha particles at a rate of 50,000 per cm^2 per sec show that, as the grain size increased in a series of commercial emulsions, the percentage of developable grains increased for a constant period of exposure.

In the Lantern Slide-type emulsion, commonly employed in the autoradiography of weak sources, the grain diameter is about 6 times greater than in the nuclear-type emulsions. By sacrificing track definition and resolving power, a 5-fold increase in photographic density is secured through the use of the coarser-grained emulsion. This factor is due to the alpha-ray component only, and the blackening is further augmented if the source also emits beta particles, as the coarse-grained emulsions are also activated by them.

Pinhole Autoradiography. It is not practical to study the surface distribution of very active preparations by the methods of contact autoradiography. In manipulating a source of 1 curie strength the total exposure must be kept below 0.001 sec. To avoid excessive blackening an elaborate mechanism would be necessary in making and breaking contact with the emulsion.

The fact that in an evacuated system the alpha particles travel in straight lines without absorption or scatter permits the recording of a picture of the source by means of a pinhole camera. An inverted image is produced, its size dependent on the ratio of the distances of the diaphragm between the source and the recording

medium, and its definition improving with diminishing size of the orifice. The pinhole support must exceed a thickness of 50 microns in order to serve as a complete barrier for ThC′ alpha particles.

With a pinhole of diameter d set parallel with respect to the source, and the emulsion at an equal distance R, the time of exposure in seconds is approximated by $16R^2f/qd^2$, where q is the activity of the source in curies per square centimeter and f is the number of alpha particles necessary for the production of a visual image on unit area of the particular type of emulsion. In a camera constructed so that $d = 0.05$ cm, $R = 5$ cm, and utilizing a fine-grain emulsion with $f = 10^7$ tracks per cm^2, the exposure for 1 curie of polonium per cm^2 is about 43 sec. By extending the exposure to 100 hours the method becomes applicable to weaker sources of about 0.1 millicurie per $cm.^2$ Because the polished surface of the richest uranium ores has an activity of only $\sim 10^{-8}$ curie, the exposure is rendered impractically long (about 100 years).

The method has been applied by Morris and Lockenvitz [M41] in a study of the distribution of polonium on thin films of silver and bismuth. Pinhole autoradiography has also proved serviceable in defining the uniformity of polonium deposits employed as test films for electrical resistivity measurements by Maxwell and coworkers.[M42]

Chapter 2 · COMPARISON OF SCINTILLATION AND PHOTOGRAPHIC METHODS

Those who have to guide the destinies of nations might do worse than take a peep through the lens of a spinthariscope and spend the rest of the day in the contemplation of its implications. Even scientific men, who, of all people, might be expected to be the first to realize the consequences of their own discoveries, in their private lives still think, act and counsel others as though it is only by the most heroic exertions that anyone survives in the struggle for existence. For generations now, and, indeed, ever since the harnessing of ordinary fuels, the struggle has, like the Oxford and Cambridge boatrace, been of traditional and symbolic rather than physical significance. After having struggled so long to exist, humanity now exists to struggle.—Frederick Soddy, 1932

It is informative to consider the scintillation method of alpha-particle detection, as this almost forgotten technique has many features in common with the emulsion method for recording the tracks of ionizing particles. The translation of the energy of the impinging alpha particle into light by zinc sulfide or photochemical activity in silver bromide is probably governed by similar mechanisms. It is also desirable to call attention to this simple method of radiation detection if for no other reason than to dispel a prevailing notion that elaborate instrumentation is invariably a prerequisite to modern nuclear research. When one considers that many of the basic laws of radioactivity were formulated and the first evidence for artificial nuclear disintegration was secured with the aid of a coating of zinc sulfide, it becomes evident that the results achieved, and not the complexity of the apparatus, are of moment.

SCINTILLATION METHOD

Certain natural crystals like willemite and diamond, and laboratory preparations of barium platinocyanide and zinc sulfide, are rendered luminous on exposure to strong sources of alpha or

beta radiation. Sir William Crookes[C27] and, independently, Elster and Geitel[E2] found that, on microscopic examination of the irradiated zinc sulfide screen, the luminosity was not continuous, but that each impact of an alpha particle produced a flash discernible by a dark-adapted eye. Crookes devised a simple instrument termed a spinthariscope consisting of a thin film of zinc sulfide and a low-power magnifying lens focused on the screen, which renders the scintillations visible from a close-by alpha-active source.

The scholarly-minded Crookes derived the name for this instrument[C28] from the Greek word σπινθᾶρις, as used by the poet Homer in the Hymn to Apollo: "Here from the ship leaped the far darting Lord Apollo, like a star at midday, while from him flitted scintillations of fire, and the brilliancy reached to heaven." Half a century after Crookes' discovery, Henry D. Smyth,[S30] reporting an epochal experiment on the first divergent nuclear chain reaction, is also moved to Homeric expression: "At the appointed time there was a blinding flash lighting up the entire area brighter than the brightest daylight. A mountain range three miles from the observation post stood out in bold relief. Then came a tremendous sustained roar and a heavy pressure wave, . . . thereafter a huge multicolored surging cloud boiled to an altitude of over 40,000 feet."

A spinthariscope adapted to the visual detection of radioactive inclusions in polished mineral sections is described in Fig. 4. In the absence of electrical counting instruments it serves as a rapid means for establishing the presence of alpha-ray-emitting elements and with adequate experience furnishes a guide for estimating the proper exposure period in subsequent measurements with fine-grained emulsions. The tests are made in a darkened room, and observations are best delayed for several minutes until the eye becomes dark adapted. It is good practice to initiate observations on a polished section of known radioactivity, and when the flashes become discernible to replace the test section by the specimens under investigation. Conclusions are unambiguous when flashes are observed at a rate exceeding 1 per min. When the segregate has an exposed area of 1 mm^2, statistically about 2 scintillations per sec can be observed when the uranium content is above 50 per cent.

The experiment can be conducted quantitatively by supporting a zinc sulfide screen at a distance d above the center of a circular thin film of the preparation having a radius a, and focusing on the screen with a 6× objective and a 5× wide-field ocular. If

A is the area of the screen covered by the microscopic field, n the number of scintillations observed per second, then the number of alpha particles emitted per second δ from 1 cm² of the source is, according to Rutherford: [R18]

$$\delta = \frac{2n}{A\left(1 - \frac{d}{\sqrt{a^2 + d^2}}\right)} \tag{5}$$

With sufficient care and patience the scintillation method can yield accurate results, as evidenced by Rutherford's determination of the rate of disintegration of uranium and thorium [R18] and the determination of the decay constant of radium by Geiger and Werner.[G8] The disintegration rates evaluated from scintillation counts are about 5 per cent lower than the values obtained by modern electrical counting devices. Methods for the preparation of zinc sulfide screens are described in Chapter 3.

FIG. 4. Spinthariscope for detecting alpha particles from polished sections.

a. Scintillation screen with deposit of activated zinc sulfide, ZnS·Cu.

b. 10× lens, focused on zinc sulfide layer.

THE SCINTILLATION MECHANISM

The production of scintillations is commonly attributed [R20] to a network of fine strains in the crystal lattice caused by the presence of the activating ions in the phosphor. The passage of the alpha particle releases the strains along a cylindrical volume.* This space is delineated by the range of the alpha particle in the solid phosphor and its effective cross section, which is proportional to the radius of action. This view is consistent with the gradual decay of the luminosity of the screen under prolonged bombardment and is similar to the phe-

* Other densely ionizing particles as the proton also produce individually discernible scintillations on traversing the phosphor. In his classical work on the disintegration of nitrogen by alpha-particle bombardment, Rutherford notes that the long-ranged protons arising from the reaction produce flashes of lesser brilliance than the bombarding alpha particles. This is analogous to the difference in grain densities of the tracks produced by protons and alpha particles in emulsions and reflects the different ionizing properties of the two particles.

nomenon of solarization produced in emulsions on prolonged high-flux alpha-particle exposures. Assuming that an active center of the phosphor is destroyed once it has taken part in the emission of light, Rutherford [R19] found that the radius of action of the alpha particle is about 7×10^{-8} cm. In nuclear emulsions the radius of action is about 10^{-5} cm, the more effective cross section and greater visibility having arisen during the development process, which reduces the entire grain to silver and not merely the channel through which the alpha particle plowed its way.

It has been observed [Y17] that the zinc sulfide employed in the preparation of screens is triboluminescent and, like many forms of naturally occurring sphalerite, produces flashes of green light on abrasion in the dark. If the screen is compressed against or moved across a non-radioactive surface, under the microscope are observed numerous bright green flashes which are difficult to distinguish from the scintillations produced by a radioactive source separated from the stationary screen. The passage of the alpha particle produces momentarily an extremely high temperature in the space it traverses even when a small part of its energy is converted into heat. The scintillations may possibly originate from the transformation of the localized heat into light by the triboluminescent zinc sulfide. A similar "point-heat" mechanism has been postulated in the explanation of the biological action of alpha radiations in tissues.[L24]

Spectrographic analyses of the scintillations produced in ZnS·Cu phosphors show that the light covers a wide band between 4000 and 6000 A with two maxima at 4500 and 5200 A. The latter peak corresponds closely to the 5050 A line at which the dark-adapted eye is most sensitive. This fortunate distribution of the luminescence is an important factor in the sensitivity of the method which permits the visual detection of the passage of an alpha particle. The brilliance of the flash is dependent on the residual energy of the alpha particle at the time it strikes the screen. The flashes produced from thorium minerals are in general more brilliant than those initiated by the alpha rays of uraniferous materials. This is in accord with the general higher energy of the alpha particles associated with the thorium disintegration series. The length of a track recorded in an emulsion is likewise dependent on the residual energy of the particle at the moment of entry into the recording medium.

By examination of the scintillations produced in large grains of zinc sulfide or continuous cleavages of willemite [G7] or diamond [C11] at about 800× the flash can be resolved as a distinct track. The range of the luminous tracks of polonium alpha particles in a willemite crystal has been estimated at 20 microns.[K19] In nuclear-type emulsions the track length is of the same order of magnitude.

Several homogeneous transparent cleavages of sphalerite have been investigated [Y17] for sensitivity to alpha radiation. Of the crystals tested none exhibited scintillations or tracks. The trace constituents essential to the scintillation mechanism were probably absent in the clear transparent mineral specimens tested. A continuous screen is advantageous in quantitative measurements, as with powder screens a correction must be made for the voids between crystal grains. It is noteworthy that the emulsion is also essentially a discontinuous medium, and alpha particles of low residual range may at times spend the greater part of their energy in the gelatin only.

PHOSPHOR SCREENS FOR BETA PARTICLES

Mineral phosphors vary considerably in their luminous response to radioactive radiations. Zinc sulfide is activated chiefly by alpha particles. Scheelite (calcium tungstate)* and barium platinocyanide are especially sensitive to beta and gamma rays. Willemite (a zinc silicate activated by manganese) shows about equal response to all three radiations. According to Thompson [T12a] strontium sulfide activated by cerium and samarium exhibits high luminosity on beta-ray irradiation.

These luminescent phenomena suggest that the sensitivity of photographic emulsions to beta radiation might be enhanced by the incorporation of suitable phosphors in the gelatin, the fluorescent light thereby augmenting the actinic action on the silver

* Screens of the mineral scheelite and special chemical preparations of calcium tungstate luminesce with a bluish color under beta-particle bombardment. In irradiating minerals with slow neutrons the writer has observed that scheelite of diverse geologic origin becomes persistently luminescent; the intensity of the glow diminishes slowly but is still pronounced several hours after the bombardment. The phenomenon is probably caused by the emission of beta particles from radiotungsten, formed by neutron capture, which activate the calcium tungstate molecules to luminescence.

halides. These potential improvements in emulsions intended for use in beta-ray autoradiography are discussed in Chapter 10.

CONDUCTIVITY PULSES INDUCED IN PHOSPHORS

The investigations of van Heerden [V1] on the use of certain crystalline solids as ionization media for the measurement of conductivity pulses initiated by radioactive radiations are causing renewed interest in the use of crystals for the detection and differentiation of nuclear radiations. Van Heerden observed that alpha particles produce ionization in crystals of silver chloride of sufficient magnitude that the voltage pulse of every single particle, if sufficiently amplified, can be observed and measured. At the temperature of liquid nitrogen the voltage pulse induced in synthetic crystals of silver chloride is proportional to the energy of the particle. The crystal counter permits the measurement of the energy spectrum of any radioactive radiation that it can detect. Crystal counters are particularly effective in the study of gamma radiation because of their high absorption per unit volume. Likewise, beta rays of fixed energy produce ionization pulses the magnitude of which is a measure of the incident energy.

The formation of conductivity pulses in single crystals of silver chloride is also of interest in conjunction with the emulsion technique. At low temperatures the crystal probably records a latent image. Efforts have been made [Y17] to develop the latent alpha-particle image in specimens exposed tangentially to polonium alpha particles by means of standard elon-hydroquinone developing solutions. Individual tracks could not be observed owing to the deposition of a mirror-like film of metallic silver on the exposed surface. The silver chloride was employed in the form of thin rolled sheets, and the mechanical strain was probably the cause of the heavy silver deposition. It is problematical whether the latent image of densely ionizing radiations can be developed successfully in pure silver chloride in the total absence of gelatin and its associated traces of sulfur compounds.*

* It is possible that crystals of the native silver halides, carrying traces of activating ions, may operate as crystal counters at room temperature. Native crystals of cerargyrite—AgCl, bromyrite—AgBr, iodyrite—AgI, embolite—Ag(Br,Cl), and iodobromite—2AgCl·2AgBr·AgI carry traces of metallic ions and provide convenient specimens for further investigation.

Hofstadter, Milton, and Ridgway [H31] have studied the behavior of six synthetic silver chloride crystals. One specimen did not record pulses, and the energy per ion pair in the other five crystals ranged between 13 and 500 ev. They suggest that strained regions in the crystal probably act as electron traps and reduce the range of electrons in the conduction band. These erratic strains might be responsible for the large variation in the energy per ion pair in different specimens.* Hofstadter attributes the individual pulses induced by gamma radiation to the formation of high-speed beta particles in the silver chloride by the incident radiation. Hofstadter [H32] has investigated the recording properties of a crystal composed of 40 per cent thallium bromide and 60 per cent thallium iodide. After annealing to remove strains and chilling with liquid nitrogen the crystal gave satisfactory pulses on exposure to gamma radiation. Crystals of high density composed of heavy nuclei favor ion-pair production by feebly ionizing radiations. These experiments with thallium halides suggest that emulsions of these compounds may prove satisfactory recording media for the tracks of nuclear particles. These novel emulsions would be of chief interest in conjunction with fissionability studies on thallium isotopes.

Wooldridge, Ahearn, and Burton [W27] found that certain diamond specimens exhibit the phenomenon of radiation-induced conductivity and that the pulses can be measured with the specimen at room temperature. This simplification makes the crystal counter exceptionally useful because of its small size, low operating voltage, and rapid counting rate. It is noteworthy that van Heerden, experimenting with only one diamond crystal, found that it did not record conduction pulses. Also, Curtis and Brown [C35] report that apparently only water-white diamonds free from obvious flaws serve as satisfactory radiation detectors. This suggests that the induced conductivity pulse, like the luminescent properties of many phosphors, may be dependent on crystal structure or the presence of suitable activating ions in the lattice. The

* According to N. F. Mott, ion-pair production in solids like silver bromide requires a smaller expenditure of energy than in gases, for which the rate is about 30 ev per ion pair. Demers [D9] states that the energy of an ionizing particle should be spent ultimately in bringing electrons into the conduction band, at an expenditure of about 5 ev. It is noteworthy that in one of the silver chloride crystals tested by Hofstadter the energy per ion-pair production was significantly lower than in air.

work of Raman[R1] on the fluorescent properties of diamonds shows that specimens with tetrahedral symmetry fluoresce blue under filtered 2537 A ultraviolet light. Crystals with octahedral symmetry are non-luminescent, and diamonds in which the tetrahedral and octahedral structural types are intimately mixed exhibit the greenish-yellow type of luminescence. Similar studies * on crystals exhibiting conductivity pulses may provide a simple guide for the selection of specimens for use in crystal counters. In this connection it is also of interest that Chariton and Lea[C11] observed scintillations in alpha-particle-bombarded diamond chips.

ELECTRONIC SCINTILLATION COUNTERS

The humble scintillation screen has recently been incorporated into new types of radiation detectors. In these devices the eye is relieved of the task of viewing the individual flash, and in its stead a photomultiplier tube circuit enhances the initial light quanta from the phosphor sufficiently for a pulse to be observed on an oscilloscope screen. The circuit can also be arranged so that each alpha-particle scintillation produces a click in a headphone or loudspeaker.

Sherr[S26] has described an instrument that exhibits selective response to alpha particles. It employs a zinc sulfide phosphor activated by silver as the detection screen. The phosphor is covered by two thin aluminum foils having a thickness equivalent to 1 mm of air, which serves to prevent access of light. With this arrangement Sherr observed the range of the polonium alpha particles to be 3.65 ± 0.05 cm using headphones and 3.70 ± 0.02 cm with an oscilloscope. Since the mean range of the radiation is 3.84 cm, these values indicate that the instrument can detect alpha particles with a residual energy of about 0.2 air-cm, which represents a marked improvement over visual detection of the scintillation. By employing more elaborate electronic equipment and optical focusing of the flash, Sherr believes that it should be possible to detect alpha particles with a residual range below 0.1 Mev. This scintillation counter, like the nuclear-type

* Studies by Friedman, Birks, and Gauvin[F15a] indicate that diamond specimens that exhibit good pulses transmit ultraviolet light well below 2536 A.

emulsions, is relatively insensitive to gamma and beta rays. An external source of 1.8 millicuries of radium increased the background hiss but did not give rise to distinguishable pulses.

Another type of photomultiplier radiation detector, described by Coltman and Marschall,[C20] also responds to less densely ionizing radiation such as beta, gamma, and x-rays. The luminescence induced by the beta radiation is concentrated with the aid of a spherical mirror onto the sensitive area of the photocathode of a multiplier tube. The initial quanta emitted by the phosphor are passed through several stages of amplification until the output pulses are sufficient to operate the amplifier of an oscilloscope. Comparative tests on the detection of gamma and beta rays and 8-kv x-rays show that the photomultiplier tube is twice as efficient as Geiger counters designed for the measurement of the particular radiations.

The beta-ray pulses have a duration of about 25 microseconds. This limits the maximum counting rate to 10^4 beta particles per sec. The duration of the pulses induced by alpha particles ranges between 1 and 5 microseconds, the period depending on the nature of the phosphor screen. It has also been possible to count neutrons with this detector by incorporating boron compounds with the fluorescent powder. The slow neutrons are captured by B^{10} with emission of alpha particles on disintegration of the compound nucleus. These alpha particles give rise to scintillations which generate pulses after suitable amplification.* For purposes of beta-particle detection the most efficient response is produced by a Patterson-D x-ray screen, carrying a $ZnS \cdot Ag$ phosphor fluorescing in the blue region.

Moon[M43] has investigated a series of natural and synthetic crystals as scintillation media for the counting of ionizing radiation and quanta. Among 28 specimens tested, scheelite, fluorite, spodumene, Al_2O_3, and LiF gave excellent responses. Other crystals, including quartz and mica, produced no detectable pulses, the remaining materials giving reactions of intermediary intensity. Many of the native crystals caused spurious pulses

* The efficiency of this neutron-detection mechanism might be increased by substituting zinc or cadmium borate phosphors for the zinc sulfide screen. If these phosphors could be sensitized to low-energy alpha particles, the efficiency would be increased by the greater abundance of boron nuclei and the absorption of the particles in the phosphor.

in the photomultiplier tube owing to residual phosphorescent reactions. The pulses were eliminated by chilling with solid CO_2, or destroyed by heating and subsequent cooling in the dark. With these precautions the background count could be reduced to the normal level of about 1 per sec.

In comparing a scheelite crystal with naphthalene, the mineral phosphor gave a better response to gamma radiation from Ra, but the two materials were equally sensitive to electrons from a RaD + E source. In a comparative test with a G-M counter the scheelite crystal proved to be 125 times more sensitive than naphthalene as a gamma-ray detector.

Hofstadter [H32a] finds that alkali halide crystals activated by about 0.1 per cent thallium are efficient scintillation counters. In a synthetic crystal of NaI·Tl alpha particles produced pulses comparable in intensity to those from a ZnS·Ag phosphor. This crystal also proved to be a more efficient detector for gamma radiation than a clear piece of naphthalene of comparable size.

It is of interest that Hofstadter secured a measurable photographic blackening by placing the crystals on Eastman-type 103-O plates, using a thin quartz intermediary filter, and exposing to penetrating radiation. Discernible images produced by the light in the crystals developed after a 30-min exposure to the gamma rays of 1.8 millicuries of Ra kept at a distance of 1 meter from the detector. Mineral-phosphor screens for the photographic detection of slow and fast neutrons, proposed by Kallmann, are described in the section on neutron radiography, p. 246.

Chapter 3 · LABORATORY MANIPULATIONS

Trifles make perfection, and perfection is no trifle.
—Leonardo da Vinci, 1500

GENERAL ASPECTS OF SAMPLE PREPARATION

The methods for the preparation of plane polished surfaces of inorganic materials for microscopic study are in general also suitable for purposes of autoradiography. The polishing of metals and minerals, and the preparation of thin sections of biological tissues, are highly developed arts. Details are recorded in works on metallurgy,[K8, B16] petrography,[S28, K15] and histology.[M20] The polishing of complete ore bodies containing components of extreme degrees of hardness has been the subject of considerable study. Techniques have been developd for the preparation of specimens with mirror-like surfaces in which the soft and hard components reside in the same plane and are essentially scratch free even at magnifications above 500×. Perfectly polished surfaces of this character, as developed by the Harvard School of petrographers,[G20] are usually unnecessary for radiographic study, as the resolving power of the emulsion is seldom equal to the mechanical definition of the segregates.

In the cutting, mounting, and polishing of radioactive material considerable care must be taken to avoid contamination of the specimens. The customary concepts of chemical cleanliness are not adequate, and a new set of habits must be acquired in order that the specimens remain radiochemically unaltered. In tracer work with radioactive isotopes the routine histological methods of fixation and dehydration may lead to the loss of water-soluble materials, and if proper corrective measures are not taken the autoradiographic pattern may be fallacious.

The true surface area of the section invariably exceeds its geometric area. The polished surface is the final result of angular cuttings removed by the abrasive grains. As the grains are made successively finer, the depth of penetration diminishes, and the number of serrations per unit area increases. Measurements of

the absolute surface of metals subjected to different mechanical treatments show, from the work of Erbacher,[E8] that the area is practically independent of the size of emery paper used, and that it is about 2.5 times as great as the geometric surface. Hahn [H3] attributes the lower surface-area ratio after polishing to the

Polishing Process	Ratio of Absolute to Geometric Area
Finished with coarse emery	2.49
Finished with fine emery	2.53
Finished with precipitated chalk	1.72

softness of the chalk and to its smaller angular effect in producing a striation mark. It is also possible that with very fine dry abrasives the surface film tends to flow and reduces the number of furrows. These considerations on absolute surface area are of particular importance in polishing radioactive minerals, as the loss of emanations is a function of surface area. Where quantitative comparison of activity is to be made among different specimens, a standardized polishing procedure must be adhered to.

The common methods of surfacing and polishing using revolving wheels covered with a slurry of emery are not conducive to maintenance of radiochemical purity. Active specimens contaminate the metal laps as a result of electrochemical replacements and deposition of radiocolloid aggregates. The usual water rinse does not free the lap from radioactive deposits, and there is danger of contaminating other samples. Dry polishing papers eliminate these difficulties as they are readily discarded after each operation.

PREPARATION OF PLANE SURFACES

Massive Materials. Metallic samples and firmly coherent rock and mineral specimens do not require a preliminary impregnation with binding agents. A slab about 5 mm thick and of 4 cm^2 cross-sectional area is removed from the sample using a hacksaw on malleable material and a diamond wheel on rocks. The cutting tools should be specially marked and used on specimens of about equal degrees of activity. Contaminants incorporated into the surface at this stage are usually eliminated in the preliminary stages of dry polishing on emery papers.

The rough-surfaced chip should be mounted in a plastic base like Bakelite or Lucite. This serves to standardize the dimensions of irregular-shaped chips and is of great convenience in subsequent microscopic examination of the specimen and its pattern. The plastic shields the hand from alpha and beta radiation during polishing and likewise prevents the registration of these radiations from the sides of the specimen.

Bakelite molding powder BM 120 is commonly employed. To prevent contamination of the mold and facilitate the removal of the biscuit, a disk of waxed filter paper should be inserted between the steel base plate and the specimen. The weight of molding powder is adjusted to yield an extrusion of nearly constant volume. The die is compressed to a pressure of 1000 lb per in.^{2}, heat is applied, and the pressure is augmented to 3000 lb. When the temperature reaches 160° C polymerization is complete. The die is chilled with an aluminum jaw-block to about 80° C and the mounted specimen is extruded.

Polishing is effected through the successive use of graded "metallographic" emery papers. The specimen is abraded on No. 2 paper until the waxed-paper separator is cleared and the specimen surface comes to view. This may be performed manually, supporting the abrasive paper on a sheet of plate glass, or a 9-in. square of the paper can be attached to the center of a rotating horizontal disk by means of a cap screw and washer. Considerable dust is generated at this stage, and the operation must be conducted with adequate ventilation. The periphery of the paper is not attached, the rotation at 2000 rpm keeping the paper flat. The specimen is moved slowly from the center towards the periphery using just sufficient pressure to hold the specimen against the wheel. When the surface markings from the cutting process are obliterated, the abrasion is continued using a No. 1 grade paper, holding the specimen so that a series of parallel grooves is cut at right angles to the first series. This process is continued through successively graded emery papers, 0, 00, 000, and 0000. In passing from one grade to the next the specimen should be cleaned with a dry soft tissue. Any film of abrasive adhering to the surface after the last stage is removed by gentle rubbing against a sheet of lightly waxed blotting paper.

Where a lower temperature is desirable to avoid phase changes or possible shattering of hydrated materials the specimen can

be embedded in Lucite, or in atmospheric-pressure-setting compositions of methyl methacrylate, like Ward's Bioplastic. Water-soluble crystals can be mounted with the aid of paraffin or montan wax.[Y10] A solid Bakelite form is molded into a shell as indicated at *b* in Fig. 5. The roughly surfaced specimen is placed on a flat sheet of aluminum, centered beneath the Bakelite shell, and the prewarmed unit is filled with molten wax. Low-melting-point alloys, as Wood's metal, m.p. 66° C, are employed advan-
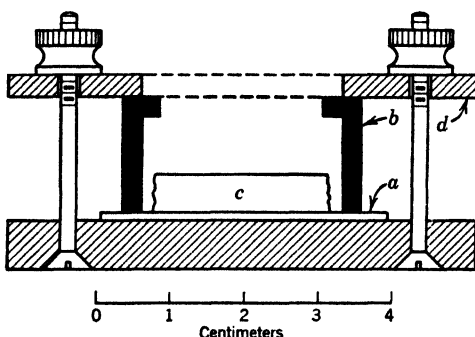
FIG. 5. Frame for wax mountings.

a. Flat aluminum sheet about 1 mm thick.
b. Plastic shell or Bakelite screw cap.
c. Slab impregnated with wax.
d. Brass clamping bar with hole for admission of wax.

tageously in the mounting of hard, thermal-sensitive specimens. These methods have permitted the polishing of single crystals of $CuSO_4 \cdot 5H_2O$ grown from saturated solutions of copper sulfate after neutron bombardment, and of ammonium bichromate crystallized from a solution carrying polonium. Typical specimens mounted for autoradiography are illustrated in Fig. 6.

Sulfur is worthy of consideration as a mounting medium for specimens of very low alpha-ray activity. The commercial product has a low radioactivity and is readily purified in the laboratory by sublimation. It has been recommended by Epstein[E7] as a mounting medium for dental alloys and steel specimens. It melts at 120° C, hardens quickly after solidification, and is inert to acid etching solutions. Mounting is effected with the aid of the frame described in Fig. 5, substituting a filter paper for the thin aluminum backing. Dry sulfur does not appear to react with silver halide emulsions even after a contact period of one month.

Friable Materials. Samples of a porous or crumbly nature require reinforcement by infiltrated binders to prevent grains working loose during polishing:

Place a suitably sized lump of ore or bone in a small beaker and cover with a 5 per cent solution of Lucite powder dissolved in acetone. Cover with a bell jar and reduce pressure cautiously. When foaming ceases, transfer material to a waxed disk of paper and allow solvent to evaporate
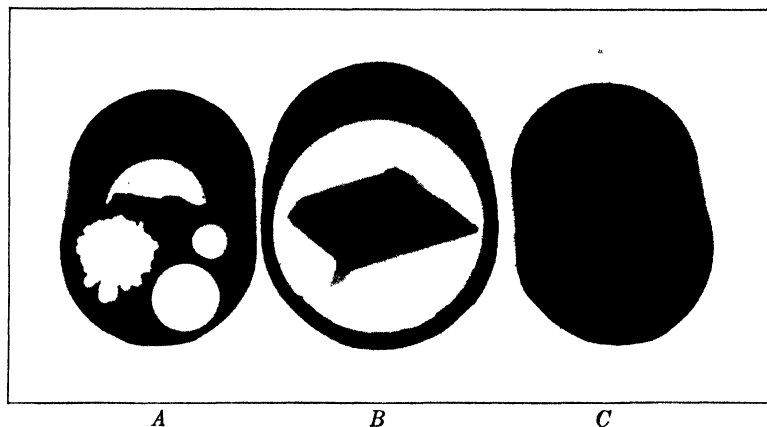
Fig. 6. Specimens mounted for autoradiography.

A. Metals mounted in Bakelite.
B. Crystal of $CuSO_4 \cdot 5H_2O$ embedded in montan wax and supported by screw-cap frame.
C. Copper-ore section impregnated with wax and molded in Bakelite.

slowly at room temperature. When the outer coating hardens the unit is placed in the die and molded in either Lucite or Bakelite. After preliminary abrasion on No. 2 paper, examine exposed surface for complete impregnation. If loose grains are evident, cover the surface with a layer of Lucite solution, infiltrate under reduced pressure, dry, bake for several hours at 100° C, and continue with the polishing.

An alternative procedure, advisable in the sampling of large lumps, is to impregnate superficially with Lucite solution and to allow the mass to dry on a rectangular board about 1 cm thick. When the solvent has evaporated, drip molten montan wax over the specimen until it is covered and attached firmly to the wooden support. Cut into slabs about 5 mm thick, remove wooden slats, trim slabs to fit die, wash, and wipe dry. Films of adhering wax

do not interfere with subsequent mounting in Bakelite. In the absence of hydraulic mounting equipment, or where it is desirable to avoid high pressures, the slabs can be mounted in a Bakelite shell or bottle screw cap as shown in Fig. 5:

Assemble the press with the specimen centered in place and warm on a hotplate until the wax surrounding the slab begins to melt. Place on level board, fill screw cap with molten wax, using a medicine dropper, and allow to solidify. Remove aluminum backing (*a*) by warming momentarily on a hotplate. Polish as described in the section entitled Massive Materials. The supply of montan wax was obtained originally from I. G. Farben Ind. and is now no longer available. Domestic montan waxes exhibit a minute shrinkage on solidification and, though satisfactory as impregnants, are not serviceable for mounting in screw caps. Halowax 2025 furnished by the Halowax Corporation, New York City, is satisfactory both as an impregnant and as a mounting medium. It melts to a mobile fluid at about 110° C. The vapors of this chlorinated hydrocarbon are somewhat toxic, and the wax should be liquefied under a hood.

It is occasionally advantageous to examine the specimen by transmitted as well as by reflected light. Also, in beta-ray autoradiography the pattern is more sharply delineated by using a thin polished section. The Canada balsam commonly employed as a cementing medium produces pseudophotographic effects. Glycol phthalate provides a satisfactory mounting medium for thin rock sections. Details of the method are described by Kennedy[K7] in the preparation of thin ore sections on wet emery-charged laps. To avoid radioactive contamination the grinding can be effected manually on small squares of plate glass which are reserved for specimens of different levels of radioactivity, or preferably are discarded after use:

A parallel-faced slice about 3 mm thick is cut and surfaced with grade 600 Carborundum. Place the dry specimen and a glass slide side by side on a sheet of brass and warm to about 120° C. Run a stick of the thermoplastic over the hot slide so that a thin layer melts onto it. Center the polished surface over the melt, pressing out air bubbles, and allow to cool. The chip is thinned in three stages, first in a slurry of F-Carborundum until it is reduced to about 60 microns, followed by 600-Carborundum on a separate glass plate until it reaches a thickness of 35–40 microns. The final stage of grinding is effected on a glass plate charged with 600-Alundum. Polishing is done on duck cloth by means of stannic oxide. Further details on the specialized technique of thin-rock-section preparation are described by Head.[H19]

In the study of the distribution of incorporated radioisotopes in alloy melts, thin metallic sections can be prepared by the methods developed in the field of x-ray microradiography by Zimmerman [Z7] and McCutcheon: [M21]

Flat samples about 5 to 10 mm thick are removed by hacksaw cuts and one surface is polished as usual. After molding in Lucite, with the unprepared surface facing outward, the specimen is turned down in a lathe by cuttings parallel to the interior polished face until a slab about 0.3 mm remains. The unit is now polished by hand, starting with grade 0 paper, until the thickness is reduced to about 120 microns. If the specimen should loosen in the Lucite before this stage is reached the thin disk is remounted on a rubber stopper with the aid of Cenco label varnish and the reduction in gauge continued. The foil-like specimen is removed from the Lucite mounting by beveling off the surrounding edge of plastic and prying with the aid of a razor blade, or chilling on Dry Ice. Cutting tools should be tested for activity after use and properly marked. Filings and turnings are collected in a tray and should not be allowed to remain in the instrument shop. These operations are best conducted in a separate room so as to avoid contamination of machinery in the main shop.

An alternative procedure for the preparation of thin metallic foils is given by McCutcheon.[M21] A parallel-faced slab of the specimen about 2 mm thick is polished on one face and mounted on a flat steel disk with de-Khotinsky cement. The opposite face is then filed down to about 0.3 mm. The thin disk is removed with the aid of alcohol, transferred to a No. 9 rubber stopper, and caused to adhere with a thin layer of rubber cement. It is then abraded down on fine emery paper until it is about 25 microns thick.

Biological Tissues. After embedding of the fixed and dehydrated tissue in paraffin, the microtome-surfaced block is in many respects identical with the polished inorganic sections mounted in plastics. The study of ingested alpha-ray-emitting elements as radium, polonium, and plutonium is facilitated by direct contact of the faced block against a nuclear-type emulsion. Comparison of the developed alpha-ray pattern with the tissue structures is effected with the aid of an adjacent stained thin section. In the study of macro segregations in whole organs this simple procedure is particularly effective, as the embedded massive tissue suffers but little distortion in cutting and usually exhibits better definition of macro structures than a radiograph from a thin ribbon section. The surface of the block must be perfectly dry to avoid fixation to the gelatin of the emulsion. Clamping

is unnecessary, as a slight pressure on the block causes the paraffin to adhere to the plate.

In the preparation of tissue for autohistoradiography it is important to employ methods which retain water-soluble salts and minimize their migration by diffusion processes. The radioisotopes of the heavy metals, like RaF, Ra, ThC, and ThX, have a tendency to form radiocolloid aggregates (see Chapter 6) which are strongly adsorbed on the walls of capillary structures or precipitate as organometallic complexes in the tissue. There is little danger of losing these particular constituents following routine histological procedures of tissue staining. The synthetic radioactive isotopes of the elements of low atomic number do not have as marked a tendency towards aggregation. On contact with water, tagged compounds such as $Na_2HP^{32}O_4$, KI^{131}, or $Na^{24}Cl$, are very likely to be lost or dislocated from their *in vivo* site of deposition.

The identical problems occur in the preparation of tissue for the study of the deposition of total ash content in plant and animal sections by the microincineration method. These methods, developed by Policard [P26] and studied in great detail by Scott [S14] and Gersh,[G10] also offer a desirable experimental approach for historadiographic studies. Indeed, the microincineration method itself is worthy of consideration as a working tool, as it offers the possibility of obtaining individual radiographs of systems containing multiple radioactive tracers. Thus, if an animal is injected with a mixture of radiocarbon and radioiron, the radiograph of the original tissue would reveal the location of the joint activity, and a print of the microincinerated tissue would exhibit the distribution of the non-volatile iron compounds, as almost all carbon derivatives are destroyed in the incineration. The method also permits the use of thicker tissue sections without loss in definition, as the ashing produces an extremely thin film of residual solids. This incineration process concentrates the activity, and the removal of all organic matter reduces scattering.[Y17]

The tissues are removed from the animal under anesthesia and plunged directly into isopentane chilled by liquid air. The solid tissue is transferred to a cryostat maintained at −70° C, and gradually warmed to −32.5° C. At this temperature the ice has an appreciable vapor pressure

and the tissue can be dehydrated in an evacuated system. The desiccated tissue is then plunged into molten paraffin and infiltrated under reduced pressure. The tissue blocks are embedded and prepared for cutting in the routine fashion. Sections are placed on clean, dust-free slides and pressed down with the ball of the thumb. For purposes of microincineration no fixative is necessary. Details of the method are described by Scott in McClung's *Handbook of Microscopical Technique*.[M20]

A simplified technique for the microincineration of plant tissue is described by Struckmeyer.[S45] The tissue is fixed for 24 hours in a mixture of 1 part of formaldehyde and 9 parts of absolute alcohol. Dehydration is effected by several changes in absolute alcohol. The plant tissue is cleared in xylol, infiltrated with paraffin, and cut into sections 15 microns thick.

Elaborate combustion trains are not essential for the preparation of good microincinerated sections. A crucible-type muffle furnace is adequate if lined with Monel metal to equalize the temperature and to prevent fragments of the ceramic from falling on the tissue. The slides are placed in the cold muffle, and the current is adjusted so that a maximum temperature of 400° to 500° C is achieved in about 3 hours. Combustion is then complete, and the slides are removed about 2 hours later when the temperature drops to about 30° C. Original tissue structures can be recognized in the resultant spodogram when the slides are examined under dark-field illumination at magnifications up to 200×.

For purposes of autoradiography the thin sections should be freed of paraffin by immersion in xylol and reimpregnated with a dilute solution of Parlodion so as to produce a protective film about 1 micron thick. The extraction of the paraffin prior to exposure is not essential, but it permits more effective contact with the emulsion. The Parlodion film is also a protective measure against fogging by pseudophotographic agents. Care must be taken to avoid contamination of the ribbons. Separate microtome knives should be used on paraffin blocks containing high and low concentrations of radioelements. Certain elements, polonium, for example, are likely to deposit electrochemically on the steel knife. Adapters for standard razor blades are convenient in sectioning highly active blocks, as the blades can be discarded after cutting.

Thin sections of such hard tissues as teeth and bone can be prepared by grinding the fixed and infiltrated organs, treating the material as a friable inorganic solid. Special methods for cutting undecalcified bone for purposes of autoradiographic study are described by Axelrod.[A6,7] Standard procedures involving

decalcification by acid washing cannot be employed, as the inorganic tracer atoms are washed out along with the calcium.

In a noteworthy advance in technique described by Bélanger and Leblond[B15] a layer of emulsion is poured on the stained section and the autoradiograph becomes an integral part of the slide. This greatly simplifies the microscopic localization of the radioactive areas, as the image and the tissue are always in point-to-point correlation, and each is brought into view by proper focusing. The method is somewhat laborious as the emulsion layer has to be prepared by remelting commercial dry plates and applying the fluid to the tissue under red-light illumination. An alternative procedure yielding excellent results with tissues carrying alpha-ray-emitting elements was developed by Endicott.[E4] Here advantage is taken of the poor light sensitivity of nuclear-type emulsions and their selective response to alpha radiation:

The tissue ribbon is floated off alcohol onto a 1 × 3-in. length of Eastman NTA plate, dried, and stored in a desiccator for a suitable exposure period. The paraffin is extracted by xylol, and the plate with the adherent tissue is developed in D19 for 2 min, rinsed in water, fixed for about 30 min in F5, washed, and dried. The tissue is then stained with the aid of Delafield's iron-hematoxylin for 2 min, washed in tap water for 5 min, dehydrated in 3 changes of acetone, cleared in 1:1 acetone-xylol and in 3 changes of xylol. A drop of xylol-clarite is placed on the tissue, and the preparation is covered with a glass cover slip. The characteristic alpha-particle tracks reside in the plane of the emulsion, and by focusing upwards the superimposed tissue is brought into view. The method permits resolution of radioactive structures at 1000× magnification.

A similar method was developed independently by Evans[E16] for the localization of radioiodine in tissues. The ribbon is superimposed on a portion of lantern-slide plate which after exposure and development is stained and examined at low power for blackening produced by the beta radiation. Evans' improved procedure[E17] is as follows:

The thin section is spread in a petri dish on water at 42° C. When the ribbon is smooth the small dish is placed in a large bowl of cool water illuminated with a red light and the section is floated onto a 2 × 2-in. Lantern-Slide plate. After 24 hours, when the unit is dry, the paraffin is removed with xylol and the exposure is continued for a sufficient period as indicated by a Geiger count. After development, fixation, and washing the plate is stained with Harris' hematoxylin solution by the following route:

Overstain → wash → acid water → wash → alkaline water → wash → counterstain with eosin. The stained preparation is dehydrated in alcohols, cleared in xylol, and mounted in clarite or balsam. Evans cautions on the use of ferric alum as a differentiating agent after hematoxylin staining, as the reagent reduces the intensity of the silver deposit. Its application is serviceable only when the photographic image is too dense from overexposure. The developed silver grains in nuclear-type emulsions are par-
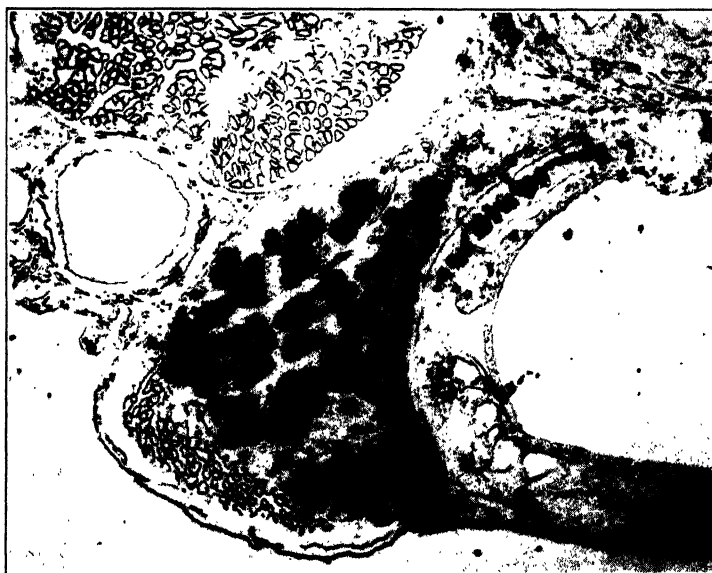
Courtesy of S. R. Pelc

FIG. 7. Localization of radioiodine in unstained tissue. Example of stripping-film technique autoradiography described by Pelc. Contrast phase microscopy; 35× magnification.

ticularly sensitive to acid solutions owing to their fine state of division. It is good practice to test the staining solutions for silver solvents by running a trial alpha-ray-exposed emulsion through the staining procedure.

Another useful modification of these techniques involves the adhesion of a thin film of dry stripping emulsion to the tissue section. The stripping emulsion consists of a layer of emulsion on an extremely thin coating of cellulose base which can be peeled readily from the temporary glass or plastic backing. In the method described by Pelc [P7,8] a 2 × 2-cm portion of emulsion is stripped off the special backing and floated on water with the side that formerly adhered to the support facing upwards. After

a few minutes the slide carrying the section, freed from paraffin, is slipped underneath the water-stretched emulsion, and the unit is dried in a dust-free air stream. The developed autoradiograph depicts minute radioactive inclusions with great clarity, as shown in Fig. 7, and a resolution of 3 to 5 microns can be attained. The Ilford Halftone dry stripping film employed by Pelc necessitates the use of special "subbed" slides in order to secure good adherence of the emulsion to the tissue and glass. The structure of the underlying tissue is delineated with the aid of contrast-phase microscopy, as it is difficult to stain the tissue through the residual film of gelatin.

In an alternative procedure, devised independently by Endicott and Clark,[E5] the prestained section is covered with Duco cement diluted 1:20 with ethyl acetate, and the cellulose side of the stripping film is pasted onto the tissue. After proper exposure the unit is developed and fixed as usual. The intermediary waterproof film of cement prevents discoloration of the stained tissue. Though this protective film introduces a small loss in resolving power, it is advantageous in preventing the diffusion of water-soluble radioactive constituents and minimizes pseudo-photographic effects on the emulsion. It also permits the use of more varied staining methods, as the tissue is not acted on by the developing and fixing reagents.

Nuclear-type emulsions are also available on stripping-film supports. These can be employed advantageously in studying the localization of alpha emitters in conjunction with Endicott's prestaining technique. Care must be taken that the intermediary layer of Duco cement does not exceed 5 microns, to avoid absorption of short-ranged alpha particles.

PREPARATION OF THIN FILMS

Quantitative measurements on the rate of disintegration are effected by measuring the ionization produced by the radiation escaping from thin weighed deposits of the sample. Because of the short range of alpha particles in solids the film must be especially thin so that a large fraction of the particles ejected from it will have sufficient residual energy to activate the detection apparatus. For the measurement of energetic beta particles and gamma radiation, an extra thin powder sample is not essential as the radiations spend comparatively little energy in the source.

The beta particles emitted in the decay of C^{14}, however, have upper energy limits of only 0.15 to 0.17 Mev, and the use of thin uniform films is desirable in its exact assay.

In the quantitative determination of the rate of alpha-particle emission with nuclear-type emulsions it is especially important that the sources be thin and uniformly deposited, as the longer the recorded track length the more readily is the event discerned microscopically. The following is a summary of proven methods of thin film preparation. The Parlodion ignition method is of comparatively recent origin,[Y17] and preliminary tests indicate that when applicable it is the most reliable with respect to uniformity and controlled thickness.

Sedimentation Method. This method, initially described by McCoy in 1905, consists in grinding an approximate weight of powder with a volatile organic liquid and depositing the suspension onto a preweighed support. After drying, the exact weight per unit area is determined by difference. Using chloroform or alcohol as suspension fluids McCoy[M19] was able to make films of U_3O_8 having a thickness of 0.5 micron. Essentially similar methods were employed by Boltwood in measurements on the decay rate of radioactive mineral fractions, and by Rutherford in the determination of the disintegration constants of uranium and thorium. Evans[E14] has improved on the method by providing a circular well with a thin rubber gasket above a weighed aluminum disk, so that the solid can deposit on an area of fixed dimensions. A layer of alcohol is placed in the well, and the finely ground suspension is poured onto the aluminum. The alcohol is evaporated in an electrically heated balance case continuously flooded with radioactively dead nitrogen. Powder films of circular cross section can also be deposited with the aid of frame *A* illustrated in Fig. 8.

The deposits prepared by these methods have adequate adherence but must be handled with care and cannot be placed in direct contact with emulsions. The films are usually deposited uniformly, except at the periphery, where the capillary forces tend to drag the suspension and produce an appreciable piling. On rare occasions, possibly owing to the condensation of atmospheric moisture, the film reticulates, and the preparation must be repeated. For samples in radioactive equilibrium and produc-

ing emanations Evans suggests the use of a thin covering film of cellulose acetate in order to retain the radon and thoron.

A rectangular-shaped source is preferable in measuring track populations on nuclear emulsions. The shape facilitates track

FIG. 8. Apparatus employed in thin-film preparation.

Front. Micro mortars of mullite and agate for grinding powders with ether. The fines are transferred by suction tubes into graduated cylinder on right.

Center. Circular (*A*) and rectangular (*B*) frames for evaporation of suspensions. In the Parlodion method the glass slide (*C*) is supported on a thermally insulating layer of cork.

Rear. Solvent evaporation is effected beneath bell jar, whose mouth is covered by a disk of filter paper.

counting in conjunction with the standard two-directional mechanical stage. Using ether as suspension fluid, numerous trials on diverse compounds like uranium oxide, beryl, zinc beryllium silicate, and a manganese dioxide carrier demonstrated that uniform deposits can be obtained with the aid of a rectangular

trough (item *B*, Fig. 8). It is important to have a 2-mm layer of ether in the trough, and the suspension must be poured unhesitatingly in one continuous stream. If the last drop hanging from the lip of the cylinder falls after the major stream is delivered, the uniformity of the film is disturbed. Surrounding the frame with a bell jar is essential to the technique as it prevents air currents from disturbing the sediment, and the surrounding atmosphere of ether minimizes condensation of moisture. The weight of the deposit is invariably less than that of the powder introduced into the mortar, and a 20 per cent allowance for loss should be made when aiming at a film of specified thickness. It is good practice to pipette the ground suspension into a tube, allowing the coarse particles to settle in the mortar, and to pour the well-shaken fines into the trough. Evaporation of the ether is completed at room temperature in about 2 or 3 hours.

When perfect film uniformity is not essential these methods can be simplified by grinding the powder to a pasty consistency and painting the suspension on a weighed backing with the aid of a small hair brush or a dab of cotton. The suspension can also be deposited on paper by filtration processes. Confined spot-test papers employed in microchemical procedures [Y3,4,8] are particularly convenient, as aqueous suspensions can be employed and the confining ring embedded in the paper serves as a microfunnel. Details of this semiquantitative spot-test technique are described by Feigl.[F6]

Electrolytic Method. Though the quantity of sediment introduced into the suspension can be reduced indefinitely, a point is reached, when the film weighs about 0.5 mg per cm^2, where the sedimentary deposit ceases to be uniformly thin. It is difficult to grind powders much finer than about 10 microns, and effort expended in that direction is usually offset by recoalescence and clustering of the fine particles into large-sized aggregates during subsequent manipulations. The clumps cause internal absorption of alpha particles, and introduce other complicating factors which are difficult to allow for, on purely geometric considerations, in the equations correlating film thickness with disintegration rate. In making absolute determinations of decay constants, as in the work of Schiedt [S4] on the disintegration rate of uranium, resort is made to electrolytically deposited films.

An ignited platinum foil of known weight is connected to the cathode on a base plate confined by a glass cylinder carrying the electrolyte. Spe-

cially constructed electrolytic cells are described by Schiedt[S4] and also by Francis.[F13] Russell[R15] describes an electrolyte suitable for the deposition of about 100 mg of uranium. An equivalent amount of uranyl acetate is dissolved in 125 ml of water acidified with 0.1 ml of 30 per cent acetic acid. The solution is warmed to 70° C and electrolyzed for 6 hours using a current of 0.04 ampere per 100 cm^2 of cathode surface.

Francis[F13] dissolves 10 mg of radiochemically purified U_3O_8 in dilute nitric acid, evaporates the solution to dryness, and redissolves the uranyl nitrate in 2.25 ml of 1 N acetic acid, 2.0 ml of 1 N NH_4OH, and dilutes the mixture with 15 ml of ethyl alcohol. A 7-cm platinum disk serves as cathode, and a rotating spiral of platinum wire is employed as anode. The electrolyte is maintained at 60° C with the aid of a microflame. The alcoholic medium favors the deposition of adherent films.

The uranium is deposited as $U_3O_8 \cdot 3H_2O$, which can be ignited to a compound whose composition approximates U_3O_8. In studies aiming at utmost accuracy the exact weight of the uranium must be determined, at the conclusion of the activity measurements, by suitable microchemical analyses. Hecht[H20] has devised a method for the microgravimetric determination of uranium oxide films based on its resolution in nitric acid and conversion of the uranyl nitrate to the 8-hydroxyquinoline derivative.

Electrolytic methods described by Haissinsky[H9] are also applicable to the preparation of thin sources of polonium, radium D, radium C, and thorium C, and possibly to certain transuranium metals.[H16] The deposition is effected electrochemically without the aid of an external electromotive force by rotating disks of copper (for RaF), nickel (for RaE), or silver (for RaC) in electrolytes of proper acidity. It is convenient to mount the metal disks in Bakelite and to polish the surface prior to electrodeposition of the radioelement.

Volatilization Methods. When samples of the pure metal are available, exceptionally thin films can be prepared on backings of glass, mica, or collodion by passing a heavy current through a wire or fragment of the metal and allowing the vapor to condense in an evacuated system. Films of this sort are essential in accurate measurements of alpha-particle ranges[R2] and in preparing deposits for scattering experiments.* An apparatus for volatilizing polonium and collecting the deposit on a minute area has been described by Rona.[R8] The method is serviceable

* A spot-test method for estimating the quantity of metal deposited on unit area of backing has been devised by Yagoda and is described briefly in the studies of Cox and Chase[C25] on the scattering of electrons by aluminum.

in preparing intense alpha-particle sources for experiments requiring collimated beams.

Parlodion Ignition Method. In the course of measurements on the decay rate of uranium Y14 a method was devised for the preparation of extra-thin uniform films of uranium trioxide, which shows promise of development into a method of fairly general utility:

A weighed quantity of radiochemically purified U_3O_8 is converted to uranyl nitrate, which is dissolved in absolute alcohol and transferred quantitatively to a volumetric flask. An aliquot of this solution is mixed with a 1 per cent solution of Parlodion dissolved in equal volumes of ether and alcohol, adjusting relative proportions so that the weight of the solute and the cellulose nitrate compound are about equal. A clean 2×3 in. slide is supported on a level cork platform as illustrated at C in Fig. 8, beneath a bell jar, and 1.00 ± 0.05 ml of the solution is delivered to the center of the slide. After evaporation of the solvents, a thin film of the mixed solids is produced, the Parlodion inhibiting marked migration of the uranyl nitrate towards the edges of the plate. The dry slide is placed in a cold muffle and the temperature is raised slowly to about 500° C until the cellulose nitrate is burnt off. Parlodion is a particular cellulose nitrate ester which does not burn with explosive violence.

When the weight of uranium is appreciable (1 mg per cm^2) the cold residual film has a yellow color indicative of the formation of UO_3. The film is strongly adherent but can be scratched off the glass by a decided effort. As the quantity of metal is reduced, the film loses its yellow color and exhibits interference colors typical of monomolecular oil films on water. Uniform films, weighing 5×10^{-8} g per cm^2, which emit alpha particles at the rate of only 50 per cm^2 per day, have been prepared by this method.

These films can be placed in direct contact with the photographic emulsion without danger of portions adhering to the gelatin. The quantity deposited can be controlled accurately within the limits of volumetric error. The method avoids grinding in mortars with the attendant danger of contamination. Careful measurements show that these films also exhibit an edge effect produced by migration of the solute during the evaporation, which must be corrected for in experiments of extreme accuracy. The method is seemingly applicable whenever the nitrate compound is soluble in absolute methyl or ethyl alcohol. When very thin films are desired, the solubility of even "insoluble" nitrates is usually adequate in providing sufficient solute

The method has been applied successfully in the preparation of thin films of UO_3, ThO_2, Sm_2O_3, and mixed rare-earth oxides.[Y17]

Mass-Spectrograph Films. Mass spectrographs which operate with crossed magnetic and electric fields bring accelerated ions of given mass, charge, direction, and velocity into focus on a photographic plate. If the direction and velocity of the beam are maintained within narrow limits, a line spectrum is obtained in which each band corresponds to a given ratio of atomic mass to charge. Radioactive isotopes can be differentiated from stable ones by exposing the collector plate against an emulsion of suitable sensitivity. After development the images on the collector plate exhibit the location of all isotopes, and the radioactive ones are designated by corresponding blackening on the autoradiograph. The method is proving a useful tool in determining the mass number of beta-ray-emitting isotopes, a description of which is presented in Chapter 11.

In an allied method, the alpha particles emitted from an external source are sorted out by means of a powerful magnetic field so that those of different energy enter the emulsion and record tracks along separated bands. Under these conditions the emulsion serves as an alpha-particle counter for estimating the relative number of particles of different initial velocity of emission. This method has been applied successfully by Chang[C10] in studies of the alpha-particle spectra of polonium and radium. The fine structure of the alpha spectrum of protoactinium has likewise been investigated by Rosenblum.[R22]

When the alpha particles from a thin source are analyzed spectrographically the principal body of monoenergetic particles produces a visually discernible line on the developed nuclear emulsion. Microscopic examination of the adjoining areas establishes the presence or absence of minor alpha-particle groups of energy different from the main group. Under conditions of steady magnetic field strength the half-width of the main line is less than 0.5 mm, corresponding to an energy resolution of about 0.01 Mev. A spectrographic analysis of the magnetically deflected alpha particles emitted by polonium shows that every million particles of 5.303 Mev are accompanied by a total of 717 particles of lesser energy. These fall into 12 groups differing in energy from the main body by 0.190 to 1.618 Mev.

During long exposures in an evacuated system the gelatin is desiccated and the emulsion tends to crack and peel away from the backing. Chang finds that this can be minimized by coating the edges of the plate with collodion solution. Peeling can also be reduced by incorporating a

plasticizer in the emulsion prior to vacuum exposure.[Y18] The plate is bathed for about 15 min in a 5 per cent solution of glycerine in water. After drying at normal pressure in dehydrated air, the imbibed non-volatile glycerine inhibits cracking of the emulsion layer under reduced pressure. Cotton[C23] has observed that as a result of camera evacuation and loss of water the stopping power of the emulsion is altered by about 2 per cent. In making precise track-length measurements the calibration curve must be constructed from tracks of known origin recorded in emulsions that received the same drying treatments as the experimental plates.

Dry Adhesion Films. Satisfactory thin films for alpha-particle counting can be prepared by dusting the dry powder onto a tacky basis, such as "Scotch tape." The weight of the deposit is dependent on the density and particle size of the powder and its mode of application. For a large number of carrier preparations the saturation pickup by the adhesive is in the range of 0.5 to 2.0 mg per cm^2, which provides a convenient method of thin film preparation suitable for routine activity measurements.

A cardboard frame about 0.5 mm thick and of the same external dimensions as the photographic plate is provided with a rectangular window measuring 2×5 cm. This frame is pressed onto a sheet of flat Scotch tape, and the unit is weighed to ± 0.1 mg. The exposed tacky surface is covered with a layer of the finely divided powder. Excess powder is shaken off by tapping the backing until all loose particles are dislodged. Any residual bare spots can be covered by applying a second layer of powder and repeating the process. Particles which adhere to the cardboard frame are wiped off with a dab of cotton, and the unit is reweighed.

These films are not as uniform or compact as the ones made by the ether sedimentation method, but the procedure is rapid and minimizes contamination by its modest demands on auxiliary apparatus. In its application to ignited precipitates even the use of a mortar can often be avoided by the addition of filter-paper pulp to the precipitate just before its filtration. This results in a finely divided ignition product which falls to a loose powder on being rubbed with a microspatula against the walls of the crucible. The manipulation of the dry powder creates dust particles, and care must be taken to avoid its inhalation and its settling on the laboratory equipment. The operation should be conducted under a hood, the bench being covered with a separate paper liner for each sample.

Preparation of Scintillation Screens. As is well known, pure zinc sulfide will not fluoresce under ultraviolet light, and the compound will serve as a phosphor only when traces of certain metals are incorporated in its crystal lattice. The presence of activating metallic ions is also essential for the production of scintillations by incident alpha particles. The most brilliant flashes are produced when the activator is copper, present in about 0.01 per cent of the zinc content. Specially activated zinc sulfide preparations are available from the Hammer Laboratories, Denver, Colorado. The material phosphoresces strongly after exposure to sunlight, and once the screens are prepared they should be stored in the dark in order to avoid a luminous background at the time of observation.

The powder consists of crystals ranging between 5 and 50 microns, and Rutherford [R20] recommends that a fraction between 20 and 30 microns be separated by suitable screening. The size of these coarse crystals corresponds to the range of RaC′ alpha particles in the phosphor, but when applied as a thin film the screen has numerous voids whose area must be corrected for in quantitative counting. The early workers [M2] secured the zinc sulfide to the glass backing with the aid of a tacky film of Canada balsam. A more uniform preparation results by depositing the phosphor directly onto the glass, employing the sedimentation method described in the section entitled Preparation of Thin Films.

To prepare a screen of 5-cm^2 area, suspend about 15 mg of the phosphor in 2 to 3 ml of ether, and pour the mixture into the circular well, Fig. 8, *A*, framing the glass slide. On evaporation of the solvent, an adherent uniform film results, uncontaminated by binding matter. A more durable screen can be prepared by precoating the glass with a thin layer of gelatin. A portion of plate from which the silver compounds have been removed by bathing in sodium thiosulfate, washing, and drying is satisfactory. During the evaporation of the ether traces of moisture soften the gelatin and the zinc sulfide grains become embedded superficially.

EXPOSURE AND PROCESSING OF EMULSIONS

Radiographic Cameras. The basic camera for clamping a polished section against an emulsion is described in Fig. 9. In constructing these units it is convenient to standardize on 3-in.-length plates, as these fit the standard mechanical microscope

stage. Individual plates are readily identified by scribing on the gelatin with a steel needle. Wood or aluminum should be avoided as construction materials as they tend to fog certain beta-ray-sensitive emulsions. Certain plastics, such as Lucite, are particularly advantageous because of their low content of radioactive impurities.

The nuclear-type emulsions employed in alpha-particle exposures (NTA or C2) have an extremely low sensitivity to light, and the camera can be assembled in a room illuminated with a
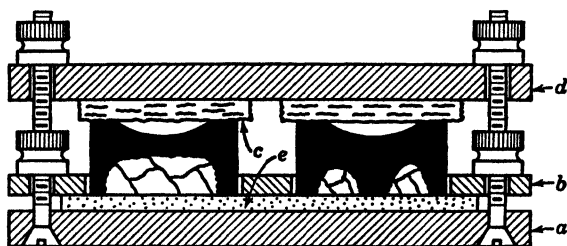
FIG. 9. Basic camera for exposing polished sections.

a. Plastic frame.
b. Centering frame.
c. Cotton or sponge-rubber pressure equalizers.
d. Clamping plate.
e. Emulsion.

yellow or amber light. A frosted 25-watt bulb mounted in a wide-mouth amber glass bottle makes an excellent lamp. Its light should be diffused by a surrounding envelope of tissue paper. Orthochromatic plates or x-ray film, employed in beta-ray autoradiography, must be handled with a red safety lamp. The assembled camera is kept inside a Bakelite box, or one constructed of wood impregnated with paraffin. In exposures of long duration, a dish of anhydrous calcium chloride should be placed in the box as the persistence of the latent alpha-ray image is prolonged by reducing the moisture content of the air. In exposures exceeding one day it is advantageous to store the camera in a desiccator kept in a refrigerator at about 5° C.

In exposures of long duration lacquered iron cans, like 1-lb pipe-tobacco containers, provide convenient miniature darkrooms. The thin metal walls facilitate heat transfer when the cans are removed from the refrigerator before development. After exposing samples of high emanating power therein, the cans should be discarded.

In counting alpha particles from strong sources, brief, accurately timed exposures must be made. These are facilitated by the use of the special plate holder described in Fig. 10. The glass slide carrying the source is placed inside a snugly fitting box into which the plate holder fits loosely. The thin ribs on
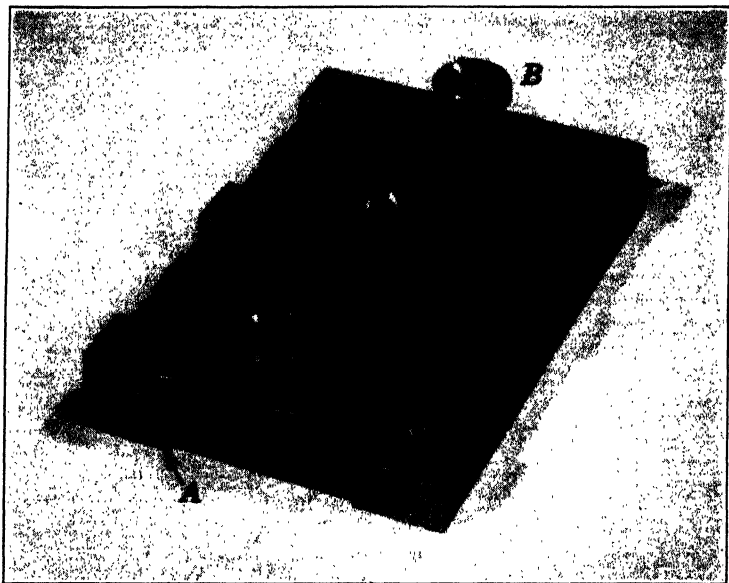
Fig. 10. Plate holder for exposures at a fixed distance from source. The frame has outside dimensions of 2×3 in. The machined elbows *A* are 0.5 mm thick and support the plate measuring $1\frac{1}{4} \times 3$ in. with the aid of set screws *B*. The bottom of the frame is ground flat and rests on a 2×3 in. glass slide carrying the rectangular-shaped source.

the plate holder prevent direct contact of source and emulsion, and contact and separation can be effected with a timing uncertainty of ± 2 sec.

Development and Fixation. Emulsions employed in beta-ray autoradiography usually do not require special processing, and the specifications for the development of the optical image are directly applicable. When the radioisotope decays by gamma emission, only a small fraction of the incident radiation is absorbed by the emulsion. The low activation is compensated for by the use of coarse-grained emulsions and by overdevelopment.

According to Barrett [B6] excessive fog is prevented in the over-development of x-ray film activated by gamma radiation by the addition of 20 mg of potassium iodide per liter of Eastman x-ray-film developer. At 18° C development may thus be prolonged up to 10 min without appreciable increase in background fog.

Investigations by Pelc [P7] indicate that background fog in beta-ray autoradiographs can be reduced by developing the emulsion for 10 min at 18° C by means of ferrous oxalate. The developer is composed of two solutions and is prepared prior to use by pouring 20 ml of *B*, with rapid stirring, into 70 ml of component *A*.

A. Dissolve 120 g of neutral potassium oxalate in warm water and dilute to 500 ml.

B. Dissolve 120 g of ferrous sulfate crystals in warm water, acidify with 1.5 ml of concentrated sulfuric acid, and dilute to 500 ml.

The nuclear-type emulsions develop satisfactorily in elon-hydroquinone developing solutions. The temperature of development between 18° and 25° C is not critical for purposes of autoradiography. Tracks whose latent image suffered partial fading as a result of delayed development are rendered developable with increase in temperature of the bath.[M29] Using the old Eastman Fine Grain Alpha plates it was found that reproducible photographic density of visual alpha-ray images could be obtained only by warming the developer to 32° C. Eastman NTA emulsions of current manufacture develop satisfactorily at 20° C. Fog and artifacts are diminished by cleaning the *glass* developing dish frequently and filtering all processing solutions before use. The composition of the solutions recommended by Eastman and Ilford for the development of their respective nuclear-type emulsions are as shown. These stock solutions are stable for long

	Eastman D19	Ilford ID19
Water warmed to 50° C	2 liters	2 liters
Elon	8.8 g	8.0 g
Anhydrous sodium sulfite	384 g	300 g
Hydroquinone	35.2 g	32 g
Anhydrous sodium carbonate	192 g	148 g
Potassium bromide	20 g	20 g
Dilute with water to	4.0 liters	4.0 liters

periods of time when stored in brown bottles at a low temperature. It is good practice to use small-sized fresh portions of prefiltered solution for each plate developed.

After development the plate is rinsed in distilled water for about 1 or 2 min and fixed in a bath of either Eastman F5 or a 30 per cent solution of sodium thiosulfate crystals. The nuclear emulsions carry unusually large quantities of silver bromide whose removal necessitates a 30- to 60-min fixation period. The wet plates appear opalescent even after complete solution of the silver bromide. The turbidity probably results from the voids in the residual gelatin formed on extraction of the silver salts, as, after washing and drying, the gelatin layer clears.

In the study of cosmic radiation it is advantageous to employ exceptionally thick emulsions. These plates are from 50 to 200 microns thick and present unusual difficulties both in the development and fixation steps. In order to secure uniform depth development it is often necessary to preswell the gelatin to facilitate access of the developer to the deepest grains. Fixation is expedited by the use of continuous mechanical rocking devices. The methods of processing have not been standardized and must be modified in accordance with the sensitivity of the emulsion and the objectives of the exposure. Tracks of low grain density, such as those of mesons, are made more readily visible by overdevelopment. This, however, increases the size and clumping of the developed grains in the tracks of protons and alpha particles, rendering their differentiation more difficult. The following procedures are representative of good experimental practice in the depth development of thick nuclear emulsions:

Method I: The Ilford C2 and the Eastman NTA plates with coatings up to about 100 microns are processed in the following steps:

(*a*) Keep for 15 to 30 min in 1 volume of D19 stock diluted with 4 volumes of water at 20° C, with continuous agitation.

(*b*) Wash in running water for 5 min.

(*c*) Fix in 30 per cent sodium thiosulfate until plate appears clear.

(*d*) Complete fixation and harden by a 15-min treatment in a bath of Eastman F5.

(*e*) Wash and dry.

Method II: The Eastman Research Laboratories recommend the following procedure for their 100-micron-thick NTA and NTB plates. Preswell the emulsion in water at 80° to 85° F for 10 min, develop immediately for 10 min in full-strength D19 at room temperature, and then continue with steps (*b*) to (*e*) as described in Method I.

Method III: The preswelling in water involves the danger of weakening of the latent image, particularly if dissolved air is present in the bath. This is avoided by soaking the plate in water containing 0.5 ml of D19 per

100 ml for 10 min at 28° C. Development is then completed as in Method II. Appreciably better track differentiation is secured by continuing the development of the preswollen emulsion by Method I.

Method IV: The Bristol investigators[D16] aim at uniform depth development by saturating the plate with a cold developer and then instigating chemical action by warming the bath:

(*a*) Cover the plate with a shallow layer of developer (1 part D19 + 1 part water) chilled to 5° C, agitating occasionally during a period of about 30 min.

(*b*) Transfer the glass developing tray to a water bath at 20° C, and add 2 parts of water at 15° C. The tray is agitated slowly for about 10 min to produce uniform mixing and temperature equilibration. When the solution reaches 20° C development is continued without agitation for 25 min.

(*c*) Transfer the plate to an acid stop bath containing 1 to 2 per cent acetic acid at 15° C, and agitate for about 25 min.

(*d*) Rinse in water at 15° C for several minutes.

(*e*) Fix in 40 per cent by weight of sodium thiosulfate with an addition of 25 ml per liter of Eastman hardener solution until plate clears. With continuous agitation at 20° C fixation is complete in about 1 hr when the coating is 100 microns thick. This period increases rapidly with emulsion thickness, and 5 hr are necessary when the plate is 300 microns thick.

(*f*) Wash for 4 hr in cold water. Dry the plate by placing it horizontally, emulsion side up, in a tube through which air is blown at 27° C.

(*g*) Remove surface layer of amorphous silver by rubbing with a xylol-dampened chamois skin.

Method V: An alternative method for the development of 200-micron-thick plates is described by Blau and De Felice.[B26a] Surface development is avoided during penetration of the gelatin by omitting the alkali from the solution; reduction of activated grains is then instigated by means of an extra-alkaline solution of elon and hydroquinone.

Solution A: elon 1.1 g, Na_2SO_3 24.0 g, hydroquinone 4.4 g, KBr 2.0 g diluted to 2 liters.

Solution *B:* 400 ml of Eastman D19 stock diluted with 1600 ml of water and fortified by an additional 16 g of Na_2CO_3.

(*a*) Soak plate in water at 20° C for 10 min.

(*b*) Transfer to solution *A* and agitate occasionally for 30 min.

(*c*) Transfer to solution *B* and maintain at 20° C for 30 min without agitation.

(*d*) Complete processing as described either in steps *c* to *f* of Method IV, or steps *b* to *d* of Method I.

Owing to the unusually thick layers of emulsion and the stronger development, Methods I to V produce an exceptionally high fog background, and the plates cannot be examined satisfactorily under dark-field illumination. For purposes of autoradiography and track counting from external sources thinner

emulsions of 25 to 50 microns are adequate, and a superficial development (2–3 min in D19 at 20° C) is satisfactory. When counting tracks in loaded emulsions complete depth development is essential and Method I is recommended, reducing the time in the developer to 15 min when employing the thinner-type emulsions.

Van der Grinten [V17] has suggested a new approach to the development of nuclear-type emulsions aiming at a developed grain size proportional to the degree of activation imparted to the silver bromide grains. This technique, designated *grain gradation,* produces a thin track when the emulsion is traversed by a particle of low specific ionization, and tracks comprised of larger and more opaque silver grains result from a greater density of ionization. In a private communication Van der Grinten recommends the following method for the development of Ilford B1 plates:

Method VI: Develop for 10 to 20 min at 60° to 70° F, in a freshly prepared solution containing 0.5 g hydroquinone, 10 g Na_2SO_3, 0.5 g KBr, and 1.0 g KOH per liter of distilled water.

This method has been applied successfully by the author in the development of alpha, triton, and proton tracks in the Ilford C2 and B2 and the Eastman NTA emulsions of current manufacture. In 50-micron plates development is complete throughout the entire depth, the fog background is low, and the plates are readily examined by dark-field illumination. With this developer formula the tracks of protons are rather thin, suggesting that meson particles may not record recognizable tracks. Examples of grain gradation development are represented by Figs. 58 and 62, Chapter 12. By extending the period in the bath to 30 min and increasing its temperature to 20° C 100-micron-thick plates develop uniformly and the tracks of protons and mesons are more readily evident. The stronger development, however, also augments the size and number of the background fog grains. It is noteworthy that this simple hydroquinone developer does not cause the deposition of loose surface silver films, which are often produced when Ilford plates are developed with the more powerful D19 formula. The method is also applicable in the development of emulsions 200 microns thick by the following modification: [Y18]

Method VII: Immerse the plate for 1 hour in the grain gradation developer chilled to 8° C. Add small portions of fresh solution at about 25° C until the tray and contents are brought to 20° C and maintain at this temperature for 15 to 30 min, depending on the desired track discrimination. Siphon off the developer, and rinse the plates with two changes of distilled water, rocking the tray gently for about 3 min between rinsings. Cover with 30 per cent sodium thiosulfate and rock until clear

(about 3 hours). The gelatin is then hardened by a 30-min treatment in Eastman F5 fixing solution. Wash in filtered running cold tap water (if chlorine-free) or in distilled water for 3 hours. Rinse for 10 min in a bath containing 1 per cent glycerine and 0.1 per cent of an aqueous wetting agent. Drain thoroughly and allow to dry slowly with the plate supported in a horizontal position. The thick layer of dry gelatin tends to peel under conditions of low humidity. The glycerine incorporated in the last water rinse prevents cracking of the gelatin film, but to insure a permanent preparation the edges of the plate should also be painted with shellac.

This method is not applicable to emulsions loaded either with heavy metals or compounds such as lithium borate which exert a buffering action on the developer. The hydroxyl-ion concentration is depleted by precipitation of metallic hydroxides, and the surface deposits of these gelatinous compounds inhibit diffusion of fresh developer. Loaded plates develop more satisfactorily with elon-hydroquinone solutions as described in Methods I to III.

Washing is effected in a slow stream of filtered tap water. A glass tube filled with alternate layers of absorbent cotton and sand provides an adequate filter. The plates are set lengthwise with gelatin side up in a horizontal snug-fitting glass tube, and the filtered water is allowed to flow for about 1 hour. The plates are drained and supported in a large cabinet containing a dish of calcium chloride. Exceptionally thick emulsions can be dried more effectively by replacing the imbibed water with alcohol, rinsing the plates successively for about 2 min in 25, 50, 75, and 95 per cent ethyl alcohol. It is usually unnecessary to protect the dry gelatin with a cover glass. In measuring grain spacings with oil-immersion objectives, the oil can be removed without scratching the gelatin by immersing the plate in carbon tetrachloride.

MICROSCOPY OF RADIOGRAPHIC PATTERNS

A flexible system of microscopic illumination suitable for the observation of both macro images and individual alpha-particle tracks is illustrated in Fig. 11. A 6-volt ribbon-filament lamp is mounted rigidly on a common base with the microscope at a distance of about 18 in. from the mirror. The lamp should be provided with an adjustable spherical lens *L* and a variable diaphragm *D*. A long-focal-length Abbe condenser provided with a central stop *F* is satisfactory for low-power dark-field

illumination and will also give satisfactory performance with bright-field illumination at higher powers by simply removing the central stop. To achieve maximum resolution in conjunction with Köhler illumination a second condenser with a numerical
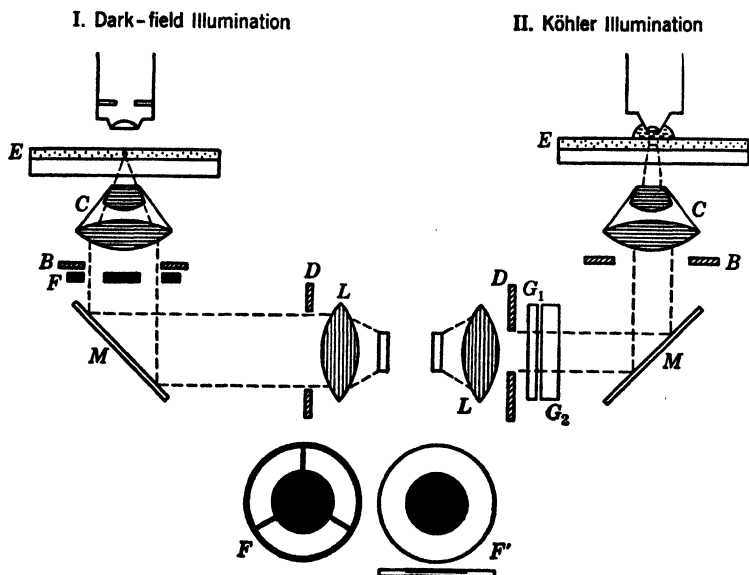
FIG. 11. Illuminating systems employed in nuclear emulsion microscopy.

I. Dark-field illumination by means of a central stop in the substage condenser. Stop F is standard with most biological-type microscopes. A differential color stop F' which produces a green image of the tracks on a dim red background can be improvised by painting a film of red semi-opaque lacquer on the center of a thin glass disk and tinting its periphery with a transparent green lacquer. The method employs achromatic objectives of 21 and 44× magnification. The aperture of these lenses should be reduced either by a variable-iris diaphragm or by insertion of washers.

II. Standard Köhler illumination for use in conjunction with 40× fluorite or 100 apochromatic objectives. G_1 is a gray-tinted filter for reducing light intensity, and G_2 is a green filter for toning color of field.

aperture comparable to that of the objective should also be available.

After the optical system is properly centered, open D to full aperture and focus image of filament by means of L onto diaphragm B of the Abbe condenser. To secure dark-field illumination insert central stop F and focus with a low-power objective on tracks in emulsion E. Adjust to

optimum brilliance by manipulating condenser C, tilting mirror slightly until entire field is uniformly illuminated. In plates where the fog background is not excessive the tracks will appear silver bright on a black background. By employing central stop F' other differential color contrasts can be obtained which are useful in securing adequate illumination for coordinate nets or scales set in the ocular. Dark-field illumination is advantageous only when the emulsion is less than 50 microns thick.

To switch to bright-field illumination remove the central stop, place a drop of non-hardening oil on the slide, and lower an apochromatic objective into the oil. Reduce the lamp diaphragm D to about 2 mm, focus on a track, and adjust condenser C so that the image of the light orifice is also in sharp focus. Open D slowly until the entire field is uniformly illuminated. If this light proves too brilliant, lower the voltage on the lamp, or absorb some of the light by a gray-tinted polished glass filter G_1. When the gelatin layer is exceptionally thick, the condenser C is best adjusted so that the image of D is in the same focal plane as the particular track under study. This is essential only to secure optimum illumination for purposes of photomicrography, and one median plane setting is adequate for track-counting purposes.

Examination of Macro Images. The autoradiographic pattern is a mirror image of the radioactive inclusions in the polished surface. In correlating the blackening with the segregates, the plate is inverted gelatin side down, in order to match points. Images that outline the shape of visible inclusions are readily correlated by inspection at low magnification. At higher magnifications, in excess of 100×, photomicrographs of identical areas facilitate comparison and interpretation of results. Illumination of opaque sections of metals and ores is effected by reflected light. Annular illumination, exhibiting the segregates in their normal colors, is aided by the use of long-working-distance objectives but limits the magnification to about 150×. Better resolution is achieved by means of vertical illumination. Transparent tissue and rock sections are examined by transmitted light and are readily compared with the radiograph either under bright- or dark-field illumination.

The execution of two exposures on the same plate often facilitates the quantitative interpretation of the pattern. One exposure is made of sufficient duration so that a dense, well-defined image develops. At the termination of this exposure the specimen is moved a precise distance, without rotation, to an adjacent collinear portion of the emulsion and exposed briefly so that only a small number of tracks from each segregate are recorded.

After the location of a particular structure in the visual image, a measured translation of the stage brings the identical, briefly exposed area into view. By inserting a disk with a ruled net in the ocular, and counting the tracks, the alpha-ray activity of individual segregates can be evaluated accurately. When the segregates have appreciable dimensions the two exposures can be made with the aid of the basic camera shown in Fig. 9. When the structures are very minute, as in the estimation of the activity of radiocolloids, the dual exposures must be made on a frame constructed with great mechanical precision, and only the following procedure has proved practical:

Replace the microscope objective with an extension collar filled with modeling clay. Insert a slide in the mechanical stage, and orient the polished section. Lower the microscope tube so that the clay makes contact with the specimen top and holds it securely. Bring the assembly into a darkroom, elevate the specimen about 7 cm above the stage, and replace the slide with a nuclear-type emulsion. Place a sheet of paper near the plate, lower the specimen close to it, remove the paper, and complete contact with emulsion by means of the vernier adjustment. At the completion of the first exposure, raise the specimen about 1 mm, reinsert the paper, and translate the mechanical stage a *precisely measured distance* sufficiently long to clear the initial image. Remove the paper, reestablish contact, and expose for from 15 to 30 min. When the developed plate is replaced in the same microscope stage corresponding areas on the two images can be located with a precision of ±0.1 mm. The microscopic appearance of two collinear exposures of a radiocolloid is exhibited in Fig. 24, p. 125.

Microscopy of Single Tracks. At magnifications exceeding 100×, individual tracks of the more energetic alpha particles become discernible. For quantitative track counting, magnifications above 500× are essential. Dark-field is preferable to bright-field illumination as it reduces strain during prolonged counting. Adequate illumination is secured with the Abbe condenser fitted with a dark-field stop. A 44× dry objective provided with a variable-iris diaphragm is employed. In the absence of this special lens the aperture can be reduced by placing metal washers inside the objective. A 15× ocular fitted with disks delineating a measured area of the emulsion by a centrally located slit completes the optical system.

Track length, grain spacing, and dip are measured microscopically at magnifications in excess of 1000× using high-resolution

oil-immersion objectives and oculars fitted with engraved linear scales. The grain structure of tracks produced by particles of different ionizing power, as protons, alpha particles, and fission fragments, is differentiated by transmitted light. In nuclear-type emulsions the grain diameter and grain spacing are only a small fraction of a micron, and an optical system of high resolving power is essential for their accurate measurement. By employing a blue filter transmitting light of 4800 A, a 1.4 N.A. condenser in conjunction with an 1.3 N.A. 90× apochromatic objective, and a 12.5× compensated eyepiece, Demers [D9] attained a resolving power of 0.24 micron. A film of oil must be placed between the condenser and the glass backing and also between the gelatin and the objective lens.

Powell and Champion [P33] describe a microscope fitted with a vertical vernier-micrometer depth gauge for measuring the dip of tracks in the emulsion. By making suitable correction for the shrinkage of the gelatin (see Chapter 12) after fixation and drying, the measurement permits the reconstruction of the original track orientation in the dry emulsion. Other methods of defining the spatial orientation of tracks based on the use of universal stages are described in the work of Zhdanov [Z1] and Myssowsky.[M37] Martin and Wilkins [M13] describe a special stereoscopic camera which makes it possible to measure directly the lengths and angles from a true scale reconstruction of the original tracks. Microscopes fitted with special precision stages are available commercially as illustrated in Fig. 12. These have micrometer screw feeds which facilitate range measurements, particularly of long tracks that extend over several fields.

The exploration of exceptionally thick emulsions is rendered difficult by the small working distance and limited depth of focus of the commonly available refracting objectives. These difficulties have been circumvented by means of a reflecting objective designed by Burch.[B50] According to Feld,[F19] at the highest magnification the reflecting microscope has a working distance of 5 mm, which is about 25 times greater than that of refracting objectives of comparable magnification.

Bates and Occhialini [B51] describe several interesting applications of thick nuclear emulsions rendered practical by the reflecting microscope. The instrument can focus through the 1-mm glass backing and permits the observation of tracks in the gelatin layer. This inverted mode of observation is often useful in observing details of a nuclear evaporation which are obscured by
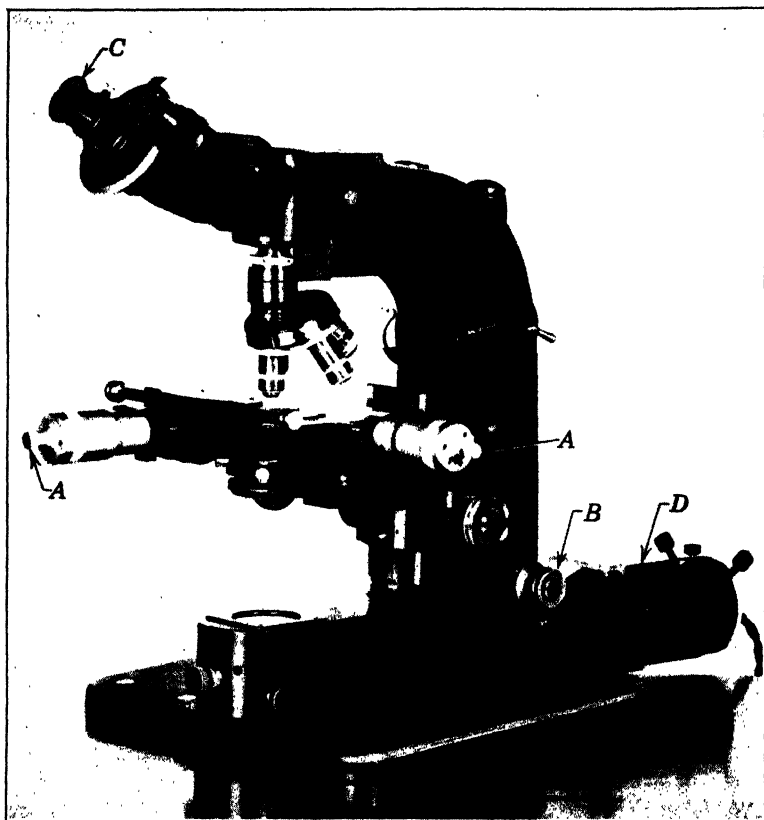
Courtesy of R. Y. Ferner Co., Boston, Massachusetts

FIG. 12. Nuclear research microscope.

A. Micrometer screws for controlling the movements along the x and y axes. These can be read to 0.005 mm and facilitate measurement of long tracks.

B. The fine-focusing adjustment is graduated in 0.001 mm. It is employed in making depth measurements along the z axis.

C. Protractor ocular, graduated in degrees, can be read by a vernier to 15 min.

D. Built-in illuminating system.

the center portion as viewed by normal microscopic methods. The instrument also permits the simultaneous examination of two emulsions which have been exposed face to face. Ionizing particles which leave the emulsion of one plate can thus be followed into the second plate:

Register is secured by marking the sandwich with a grid photographed by x-rays before development. The writer has found that register can also be effected by drawing a line over one of the emulsions, prior to dual exposure, either with a needle coated with polonium, or a pen using uranium or thorium solutions as ink. On completing the sandwich the upper plate will carry an autoradiograph of the infected scratch line. These internal lines also provide alpha-particle tracks whose grain density is useful as a measure of the extent of fading during prolonged cosmic-ray exposures. After development the plates are cemented together with the aid of a film of Clarite or dammar. Owing to imperfect contact and alignment, corresponding portions of a track may appear displaced by 50 to 100 microns. However, in multiple events with a common center, such as alpha stars or nuclear evaporations, the component parts of the trajectories are readily matched by their directional correspondence and equality of dip. The sandwich can be assembled and examined with the aid of a 21× refracting objective, which provides adequate working distance, but the resolution is poor.

The reflection microscope should also prove useful in the joint examination of thin stained sections with their autoradiographs and facilitate the search for individual alpha-particle tracks in emulsions to which the stained tissue section is secured permanently. As a variation on the dual-contact exposure Powell and Rosenblum [P36] separate the two plates so that there exists a measured gap which can either be evacuated or be filled with a gas of known composition. The unit can be exposed between the poles of a magnet, and as in the analogous method with the cloud chamber the magnetic deflection of the light particle traversing the air gap serves as a measure of its mass.

In a magnetic deflection method of track study described by Barbour [B59] the use of special reflection objectives is avoided by employing thin glass plates, both faces of which are coated with emulsion. The double coating equalizes the stresses produced by the gelatin permitting the use of supports 50 to 150 microns thick. The thin plates can be examined by means of refracting objectives of high numerical aperture.

The photomicrographic reproduction of long tracks in thick nuclear emulsions is also beset with technical difficulties. Since the tracks rarely reside in a single plane, small portions of the trajectory must be photographed and the individual portions assembled as a mosaic. In order to secure optimum conditions of resolution for each component the condenser should be adjusted for optimum illumination at each focal setting. The preparation of mosaics is facilitated by the technique described by Morrison and Pickup.[M48] The image is projected onto a
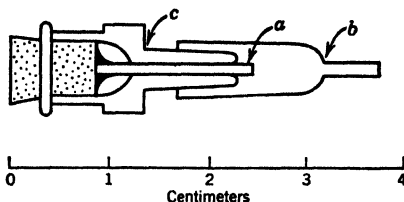
FIG. 13. Collimated alpha-particle source.

a. Palladium wire with polonium deposited on polished tip and cemented into standard taper serological tip.

b. Source collimated with cutoff blood needle. Full-energy alpha particles are recorded by conducting the exposure in a vacuum.

c. Standard taper coupling.

horizontal surface with the aid of a prism and mirror system. Each track is recorded on a strip of film in a holder fitted with two slides which can be moved to expose short successive intervals. Each portion is brought successively into focus on the top surface of one of the opaque slides, and the image is then allowed to activate the film.

POINT SOURCE OF ALPHA RADIATION

A source of polonium alpha particles serving many useful functions in the calibration and study of nuclear-type emulsions can be assembled, as shown in Fig. 13. The following procedure is designed especially for minimizing contamination of the laboratory:

Coat a palladium wire 1 cm long and 1 mm in diameter with hot sealing wax, holding the wire vertical so that a globule of wax collects at one end. Abrade the globule on emery paper until the metal is exposed, and continue polishing until the surface is scratch free. Insert the opposite end

of the wire in the rubber eraser of a lead pencil, and support the unit above a 30-ml cone flask containing about 5 ml of water. Bubble a slow stream of hydrogen through the water, and, when a steady rate free from spattering is attained, deliver 2 ml of a polonium solution in concentrated hydrochloric acid having a strength of about 1 millicurie per milliliter. Lower the pencil so that the polished surface of the palladium wire and its protecting side coat of wax is submerged below the level of the liquid. A saturation electrochemical replacement film of polonium will deposit in about 30 min.

Stop gas flow, remove pencil, and wash wire with water. Using forceps, insert the wire in a standard taper metallic serological tip, as shown in Fig. 13, *a*. Droplets of Duco cement applied to the cork base and the mouth of the adapter secure the wire in place. Some polonium is adsorbed by the wax coating during immersion. Scrape the wax away with a sharp razor blade mounted in a handle of suitable length. The resultant deposit is a close approximation to a point source of monoenergetic alpha radiation. It is collimated by simply slipping a blood-drawing needle over the standard taper joint supporting the wire. Since these needles are available in a variety of bores and can be cut to any desired length, nearly parallel alpha-particle beams of varying intensity are readily obtained. When not in service the source is covered with a long needle reserved for the purpose, and should not be left covered by calibrated collimating tubes in order to avoid their contamination by creeping. To avoid contamination of the hands and laboratory, the pencil employed as a support in the plating process should be incinerated.

The polonium can be isolated from uranium minerals, or can be extracted from old radon needles with acid. The simplest procedure, however, is to order a 10-millicurie solution from the Canadian Radium and Uranium Corp., which recovers the element routinely in working up pitchblende for radium.* The absolute strength of the source is determined by covering the deposit with a collimator needle having a measured bore a of about 0.5 mm and a length h from tip to source of 10 mm. Incline the needle at about 45° with the plane of the emulsion, and make a series of exposures, varying the time from 10 sec to 3 min. Each exposure is confined to an elliptical area, and the track population in some one of the exposures may be convenient for counting. Photograph this complete elliptical area at 200×, and determine the number of tracks on the negative, or make the estimate by viewing it on a projected screen.

* When purchased by weight, polonium is probably the most expensive commodity in commerce, selling for $4,660,000,000 a gram. As only 10^{15} atoms of the element are employed, the capital investment is about $50.

From the precise values of a, h, and $k = \sqrt{a^2 + h^2}$, the number of alpha particles emitted per square millimeter of source N_0 can be computed from the track count C with the aid of the first terms of equation 6, as derived by Kovarik: [K20]

$$\frac{C}{N_0} = \pi a^2 \left(\frac{h}{a}\right) \left\{ \frac{1}{2}\left(\frac{a}{h} - \frac{a}{k}\right) + \frac{3}{16}\left(\frac{a}{k}\right)^3 \left[\left(\frac{h}{k}\right)^2 - 1\right] - \frac{5}{128}\left(\frac{a}{k}\right)^5 \left[7\left(\frac{h}{k}\right)^4 - 10\left(\frac{h}{k}\right)^2 + 3\right] + \cdots \right\} \quad (6)$$

When employing a tube with the precise dimensions of 0.50 and 10.0 mm for a and h, respectively, equation 6 evaluates to $N_0 = C/0.000495$. By recording the date of the exposure, the strength of the polonium source N after the elapse of t days can be computed from the decay law, $N = N_0 e^{-0.0051t}$.

In reviewing this chapter for omissions of pertinent techniques it was noted that, though considerable preparatory work is to be performed by the biologist, chemist, and petrographer before the exposure can be made, there are no troublesome tasks for those who employ the emulsion in the study of cosmic radiation. At one time these experimentalists had to be adept at mountain climbing, but since the routine event of prolonged high-altitude flights by airplanes and ascension to even greater heights by balloons and rockets, this invigorating technique is no longer of scientific interest. The enviable freedom from laboratory detail recalls a statement, once read in a source long forgotten, whose substance is that *science has its caste system, with the mathematician seated like a brahmin on the apex of the scientific pyramid. He looks down contemptuously at the chemist and physicist, and they in turn are united in the relegation of experimentalists in the less exact sciences to the pariah class.* If the burden of detail involved in the solution of a problem be an index of caste classification, this laborious chapter appears to be proof of the existence of the pyramid.

Chapter 4 · ALPHA-PARTICLE PATTERNS ON NUCLEAR EMULSIONS

Just as a waterfall, instead of taking one plunge into a lake, may cascade in a series of successive leaps from pool to pool on the way down, so a radioactive element like radium passes in its change through a long series of intermediate bodies, each produced from the one preceding and producing the one following.

—Frederick Soddy, 1922

PROPERTIES OF ALPHA PARTICLES

The naturally occurring elements of atomic numbers 83 to 92 have unstable isotopes which decay with the emission of a massive nuclear fragment termed an alpha particle. This disintegration product has a mass of 6.6442×10^{-24} g, carries initially a double positive charge, and, when it is slowed down by encounters with atoms of the medium it traverses, reverts to a neutral atom of helium with a chemical atomic weight of 4.0028. The alpha disintegration of an element of mass M and atomic number Z results in the production of a daughter atom of mass number $M - 4$ and atomic number $Z - 2$. The spontaneous reaction is exoergic, and the energy is shared between the alpha particle and the newly created recoil atom. Since the mass of the alpha particle is small compared with that of the recoil fragment, it is accelerated with the bulk of the disintegration energy. The energy liberated in the spontaneous decay of heavy nuclei ranges between 4.2 and 9 Mev. The alpha particles are ejected with initial velocities about $\frac{1}{20}$ that of light.

The alpha particle and the recoil atom separate in opposite directions and traverse a characteristic distance known as their range. The range is measured in standard dry air at 15° C and 1 atmosphere pressure. Because of the discontinuity of the matter traversed, alpha particles of identical energy do not invariably have identical ranges. Small variations will be observed, depending on the number and varieties of atoms encountered and the amount of work expended in traversing their electronic orbits.

TABLE 2. ALPHA-RAY-EMITTING ELEMENTS PRESENT IN MINERALS *

Atom	Branching Ratio	Z	A	λ sec^{-1}	T	Mean Range, cm 15°	Energy in Mev: Alpha	Energy in Mev: Recoil
UI	1	92	238	4.86×10^{-18}	4.51×10^{9}y	2.65	4.20	0.06
UII	1	92	234	9.43×10^{-14}	2.33×10^{5}y	3.21	4.67	0.09
Io	1	90	230	2.65×10^{-13}	8.3×10^{4}y	3.09[a]	4.59	0.08
Ra	1	88	226	1.38×10^{-11}	1590y	3.26	4.79	0.09
Rn	1	86	222	2.10×10^{-6}	3.825d	4.05	5.48	0.10
RaA	1	84	218	3.79×10^{-3}	3.05m	4.66	6.00	0.11
RaC	0.0004	83	214	2.34×10^{-7}	. .	4.0	5.48	0.10
RaC′	0.9996	84	214	4.61×10^{3}	1.5×10^{-4}s	6.91	7.68	0.15
RaF	1	84	210	5.73×10^{-8}	140d	3.84	5.30	0.10
AcU	1	92	235	3.11×10^{-17}	7.07×10^{8}y	3.0	4.52	0.08
Pa	1	91	231	6.86×10^{-13}	3.2×10^{4}y	3.57[b]	5.06	0.10
RdAc	1	90	227	4.26×10^{-7}	18.9d	4.60	6.00	0.10
Ac	0.01	89	227	1.63×10^{-11}	[c]	3.5[d]	5	0.1
AcX	1	88	223	7.18×10^{-7}	11.2d	4.29	5.72	0.10
An	1	86	219	0.177	3.92s	5.67	6.83	0.12
AcA	1	84	215	3.78×10^{2}	1.83×10^{-3}s	6.46	7.37	0.14
AcC	0.9968	83	211	5.3×10^{-3}	2.16m	5.36	6.61	0.13
AcC′	0.0032	84	211	139	0.005s	6.52	7.44	0.14
Th	1	90	232	1.58×10^{-18}	1.39×10^{10}y	2.60[e]	4.1	0.07
RdTh	1	90	228	1.16×10^{-8}	1.90y	4.00	5.42	0.10
ThX	1	88	224	2.21×10^{-6}	3.64d	4.32	5.68	0.10
Tn	1	86	220	0.0127	54.5s	5.00	6.28	0.12
ThA	0.9999	84	216	4.38	0.158s	5.64	6.78	0.13
ThC	0.337	83	212	6.4×10^{-5}		4.73	6.04	0.12
ThC′	1	84	212	2.3×10^{6}	3×10^{-7}s	8.57	8.78	0.17

* Recent measurements indicated below are probably more accurate than the data in the table.

[a] The range of ionium alpha particles is 3.110 cm (Joliot-Curie[J4]).

[b] The alpha spectrum of protoactinium has a principal line at 3.511 cm, with minor components at 3.23 and 3.20 cm (Tsien[T22]).

[c] The half-life of actinium measured by Joliot-Curie[J3] ranges between 21 and 21.7 years.

[d] The principal group of actinium alpha particles has a range of 3.46 cm (Gregoire and Perey[G23]).

[e] Measurements by Faraggi[F2] indicate that thorium alpha particles have a range of 2.43 ± 0.03 cm.

As a result of straggling the average of a large number of range measurements is the defining entity, which is called the mean range of the particle. The magnitude of the mean range for the alpha particles emitted in the decay of members of the uranium,

actinium, and thorium series is recorded in Table 2 together with other pertinent properties of these nuclear projectiles.

The number of disintegrations δ is proportional to the number of atoms of the element present in the system. The disintegration constant λ is simply a ratio expressing the number of atoms decaying per unit time to the total number of parent atoms in the system, i.e., $\lambda = \delta/N$. During the decay of an isolated radioelement the number of disintegrations per unit time becomes less as the stock pile of parent atoms diminishes. If N_0 represents the number of atoms at some initial time, then the number of atoms N which remain undecayed after a time t is expressed by:

$$N = N_0 e^{-\lambda t} \tag{7}$$

As the element decays, a time comes when only half the original number of atoms remains unaltered. This time T is known as the half-life of the element, and it is related to the decay constant by:

$$\lambda T = 0.693 \tag{8}$$

The magnitude of the half-life varies enormously from element to element, being only 10^{-11} sec for ThC′ and 4×10^{18} sec for samarium. In no other field of physical measurements is so extensive a gamut encountered. In a given mass, any one atom may exist unchanged for an interval varying between zero and infinity. However, the "average atom" has a statistical life expectancy θ which is numerically equal to the reciprocal of the decay constant. In a series of radioactive elements the range of the alpha particles emitted by the several members is related to the rate of disintegration by an empirical relationship,

$$\log R = a \log \lambda + b \tag{9}$$

known as the Geiger-Nuttall law.

Precise modern measurements on the mean ranges of alpha particles show that the velocity of emission is seldom of a purely monoenergetic character, and that, in general, the alpha particles from a given element show a spectrum whose energy levels are often associated with the gamma-ray spectrum accompanying the decay of the atom. Thus, for every million alpha particles from RaC′ of normal range 6.91 air-cm there are 22 emitted with a range of 9.00 cm. Likewise, in the decay of ThC′ there are 34 particles of 9.69 air-cm range and 190 of 11.54 air-cm for every

million alpha particles of mean range 8.57 air-cm. The last group of rare alpha particles represents the most energetic nuclear projectiles available from natural sources. In the decay of certain elements as RdAc the number of abnormal alpha particles constitutes a large fraction of the total, but the fluctuations in range amount to only a few per cent. For most purposes of radiochemical computation the range of the alpha particles emitted by a given radioisotope is represented with adequate precision by the weighted average of the several components.

Old unaltered radioactive minerals constitute a complex system of radioisotopes which are classified into three principal radioactive series. The members of the uranium, actinouranium, neptunium, and thorium series are represented graphically in Fig. 14 showing their genetic relationships. Solid circles ● denote decay by alpha-particle emission, ○ a beta-ray transformation, and ◐ nuclei which exhibit branching and decay by emission of both alpha and beta particles. Members of the same column are isotopic and cannot be separated from each other by ionic chemical reactions. Of the radioactive elements only uranium and thorium are available in sufficient abundance in minerals for their direct determination by the usual analytical procedures. The other radioelements can be separated as isotopic groups, or pleiads, as termed by Fajans,[F1] by coprecipitation on an insoluble compound of an homologous non-radioactive element.

In a state of radioactive equilibrium the number of atoms produced per unit of time is equal to the number disintegrating in the same interval. Since the number of disintegrations $\delta = \lambda N$, is follows that:

$$\lambda_1 N_1 = \lambda_2 N_2 = \cdots \lambda_k N_k \qquad (10)$$

Under these conditions the more slowly decaying members accumulate in greater abundance, and the very active ones are present in proportionately smaller quantities.

Most radioactive minerals contain both uranium and thorium as major constituents, fostering a total of 41 radioactive isotopes and three stable isotopes of lead which accumulate as the end products of the three chains. Pitchblende and carnotite are essentially devoid of thorium; and certain thorium minerals, such as monazite, contain only minute amounts of uranium. There are no minerals known which contain actinouranium as an exclu-
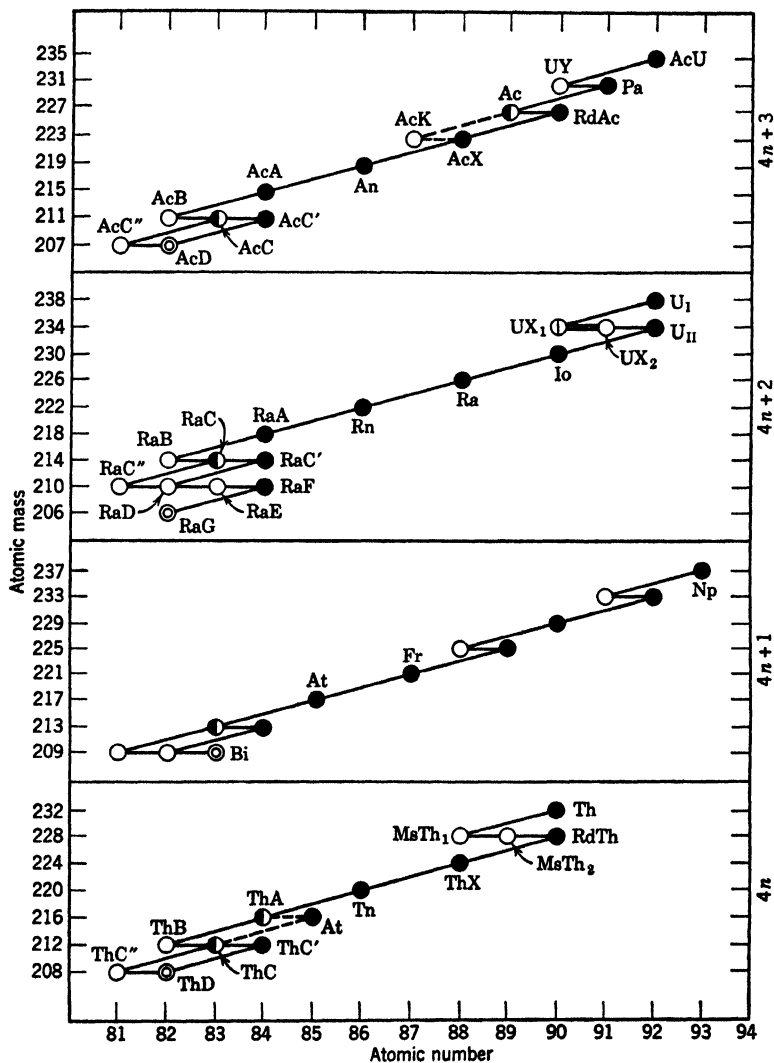
FIG. 14. Disintegrations in the Th ($4n$), Np ($4n+1$), U ($4n+2$), and AcU ($4n+3$) series.

sive primary constituent.* Actinouranium is present in all uranium minerals to the extent of 0.719 per cent of the total uranium content.

Knowing the relative abundance of the two principal uranium isotopes, UI of mass 238 and AcU of mass 235, and their rates of disintegration, the equilibrium quantities of the other members of the series can be computed.

A sample of pitchblende containing 85.4 per cent of U_3O_8 may be expected to contain the following quantities of radium and protoactinium, viz.:

$$W_{Ra} = 0.854 \times 0.848 \times 0.9928 \times \frac{4.86 \times 10^{-18}}{1.38 \times 10^{-11}} \times \frac{226}{238}$$

$$= 2.40 \times 10^{-7} \text{ g Ra per g}$$

$$\frac{Ra}{U} = \frac{2.40 \times 10^{-7}}{0.854 \times 0.848}$$

$$= 3.32 \times 10^{-7} \text{ g Ra per g of U (measured } 3.38 \times 10^{-7})$$

Likewise, the weight of protoactinium in the mineral is computed to be:

$$W_{Pa} = 0.854 \times 0.848 \times 0.00719 \times \frac{3.11 \times 10^{-17}}{6.86 \times 10^{-13}} \times \frac{231}{235}$$

$$= 2.31 \times 10^{-7} \text{ g Pa per g}$$

$$\frac{Pa}{U} = \frac{2.31 \times 10^{-7}}{0.854 \times 0.848}$$

$$= 3.20 \times 10^{-7} \text{ g Pa per g of U (measured } 2.74 \times 10^{-7})$$

These values are in close agreement with the measured quantities found in a radiochemical analysis of pitchblende by von Grosse.[V6]

Complete equilibrium is attained only after the elapse of an infinite period of time. For practical purposes, conditions of

* Pleochroic halos have been observed whose ring structures can be attributed only to the exclusive decay of actinouranium. This puzzling phenomenon is now explicable on the assumption that plutonium of mass 239 existed during the earth's past in appreciable quantity. Its alpha decay provides a source of actinouranium free from the other uranium isotopes.

essential equilibrium prevail after the longest-lived daughter member of the chain has accumulated for an interval 10 times the duration of its half-life. Because the uranium isotopes are inseparable by normal geochemical alteration processes, the relative abundance of radium will be dependent on the accumulation of its non-isotopic parent, ionium. Thus, if the mineral was altered ($10 \times 83{,}000$) years ago the U-Ra series will be in equilibrium. In the laboratory, when radium sulfate is freshly precipitated from a boiling solution of a uranium mineral it emits 3.7×10^{10} alpha particles per sec per g of Ra. About 1 month or (10×3.825) days later, when the radon accumulates in equilibrium amount, this rate is increased to $4 \times 3.7 \times 10^{10}$ by the additional alpha radiation emitted by Rn, RaA, and RaC′. Since RaD has a half-life of 22 years, radium salts of recent manufacture will not contain the equilibrium amount of polonium until they have aged about 220 years.

Besides the members of the three principal radioactive series, samarium is the only other naturally occurring element that decays with the emission of an alpha particle. Certain isotopes of the transuranium elements, whose properties are recorded in Table 3, also decay with the emission of alpha particles. Pu^{239} is the most important of this group because of its large-scale synthesis in uranium-pile reactors. Traces of plutonium have been reported by Seaborg[S17] in pitchblende and carnotite. Its presence is attributed to neutron capture by U^{238}, which by successive beta decay results in the long-lived Pu^{239}. The neutrons originate from the spontaneous fission of uranium, possibly augmented by other neutrons resulting from the capture of alpha particles by certain light nuclei as Al, Na, and Be present as minor constituents in uranium minerals.

When Th^{232} is bombarded with neutrons a compound nucleus is formed which decays by successive beta emission to U^{233}. The alpha decay of this uranium isotope fosters a new series of radioelements whose interrelationship is shown in Fig. 14. The parent of this $4n + 1$ series is Np^{237}, and in its decay to stable Bi^{209} eight alpha-particle-emitting isotopes of the heavy metals are produced. There is no evidence for the existence of the neptunium series in uranium or thorium minerals.

Almost all analyses of pitchblende report minor amounts of bismuth. This is probably not of radioactive origin as bismuth sulfide minerals are

intimately admixed in pitchblende deposits. Two old analyses report traces of bismuth in unaltered thorianite and bröggerite. This suggests a possible radioactive origin, and it may be worth while to include Bi/Th ratios in the analysis of minerals for their Pb/U ratio.

TABLE 3. SYNTHETIC ALPHA-RAY-EMITTING ISOTOPES

Element	Z	A	T	λ sec^{-1}	Energy, Mev	Air-Range, cm
Bismuth *	83	213	46m	2.51×10^{-4}	5.86	4.2
Polonium	84	213	4.4×10^{-6}s	1.58×10^{5}	8.336	7.8
Astatine	85	211	7.5h	2.57×10^{-5}	5.94	4.3
		216	Brief		7.64	6.8
		217	0.02s	34.7	7.023	5.9
		218	710s	9.76×10^{-4}	6.63	5.2
Francium	87	221	4.8m	2.41×10^{-3}	6.30	5.0
Actinium	89	225	10.0d	8.04×10^{-7}	5.801	4.4
Thorium	90	229	7000y	3.1×10^{-12}	4.825	3.3
Uranium	92	232	30y	7.4×10^{-10}	5.31	3.8
		233	1.63×10^{5}y	1.35×10^{-13}	4.83	3.3
		236	10^{7}y			
Neptunium	93	237	2.25×10^{6}y	9.8×10^{-15}	4.77	3.3
Plutonium	94	236			5.75	4.3
		238	50y	4.4×10^{-10}	5.52	4.08
		239	2.411×10^{4}y	9.13×10^{-13}	5.144	3.68
		240	10^{4}y	2×10^{-12}	(5.3)	3.8
		241			(5.23)	3.7
Americium	95	241	500y	4.4×10^{-11}	5.47	4.0
Curium	96	240	30d	2.68×10^{-7}	6.25	4.9
		242	150d	5.35×10^{-8}	6.0	4.6

* Branching ratio estimated at 0.02 to 0.04 for alpha disintegration.

The number of nucleids decaying by alpha-particle emission has been further augmented by the synthesis of collateral radioactive chains in the uranium, thorium, and actinium series. By bombarding thorium metal with 19-Mev deuterons or 38-Mev alpha particles Studier and Hyde [S55] isolated a beta-active protoactinium fraction whose decay results in the production of four new alpha-active nuclei:

$$Pa^{230} \xrightarrow[17d]{\beta^-} U^{230} \xrightarrow[20.8d]{5.85\alpha} Th^{226} \xrightarrow[30.9m]{6.30\alpha} Ra^{222} \xrightarrow[38s]{6.51\alpha} Em^{218} \xrightarrow[0.019s]{7.12\alpha} RaC'$$
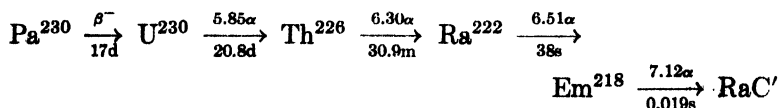
This protoactinium series is of interest in providing a short-lived isotope of uranium of potential use in tracer studies, and in intro-

ducing a fourth radioactive gas, Em^{218}. The emanation decays by alpha-particle emission via the classical RaC′ chain to form stable RaG (Pb^{206}).

By bombarding thorium metal with 80-Mev deuterons accelerated in the Berkeley 184-in. cyclotron, Ghiorso, Meinke, and Seaborg[C38] isolated another protoactinium fraction which exhibited the following decay scheme:

$$Pa^{227} \xrightarrow[38m]{6.46\alpha} Ac^{223} \xrightarrow[2m]{6.64\alpha} Fr^{219} \xrightarrow[10^{-4}s]{7.30\alpha} At^{215} \xrightarrow[10^{-4}s]{8.00\alpha}$$

$$Bi^{211}(AcC) \xrightarrow{\alpha} Tl^{207}(AcC'') \xrightarrow{\beta^-} Pb^{207}$$
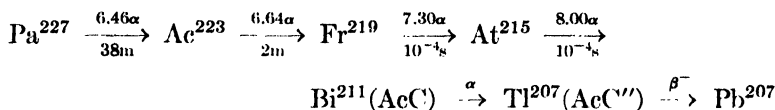
The decay of Pa^{227} gives rise to four alpha emitters which are members of a collateral branch of the $4n + 3$ family. Following the decay of the initial activity fostered by Pa^{237} a second group of alpha-particle emitters was detected stemming from a longer-lived protoactinium isotope Pa^{228}:

$$Pa^{228} \xrightarrow[22h]{6.09\alpha} Ac^{224} \xrightarrow[\sim 2.5h]{6.17\alpha} Fr^{220} \xrightarrow[30s]{6.69\alpha} At^{216} \xrightarrow[10^{-3}s]{7.79\alpha}$$

$$Bi^{212}(ThC) \xrightarrow{\alpha} Tl^{208}(ThC'') \xrightarrow{\beta^-} Pb^{208}$$

$$Bi^{212}(ThC) \xrightarrow{\beta^-} Po^{212}(ThC') \xrightarrow{\alpha} Pb^{208}$$
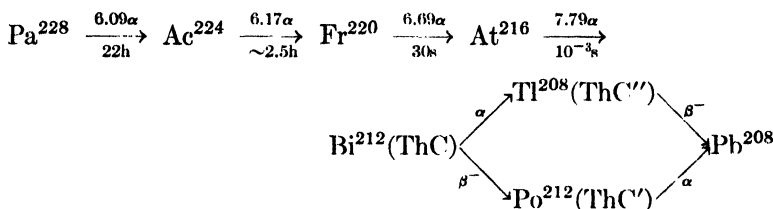
The synthesis of the astatine isotope of mass 216 confirms the claim of Karlik and Bernert[K28] of the existence in nature of a radioactive ekaiodine emitting 7.64-Mev alpha particles which they attributed to beta-branching in the decay of ThA.

In a series of radioactive elements the energy of the alpha particles is related to the rate of disintegration. The most familiar of these relationships is that formulated by Geiger and Nuttall stating that in a family of radioelements log λ is approximately a linear function of log R. Isotopic nuclei which decay by alpha-particle emission exhibit another quantitative relationship between their decay energy and atomic mass. It has been observed by Fournier[F22] that, when the velocity of the alpha particles is plotted against the atomic weight of the parent atoms, the members of isotopic groups fall on a series of lines. In testing this relationship on the newly discovered alpha emitters it was ob-

served [Y17] that the general precision of this empirical relationship is improved utilizing $E/(A - Z)$ and A as parameters. The loci in Fig. 15 show that this formulation fits the available data for all members of the four principal series and their collateral chains. Only RaF, AcC′, and At^{211} exhibit abrupt departures from linearity and the correlation is poor for U^{238} and Th^{232}. Although the physical significance of this regularity is obscure, it offers an
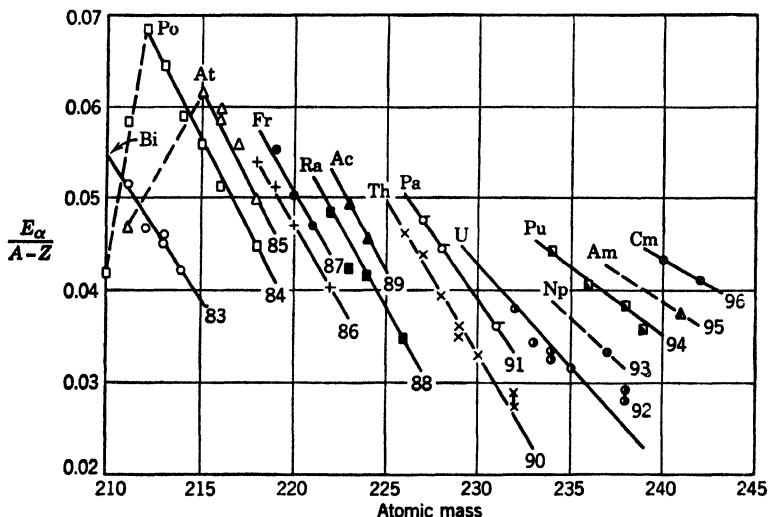
FIG. 15. Relationship between disintegration energy and mass for alpha-emitting nuclei.

additional means of extrapolating the decay energy of other alpha emitters that may be produced in the bombardment of heavy metals with fast charged particles.

RANGE OF ALPHA PARTICLES IN SOLIDS

Range measurements of densely ionizing particles are usually made in air or other gases of low stopping power. In quantitative autoradiography the range of alpha particles in solid sources must be known and, in particular, their range in the heterogeneous mixture of silver halides and gelatin constituting the recording medium for the tracks. Direct measurements in solids are available for several pure metals and an even smaller number of com-

pounds. The range in a solid can be estimated, however, from a simple empirical rule formulated by Bragg and Kleeman.[B39] This states that the stopping power of an atom is proportional to the square root of its atomic weight. The relative atomic stopping power s of an element of density d, thickness t, and atomic weight W is expressed by $s = d_0t_0W/dtW_0$, in which the symbols with subscripts 0 refer to the standard substance for which the stopping power is taken as unity. Likewise, the relative stopping power of a complex molecule is defined by d_0t_0M/dtW_0, where M is its molecular weight.

Bragg and Kleeman observed that $s/\sqrt{W}$ is approximately a constant for all the elements and that their rule also held for polyatomic solids when the stopping power is taken as the sum of the stopping powers of its constituent atoms. Rutherford[R20] states that this additive rule is a serviceable approximation only when the alpha particle spends most of its energy in acting on the individual atoms and not in dissociating or exciting the molecule. For purposes of direct conversion of air ranges into ranges in a particular solid it is convenient to formulate the Bragg-Kleeman rule by equation 11:

$$\frac{R_a d_a}{R_s d_s} = \frac{\psi_a}{\psi_s} \tag{11}$$

In this expression ψ is the permeability of the medium to alpha particles defined in terms of its atomic composition. If a medium is composed of atoms $A, B, C \cdots$, in the relative proportions by weight $a, b, c \cdots$, then the permeability of the medium is:

$$\psi = a\sqrt{W_A} + b\sqrt{W_B} + c\sqrt{W_C} + \cdots = \Sigma n\sqrt{W_N} \tag{12}$$

Thus, the permeability of standard dry air is as tabulated:

Atom	Composition	$\sqrt{W}$	Permeability
Oxygen	0.23024	4.000	0.921
Nitrogen	0.75539	3.742	2.827
Argon	0.01437	6.324	0.091
	1.00000		$3.839 = \psi_{air}$

Since the density of dry air at 15° C and 760 mm of Hg is 0.001226 g per ml, the range of an alpha particle in any other medium R_s is obtained as a first approximation by equation 13:

$$R_s = \frac{R_a d_a \psi_s}{d_s \psi_a} = 0.0003194 \frac{R_a \psi_s}{d_s} \quad \text{cm} \tag{13}$$

The stopping power of a number of metals has been measured by von Traubenberg,[V15] and more recently by Walker.[W1] Von Traubenberg employed the scintillation method for the detection of the emergent alpha particles. The particles originating from a wire coated with RaC + RaC′ passed through an accurate wedge of the metal, and a point was determined where the scintillations were no longer detectable. The extrapolated thickness of metal penetrated by the RaC′ alpha rays (formed as a result of the beta decay of RaC to RaC′), corrected for air absorption between source and wedge, is compared in Table 4

TABLE 4. COMPARISON OF MEASURED AND COMPUTED RANGES OF RaC′ ALPHA PARTICLES IN METALS

				Measured Range, cm		Computed Range, cm
Z	Metal	ψ	d	von Traubenberg[V15]	Walker[W1]	
3	Li	2.64	0.534	0.01291	0.01410	0.0110
4	Be	3.01	1.85	....	0.00428	0.0036
6	C	3.47	2.25	....	0.00351	0.0034
12	Mg	4.94	1.741	0.00578	0.00595	0.0063
13	Al	5.20	2.699	0.00406	....	0.0043
14	Si	5.31	2.35	....	0.00472	0.0051
19	K	6.25	0.87	....	0.01500	0.0160
20	Ca	6.34	1.54	0.00788	....	0.0092
26	Fe	7.46	7.86	0.00187	0.00194	0.0021
28	Ni	7.66	8.75	0.00184	....	0.0019
29	Cu	7.99	8.93	0.00183	0.00182	0.0020
30	Zn	8.09	7.19	0.00228	....	0.0025
47	Ag	10.39	10.6	0.00192	0.00198	0.0022
48	Cd	10.61	8.67	0.00242	....	0.0027
50	Sn	10.90	7.30	0.00294	0.00301	0.0033
78	Pt	13.99	21.37	0.00128	0.00131	0.0015
79	Au	14.02	19.33	0.00140	....	0.0016
81	Tl	14.29	11.86	0.00233	....	0.0027
82	Pb	14.40	11.35	0.00241	0.00256	0.0028

with the value computed from equation 13. The study shows that the method yields estimates of the range which are in fair agreement with the available measurements but that, in general, the computed results are about 10 per cent high. The range of alpha particles other than those emitted by RaC′ can be approxi-

mated by assuming a linear proportionality between the measured air ranges and the corresponding range in the solid.

This assumption is valid only for alpha particles of approximately the same energy as RaC′. Alpha particles of very short range and those of very high energy cannot be compared accurately by a simple proportionality. The range of an alpha particle is a complex function of its velocity. At the velocities of emission from nuclei in the uranium, actinium, and thorium series the range is proportional to the cube of the initial velocity. The early studies of Geiger showed that when the decay energy resided between 4.5 and 8.8 Mev the air range of the particles could be formulated by $R_a = 9.67 \times 10^{-28} v^3$. With increasing velocity, the range varies more nearly as v^4, and at lower energies the range varies very nearly as the $3/2$ power of the initial velocity.

TABLE 5. RANGE OF ALPHA PARTICLES IN COMPOUNDS

Compound	Alpha Particle	Measured Range, cm	Computed Range, cm
Mica	RaC′	0.0036 [W1]	0.0037
Willemite	RaF	0.0020 [G7]	0.0020
Water	RaC′	0.0060 [W1] *	0.0081
Water	RaF	0.0032 [M19]	0.0045

* An identical range of 0.0060 cm was observed by Philipp.[P21]

Direct-range measurements within polyatomic solids and liquids are very few in number. Available data are summarized in Table 5 together with the corresponding value computed from the Bragg-Kleeman rule. The agreement is good for mica and willemite but is about 30 per cent high for water. Other physico-chemical measurements on water indicate that the molecules in this liquid are associated in units of two or more. The trajectory of alpha particles in water is possibly reduced by partial expenditure of their energy in dissociating these complex molecules.

It is of interest that Glasson[G12] has demonstrated that the atomic stopping power is proportional to the $2/3$ power of the atomic number. Hume-Rothery[H37] and Yagoda[Y1] have demonstrated that in a periodic group of elements the ionization potential V is closely approximated by

$$n^2V = aZ^{2/3} + b$$

where n is the total quantum number of the valence electron, and a and b are constants for a periodic group. This is in agreement with prevailing concepts that in the passage of alpha particles through the orbital electrons energy is expended chiefly in producing ionization. Von Hevesy[V14]

finds that the atomic stopping power is related to the atomic number by the expression $s = 0.563Z/\sqrt{Z+10}$. The application of these formulations might possibly lead to more accurate estimates of the range of alpha particles in solids. In view of the paucity of experimental data and their low precision, there is little to be gained from the application of these somewhat more complex relationships.

Measurements on the variation of the ionization along the trajectory of an alpha particle in air show that it increases gradually with the distance from the source, reaches a maximum near the end of the range, and then rapidly diminishes to zero. In the passage of an alpha particle through a solid, the ionization maxima near the end of the trajectory produce an enhanced localized chemical action on the crystal lattice. In biotite mica the ferrous iron is oxidized to the trivalent state, and an intensified brownish color appears near the range termination. The occurrence of minute radioactive inclusions in mica results in a series of concentric colored spherical shells produced by the alpha radiations over geologically long periods of time.

TABLE 6. RADII OF PLEOCHROIC HALOS AND RANGES OF ALPHA PARTICLES IN MINERALS

	Biotite Mica[H22]		Fluorspar[G28]	
Alpha Ray	Halo Radius, microns	Computed Range, microns	Halo Radius, microns	Computed Range, microns
UI	12.7	14.1	14.0	13.8
UII			14.4	17.3
Io	15.3	16.9	15.8	16.6
Ra			16.9	17.6
RaF }	19.2	21.0	{ 19.5	20.7
Rn }			20.5	21.8
RaA	23.0	24.8	23.5	25.2
RaC′	34.2	36.8	34.5	37.3
Permeability	5.19		5.37	
Density, g per ml	3.12		3.18	

When a thin cleavage plane of the mica, embodying a major diameter of the spheres, is observed microscopically a series of concentric colored rings termed pleochroic halos may be seen about the central inclusion. Measurements of the radii of these halos afford an independent estimate of the ranges of alpha particles in solids, as the ionization peaks are reasonably close to the

true track terminations. Table 6 compares the halo radii in mica and fluorspar with the estimates provided by the Bragg-Kleeman rule for these compounds. The measurements and the computed ranges are in good agreement, the average 10 per cent deviation being usually in accord with the lower value to be expected from the halo dimension.

Fortified by these considerations, an estimate of the range of alpha particles in photographic emulsions can now be attempted. As a first approximation, the emulsion can be considered as a dispersion of silver bromide in gelatin, neglecting the small variable amounts of residual potassium nitrate and water which are also present. The range of an alpha particle is then defined by the permeabilities, densities, and relative proportions of silver bromide and gelatin. The distances traversed in the two components is proportional to the volumes occupied by them. The volumes can be estimated from the weight proportions of the two ingredients, assuming that their densities in the emulsion are the same as in the unmixed state. The composition of the emulsion can be ascertained precisely by suitable gravimetric methods of analysis, but data of ample accuracy are secured by the following simple procedure:

Condition a 5×8 cm plate over a desiccant and determine its total weight. Extract the silver halides by means of 30 per cent sodium thiosulfate, and wash repeatedly with distilled water until all soluble salts are removed. The loss in weight by the reconditioned plate closely approximates the weight of the silver halides. Soak the gelatin-coated slide in concentrated hydrochloric acid for about 5 min and dissolve the hydrolyzed coating in hot water. Dry and weigh the glass backing, obtaining the weight of the gelatin by difference.

TABLE 7. COMPOSITION OF PHOTOGRAPHIC GELATIN

Element	Mees[M23]	Perfilov[P15]	Yagoda[Y17]
Carbon	50.5	52.5	49.4
Hydrogen	6.8	7	6.8
Nitrogen	17.5	17	18.0
Oxygen	25.2	21.5	25.0
Sulfur		2	0.7

The permeabilities of silver bromide and of gelatin are readily calculated from their atomic composition. The composition of the purified gelatin employed in the manufacture of photographic emulsions is indicated by the analyses recorded in Table 7.

Analysis of an Eastman NTA emulsion revealed the presence of AgBr : gelatin as 80 : 20 by weight. On a basis of 6.47 and 1.31 for the specific gravities of the respective compounds, the analysis indicates a composition by volume of 44.7 per cent AgBr and 55.3 per cent gelatin. The calculated ranges of the alpha particles from RaC′ in the individual components and in the emulsion are as tabulated.

Medium	ψ	d	Range, microns
AgBr	9.78	6.47	33.3
Gelatin	3.50	1.31	58.9
Emulsion	6.30	3.62	38.4

Microscopic measurements of the tracks of RaC′ alpha particles in the same emulsion showed an average length of 41 microns. This is in reasonably close agreement with the computed value in view of uncertainties in the several measurements, the lack of precision of the Bragg-Kleeman rule and the straggling in range of alpha particles. The computed range of 38.4 microns indicates that the emulsion has a stopping power for alpha particles 1800 times greater than air.

CHARACTERISTICS OF NUCLEAR EMULSIONS

Historical Development. The early work of Kinoshita, Makower, and Walmsley on alpha-particle recording was done with optical-type emulsions. These emulsions have a thickness of a few microns and will record complete tracks only of particles entering at glancing incidence. To record the full trajectory of low-energy alpha particles at all angles of incidence an emulsion thickness of about 50 microns is essential. Thick-layered emulsions were prepared by Myssowsky [M36] in 1927. They were applied by Baranov [B2] in the study of the distribution of radioactive inclusions in rocks and plants and were also applied by Alexandrov [A1] in the study of the Russian radium deposits at Tyuya-Muyun. Improved thick-layered emulsions were studied by Zhdanov [Z2] at the State Radium Institute in Russia, and by Blau and Wambacher [B22] at the Radium Institute in Vienna. The latter observed that their extremely fine-grained emulsions were very insensitive to white light and reacted anomalously after treatment with sodium nitrite. This compound has a hyper-

sensitizing action on plates exposed to white light. Blau and Wambacher found that the reagent diminished the sensitivity of their thick-layered emulsions to alpha particles.

Interest in these early nuclear-type emulsions increased when Blau[B21] and Wambacher[W2] discovered that energetic protons recorded tracks in emulsions sensitized with pinakryptol yellow. Low-energy protons produced by the collision of alpha particles with hydrogen nuclei could be recorded on normal plates, but the more energetic recoil protons resulting from the neutron bombardment of metallic foils registered tracks only when the emulsion was sensitized with dyes having structures similar to pinakryptol yellow. According to these investigators, the dye alters the outer surface of the silver bromide grains so that they are rendered more readily developable after impact by a proton. As a result of oxidation, the dyes rapidly lose their sensitizing property, and it was found necessary to conduct the exposure either in a vacuum or in an oxygen-free atmosphere. Zhdanov[Z1] found that the grain size of the silver bromide was critical for the registration of proton tracks, and that by keeping the grain diameter between 0.5 and 0.8 micron satisfactory proton tracks would record without the aid of dye sensitization.

Zhdanov prepared emulsions sensitive to protons by adding a solution of 5 g $AgNO_3$ and 1.75 g gelatin in 52.5 ml of water to a second one consisting of 4 g KBr, 3.5 g of gelatin, and 52.5 ml of water. The solutions are maintained at 60° C and stirred while mixing. The properties of Zhdanov's E1 emulsion have been confirmed in investigations by Demers.[D5]

As a result of the widespread application of these emulsions in the study of cosmic radiation and in the detection of densely ionizing particles originating from nuclear reactions, the Ilford Laboratories in England developed similar plates on a commercial basis.

The early nuclear-type emulsions were experimental and subject to fluctuation in properties. The Ilford R1 plate was a fine-grained emulsion sensitive to alpha particles, with very little background fog, but insensitive to protons. Their R2 plates was proton sensitive but had an increased number of background grains rendered developable. After further experimentation, Ilford developed a "New Halftone" emulsion which was sensitive to both alpha particles and high-energy protons.

Collaboration between C. F. Powell and the Ilford Laboratories has resulted in a series of nuclear emulsions containing about eight times the normal concentration of silver halides. In the preparation of these concentrated emulsions, care is taken to prevent the background density of fog grains from increasing in proportion to the increased silver content. These Nuclear Research emulsions are available in different types desig-

nated B2, C2, E1, and D1. The B2 type is the most sensitive emulsion of the series and records tracks of alpha particles and energetic protons. Type C2 is of finer grain than B2 and is suited for accurate track-length measurements. According to a statement from Powell, the C2 emulsion is the most suitable grade for the registration of alpha-particle tracks for purposes of autoradiography. The E1-type emulsion is serviceable for the differentiation of alpha-particle and proton tracks, as the latter record poorly. The finest-grained emulsion of the series is the D1. This emulsion does not record proton tracks, records alpha-particle trajectories poorly, and is serviceable as a medium for the registration of fission fragment tracks. The general composition base of these emulsions is compared with that of other nuclear types in Table 8. A comparative study of the Ilford C2 and the Eastman NTA emulsions, described in Fig. 16,
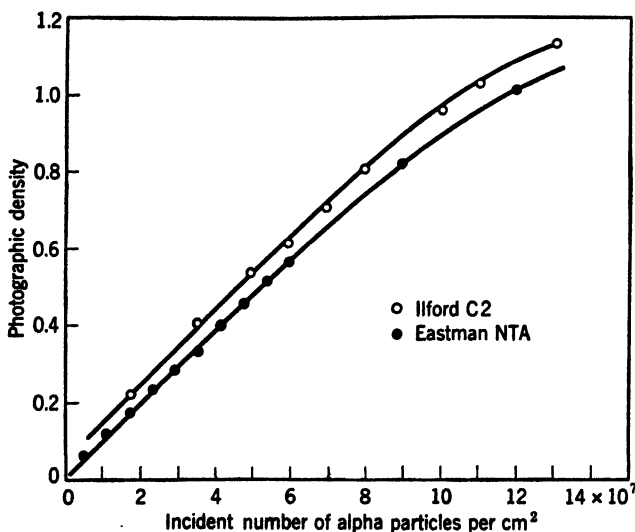
FIG. 16. Relationship between photographic density and alpha-particle exposure. Emulsions exposed to RaF alpha particles and developed in D19 for 2 min at 25° C. Alpha-particle flux during exposure approximately 10^6 per sec per cm^2.

shows that both media have very nearly the same density developed after exposure to an identical source of alpha particles.[K4]

In collaboration with T. R. Wilkins the Eastman Kodak Laboratories produced a series of experimental nuclear-type emulsions designated as Fine-Grain Alpha-Particle plates. These media had a coarser grain size and a lower concentration of silver halide than their present NTA emulsions. The Eastman Nuclear Track emulsion has its stopping power augmented by the use of a high silver bromide to gelatin ratio, and the coating ranges between 25 and 40 microns in thickness. After fixation, the

residual film of gelatin is about 15 microns thick. This is advantageous in counting tracks and in exploring the plate for rare nuclear events, as almost all the developed tracks reside in very nearly the same focal plane.

The Agfa Laboratories in Germany developed a nuclear-type emulsion designated as the "K-plate," which according to Wambacher[W5] showed a marked difference in the grain density of recorded proton and alpha-particle tracks. Cüer[C29] has described the recording properties of two emulsions of French manufacture. Polonium alpha particles record tracks of 23.5 microns in the "micro" emulsion and 25.0 microns in the "Tous noirs" plate.

TABLE 8. COMPOSITION OF NUCLEAR-TYPE EMULSIONS

Designation	Eastman Fine-Grain	Eastman Improved	Eastman NTA	Ilford C2
Emulsion No.	276,296	329,489	350,773	
AgBr, %	44	73	82	85.1
Gelatin, %	56	27	18	14.9
Emulsion weight, mg/cm^2	5.4	7.2	8.8	16.8
Thickness, microns	40	24	30 *	44

* The Eastman nuclear-type emulsions are now available in different emulsion thicknesses of 25, 50, and 100 microns. The 25-micron coating is best suited for alpha-particle counting and alpha-ray patterns. Plates with heavier coatings are employed chiefly in the study of cosmic radiation. According to the Eastman Co. their NTA and NTB emulsions are composed of 17.50 per cent gelatin and 82.49 per cent silver halides (97 parts AgBr and 3 parts AgI by weight). The Ilford nuclear research plates are available with coatings 50, 100, 200, and 300 microns thick and have the same chemical composition as the Eastman NTA emulsion.

The commercial availability of the nuclear-type emulsions is of considerable advantage in their practical application in radioactive measurements. Unfortunately, details on the sensitization of these emulsions are not disclosed. Investigators using these plates, therefore, do not have access to information on minor constituents, such as light-desensitizing dyes or proton-sensitizing agents, which may have a significant bearing on the properties of the emulsion. Thus, Schäfler[S3] has found that traces of pinakryptol yellow, added as a proton sensitizer to Agfa plates, cause an increased fading of the latent image. The preparation of thick-layered, fine-grained emulsions has not been standardized. Their recording properties are therefore subject to fluctuation as a result of modifications in the manufacturing formulae. In this way the stopping power of the Eastman nuclear-type emulsions has increased progressively from 1300 to

about 1750 during the past few years. This alteration diminishes the length of tracks but increases their microscopic discernibility because of closer grain spacing. For purposes of autoradiography the increased stopping power also improves the resolving power of the emulsion for minute radioactive inclusions.

However, potential changes in emulsion composition necessitate new calibration data for each lot of plates. Until their properties become more highly standardized, new plates must be investigated to determine whether their characteristics have been altered appreciably. In particular, generalized statements concerning stopping power, resolution, and sensitivity to other radiations such as light, beta particles, and x- and gamma-rays must be interpreted as a trend for the type emulsion and not always as indicative of the precise characteristics of a particular shipment. The emulsions keep well when stored in an air-conditioned room kept at low humidity. It is advantageous to order a supply of one emulsion number adequate for about a year's use. Toward the end of this period the developed plates are likely to show an appreciable population of cosmic-ray events even when the laboratory is located near sea level.

Formulae for the laboratory preparation of nuclear-type emulsions have been described by Demers.[D4] This work is of particular importance as it provides direct information on the composition of nuclear-type emulsions. Demers' researches demonstrate that emulsions of markedly different sensitivity can be prepared by altering the size and spacing of the silver bromide grains without resorting to their sensitization by dyes. An emulsion that records tracks with grain spacing sufficiently distinctive for the differentiation of alpha particles, protons, and fission fragments is prepared as follows:

Thirty milliliters of 60 per cent silver nitrate and an equal volume of 42 per cent potassium bromide are added dropwise to 75 ml of a 6 per cent gelatin solution. The gelatin solution is maintained at 40° C and is stirred continuously during the slow simultaneous addition of the salt solutions, whose flow is adjusted to about 1 ml per min.

In an improved formula (Emulsion II) Demers[D9] describes emulsion preparation in greater detail. In this formula alcohol is employed to prevent the formation of clumps and coarse grains. The gelatin (4.5 g) is dissolved in 50 ml of warm water, and when complete solution is effected 25 ml of ethyl alcohol is stirred into it, maintaining the temperature at 40° C. The silver bromide is incorporated by allowing two

solutions, the first containing 18.6 g $AgNO_3$ diluted with water to 30 ml, and the second containing 12.8 g KBr diluted to 30.5 ml, to flow dropwise into the gelatin solution under constant vigorous stirring. The burettes for the delivery of the solutions are fitted with capillary tips, or stainless-steel needle-valves that provide an outflow of 1 ml per min. It is desirable to have the bromide ion in slight excess over the silver during precipitation, and the potassium bromide flow should be about 0.5 to 1 ml ahead of the silver nitrate solution.

The resultant emulsion is poured into a flat tray, 12 × 18 in., and the thin layer is jelled by cooling the vessel in ice water. The gel is then washed in running cold water for about 8 hours to remove the potassium nitrate. After washing, the emulsion is remelted and coated on individual 1 × 3 in. clean glass slides. By delivering 1 ml of emulsion, on drying, a layer measuring 40 microns at the center is produced. Peeling of the emulsion is prevented by allowing the gelatin to set in an atmosphere of 60 to 80 per cent relative humidity. The emulsions are not very sensitive to light. Hence, they can be prepared in a room illuminated with red or amber light. Demers cautions that owing to syneresis Emulsion II may occasionally not melt after the washing process. This difficulty has not been encountered in the preparation of the alcohol-free emulsion. The characteristics of these laboratory-prepared emulsions are compared with commercial nuclear-type plates in Tables 9 and 10.

TABLE 9. PHYSICAL CHARACTERISTICS OF NUCLEAR EMULSIONS

Emulsion	Composition by Weight: AgBr	Composition by Weight: Gelatin	Coating: mg/cm²	Coating: microns	Stopping Power	Developed Grain Diameter,[a] micron
Eastman Alpha	56[b]	44	5.4	40	1400	0.6
Eastman NTA	84[b]	16	12.6	38	1750[b]	0.6
Eastman NTC[c]	66[b]	34	8.0	27		
Ilford Halftone	40.6[d]	59.4			1400[a]	0.5
Ilford Conc.	80[e]	20	20.0	50	1700	
Demers	81.6[a]	18.4		40	1600	0.1–0.3

[a] Characteristics determined by Demers.[D8]
[b] Characteristics determined by Yagoda.[Y17]
[c] An experimental emulsion intended for the registration of fission tracks.
[d] Characteristics determined by Choudhuri.[C13]
[e] Characteristics described by Ilford Co.

Knowles and Demers[K16] have studied the grain size of several undeveloped emulsions employed as track-recording media. Their results, summarized in Table 10, show that the nuclear-type emulsions have a grain size about 5 to 10 times smaller than the Lantern-Slide plates employed as recording media for beta particles. Electron-microscopic examination of the original

emulsions exhibits the grains as regular hexagons of nearly uniform size. A layer of adsorbed gelatin 0.01 micron thick is visible around the grains. Their studies indicate that each developed grain, after passage of an alpha particle, arises from about 30 original silver bromide grains surrounding the one traversed.

TABLE 10. ORIGINAL GRAIN SIZE OF PHOTOGRAPHIC EMULSIONS *

	Designation	Grain Diameter, micron
Eastman	V-O	0.25
	Fine-Grain Alpha	0.28
	Microfilm	0.42
	Lantern-Slide	0.60
	548-Microradiographic	0.03
Ilford	D	0.12
	C1	0.16
	C2	0.16
	B1	0.21
Demers		0.04–0.08

* Based on electron microscope measurements by Knowles and Demers.[K16]

Hälg and Jenny[H42] describe the preparation of a silver bromide-iodide nuclear-type emulsion utilizing Demers' precipitation technique. The role of small quantities of admixed silver iodide is not fully established. According to Mees[M23] the addition of 1 to 5 per cent silver iodide to a silver bromide optical-type emulsion increases the sensitivity to light and reduces background fog. Demers, however, found that when 25 per cent of the bromine atoms were replaced by iodine the sensitivity was diminished to the point where only the tracks of fission fragments recorded. With a smaller replacement by either iodine, chlorine, or both Demers observed no worthwhile improvement in sensitivity. The present-day Eastman and Ilford emulsions are of mixed halide type with AgBr:AgI = 97:3. In a personal communication, Hälg states that in his emulsion (67 AgBr + 1 AgI + 22 gelatin + 10 parts of glycerine by weight) the latent image of alpha particles persists for 100 days with but little diminution in grain density on delayed development. Thus, the admixed iodide may play an important role in latent image retention.

The investigations of Hälg and Jenny are of interest in providing specific information on minor constituents of the emulsion

and in furnishing technical details on emulsion washing, stabilization, and the pretreatment of the glass backing for adequate emulsion adherence. They employ solutions of the following composition:

A. Soak 6.5 g of gelatin in 70 ml of distilled water at room temperature for 1 hour and then dissolve by gentle stirring and warming to 50° C.

B. Dissolve 14 g of KBr in 23 ml of water and add 5 ml of 10 per cent $CdBr_2 \cdot 4H_2O$ and 2 ml of 10 per cent KI.

C. Dissolve 18 g of $AgNO_3$ in 30 ml of distilled water.

D. Dissolve 2 g of chrome alum in 78 ml of water; add 60 ml of ethyl alcohol, 42 ml of glycerine, and 0.75 ml of 10 per cent KBr.

E. Dissolve 2 g of gelatin in 150 ml of water at 35° C; add 5 ml of 0.2 per cent aqueous wetting agent and 2.5 ml of 2 per cent chrome alum, and filter.

Solutions *B* and *C* are delivered simultaneously to solution *A* with constant stirring at a rate of about 1 ml per min, adjusting the position of the stirrer so as to avoid foam production. The emulsion is ripened for 45 min at 50° C with slow stirring, and is then transferred to a chilled porcelain dish and cooled in an ice bath for 6 hours. The gel is cut with a spatula, transferred to cheesecloth, and washed for about 16 hours until free from potassium nitrate. The writer has found that small batches of emulsion can also be washed satisfactorily by pouring the emulsion directly into a 1-liter flask and allowing the gel to set on the walls by rotating the flask in an ice bath. This produces a layer about 3 mm thick from which the soluble salts can be removed by filling the flask with chilled distilled water, agitating for several hours, and renewing the water until the last wash gives a negative ring test for nitrate ion.

The washed gel is melted at 35° C and at this stage 9 ml of solution *D* and 5 ml of a 0.2 per cent aqueous wetting agent are added. The incorporated potassium bromide serves as a stabilizer against grain growth, the chrome alum hardens the gelatin, the alcohol lowers the setting point, and the glycerine serves as a plasticizer preventing peeling of thick emulsion coatings under conditions of low humidity. The over-all sensitivity of the emulsion can be increased by the further addition of 1 ml of 2 per cent aqueous acridine orange. The dye increases the light sensitivity of the emulsion necessitating the handling of the plates in a yellowish-red light.

Prior to coating, the acid-cleaned glass is subbed with solution *E*, using about 2 ml on each 2×3-in. plate. When this layer of hardened gelatin has dried the slides are supported horizontally on a glass frame whose bottom can be chilled with ice water. A coating approximately 50 microns thick is obtained by delivering 5 ml of the gel at the center of the slide and pushing the fluid towards the edges with the aid of a fire-polished glass rod. It is good practice to filter the molten gel through glass wool to remove any clotted material. When the temperature is lowered setting takes place in about 10 to 30 min, after which the plates are dried in filtered air.

Response to Nuclear Particles. The nuclear emulsion is in many respects similar to a Wilson cloud chamber in its ability to differentiate between different types of nuclear fragments. In the cloud chamber, ions produced in the gas through which the particles traverse act as nuclei of condensation for water vapor. Under suitable illumination the resultant micro water droplets outline the path of the radiation. The length of the transient
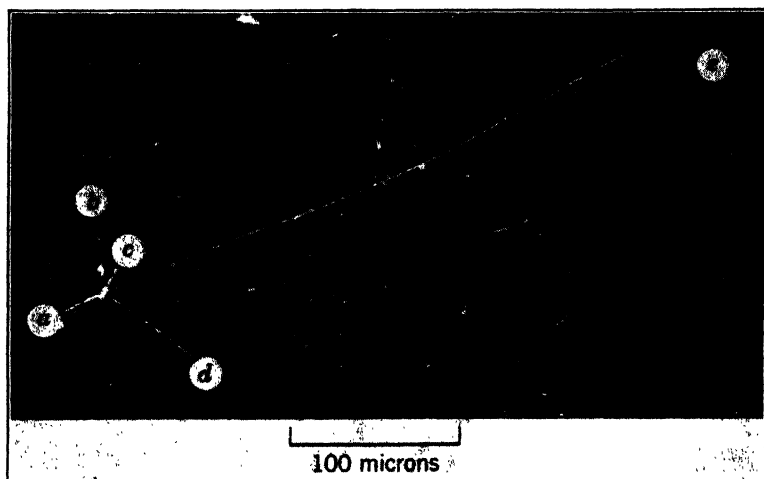
FIG. 17. Nuclear evaporation recorded in an emulsion exposed at high altitude.

tracks corresponds to the range of the particles, and their thickness serves as a measure of the density of ionization. Cloud chamber photographs of alpha-particle tracks show that they travel in a straight line, with an occasional deflection near the track termination owing to a chance collision with an atomic nucleus.

Similar features are depicted when ionizing particles traverse nuclear-type emulsions. The general linearity of path of densely ionizing particles is clearly revealed by tracks *a*, *b*, *c*, and *d* of the cosmic-ray star shown in Fig. 17. Track *e*, however, exhibits both small-angle scatter along the trajectory of the particle, and large-angle scatter close to the end of the particle's range. In instances of large-angle scatter observed even in the tracks of low-energy alpha particles near the end of their range, the projec-

tile penetrates deeply into the electronic structure of one of the atoms in its path and is deviated on approaching close to its nucleus. In traversing the emulsion the particle will more often receive a large number of very small deflections, each of about the same order of magnitude, and the track will exhibit at high magnifications a series of gradual curvatures. This latter process is known as multiple scattering, and the average small-angle deviation along the trajectory is a measure of the mass of the particle. The small-angle scattering is measured by dividing the track into segments of equal length and measuring the angle between adjacent segments.[G32] The average angle along the trajectory is a statistical function which varies directly with the velocity of the particle, the number and charge of the nuclei constituting the emulsion, and is inversely proportional to the kinetic energy of the particle. For a given velocity particles of small mass, like electrons and mesons, will exhibit greater multiple scattering than the more massive proton or alpha particle.

In the interpretation of scattering it is important to note that under severe conditions of exposure the emulsion may record distorted tracks. Spurious effects are particularly noticeable when thick emulsions are exposed at high altitudes under conditions of reduced pressure and elevated temperature. Micro air bubbles trapped in the sensitive layer introduce stresses in the gelatin owing to expansion of the gas. These result in localized distortions of the gelatin layer during photographic processing. Particles ejected linearly in the vicinity of the stressed areas and directed through the thickness of the emulsion will exhibit an S-shaped track. Such occasional complications can be minimized by providing temperature and pressure control during the stratosphere flight and by exercising exceptional care in the manufacture and processing of thick-layered emulsions. The plates should be supported horizontally in all reagent solutions and during the final washing. The addition of a wetting agent in the last stages of washing facilitates uniform drainage of water droplets and avoids distortion in the swollen gelatin caused by uneven drying.

The developed grain density along the track serves as a measure of the ionizing power of the particle and is useful in differentiating trajectories produced by particles differing in charge or mass (see p. 258). In a cloud chamber the track of an alpha particle is observed to be more dense close to the end of its range owing to the greater ionization as the particle slows down. This effect is not generally noticeable in tracks recorded in the emulsion by low-energy alpha particles as the normal development

process is sufficiently strong to reduce all grains traversed to silver once a minimum amount of energy has been expended in them. The variation in ionizing power along the tracks of fast protons and alpha particles is depicted by a variation in grain density, as the interaction between a fast particle and the silver halide grains is not always adequate for latent-image formation and only the more sensitive ones are rendered developable.

TABLE 11. COMPARATIVE IONIZING POWER OF NUCLEAR FRAGMENTS

Particle	Charge	Mass	Energy, Mev	e^2M/E	Relative Ionization
Alpha (RaF)	2+	4	5.30	3.02	1
Recoil atom (RaG)	1+	206	0.10	2060	680
Light fission	(10) *	95	97	98	32
Heavy fission	(11+) *	139	65	259	86
Slow electron	1−	$1/1840$	0.02	0.027	0.009
Beta particle	1∓	$1/1840$	2	0.00027	0.00009
Light meson	1∓	$200/1840$	2	0.054	0.018
Heavy meson	1∓	$316/1840$	2	0.086	0.028
Proton	1+	1	2	0.5	0.17

* The charge of fission fragments decreases with diminution of velocity. According to Evans [E15a] the initial charges at the instant of splitting are about 20+ and 22+ for the light and heavy fragments, respectively. On the basis of average charges of 10+ and 11+ the relative ionization along the fission track is about 60 times that produced by a polonium alpha particle. Perfilov [P15] has estimated that the relative ionization of fission fragments exceeds that of an alpha particle by a factor of 30 to 40.

In general, the ionization produced per unit length of path I by a particle of charge e and velocity v is approximated by $I \propto e^2/v^2$. The ionization is independent of the mass of the particle, but in order to compare the over-all ionization over the complete trajectory for particles of mass M ejected with kinetic energies E, the function e^2M/E serves as a convenient index for the type of track the particle can produce. Values of this index for particles of interest in nuclear physics studies are compared in Table 11. Using polonium alpha particles as a reference standard, it is observed that heavy recoil atoms and fission fragments have high specific ionizations. Although the short range of RaG recoil atoms in the emulsion (~0.01 micron) precludes track formation, other heavy particles ejected in the explosive disintegration of nuclei record exceptionally heavy tracks. With normal development fission tracks are not very much more robust than the alpha-particle tracks. In sensitive emulsions the energy

expenditure of the alpha particle is adequate to ionize almost every grain traversed, and the fission fragments can do but little more. However, the greater ionizing power of the fission fragments can be made manifest by employing emulsions of lower sensitivity, by partial destruction of the latent image, or by employing a weak developer. Under these conditions alpha-particle tracks no longer appear whereas those of the fission fragments develop as nearly continuous lines.

Among the singly charged particles, for a given energy the massive proton produces tracks of greater density than meson particles or electrons. Fast beta particles have comparatively little action on the emulsion, but will cause enhanced fog on prolonged exposure. Low-energy beta particles (0.02 to 0.1 Mev) have a sufficient ionizing power to produce recognizable tracks in the more sensitive emulsions such as Eastman NTB and Ilford B2. These electron tracks have a low grain density and are easily differentiated from proton- and alpha-particle tracks by their large scatter. Because of the high specific ionization of low-energy alpha particles the nuclear emulsions provide virtually selective recording media in the counting of these particles.

Resolving Power of Alpha-Particle Pattern. Certain nuclear emulsions such as Eastman Fine-Grain Alpha have an extremely low sensitivity to both visible and ultraviolet light and are not activated appreciably by pseudophotographic agents. Polished surfaces can therefore be exposed in direct contact with the emulsion. The developed image is a measure of the alpha-particle activity of the surface and of the immediate thin layer above it defined by the range of the alpha particles in the particular solid. The mechanism of this selective alpha-ray pattern is represented diagrammatically in Fig. 18.

A minute radioactive point, source *A*, situated on the polished surface emits alpha particles in all directions, and those directed towards the emulsion are capable of photographic action over a hemispherical volume defined by their range in the emulsion. For points slightly above the polished surface, *B*, the photographic action is restricted to a spherical segment defined by the angle θ and the distance h of the point source above the interface. Alpha particles originating from points within the source located at distances equal to or exceeding the maximum range in the specimen, as *C* and *D*, do not activate the emulsion.

Since the range of the most penetrating alpha particles, originating from the decay of ThC′, is seldom more than 50 microns

in solids, the resultant image is a sharply defined replica of the radioactive segregates. Microscopic examination of the image shows that it consists of a network of tracks produced by alpha particles impinging into the emulsion over a wide range of angles. The source seldom emits particles of a monoenergetic character. In a radiochemically purified uranium preparation, three alpha particles are emitted from the decay of UI, UII, and the minor
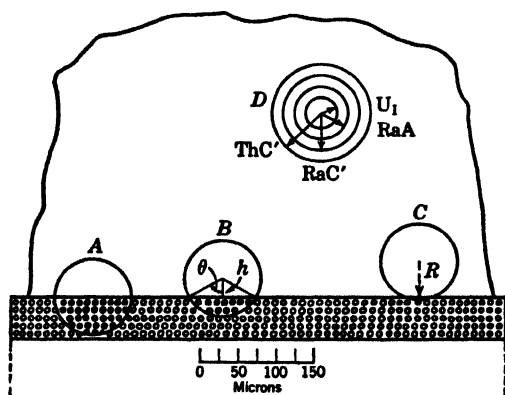
FIG. 18. Effective range of alpha radiations from radioactive mineral in contact with a nuclear-type emulsion.

quantity of AcU. Multiple alpha-ray sources can be treated as a monoenergetic source by assigning an effective range $\bar{R}$ to the constituent particles, equal to their arithmetic mean weighted by relative activity.

At the present time, uranium preparations of natural isotopic ratio contain 99.274 per cent UI, 0.00518 per cent UII, and 0.719 per cent AcU. The actinouranium has a fractional alpha-ray activity of 0.046, the residual 0.954 unit being contributed equally by the decay of UI and UII atoms. The effective range of this system of isotopes is as tabulated. The effective range

Isotope	Air Range, cm	Fractional Activity	Range × Activity
UI	2.65	0.477	1.264
UII	3.21	0.477	1.530
AcU	3.0	0.046	0.138
			$\bar{R}$ = 2.932 air-cm

in air is readily converted into an equivalent range in the solid source by means of the Bragg-Kleeman rule. Thus, the alpha particles resulting from the decay of uranium have a range of 7.7 microns in the pure metal, and a range of 17.5 microns in the oxide U_3O_8. The effective range in air of several systems of interest in radiochemistry and geology is summarized in Table 12.

TABLE 12. EFFECTIVE RANGE OF ALPHA-PARTICLE SYSTEMS

System	Radioisotopes	$\bar{R}$, air-cm
Uranium series	UI, UII, Io, Ra, Rn, RaA, RaC′, and RaF	3.96
Isolated uranium	UI, UII, and AcU	2.93
Radium series	Ra, Rn, RaA, and RaC′	4.72
	Ra, Rn, RaA, RaC′, and RaF	4.54
Thorium series	Th, RdTh, ThX, Tn, ThA, and ThC + ThC′	4.81
Actinium series	AcU, Pa, RdAc, AcX, An, AcA, and AcC	4.71
U + 0.046 AcU	Uranium mineral in equilibrium	4.00
Radon series	Rn, RaA, and RaC′	5.21
Thoron series	Tn, ThA, and ThC + ThC′	5.98
Actinon series	An, AcA, and AcC	5.83

The effective thickness of a solid can also be expressed in equivalent air-cm, that is, the number of centimeters of dry air at 15° C and 760 mm Hg which offer equal resistance to the passage of the alpha particles as encountered by it in traversing the source. If m is the mass of the source in grams, A its area in square centimeters, R_s the range in centimeters in the source, R_a its range in standard air, and d_s the density of the source in grams per cubic centimeter, then the thickness of the source τ in equivalent air-centimeters is:

$$\tau = \frac{mR_a}{AR_s d_s} \tag{14}$$

This unit of measurement is convenient in dealing with alpha particles which expend their energy in several media of different stopping power, as the distances traversed are directly additive when expressed in equivalent air-centimeters. Substituting the value of R_s from equation 13 yields:

$$\tau = \frac{3130m}{A\psi_s} \tag{15}$$

TABLE 13. RANGE OF ALPHA PARTICLES IN RADIOACTIVE MINERALS AND OTHER SOLIDS

Mineral	ψ	d	$\bar{R}$,* microns
Uraninite	13.5	9.0	19.1
Pitchblende	12.5	7.0	22.8
Thorianite	13.3	9.4	22.6
Curite	13.0	7.2	23.2
Carnotite	9.8	4.1	31.6
Torbernite	10.0	3.5	36.5
Samarskite	9.2	5.7	20.6
Betafite	8.8	4.3	26.1
Monazite	9.2	5.1	28.8
Allanite	6.3	3.5	28.7
$Ca_3(PO_4)_2$	5.21	3.14	36.5
LiF	3.90	2.30	37.3
SiO_2	4.61	2.65	38.3
$CaCO_3$	4.88	2.71	39.7
$BaSO_4$	8.75	4.50	42.7
Glass †	4.69	2.50	41.3

* $\bar{R}$ for the radioactive minerals refers to the range of the predominating system of alpha particles generated by decay processes inside the mineral. For the other solids the range is R, as computed for the RaC′ alpha particle.

† The glass employed as a support for the Ilford Nuclear Research emulsions is composed of $72SiO_2 + 14Na_2O + 9CaO + 3MgO$, and 2 per cent of minor constituents.

The effective range of the component alpha radiations in several of the more common uranium and thorium minerals is collected in Table 13. The effective range is about 20 to 37 microns and is on the average very close to the range of the radiations in the emulsion. A minute radioactive segregate located on the polished surface will generate a hemisphere of individual tracks in the emulsion which may attain a maximum diameter of 45 microns. Since the emulsion is viewed in a plane at right angles to the optical axis of the microscope, only the horizontal projections of the tracks are observed. In general, the visual annulus of diffusion about the image of the grain is less than the effective range of the alpha particles. The horizontal projection of rays entering the emulsion at 45° is equal to $\bar{R}/\sqrt{2}$, which evaluates to about 20 microns for most radioactive mineral sources.

Comparative microscopic measurements of the dimensions of mineral grains on the polished surface and their corresponding

alpha-ray patterns show good agreement with the deductions on resolving power. A diffuse annulus of about 20 microns is recorded about the autoradiographic image of the grain. The minute annulus of diffusion causes an apparent diminution in the dimensions of non-radioactive inclusions in matrices of uranium and thorium minerals which must be taken into consideration when the inclusions are very small. Thus, a gangue vein less than 50 microns wide may appear to be feebly radioactive as a result of emergent alpha rays from the surrounding matrix.

Fading of Latent Alpha-Particle Image. If a nuclear-type emulsion is exposed to a source of alpha particles of long half-life and its development is delayed for several days, its photographic density D_f will in general be smaller than that of the control image D_0 made immediately before development of the plate. The magnitude of the fading coefficient $(D_0 - D_f)/D_0$ is a complex function of the emulsion composition, the flux of alpha particles generating the image, their energy, and particularly the conditions of humidity and temperature under which the plates are stored during the period of delayed development.

The phenomenon was first observed by Blau and Wambacher,[B23,20] who state that after 14 days' delay the density is half that produced on undelayed development. Lauda,[L21] who studied the effect in considerable detail on Agfa contrast plates, concludes that after 160 days' delay in development the loss in density is 80 per cent when the plate is stored under normal ambient conditions, 60 per cent when the emulsion is maintained at 0° C, and only 8 per cent when the emulsion is kept in an evacuated desiccator.

The fading of the latent alpha-ray image is a reproducible phenomenon encountered in all nuclear-type recording media. The fading rate in Eastman nuclear-type emulsions has been investigated by Yagoda and Kaplan.[Y10,13] Under normal ambient conditions of storage, fading increases progressively with the period of delayed development, and at the end of 20 days the photographic density is reduced from 90 to 35 per cent, depending on the emulsion composition. Fading is more pronounced in emulsions of low silver bromide concentration. On delayed development the silver grains constituting individual tracks become obliterated, and in Fine-Grain Alpha plates distinct tracks are no longer observable after 5 days' aging of the latent

image. Track deterioration is considerably reduced in the Eastman NTA emulsion. That the ratio of silver bromide to gelatin is an important factor in the rate of fading is substantiated by the recent investigations of Cüer and Morand [C38a] on the retention of the latent image in the Ilford series of emulsions. Their studies likewise show that the fading rate increases with diminishing silver halide content.

Occhialini [O1] and LaPalme and Demers [L12] also report fading of track structures on delayed development. The latter find that fading occurs in all fine-grained emulsions such as the Eastman Alpha plate, type V-O and type 548; The Ilford D1, C1, and C2; and also in their own specially prepared emulsions. In each plate fading of the track is perceptible after 1 day, and is severe after 1 month. The phenomenon is especially marked when the tracks are produced by protons. LaPalme and Demers report that the fading is much faster when the plates are stored at 42°C, and that at low temperatures, such as that of Dry Ice (−85° C), the fading is too slow to be observed in several months.

On first consideration the rapid fading of the latent alpha-particle image appears to be anomalous when compared with the general stability of the optical latent image. Successful development of negatives 10, 20, and even 30 years after the initial exposure are on record.[N1] In these unusual instances the films were found in polar regions, at the camp sites of lost arctic explorers, and the favorable conditions of low temperature and humidity may have been important factors in the preservation of the optical latent image. In contrast to the general stability of the optical image on fast negative emulsions, the latent image on low-speed emulsions, particularly positive printing papers, begins to fade shortly after exposure and progresses rapidly on further delayed development.[N1]

Blair and Hylan [B27] found a distinct decrease in the optical latent image on delayed development and also discovered that the effect was accentuated in plates desensitized to light with pinakryptol yellow. The work of Lauda [L21] on pinakryptol yellow desensitized plates likewise shows that the dye accelerates fading of the latent alpha-ray image. Fading of the optical latent image was observed to increase with high temperatures of storage both in the studies of Blair [B27] and in the independent investigations of Burton.[B48] In a series of studies on the fading of the optical latent image, Emmermann [E3] observed that the rate increased as the silver iodide content of the emulsion was augmented, and that in plates of fixed composition the effect was accentuated by conditions of high temperature and humidity.

Fading is accelerated by storing the exposed plates in warm air saturated with water vapor. The experiments of Yagoda and Kaplan,[Y19] summarized in Fig. 19, show that an exposure of 10^7 alpha particles per cm^2 can be completely obliterated by overnight exposure to air at 35° C saturated with water vapor. Although the emulsion absorbs a considerable volume of water, the rapid fading of the latent image cannot be attributed to
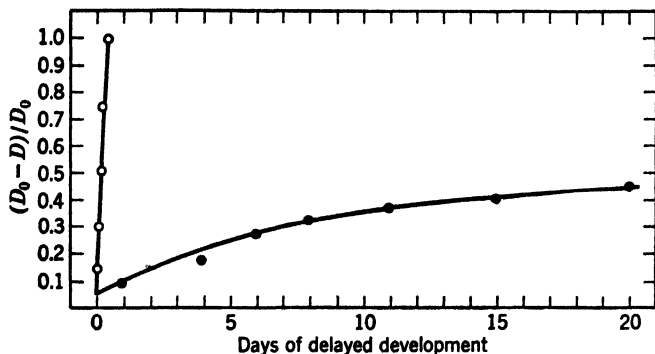
FIG. 19. Variation of fading rate with conditions of storage.

● Ambient conditions, 25° C and low humidity.

○ Eradication conditions, 35° C and saturation humidity.

Eastman NTA emulsions coated 30 microns exposed to a total of 5×10^7 polonium alpha particles per cm^2. Two exposures were made on each plate, the photographic density of the second one, made just before development, serving as a control. Test plates developed in full strength Eastman D19 at 20° C for 2 min.

swelling of the gelatin, as direct immersion of the emulsion in distilled water for 1 hour causes only a 6 per cent loss in photographic density after drying and development. This behavior suggests the occurrence of a simultaneous oxidation process. The fading rate is further augmented by introducing small concentrations of hydrogen peroxide into the water above which the plates are stored. After 4 hours' exposure above 3 per cent hydrogen peroxide the latent alpha-particle image is completely obliterated. After this treatment, desiccation of the plate restores the emulsion to its original sensitivity.

Mechanism of Spontaneous Fading. In her original description of the fading phenomenon Blau [B20] suggests that the alpha particles cause disturbances in the crystal structure of the silver

bromide which reach a maximum after initial passage of the projectile, and then, by a recrystallization effect, the original distortion diminishes and causes fading of the image on delayed development. LaPalme and Demers [L12] are of the opinion that fading should result in part from evaporation of active specks in the silver bromide crystals.

The pronounced acceleration of fading caused by traces of hydrogen peroxide suggests that this reagent might be an important factor in the spontaneous fading of track structures. Hydrogen peroxide is produced during the decomposition of water by alpha particles. Under normal conditions the emulsion contains about 5 per cent moisture. Calculations based on an assumption of a yield of one molecule of H_2O_2 per ion pair show that in the minute channel of 3.5×10^{-17} ml traversed by the polonium alpha particle a concentration of about 2 per cent H_2O_2 can be generated during the radiochemical decomposition of the water. On delayed development the hydrogen peroxide has opportunity to diffuse into the silver bromide grains. Colloidally dispersed silver is known to dissolve readily in hydrogen peroxide, and the fading is probably caused by resolution of the silver specks believed to constitute the latent image.

This mechanism is consistent with the higher rate of fading observed when the plates are stored in warm humid atmospheres. It also conforms to observations that fading is more pronounced in emulsions of high gelatin content. The proposed mechanism explains the greater stability of the latent alpha-particle image when the dry plate is stored in a desiccator at reduced temperature. The radiochemical behavior of other densely ionizing radiations on water has not been investigated, but it is possible that protons also furnish an appreciable yield of hydrogen peroxide, as this compound has been detected among the decomposition products of water irradiated by x-rays and beta particles.

Preservation of the Latent Image. The fading of the latent image does not enter as a significant factor during short exposures of sources of appreciable activity. The question arises, however, if a fading of the older tracks takes place in continuous exposures of long duration. Experiments with radioactive minerals emitting about 20 alpha particles per sec per cm^2 show that the photographic density of the image increases linearly during a period of over 2 months, if the camera is kept in a desiccator

charged with anhydrous calcium chloride. However, fading can be very serious in exposures made during the humid summer months, particularly when the flux of alpha particles is low and the plate is in contact with moist air.

The investigations of Lauda [L21] demonstrate that fading is reduced by storing the plate in an evacuated vessel. In practice this method is objectionable as under prolonged reduced pressure the gelatin dries excessively and the emulsion may peel away from the glass support. Also, when radioactive minerals are exposed under reduced pressure the diffusion of their emanations is accelerated, and the loss of radon or thoron upsets the computation of the radioactive metal content which is based on the assumption that all the members of the series are present in the polished surface in their equilibrium concentrations.

Controlled exposures demonstrate that, by storing the plate in dry air at atmospheric pressure and reducing the temperature to about 5° C, the high-concentration silver bromide emulsions such as Eastman NTA do not exhibit appreciable fading, even when the disintegration rate is as low as 20 alpha particles per cm^2 per day. In order to avoid reticulation of the chilled gelatin during development at 20° C, it is good practice to remove the desiccator from the refrigerator about an hour before the termination of the exposure. Under these conditions track fading is not appreciable at the end of 66 days, and it is probable that quantitative recording could be prolonged for even longer periods. The investigations of La Palme and Demers [L12] indicate that by storing the plates at Dry Ice temperature the latent image of the tracks persists for several months. The early work of Wilkins [W16] shows that photographic emulsions can be processed successfully even after their immersion in liquid air.

It is of interest in this respect that very low temperatures have no measurable influence on the stopping power of metals for alpha radiation. On the basis of von Weizsäcker's theory of atomic stopping power, a change of about 6 per cent per conduction electron is anticipated for aluminum when the temperature decreases from 300° to 20° Kelvin. In some recent experiments by Gerritsen [G9] no variation in the stopping power of aluminum and tin for polonium alpha particles was observed even when these metals were chilled down to liquid helium temperature.

In a more recent independent study of alpha-track fading by Faraggi and Albouy [F2a] a 10 per cent fading effect was observed

when Ilford-type C2 plates were stored on ice during a period of 90 days between exposure and development. In control plates stored at room temperature the developed tracks exhibited a 70 per cent reduction in grain density after only 8 days of delayed development. Using Eastman NTA plates stored at 0°, 20°, and 40° C, Lamb and Brown[L51] report a 10 to 40 per cent reduction in track count following a 46-day delay in development. The emulsions employed in these investigations contained their normal moisture content and the appreciably greater fading rates reported are attributable to variable quantities of hydrogen peroxide generated by the radiation. It is noteworthy that the rate of hydrogen peroxide production is catalyzed by the presence of halide ions in the irradiated water. A study of the phenomenon by Krenz[K25] shows that I^- is more effective than Br^- which in turn produces a higher yield than Cl^-. The fading rate observed in emulsions may, therefore, also be dependent on the extent to which excess soluble salts are removed during manufacture.

BACKGROUND ERADICATION

Within the limitations of the fading phenomena, nuclear-type emulsions record continuously the tracks of all densely ionizing radiations that traverse the plate. At the time of development the total track count exceeds the number of particles originating from the experimental source by a complex factor dependent on the age of the plate and the duration of the fading cycle under the conditions of storage. The recorded background radiation originates chiefly from radioactive contaminants present in the glass support and the components of the emulsion layer. The autoregistration of alpha-particle tracks originating from impurities in the glass backing was first noted in the early work of Taylor.[T10] It may be augmented slightly by variable amounts of radon and thoron, which diffuse readily through the cardboard boxes in which the plates are delivered. At sea level the track contribution by cosmic radiation is negligibly small.

Owing to fading during normal storage the population of tracks is usually below 500 per cm² of blank emulsion area. The blank correction is negligible in most radiochemical analyses where the radiation from the source contributes 10,000 alpha-particle tracks

per cm^2. In autoradiography the blank population is entirely negligible in comparison with the 10^7 alpha particles necessary for the formation of a visual image. However, in making measurements on feebly radioactive materials having an activity of the same order as the background, the variable blank population becomes an important factor in the interpretation of the net track count. The proper approach to this problem is to eradicate the accumulated background tracks prior to experimental exposure. While this procedure is more laborious than the mechanical resetting of the tally meter on a Geiger counter, it can be achieved by the following procedures:

Eradication by Oxidizing Solutions. The destruction of the latent image of densely ionizing particles by processing the emulsion with dilute solutions of oxidizing agents has been investigated by Perfilov.[P13] Using the fine-grained emulsions prepared by Zhdanov, Perfilov found that the background tracks can be destroyed by bathing the plates for 15 min at 15° C in aqueous chromic acid solutions containing 0.125 to 0.333 g of CrO_3 per liter. This pretreatment did not increase the subsequent rate of fading of incident alpha-particle tracks. In a continuation of these studies, Perfilov [P14] concludes that the emulsion does not lose its sensitivity to protons as a result of background eradication with dilute solutions of chromic acid or potassium permanganate.

Powell and collaborators [P34] have likewise found that, by employing more concentrated solutions of chromic acid, the background eradication is accompanied by desensitization of the plate to protons. Treatment of Ilford plates in 2 per cent chromic acid solution renders proton tracks very diffuse without destroying the sensitivity of the emulsion to alpha particles. This technique is serviceable in recording the tracks of densely ionizing particles in the presence of predominating neutron and gamma radiations.

Liebermann and Barschall [L33] have demonstrated that the fog background of optical-type emulsions can be removed by developing the plate before experimental exposure, and by destroying the developed silver by oxidation with dilute acid-permanganate. After washing and drying, the processed emulsions are serviceable as recording media for the tracks of densely ionizing particles. Richards and Speck [R6] have applied this method of eradi-

cation to the Eastman-type 548-O emulsion. After this oxidization procedure these plates become desensitized to alpha particles but record tracks from the fission fragments of uranium.

The applicability of the Liebermann-Barschall method in the eradication of 100-micron-thick Ilford-type C2 plates has been investigated by De Felice,[D12] who showed that the oxidation alters the sensitivity of the emulsion. After eradication alpha tracks from uranium exhibited a 20 per cent reduction in grain density as compared with tracks developed in the untreated control plates.

These methods of background eradication are impractical when the emulsion is to be employed as a recording medium for low levels of alpha-particle activity. The reagents and wash waters must be specially purified in order to prevent adsorption of radioactive contaminants by the emulsion.

Eradication by Hydrogen Peroxide Vapor. In the studies of the factors controlling fading of the latent image it was demonstrated that the rate was greatly accelerated by exposing the emulsion to water and hydrogen peroxide vapors. This provides a convenient method of background eradication which avoids contact of the emulsion with solutions and thus minimizes radioactive contamination. The following procedure has proved effective:

The plates are stored at room temperature in an atmosphere saturated with water vapor containing traces of hydrogen peroxide. Slotted wooden boxes designed for the storage of 2 × 3-in. microscope slides provide a convenient housing for the eradication. The box and cover are impregnated with hot paraffin wax, and the floor is fitted with a slab of porous tile. The 3-in. plates, coated about 25 microns thick, are supported on edge by the grooves in the walls and rest about 5 mm above the tile on two glass-rod runners. The tile is saturated with full-strength 3 per cent U.S.P. hydrogen peroxide solution when rapid eradication is desired (3 to 4 hours). It is usually more convenient to eradicate the plates by overnight exposure to the vapors from a 0.1 per cent hydrogen peroxide solution. Prior to experimental exposure, sensitivity is restored by placing the slides in a large desiccator and passing a stream of dry air through it for about one hour. When this procedure is applied to emulsions 50 to 100 microns thick, peeling may occur, and the rate of air flow should be reduced to avoid excessive drying.

In making overnight eradications it is essential to reduce the concentration of hydrogen peroxide in the solution. After 18

hours above a 3 per cent solution the sensitivity of the emulsion is reduced, and alpha-particle tracks developed from subsequent exposure exhibit increased mean grain spacing. The tile should be examined periodically for the presence of mold. Mold has been observed to develop in the enclosed box during the summer months. On one occasion, when some unused plates were left in the eradicator box for several days, a mold growth was detected on the emulsion itself. This is particularly noteworthy as an apparent exception to the well-known oligodynamic effect of silver compounds on the growth of microorganisms.

Emulsions subjected to this eradication procedure exhibit a residual alpha-track population of 0 to 3 per cm^2 if developed immediately after drying. These residual tracks are probably formed during the drying period as the plate regains its sensitivity. If a series of eradicated and dried plates is stored in a desiccator at 5° C, and individual members are developed successively, the population of single tracks and alpha-ray stars increases linearly with time. The population of single tracks accumulates at a rate of about 8 to 80 per cm^2 per day. The rate varies with emulsion purity and thickness. The minimum rate was observed in a special emulsion coated on a cellulose acetate backing. This indicates that a substantial proportion of the tracks originate from radioactive impurities in the glass support. The alpha-ray stars originating from the successive decay of members of the thorium series accumulate at a rate of about 0.3 per cm^2 per day in emulsions 40 microns thick. The method of eradication does not interfere with the development of the normal background fog. These fog grains define the upper and lower surfaces of the gelatin layer, and their presence is essential in reconstructing the orientation of the particle trajectory in the original emulsion layer.

LIMITING SENSITIVITY

The rate of background-track accumulation is reconcilable with the presence of about 10^{-12} part of radium in the glass backing, and about 2×10^{-7} g of thorium per ml of emulsion coating. Though the precise values may vary somewhat in emulsions of different manufacture the lower limit of quantitative track-counting methods is set by these low levels of internal

contamination. The presence of thorium in the gelatin is indicated by the formation of alpha-ray stars with component track lengths corresponding to the ranges of members of the thorium series. If radium is present in the emulsion, it will also give rise to multibranched stars, but, owing to the aggregation of radium sulfate as insoluble radiocolloids, the bulk of this element is probably removed during the clarification of the gelatin.

Studies on track growth in eradicated emulsions coated on glass plates show that a background growth of 20 to 60 tracks per cm^2 accumulates per day as a result of autoregistration. The impurities giving rise to the tracks are distributed fairly uniformly, and the population of background tracks counted on one portion of an emulsion serves as a correction factor on measurements made on adjacent portions cut from the same plate. Emanations in the laboratory air and radioactive constituents present on the walls of the supports and the desiccator may further augment the blank alpha-track population. These external contributions can be reduced by careful attention to detail:

The traces of radon and thoron can be displaced by passing a stream of tank nitrogen through the storage vessel. Plastic materials exhibit a lower alpha-track count than wood or metals and are employed advantageously in the construction of clamps and supports for the emulsion. The effective alpha-ray activity is limited to the surface of solids, and the rate of emission can be reduced materially by heavy coatings of purified paraffin. Desiccators in which highly emanating materials have been exposed retain a layer of active deposit and these vessels must not be employed for the exposure of samples of low activity. In the measurement of activities of about the same magnitude as the background, the alpha particles originating from the impurities in the desiccant must be taken into account, and uncovered emulsions must be located so that alpha particles from the calcium chloride cannot reach the plate. By proper attention to these minutiae the total blank population can, in general, be maintained below 100 tracks per cm^2 per day of exposure.

If the exposure is limited to 10 days, and a population of 500 tracks per cm^2 is set as a lower limit for reasonably accurate track counting, the commercially available nuclear-type emulsions prove to be recording media of extraordinary sensitivity. The data in Table 14 show that for long-lived elements, as samarium, a quantity as small as 10^{-7} g can be determined quantitatively in radiochemically purified films of Sm_2O_3 weighing 1 mg per cm^2. As the half-life of the element diminishes,

the sensitivity increases. In the measurement of polonium preparations, as few as 20,000 atoms of the element suffice for its determination. Under the stipulated conditions of exposure and source thickness, disintegration rates exceeding 4×10^{-22} per sec can be estimated. In a study of the Ilford Nuclear Research plates Broda [B44] also concludes that the method is extremely sensitive and states: "Limits of not more than 10^{-23} per sec can fairly easily be set to decay constants." In properly executed exposures in which the accumulated background is eradicated and fading of the latent image is inhibited, the nuclear-type emulsions permit the detection of alpha particles emitted from elements which disintegrate 100,000 times more slowly than thorium.

TABLE 14. LOWER LIMITS OF QUANTITATIVE ASSAY IN CARRIER FILMS WEIGHING 1 mg/cm²

Element	Disintegrations per g per sec	Carrier	Pure Element, g	Percentage of Carrier
Uranium	2.5×10^4	Fe_2O_3	9.3×10^{-8}	0.009
Thorium	2.7×10^4	$Ce(IO_3)_4$	3.0×10^{-7}	0.03
Samarium	89	La_2O_3	2.6×10^{-5}	2.57
Plutonium, Pu^{239}	2.3×10^9	LaF_3	1.0×10^{-12}	1.0×10^{-7}
Radium	3.7×10^{10}	$BaSO_4$	6.3×10^{-14}	6.3×10^{-9}
Polonium	1.6×10^{14}	Te	1.4×10^{-17}	1.4×10^{-12}

Chapter 5 · QUANTITATIVE ASPECTS OF THE ALPHA-PARTICLE PATTERN

Radioactivity is the least manageable of natural processes. It will not be hurried or controlled. Nature keeps the management of this particular department in her own hands.—J. W. Mellor, 1925

ALPHA-PARTICLE COUNTING

The nuclear emulsion records tracks of all alpha particles that enter the recording medium provided that their residual energy exceeds a minimum value. Although the tracks of minimum discernibility vary with the emulsion composition, sensitivity, and the microscopic resolution, it is unnecessary to consider the complex variation in ionizing power along the trajectory and the effective area of the counting chamber which are important factors in electronic counting instruments. This simplifies the translation of the microscopically determined track count into a disintegration rate, as each track irrespective of length corresponds to the emission of an alpha particle by the source.

The processed plate carries a record of the number of tracks and also exhibits their approximate line of incidence into the original emulsion. Since the horizontal projection of the tracks is observed microscopically, and it is not practical to tilt the stage when the population is high, the visual track length will vary between the full range and a small fraction thereof, depending on the initial angle of incidence. The appearance of alpha-particle tracks under varying obliquities is shown in Fig. 20. From purely geometric considerations particles entering the emulsion at right angles should appear dimensionless. However, after fixation the gelatin dries to a very thin layer and the vertical tracks become distorted, as shown diagrammatically in Fig. 48, Chapter 12. The visibility of these erect tracks is further enhanced, under dark-field illumination, by the light scattered from the compressed column of silver grains. With thin sources weighing less than 1 mg per cm^2, over 90 per cent of the particles

enter the emulsion with energies and orientation favoring optimum track visibility. Tracks of alpha particles that spent the greater part of their energy in traversing the source are the most difficult to discern because of their short recorded length.

Even with the greatest care in manufacture and processing minute artifacts reside both in and on the gelatin layer. Occasionally, they are rod shaped and may be confused, at first glance, with alpha-particle tracks. These artifacts are differentiated by their lack of grain structure and by the color of the light scattered under dark-field illumination.
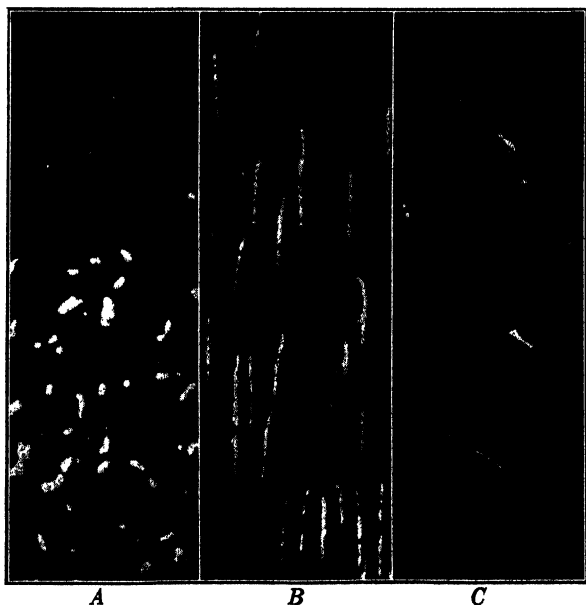
FIG. 20. Tracks recorded at varying angles of incidence. Dark-field illumination, 44× objective + 15× ocular; collimated RaF alpha particles.

A. Perpendicular incidence.

B. 45° incidence.

C. Oblique tracks of minimum discernibility produced by alpha particles traversing 3 cm of air before entering the emulsion.

Three primary sources can be employed in emulsion exposures. Two of these are common to all counting instruments, and the third is practical only by the unique properties of nuclear-type emulsions. The source may be a thin deposit of known weight

and area placed either in direct contact with the emulsion when the film is coherent, or situated a minute measured distance from it when the film is of powdery consistency. The sample may be an "infinitely thick solid" with its polished surface in direct contact with the emulsion. Finally, the source can be incorporated within the emulsion by allowing a measured volume of known concentration to evaporate on the plate. Each of these methods has its specific advantages and a set of special geometric considerations for the conversion of the track count into a disintegration rate.

It is advantageous to expose thin sources in direct contact with the emulsion in order to enhance track visibility. This is particularly important when the particles are ejected with low kinetic energy. The thickness of the film source is also governed by the disintegration rate and experimental difficulties of preparing and weighing exceptionally thin deposits.

The radiation emerging from a thick solid is composed of a large percentage of particles with reduced energy, and these sources are not conducive to precise track counting. Also, the effective range in solids must be computed from a relationship of approximate validity. This introduces an equal uncertainty in the equations connecting the track count with the rate of disintegration. The conversion factor becomes the more important the greater the film thickness, and is of maximum value for an infinitely thick solid. However, the information to be gained from measurements of the activity of individual segregates on the polished surface often compensates for the lower degree of accuracy.

The loaded-emulsion technique, when applicable, has certain marked advantages, such as ability to distinguish between single and multiple disintegrations. Since the source is disseminated ionically within the emulsion the majority of the tracks are of full energy. The technique also permits the visualization of the mechanism of nuclear reactions, the identification of the ejected particles and provides an estimate of their energies.

In the formulation of equations correlating track count with the number of disintegrations in the source, the following symbolism, more or less standardized in other counting methods, is adopted:

L = length in cm of a rectangular source.
W = width in cm of a rectangular source.
h = height in cm subtended by channel in the ocular scanning disk.
m = total mass of source in grams.
A = total area of source in cm^2.
d = density of source in g per ml.
t = time of exposure in min.
$\bar{R}$ = effective mean range of alpha particle system in dry air at 15° C.
τ = thickness of source in equivalent air-cm.
l = distance between source and emulsion in air-cm.
ρ = track length in air-cm of minimum discernibility.
C_L = number of tracks in a complete traversal along a line parallel to L using a slit h cm high.
$\bar{C}_L$ = average of a series of parallel traversals.
n_r = total number of tracks recorded during exposure.
δ = number of disintegrations in the source during exposure.
T_α = number of alpha particles escaping per second from unit surface area of an infinitely thick solid.
P = recorded population of tracks per cm^2 of emulsion surface.

THIN SOURCES

A radioactive source is considered thin when its effective thickness τ is less than $\bar{R}$. The mechanical thickness or weight per
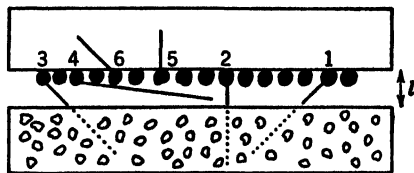
FIG. 21. Track registration from external thin sources. Showing powder film on glass backing separated from emulsion by a small air gap l. This clearance is provided by narrow cardboard or metal spacers 0.05 cm thick.

unit area varies with the permeability of the carrier but will in general reside below 2 mg per cm^2. Consider a uniform rectangular thin source separated by a small air gap from the recording emulsion as indicated in Fig. 21. Alpha particles origi-

nate from all points in this source and are directed at random towards the emulsion or into the support. Alpha particles 1, 2, and 3 will record tracks in the emulsion, whereas particle 4 originating from the bottom of the source and making a small angle with it will be absorbed internally and, like alpha particles 5 and 6, will not be recorded. Geometric considerations, the details of which are discussed by Evans[E11,14] in conjunction with the alpha pulse counter, show that:

$$\delta = \frac{2n_r}{1 - \frac{\tau + 2l}{2(\bar{R} - \rho)}} = n_r k_w \tag{16}$$

It is evident from equation 16 that l is an important factor in governing the proportion of alpha-particle tracks recorded by the emulsion. When compact films prepared by the Parlodion method are employed, l is reduced to zero, making the conversion factor k_w smaller, and enhancing the visibility of the tracks. The effect of varying l on the value of k_w is exhibited in Table 15 for several of the more common carriers.

TABLE 15. EFFECT OF AIR-GAP VARIATION ON CONVERSION FACTOR (Films weighing 1 mg/cm²)

Compound	U_3O_8	PbO_2*	Sm_2O_3
ψ	13.7	13.0	11.2
τ in air-cm	0.228	0.241	0.279
$(\bar{R} - \rho)$	2.09	3.00	0.29
	k_w	k_w	k_w
No gap ($l = 0$)	2.11	2.08	3.76
0.05 cm gap	2.17	2.12	5.77
0.10 cm gap	2.23	2.16	11.5

* PbO_2 film carrying RaD + E and RaF in equilibrium. The alpha particles from RaF are under consideration.

If it were possible to scan the entire emulsion and count each individual track no further computations would be involved. This is not a practical procedure with sources of appreciable dimensions, and n_r must be determined indirectly by a restricted count on representative areas of the emulsion. The tracks are distributed at random, and, when l is about 0.05 air-cm, 98 per cent of the tracks are confined to an area of the same dimen-

sions as the source. The distribution of the tracks can be visualized from considerations on a point source held slightly above the emulsion. The emission of alpha particles is statistically the same for any one direction, but the track population at a given point in the emulsion varies inversely with the square of the distance from the source. As a consequence, the bulk of the tracks concentrate in the immediate vicinity of the point source. When the source is of finite dimensions, the additive result of the constituent point sources is the production of a densely populated core surrounded by a penumbra with a low track population. To include all tracks, the stage is set a short distance beyond the densely populated core, and a complete traversal is made tallying all tracks C_L between the starting point and the corresponding position at the opposite end of the slide.

Studies of the track distribution along a path parallel to L and centered with respect to the source shows that the population is inappreciable at the initial and terminal points. The instantaneous population at any one point along L exhibits marked fluctuations from the mean. These fluctuations are typical of all radioactive measurements and tend to average out to a nearly constant value per complete traversal when a sufficiently large number of tracks is tallied. The total track count along different paths is constant, within the limitations of the statistical fluctuations $\pm\sqrt{C_L}$, except for the paths adjoining the extreme edges of the source.

As the gap between the source and the emulsion diminishes, the extension of the sampling plateau increases and reaches a value approximating W when both are in direct contact. Horizontal counts through the plateau region are proportional to the total number of particles directed towards the emulsion. When the air gap does not exceed 0.05 cm, and the source is 20 mm wide, the plateau extends for 5 mm on each side of the center line. The fluctuations in C_L in a series of counts through the central 10 mm of the emulsion are exhibited in Table 16. In exposures with external powder films the uncertainty in $\bar{C}$ is ± 2.3 per cent. When the counts are made on a uranium-loaded emulsion, as in analysis B, the track distribution is more uniform, and the counting error is reduced to ± 1.2 per cent.

The tracks are counted under dark-field illumination using a $44\times$ dry objective whose aperture is reduced by suitable dark-

TABLE 16. TRACK-COUNT FLUCTUATIONS

Exposure	A			B		
Source	External Film of U_3O_8			Emulsion Loaded with $(UO_2)^{++}$		
Gap	0.05 cm			None		
	C_L	$(C_L - \bar{C})$	$(C_L - \bar{C})^2$	C_L	$(C_L - \bar{C})$	$(C_L - \bar{C})^2$
	319	+23	530	235	0	0
	305	+9	81	249	+14	196
	289	−7	49	220	−15	225
	311	+15	225	239	+4	16
	320	+24	575	240	+5	25
	301	+5	25	241	+6	36
	275	−21	440	233	−2	4
	255	−41	1680	237	+2	4
	305	9	81	234	−1	1
	282	−14	196	220	+15	225
	2962	168	3882	2348	64	732
σ *	±6.58			±2.86		
$\bar{C}$	296 ± 7			235 ± 3		
Percentage Error	2.3			1.2		

* $\sigma = \pm\sqrt{\dfrac{\Sigma n(C_L - \bar{C})^2}{n(n-1)}}$, in which n represents the number of traversals.

field stops.* For track-counting purposes, ample illumination is secured with standard substage condensers provided with a dark-field disk. The tracks are counted in a restricted area of the microscope field with the aid of ocular diaphragms. An opaque disk, such as illustrated at A in Fig. 22, facilitates counting as it reduces eye shifting and prevents distraction by other occurrences in the microscope field. The mechanical height of the channel resides between 3 and 6 mm, the selection depending on the track density. When the magnification is about 500× the distance subtended on the emulsion is of the order of 0.01 cm. Its exact value h is determined with a stage micrometer or prefer-

* The reduction of the aperture is of paramount importance in quantitative track counting. It increases focal depth so that all tracks, irrespective of their position in the gelatin layer, are brought into view with one focal setting. When the exposure is made with an external source the tracks reside close to the upper surface of the gelatin. In loaded emulsions, the tracks are usually distributed throughout the entire thickness of the gelatin, and with a sharply focusing lens the tracks outside the focal plane may escape detection.

ably with the aid of a ruled grating containing 10,000 lines per in. As each track enters the channel it is recorded on a hand tally of the type commonly employed in counting dust particles or blood cells. When a track is partially obscured by the frame, it is given a full count provided a sufficient length is visible in the channel to permit its recognition as a track. In counting alpha-ray stars, as in emulsions loaded with thorium, the ocular may be rotated to a position where the multiplicity
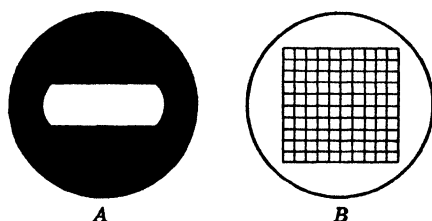
FIG. 22. Ocular disks for track counting.

A. Metal disk with narrow channel for continuous traversals.
B. Glass disk with ruled net for track counting in a fixed area of the emulsion.

of the event is in complete view and may then be brought back to its original position with the aid of markings on the lens and microscope tube.

The number of tracks recorded on the emulsion is evaluated from the average count $\bar{C}$ by the relationship:

$$n_r = \frac{\bar{C}W}{h} \tag{17}$$

The disintegration rate is expressed by:

$$\frac{\delta}{60tm} = \frac{\dfrac{2n_r}{60tm}}{1 - \dfrac{\tau + 2l}{2(\bar{R} - \rho)}} \text{ sec}^{-1} \text{ per g carrier} \tag{18}$$

When the source is deposited as a circular film of radius r, the total number of recorded tracks $n_r = \pi Cr/2h$. It is difficult to establish the exact center of a low-population circular field of tracks. Also, the conventional mechanical stage permits con-

venient sampling along only one major diameter. Because of these limitations, rectangular-shaped sources are advantageous in quantitative track counting.

When the source is 5 cm long a single traversal can be made in about 5 to 15 min, depending on the relative abundance of the tracks. The exposure should be adjusted so that the count per traversal does not greatly exceed 500. In the analysis of samples of unknown activity the first exposure is necessarily a guess. Its misjudgment can be corrected over a narrow range by altering the dimensions of the counting channel. When the emulsion is greatly overexposed, the stationary field method of counting described in the following section will yield an approximate value adequate for the calculation of a suitable exposure period. In traversing the identical path different observers usually check within ±1 per cent. The discrepancy resides in the judgment of tracks of minimum discernibility and their confusion with occasional configurations of fog grains that simulate a short track.

The magnitude of the total track count is governed by the degree of precision sought in the analysis. Almost all carrier fractions are of somewhat uncertain purity, and a precision exceeding 3 per cent is seldom justified. By counting 1500 tracks the statistical uncertainty will be below 3 per cent. A simple count of this magnitude can be made by an experienced observer in about 30 min. If the fluctuation error must be kept below 1 per cent, as is necessary in the determination of the decay constants of purified carrier-free radioelements, more than 10,000 tracks must be counted. This is an arduous task. The eye should be allowed to rest between traversals, and the color of the illumination should be altered occasionally by placing suitable filters in the optical system.

In counting tracks from feeble sources it is necessary to correct for the background tracks arising from impurities in the emulsion. In analyses of this type the center portion of a 9-in. plate serves as a monitor for background growth, and the adjoining end portions of the plate are employed in the experimental exposure. If the blank count is C_b, and the total count produced by the sample and background is C_t, then the probable error of the determination is:

$$\frac{0.6745\sqrt{C_t + C_b}}{C_t - C_b}$$

Using background-eradicated plates and an exposure of 100 hours, traversals of 0.1 cm^2 area may yield typical counts of $C_b = 10$ and $C_t = 50$ in a sample of low activity. The uncertainty of the count is over 13 per cent. By increasing the areas surveyed 10-fold, the uncertainty is reduced to 4 per cent. In order to maintain the statistical uncertainty below 3 per cent, over 1000 tracks must be tallied on the sample plate and 200 tracks on the monitor.

The smallest track length detectable by a particular emulsion and system of microscopy is best determined experimentally. A
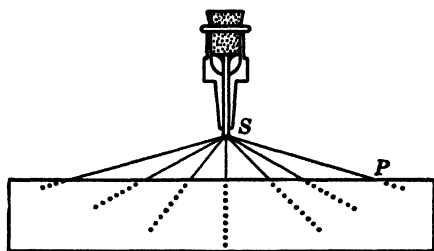
FIG. 23. Point-source exposure for determining track length of minimum discernibility.

non-collimated point source of polonium is supported a measured distance of about 5 mm above the center of the plate and exposed for about 1 hour. The exposure is made inside a desiccator, and the temperature and pressure of the dry air are noted. On development, directly beneath the source a dark spot is produced, whose visual blackening gradually diminishes over a radius of several millimeters. Two fine lines are scratched on the gelatin, intersecting at right angles through the center of the black circle, and this point is located under the microscope.

As the slide is moved away from the center the number of tracks per field and their length diminish, and a point P is reached where only short tracks are recorded, just distinguishable from the fog background. At this point the alpha particles enter the emulsion at small angles to the plane of the emulsion, and their horizontal projection is practically identical with their full lengths. To translate the residual track length into equivalent air-centimeters, calculate the distance SP of Fig. 23 as estab-

lished by the stage setting and the height of the source, and reduce this to an equivalent length at 15° C and 760 mm Hg pressure. In the Eastman NTA emulsion the tracks of minimum discernibility measure 0.84 ± 0.07 air-cm when examined under dark-field illumination at a magnification of 500×.

Electronic instruments employed in counting alpha-particle pulses respond to rays with a residual air range of 0.5 cm. Tracks of even smaller residual range, such as 0.3 air-cm, can also be differentiated from the background fog by examining the emulsion at 1000× using oil-immersion objectives of high numerical aperture. This procedure, however, is not practical in counting numerous tracks owing to the restricted depth of focus.

In exploring a heterogeneous field of tracks, such as results from a normal non-collimated large-sized source, the eye becomes accustomed to the longer tracks produced by the more energetic alpha particles, and the inexperienced observer may miss a small fraction of the shorter tracks. It is good practice to examine a field of minimum-energy tracks, under the same optical conditions employed in the counting, and to make note of the length and brilliance of these end-point tracks.

THICK SOURCES

A source is considered "infinitely thick" when its mechanical thickness exceeds the effective range of the system of alpha particles generated within the solid. In the evaluation of the number of alpha particles escaping from the surface of a thick source, it has been demonstrated by Evans [E14] that:

$$n_r = \frac{Nu(\bar{R} - \rho - l)^2}{4(\bar{R} - \rho)} \tag{19}$$

In this relationship N is the rate of production of alpha particles per unit *volume* of solid, and u is the ratio of the ranges in the solid to that in air. In direct contact autoradiography, $l = 0$, and u is expressed by $0.0003194\psi/d$, hence equation 19 simplifies to:

$$n_r = \frac{N}{4} \times 0.0003194 \frac{\psi}{d} (\bar{R} - \rho) \tag{20}$$

Converting to a rate of emission per gram of solid yields as the final relationship for the number of tracks recorded per second per square centimeter of emulsion:

$$T_\alpha = 7.985 \times 10^{-5}\psi M(\bar{R} - \rho) \qquad (21)$$

When the radioactive constituents are distributed uniformly throughout the polished surface the tracks can be counted by the continuous traversal method. More often, the surface exhibits complex segregation, and the continuous method of counting is
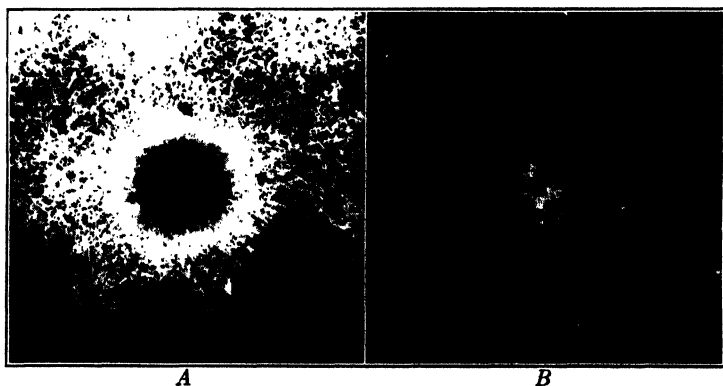
Fig. 24. Radiocolloid aggregate observed in a polished section of altered pitchblende from Cornwall, England. Dark-field photomicrographs at 110×, dual exposure technique.

A. Detail from visual image produced by 41-hr exposure. The high track population at core results in a very dense silver deposit which appears black under dark-field illumination.

B. Identical area, with lower track population resulting from a 15-min exposure. The number of tracks is countable when the area is examined at higher magnifications.

applicable only if a rough average value of the activity suffices. The principal advantage of the polished-section technique, however, resides in its ability to differentiate the variable activity of minute segregates. The track count per segregate is effected by locating the precise area on the emulsion and counting the number of tracks per unit area in the field. When the segregates exceed 1 mm in diameter, several stationary counts can be made, and the average represents a measure of the alpha-particle activity of the particular inclusion.

With the aid of a ruled ocular disk similar to *B* in Fig. 22 up to 200 tracks per field can be counted conveniently. A suitable track population is produced by a comparatively brief exposure, whose duration is dependent principally on the magnitude of *M*, the specific activity per gram of solid. In general, it is convenient to make two exposures on the same plate to facilitate the location of the tracks from a particular segregate. The initial exposure is prolonged until about 10^7 tracks per cm^2 are recorded, followed by a second exposure adjusted for the registration of about 5×10^4 tracks per cm^2. The long exposure produces a visual image of the segregates whose photographic density is an approximate measure of their activities. The second adjacent exposure has a track population that can be estimated microscopically at about 500× magnification. The dual exposures are made by the methods described in Chapter 3, the part on microscopy of radiographic patterns, section entitled Examination of Macro Images. The appearance of autoradiographic and countable exposures is exhibited in Fig. 24, as observed in a study of radiocolloid aggregates in a polished section of pitchblende.

As indicated in Chapter 3 the absolute surface of a polished specimen is not identical with its geometric area. In comparing the activity of different specimens the surfaces should have the same mechanical finish. Radioactive inclusions containing radium or thorium X may lose a fraction of their equilibrium emanations during the mounting and polishing procedures.

Comparative exposures between freshly mounted and aged polished specimens show that the track count is generally lower when the specimen is exposed immediately after its preparation. Using a compact crystal of thorianite containing 74.8 per cent Th and 8.1 per cent U the track count increased 5 per cent when a second exposure was made 1 month after the mounting of the mineral. Since it is often not practical to delay exposure until equilibrium is reestablished the T_α value of recently prepared radioactive mineral sections will tend to be lower than that calculated from equation 21. The loss in activity of grains in the same polished section is usually of about the same order of magnitude, and the resultant track counts present a fair measure of their relative activities. Measurements by Johnson [J1] show that cellulose acetate films only 0.05 air-cm thick are completely impervious to radon or thoron. This suggests that, by coating the polished surface with a thin layer of lacquer, the emanations can be retained with but little loss in the number of emergent alpha particles.

LOADED EMULSIONS

Gelatin is pre-eminently a substance with a history; its properties and its future behavior are intimately connected with its past.
—C. E. K. Mees, 1946

The atomic composition of the emulsion is controlled essentially by the relative proportions of silver bromide and gelatin. The composition of several emulsions which have been employed at different times in nuclear physics research are collected in Table 17. The constituents of low atomic weight such as hydro-

TABLE 17. ATOMIC COMPOSITION OF NUCLEAR EMULSIONS

Relative Number of Atoms

Emulsion Type	Ag	Br	H	C	N	O	S	Data
Agfa K plate	1	1	15	9.6	2.8	3.5	0.1	Wambacher[W4]
Ilford Halftone	1	1	15	10.2	3.1	3.9	0.1	Choudhuri[C13]
Ilford Nuclear Research	1	1	3.2	1.6	0.34	0.87	0.025	Ilford Co.
Eastman Fine-Grain Alpha	1	1	10	6.1	1.9	2.3	0.03	Yagoda[Y17]
Eastman NTA	1	1	2.5	1.5	0.46	0.56	0.008	Yagoda[Y17]
Eastman NTA and NTB *	1	1	2.68	1.62	0.50	0.69		Eastman Co.
Eastman NTC *	1	1	6.38	3.83	1.17	1.62		Eastman Co.

* The composition given by the Eastman Co. is expressed on the basis of an absolutely dry emulsion. When the plates are stored in an atmosphere of 50 and 70 per cent relative humidity, the emulsion contains an additional 2.2 or 4.0 per cent water content, respectively. This water pickup is equivalent to 4.5 or 8.0 weight per cent of the original dry emulsion, depending on the conditions of storage.

gen, nitrogen, and carbon are present in greatest proportion in terms of available nuclei. External sources of radiation can interact with these light nuclei, and the emulsion will record the tracks of the ejected densely ionizing fragments. Thus, fast neutrons will record proton tracks as a result of elastic collision with hydrogen nuclei. Slow neutrons cause the registration of short proton tracks arising from the $N^{14}(n, p)C^{14}$ nuclear reaction. Collision of energetic alpha particles with constituent hydrogen atoms may also record proton tracks, but more often

they will be obscured by the preponderance of alpha-particle tracks.

The nuclear-type emulsions can be employed advantageously in the study of other nuclear reactions when an adequate number of target nuclei are incorporated into the gelatin. The ions can be incorporated by adsorption, evaporation, or during manufacture of the plates.* Emulsions of this type are commonly referred to as "loaded." The term is somewhat misleading, as only a small concentration of foreign nuclei can usually be incorporated without danger of destroying the sensitivity of the emulsion.

The loading technique has received its chief application in the study of the cross sections of nuclear reactions involving the emission of heavy charged particles. The methods employed in the study of neutron flux densities, fission rates, and mechanisms are described in Chapter 12. Radioactive atoms can also be incorporated for the study of their alpha-decay rates. This procedure is advantageous, as very nearly all disintegrations are recorded by full energy tracks. The question of alpha-particle absorption within the source does not arise as the sample is dispersed ionically. When the daughter elements, produced from an initial disintegration, also decay by alpha-particle emission, the event is recorded as a multibranched star. The loaded emulsion is also employed advantageously in the study of radiocolloid aggregation in dilute solutions.

Loading by Adsorption. Loading is commonly effected by soaking the plate in a solution of the desired ions for about 5 to 30 minutes, followed by a rapid rinse in water and drying in dust-free air. The atoms are thus dispersed uniformly throughout the plane of the emulsion. The concentration adsorbed is a complex function of a considerable number of variables, and it can only be anticipated approximately from a knowledge of the

* The Ilford Research Laboratories will, on special order, incorporate 0.031 g Li, 0.0079 g Be, 0.045 g B, or 0.27 g Bi per ml of their stock C2 emulsion. The C2 emulsion contains 5 ml of glycerine added as a plasticizer per 30 g of air-dry gelatin and 190 g of silver halides. In laboratory loading operations of C2 plates part of the glycerine may be lost by diffusion into the reagent bath. The glycerine is further extracted during photographic processing, and its volume must be corrected for in estimating the emulsion thickness from microscopic measurements of the residual gelatin film (see Chapter 12).

solute concentration, pH, temperature, and time of immersion. The exact quantity adsorbed must therefore be determined by chemical analysis of a portion of the loaded emulsion. When the pickup is appreciable the quantity adsorbed may also be approximated by the following procedure:

A cardboard tray with dimensions somewhat larger than the plate is rendered waterproof by impregnation in molten paraffin. An accurately measured volume of the loading solution is delivered into the tray and the plate is immersed for 30 min. The residual solution is transferred quantitatively to a beaker; the tray is rinsed with distilled water. The quantity of unadsorbed material can then be determined by a suitable colorimetric or volumetric method of analysis for the element in question. The amount adsorbed by the emulsion is obtained by difference.

Evaporation Technique. The emulsion can also be loaded by delivering a measured volume of known concentration to the surface and allowing the solution to evaporate to dryness. The weight of the material is thus known exactly, but there may be some doubt as to the uniformity of deposition throughout the emulsion thickness. It is advantageous to incorporate a volatile solvent like methyl alcohol into the loading solution. A mixture composed of 7 parts of alcohol and 3 parts of water can be spread more uniformly over the gelatin surface, and, once deposited, it evaporates faster than pure water. The alcohol also prevents the hydrolysis of certain heavy metal salts, such as samarium nitrate, which tend to form insoluble compounds in neutral aqueous solutions.

The solution is delivered on the emulsion, covering bare spots by coalescing adjoining drops with the pipette tip. An area of about 40 cm^2 can be wetted completely by 1 ml of the solvent mixture without danger of the solution's overrunning the edges of the plate. The emulsion dries in about 2 hours when supported over a desiccant. During this period there is opportunity for internal adsorption, but some surface concentration of the solute takes place, particularly when the solution is concentrated during the last stages of evaporation. This surface deposit introduces an element of uncertainty in the evaluation of the track-disintegration conversion factor. The method consumes a minimum of solution and is commendable in the study of specially purified or rare preparations.

Effect of Loading on Sensitivity. An important factor to consider in all quantitative work with loaded emulsions is the effect of increasing quantities of heavy-metal ions on the recording properties of the medium. This problem does not arise when carrier-free radioactive sources are incorporated into the emulsion, as the concentration must be kept low in order to avoid overexposure. Trial experiments with samarium and uranyl nitrate solutions show that 0.24 mg of either Sm_2O_3 or U_3O_8 per cm^2 can be incorporated in the Eastman NTA emulsion without altering its sensitivity to the alpha particles emitted in the decay of the respective elements. With the more active elements the concentration must usually be kept below 1 microgram per cm^2 in order to avoid an excessive track population.

Chromates and high concentrations of uranyl ions have a desensitizing action on the emulsion, and it is possible that a systematic investigation would reveal the presence of numerous other desensitizers. Since emulsions of different manufacture differ in the quality of the gelatin and in the relative abundance of sensitivity specks, it is good practice to test each lot of plates after loading to make certain that the operation has not destroyed sensitivity.

The investigations of Green and Livesey [G21] and Demers [D9] show that the loading operation in saturated solutions of uranyl acetate weakens or destroys the alpha-particle tracks from the decay of uranium. Experiments by Broda [B44] show that when the plate is soaked in a solution containing 14 per cent lead and 0.012 per cent uranium the emulsion becomes completely desensitized to alpha particles. In an investigation on the fissionability of lead and bismuth, Broda [B42] established that the presence of 0.082 mg of bismuth or 0.296 mg lead per cm^2 weakened, but did not obliterate, the tracks of fission fragments from admixed uranium. Caution must therefore be exercised in applying the loading technique to alpha-particle counting when the solution contains an appreciable concentration of heavy-metal carrier ions.

As a check on the sensitivity of the loaded emulsion, it can be covered with a normal control piece, providing an air gap of about 0.05 cm between the two emulsions. The dry impregnated plate serves as an infinitely thick radioactive solid, emitting alpha particles into the monitor plate. If the sensitivity of the loaded

plate is unaltered, the track counts on both plates will yield agreeing estimates of the concentration of the radioelement. Usually, when sensitivity is destroyed, the familiar microscopic background fog is absent. The presence of alpha-active constituents will, however, be indicated by the presence of tracks on the superimposed monitor plate.

Certain constituents may have a beneficial effect on the sensitivity. According to Perkins[P17] fading of the latent image is reduced in emulsions loaded with borax. Experiments with borax-loaded NTA plates[Y18] show that it is difficult to eradicate the latent image by the usual exposure to hydrogen peroxide vapor. After 5 hours' treatment only a 20 per cent reduction in photographic density is effected, whereas in a control non-loaded plate eradication of the identical alpha exposure was complete after 3 hours. Borax combines with hydrogen peroxide to form a stable perborate, which may be a factor in the protective mechanism. In view of this behavior, however, the eradication process should precede loading.

The high-concentration silver bromide emulsions record the tracks of alpha particles during the loading operation. As a result of continuous registration during stages of variable stopping power, the track length and mean grain spacing of certain tracks recorded when the emulsion was wet will differ materially from those recorded in the normal dry state. Tracks of altered mean grain spacing are particularly noticeable when the element decays rapidly, and an appreciable track population is accumulated during the period of immersion. Alpha particles originating from layers of solution adjacent to the emulsion produce tracks of reduced length. These factors are not serious in exposures with the more stable elements, as the exposure must be prolonged in the dry state for several days and the population of the "wet" tracks is a small fraction of the total.

The range of the alpha particles emitted by actinium has been investigated by Vigneron.[V16] His technique is of interest as illustrating a general approach for rapid loading necessitated whenever the parent element decays rapidly and the daughter products are short-lived alpha emitters:

An Ilford-type C2 plate was immersed for about 1 min in a solution of actinium which had been purified from accumulated decay products 8 min earlier. Rapid drying was effected by dehydrating the loaded plate in 90 per cent alcohol for 2 min and drying in a stream of air. After 33 minutes' exposure in a desiccator the plate was developed for 5 min, and

track registration was terminated by the use of an acid stop bath. Under these conditions only a small percentage of the tracks were elongated, and among 800 actinium tracks only 40 radioactinium tracks were observed. The range distribution curve exhibited a fairly sharp maximum at 19.3 microns, which, by comparison with polonium tracks measured in a control plate, is equivalent to a range of 3.40 air-cm.

Depth Penetration. The extent of depth penetration varies with different ions and is also dependent on the nature and *p*H of the solvent. Westöö[W28] has observed that in plates loaded by immersion in 0.3 per cent thorium nitrate solution containing the associated equilibrium products the Th^{++++} and $RdTh^{++++}$ ions are confined essentially to the surface of the emulsion whereas the ThX^{++} and ThB^{++} ions penetrated into the lower depths. These observations were indicated by the presence of single alpha-particle tracks of range attributable to the decay of Th and RdTh nuclei only at the surface of the developed plates, whereas the interior exhibited stars stemming from the series decay of ThX and individual long tracks corresponding in range to the ThC and ThC′ alpha particles. By adjusting the acidity of the thorium nitrate solution with hydrochloric acid to 0.01 normal the depth penetration of the thorium ions increased. This was indicated by the registration of V-branched alpha stars initiated by RdTh with their centers a few microns below the emulsion surface. Substitution of absolute alcohol for water as the solvent reduces depth penetration, the position of the developed tracks indicating only a superficial adsorption of the thorium ions. Westöö attributes these results to variation in the swelling of gelatin, which is most pronounced in acid aqueous media, and to the relative degrees of hydration of the several metallic ions.

Ionium exhibits a similar behavior and tends to be adsorbed chiefly on the surface of the emulsion when the plates are loaded from neutral aqueous solution.[Y17] The problem of penetration is particularly important when the radioactive ions are to be identified by range measurements. It is necessary that a large proportion of the atoms decay within the emulsion in order that full-length tracks be recorded. In many instances adequate depth penetration can be secured by incorporating about 5 per cent acetic acid into the loading bath.

Loading Mechanism. The mechanism of the pickup of ions from solutions has been studied in considerable detail by Broda.[B43, 44] He employed Ilford C2 plates impregnated with uranium by immersion in solutions of uranyl acetate of variable concentration, acidity, temperature, and admixed solutes. The quantity of uranium adsorbed was determined from the population of alpha-particle tracks recorded by the test plate after a fixed period of exposure. These studies show that the velocity of uptake decreases rapidly with time of immersion and gradually approaches a saturation value. Broda observed that the absolute values of the uranium uptake exceed the values calculated from the volume of the dry emulsion. When the plates are immersed in 0.12 and 5.5×10^{-5} molar uranyl acetate dissolved in 5 per cent acetic acid, the uptake is 6.5 and 45 times greater than the imbibition volume of the emulsion. This indicates a definite adsorption mechanism in which the temporary expansion of the emulsion during impregnation is a minor factor. Further evidence favoring an adsorption mechanism was secured by studying the saturation uptake from solutions of varying concentrations at constant temperature. The track count, plotted as a function of ionic concentration, yields a curve similar in form to the well-known Freundlich adsorption isotherm.

The uptake under constant time of immersion varies with the temperature of the solution. Broda's data show that an increase in temperature from 3° to 32° C causes a 3-fold increase in the quantity of uranium adsorbed. In 5 per cent acetic acid media the uptake decreases, with diminishing uranium concentration, as follows:

Per cent U in solution	2.9	0.062	0.0062	0.0013
mg U per cm² of emulsion	0.33	0.016	0.0025	0.0009

The time spent in rinsing the plate with water does not alter the final uptake appreciably. However, if the loaded emulsion is bathed in 5 per cent acetic acid most of the uranium can be washed out.

Broda's investigations demonstrate clearly that loading is essentially an adsorption process. As such, the quantity adsorbed will depend on the relative proportions of silver bromide and gelatin, the particle size of the grains, and the thickness of the

emulsion layer. Available data, secured with a particular emulsion, are therefore only a rough guide to the probable pickup by plates of other manufacture. In loading emulsions by immersion in solutions of different composition the uptake must be studied for each particular system in order to define conditions which will yield the desired concentration.

During immersion the gelatin swells as the result of the imbibition of water. It is desirable to keep swelling at the minimum in order to reduce mechanical strain of the emulsion. Under adverse ionic environment parts of the emulsion may enter solution or even float off the backing. The effect of different compounds on the swelling of gelatin by water is well known from the classical studies of Hofmeister. His results may be summarized by stating that, for a given metallic cation, sulfates, citrates, tartrates, and acetates produce less swelling than chlorides, nitrates, or bromides. Thiocyanates and iodides should be avoided as they promote swelling and bring about an actual solution of the gelatin. When the atoms to be incorporated are available only in the form of anions, the lithium or sodium salts will tend to produce less swelling than the potassium or ammonium compound. Mineral acids and alkalies hydrolyze the gelatin, and their presence in the bath must be reduced to a minimum.

Geometric Considerations. When a radioactive source is incorporated in the emulsion for purposes of quantitative assay, it is difficult to evaluate the precise value of the factor converting the recorded track count into a disintegration rate. Atoms located in the center of a thick emulsion are in a favored position, and each disintegration records a track. Ions adsorbed in planes close to the air or glass interface record tracks only when the alpha particle is directed through a length of emulsion sufficient for the registration of a track of minimum discernibility. If it is assumed that the atoms are distributed uniformly throughout the thickness of the emulsion layer J, expressed in equivalent air-cm, then the total fraction of all disintegrations failing to record discernible tracks is $\rho/2J$. In emulsions 25 microns thick, this factor amounts to about 9.4 per cent when ρ is 0.84 air-cm, making $\delta = 1.10n_r$. This favorable counting geometry can be augmented by employing emulsions of greater thickness, but the track counting is rendered more difficult.

The emulsion thickness is not constant in different plates of the same package. In manufacture, the emulsion is poured on a single large sheet of glass. After setting, the center portion tends to be thicker than that along the periphery. When the master plate is cut, the thickness of individual test plates may vary by 30 per cent. The thickness of a particular test plate can be closely approximated by microscopic measurements on the two adjoining end pieces from which the test portion is cut. The mean of these measurements is representative of the average thickness of the center portion employed in the exposure. The emulsion thickness can also be estimated after its development from microscopic measurements of the thickness of the residual gelatin, allowing for the volume of the extracted silver halides, as described on p. 257.

In emulsions loaded by evaporation the layer adjoining the air interface may contain a higher proportion of the sample than the interior, causing a diminution in the value of the recording factor. The track-disintegration conversion factor can be determined experimentally by evaporating on a test emulsion a solution containing about the same concentration of carrier as the sample and a known quantity of uranium. The track population recorded by this monitor furnishes a conversion factor for the particular system by comparison with the known rate of uranium disintegration.

Heterogeneous Loading. An ingenious modification of the loading technique has been described by Demers.[D5,6] A thin layer of an insoluble compound of the radioelement is deposited on the surface of the emulsion and is recoated with a second layer of gelatin-silver bromide. A track-disintegration conversion factor of unity is thus achieved. The method is of particular interest in the registration of fission tracks from uranium, as the film of insoluble ammonium uranate, constituting the source, delineates the point of track origin and permits measurements of the ranges of both fission fragments. The method should prove applicable in measuring the fissionability of other heavy-metal nuclei, employing compounds like lead sulfate or thallium bromide. Since these insoluble compounds are not in solid solution there is less danger of the emulsion's losing its sensitivity.

By moistening the plate with water, minute fragments of minerals or coarse powders can be embedded in the gelatin. Insoluble grains remain fixed after photographic processing and are readily located during the microscopic examination of the plate. By focusing into the gelatin layer, radioactive fragments

decaying with the emission of alpha particles are readily identified by a halo of radiating tracks as illustrated in Fig. 25. This
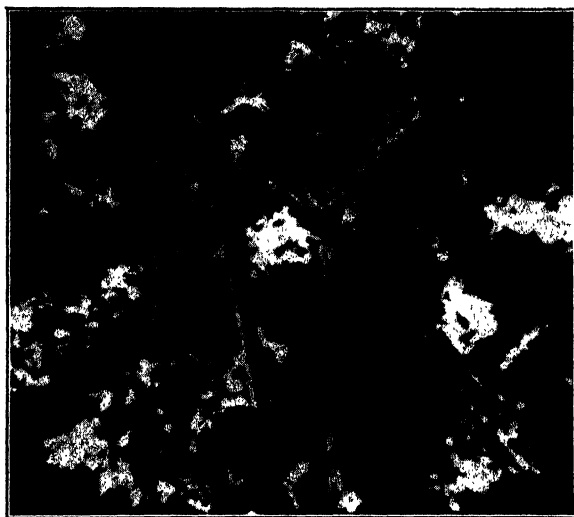
FIG. 25. Heterogeneous loading. Ash from aquatic plants sprinkled on emulsion exhibiting concentration of alpha activity in select fragments. Dark-field illumination, magnification 430×. This technique is particularly useful in testing feebly radioactive insoluble materials, as the direction of the tracks from the microscopically visible fragment eliminates possible confusion with occasional background tracks. The track-registration factor can be doubled by mixing the test powder with molten emulsion at 35° C and spreading a layer over the surface of a nuclear-type plate.

elegant method for the discrimination of radioactive and inert grains of microscopic dimensions has been applied by Tyler and Marais [T24] in the study of radioactive soil constituents.

Chapter 6 · RADIOCHEMICAL STUDIES WITH NUCLEAR EMULSIONS

We may esteem ourselves fortunate that the detection of non-radioactive substances is less sensitive than that made possible by the radioelements. If we could see how many nuclei of dirt, dust, and disease are contained in the air we constantly inhale, we might be terrified and hardly dare to breathe. Nature in her wisdom has arranged matters so that in the course from the ponderable to the imponderable the limits of visibility coincide approximately with the limits of weighability. Let us be thankful that it does not reach down to the individual atoms!—Otto Hahn, 1936

INTRODUCTION

In studies of radioactive systems containing atoms that decay with the emission of alpha particles the nuclear emulsion serves as a continuously recording counter. As such, the medium is a simple and inexpensive tool for measuring the activity of both highly radioactive and feeble sources isolated in the course of radiochemical analyses of uranium, thorium, and samarium compounds, and of preparations containing the transuranium elements. It affords an elegant means for determining the distribution of incorporated alpha-ray tracers in biological and metallurgical systems, and permits the visualization of the spatial distribution of certain trace elements in synthetic single crystals. The method finds application in the laboratory study of radiocolloid aggregation and in the detection of these bodies in altered minerals, in synthetic crystals, and in the capillary structures of plant and animal tissue.

Considered purely as a counting device for alpha particles, the nuclear-type emulsions can be substituted for electrical counting instruments in the study of diverse phenomena. When serving simply as a counter the methods will be described briefly, as they are well known and do not, in general, require modification when the activity is measured photographically. Certain methods of autoradiography indigenous to the emulsion will be discussed in detail.

The densely ionizing alpha particle permits the visual detection of a single atom in the process of radioactive decay. Even with the limitations set by the radioactive impurities in the emulsion it is possible to detect and estimate imponderable quantities of radioelements. It is therefore of the utmost importance to avoid contamination of samples by the promiscuous use of apparatus and glassware that have been in contact with solutions of high activity. In designing a laboratory separate rooms should be devoted to problems concerned with the low activity of normal rocks or tissues, radioactive minerals, and radioactive concentrates. In laboratories where work of diverse character is in progress, the traces of dust and emanations from one room may cause the contamination of the others. As an example of such contamination, an occurrence described by Hahn bears repetition: On opening a vial containing a few milligrams of radium in the chemistry laboratory sufficient radon escaped into the atmosphere to be detectable in a Wilson cloud chamber operating in the physics section several rooms away.

Unlike the cloud chamber, whose visualization is evanescent, contaminated emulsions record tracks continuously and present at the time of development an integrated picture which may seriously confuse an analysis of a feebly radioactive preparation. In assembling polonium sources care must be taken to avoid contamination of benches and auxiliary apparatus. Thin cotton gloves should be worn during source preparation and the hands washed carefully immediately after its assembly. Contamination of fingertips is readily demonstrated by contacting them with an emulsion for about 10 min. The contact softens the gelatin slightly and registers a sharp fingerprint. On development alpha-particle tracks are observed on contaminated ridges. It is good practice to provide the darkroom with a supply of lintless paper sheets. All operations with the emulsion such as cutting, marking, and the assembly of the camera are made over a fresh sheet of paper.

ACTIVITY OF CARRIER FILMS

Of the naturally occurring radioelements only uranium, thorium, and samarium compounds can be separated pure in weigh-

able amounts from laboratory-size samples of radioactive minerals. Other elements of moderate half-life such as radium, ionium, protoactinium, and plutonium can be obtained in tangible quantities by large-scale plant operations. The majority of radioisotopes are short-lived and can be manipulated chemically only with the aid of an inert carrier substance which serves as a matrix for the unweighable quantities present in the sample.

Coprecipitation Mechanisms. The science of radiochemistry is devoted to the study of diverse coprecipitation, adsorption, and extraction processes which permit the separation and concentration of radioelements. On the basis of studies made between 1898 and 1913 Fajans formulated a precipitation rule in which the basic premise is that, the lower the solubility of the compound formed by the metallic radioelement with the anion of the precipitate, the greater is the amount coprecipitated. Thus, RaE, ThC, RaC, and AcC are trapped when bismuth carbonate is precipitated from a solution carrying them as cations. If a precipitate of barium or lead sulfate is formed in acidified solutions, these radioisotopes remain in solution.

These behaviors are attributed to the similarity between properties of the radioelements and the analytical properties of the carrier. Bismuth carbonate has a very low solubility in water, whereas bismuth sulfate is soluble in acid media, and the imponderable quantities of the radioisotopes mimic these solubility relationships. In the radium pleiad, the members of which are homologous to barium, the radioisotopes coprecipitate with barium carbonate, sulfate, or chromate, as these radium compounds are insoluble in water. They are not adsorbed in the precipitation of silver chloride or chromic acid, because the chloride and oxide of radium are easily soluble.

These observations can be generalized by stating that a radioelement is carried down by a difficultly soluble precipitate when it would itself give an insoluble compound under the experimental conditions if it were present in a tangible quantity in excess of the saturation value. Paneth[P3] offers the following explanation for this behavior:

A dynamic equilibrium is envisioned between the Ba^{++} and the $SO_4^{=}$ ions with the sparingly soluble $BaSO_4$, involving a continuous replacement of these ions between the solid and liquid phases. If Ra^{++} ions are also present in the solution, on impact with the surface of the pre-

cipitate an ion exchange takes place and the radium combines with the sulfate radical to form $RaSO_4$. Since this compound has a low solubility, the probability is in favor of its retention in the crystal lattice.

With the further development of radiochemistry, exceptions to the Fajans-Paneth precipitation rules became apparent. Thus, if traces of radium are added to solutions of calcium ions and calcium sulfate is caused to precipitate, either none or only a very small fraction of the radium is carried down despite the fact that radium sulfate is one of the least soluble compounds known. Discrepancies of this character led Hahn to the conclusion that low solubility was not the sole factor determining the entrainment of traces of radioelements. Hahn differentiates between true *coprecipitation* in which the radioisotope is incorporated isomorphously in the carrier, and *adsorption* in which the separation is dependent essentially on the surface characteristics of the precipitate.

In the first entrainment mechanism, the trace and carrier ions are bound in solid solution, forming mixed crystals or systems resembling mixed crystals. The separation is independent of the conditions of the precipitation, such as the rate of precipitant addition or its final concentration in the solution. In the second method of separation, involving adsorption on a precipitate of large surface, the degree of adsorption is dependent on the surface area and its electric charge. Hahn states, "An ion, at any desired dilution, will be adsorbed by a precipitate if that precipitate has acquired a surface charge opposite in sign to the charge on the ion to be adsorbed, and if the adsorbed compound is slightly soluble in the solvent involved." In true coprecipitation the trace ion is distributed uniformly throughout the lattice of the precipitate and can be removed from it only by processes involving the resolution of the mixed crystals. Where adsorption has taken place the trace constituent can often be removed from the surface by means of solvents that do not alter the carrier solid.

It is noteworthy that these rules are also valid when the minor constituents are non-radioactive. When barium sulfate is precipitated from a solution containing the intensely colored MnO_4^- ion, the crystals possess a uniform pink color which cannot be removed either by washing with water or solutions that reduce permanganate to colorless manganous ions. The chromogenic permanganate ion is evidently held in solid solu-

tion in accordance with Hahn's concept. In developing a micro method for the estimation of barium utilizing this mechanism, Yagoda [Y8] substituted sodium permanganate as the source of MnO_4^- ion in an effort to intensify the color of the barium sulfate. It was found that, when potassium sulfate was employed as the precipitant, a pink-colored barium sulfate separated, but if the system was free from K^+ ions and the crystals were precipitated by sodium sulfate the barium sulfate separated in a colorless form. It is evident that the MnO_4^- ion does not enter the lattice by itself and is accompanied by K^+ ions. Further studies revealed that the permanganate formed mixed crystals only when the cation had an ionic radius similar to that of barium. The ionic radius of Ba^{++} is 1.35 A and is almost identical with that of the K^+ ion measuring 1.33 A, whereas the ionic radius of Na^+ of 0.95 A is markedly different. Repetition of these experiments with radioactive isotopes of potassium, sodium, and manganese may yield a further insight into the carrier properties of barium sulfate.

Purity of Carriers. In measuring activities of feebly radioactive samples it is important that the reagents, water, and carriers have an activity considerably less than that of the samples. All shelf reagents which are neatly labeled C.P. have at one time been members of the earth's crust and contain variable quantities of radioactive impurities, dependent on their previous geological history. Barium chloride is prepared by treating the mineral witherite with hydrochloric acid and crystallizing the filtered solution. Mineral waters containing traces of radium coming in contact with the native barium carbonate form a replacement deposit of the more insoluble radium carbonate. Certain commercial preparations of barium chloride may thus have a greater radium content than rocks in general.

When working with activities comparable to that of uranium minerals, the lack of purity in analytical grade reagents is readily compensated for by a blank determination on the reagent system. At lower levels it is also desirable to purify the reagents entering into the composition of the carrier. The general approach is exemplified by the following method for the radiochemical purification of barium chloride:

Dissolve 11 g of $BaCl_2 \cdot 2H_2O$ in 1 liter of water and mix with 2 ml of 10 per cent sulfuric acid. Allow the finely divided barium sulfate crystals to digest overnight on a steam bath, and then cool to room temperature. Filter this solution into a storage bottle lined with paraffin, employing a dense retentive filter paper washed with 10 per cent hydrochloric acid and a small volume of the reagent solution. One milliliter of the

purified barium chloride solution will provide about 10 mg of barium sulfate carrier.

Occasionally advantage can be taken of geochemical separation processes in the preparation of certain carriers whose purification can be achieved in the laboratory only with great difficulty. Cerium and lanthanum compounds are employed extensively as carriers for thorium and the transuranium elements. Commercial rare-earth salts, usually derived from monazite, exhibit a high alpha-ray activity owing to contamination by thorium and the presence of isomorphous actinium. Certain primary rare-earth minerals such as cerite, bastnäsite, and thortveitite contain only 0.1 per cent thorium and an even smaller concentration of uranium. As the thorium and the uranium are readily removable by analytical methods, cerium or other admixed rare-earth carrier solutions can be isolated from these minerals which are essentially devoid of actinium and mesothorium-2.

Carrier Precipitation. It is beyond the scope of this elementary treatment to enter into a detailed description of the analytical methods employed in the decomposition of samples and in the isolation of their radioelements by carrier precipitation techniques. The general approach in the isolation of a radioelement from a solution is to add a small quantity of a nonradioactive ion of similar analytical properties, and then to proceed as though this added ion alone were being separated from the other constituents of the solution. The carriers commonly employed in radiochemical separations of alpha-particle-emitting isotopes are listed in Table 18.

The number of isolation mechanisms and techniques has increased as a result of the synthesis of large numbers of radioelements isotopic with the elements of low atomic number. Also, a wealth of as yet unpublished information has doubtless been accumulated during the large-scale synthesis of plutonium. The properties of the radioisotopes occurring in radioactive minerals are described by Russell.[R15] Carrier and extraction techniques for the isolation of fission products from neutron-irradiated uranium compounds have been investigated by Hahn[H5] and Joliot.[J2] The analytical chemistry of plutonium is reviewed by Harvey.[H16,17]

TABLE 18. CARRIERS FOR RADIOISOTOPES

Z	Pleiad	Carrier and Ionic Environment	Remarks
81	AcC″, ThC″, RaC″	Tl_2S in NH_4Ac	Rapid decay, centrifuge
82	RaD, ThB, RaB	Bi_2S_3 or PbS in 0.3 *N* HCl. $Al(OH)_3$ precipitated by NH_4OH	Good for separation from radium[R15]
83	AcC, ThC, RaC	PbS in 0.3 *N* HCl	
84	RaA, ThA, AcA, RaC′, ThC′, AcC′, RaF	Bi_2S in 0.3 *N* HCl, or Te precipitated from 1 *N* HCl by $SnCl_2$	Te can be separated from Po by means of hydrazine[R15]
86	Rn, Tn, An	Carried by air or other gases	Adsorbed by charcoal and certain dust particles
87	Fr (eka-cesium)	Carried by cesium chloroplatinate	Isolation of AcK described by Perey[P11]
88	Ra, ThX, AcX	$BaSO_4$ in 0.5 *N* HCl	
89	Ac, MsTh2	Lanthanum oxalate or lanthanum fluoride	Ac can be separated from La by crystallization with Bi-Mg nitrates[M12]
90	Th, Io, RdTh, RdAc	Ceric iodate in nitric acid media [(N4)] Lanthanum fluoride Lanthanum oxalate	Th can be separated from rare earths by repeated precipitation of Th peroxynitrate in NH_4NO_3 media; also by precipitation of $Th(OH)_4$ by hexamine in NH_4Cl media[(I5)] Thorium acetyl acetone is soluble in chloroform, and the compound can be vacuum distilled[S31]
91	Pa, UX_2, UZ	Zirconium phosphate in 2 *N* HCl[(V7)] Titanium phosphate[D2] Tantalic acid[F14]	Method for isolation of Pa from rocks described by Schumb[(S11)]
92	UI, UII, AcU	$(NH_4)_2U_2O_7$ in ammoniacal solution free from CO_2 Uranyl nitrate can be extracted from ammonium nitrate media by ether	Traces of uranium are adsorbed by ferric hydroxide[(U2)] Basis of a micro method for traces of uranium described by Hecht[(H21)]
93	Np	Lanthanum or cerium fluoride	
94	Pu	Lanthanum fluoride carries tetravalent Pu	Hexavalent plutonyl fluoride can be separated from La carrier in excess HF, Harvey[(H17)]

Inhibition of Adsorption. Radioactive and gravimetric methods of analysis have much in common. The accuracy of either measurement is not limited by the counting device or the sensitivity of the balance but is largely dependent, in both methods, on the quantitative collection of the constituent in a high state of purity. The gelatinous character of many precipitates employed as carriers is conducive to the adsorption of other ions from the solution. When the entrained substance is also radioactive it will increase the total activity and render the analysis in error if the counting apparatus cannot differentiate the radiations from the carrier and its impurities. Thus, in measuring the activity of external films of U_3O_8 it is not practicable to differentiate the tracks produced by uranium alpha particles from those emitted by adsorbed polonium or ionium.

The degree of adsorption is dependent on the surface area of the carrier and the concentration of adsorbable ions. The surface area cannot be altered appreciably as it is defined by the conditions essential for the quantitative collection of the carrier. The adsorption of other radioactive ions can be reduced, however, by augmenting the ratio of isotopic inactive and active ions prior to the precipitation of the carrier. The mechanism employed in the isolation of protoactinium from pitchblende serves as an example of the "retarder" technique. The zirconium phosphate employed as a carrier is very gelatinous and tends to adsorb other radioisotopes from the solution. To inhibit the adsorption of the unweighable quantities of Ra, ThB, and RdAc about 100 mg each of Ba^{++}, Pb^{++}, and Th^{++++} is added to the pitchblende solution prior to the precipitation of the zirconium phosphate. Because the adsorption mechanism is independent of the radioactive character of the ions, adsorption is minimized by increasing the probability of entrainment of the non-radioactive isotopes.

Isolation of Radiochemical U_3O_8. Since uranium oxide serves as a primary standard in all radioactive measurements it is desirable to have a supply of this compound available for standardization purposes. The following procedure for its isolation from pitchblende also serves as an example of radiochemical purification methods:

Decompose 20 grams of high-grade pitchblende with 100 ml of 1 + 1 nitric acid in a 1-liter cone flask. Dilute to about 800 ml and saturate

with a stream of hydrogen sulfide gas. Allow the admixed acid insolubles and metallic sulfides to settle for about 2 hours, filter into a beaker, boil off hydrogen sulfide, and evaporate to a syrupy consistency. Transfer to a 250-ml platinum dish and add about 25 ml of hydrofluoric acid.*

Evaporate on a steam bath to a pasty consistency. Add 5 ml of hydrofluoric acid and 200 ml of hot water, and digest for 10 min. Cool, and filter through a platinum funnel or one of glass lined with paraffin. Receive filtrate in a paraffin-coated beaker. Clean the platinum dish by scouring it with fine steel wool and digesting it in hot 1 + 1 hydrochloric acid. Transfer the filtrate to the platinum dish; add about 50 mg of Ba^{++} ion and 20 ml of concentrated sulfuric acid. Evaporate on a steam bath and finally over an air bath until the sulfuric acid fumes. Cool, add 100 ml of water, transfer to a beaker, dilute to about 500 ml, and digest overnight at room temperature.

Filter off the mixture of barium sulfate and basic salts of iron and aluminum, catching the *clear* filtrate in a 1500-ml beaker. Dilute to 1 liter with doubly distilled water; raise to a near boil and make almost neutral with ammonium hydroxide. Add 1 + 1 ammonia dropwise while the solution is boiling, continuing its addition as long as a brown precipitate of ferric hydroxide separates and stopping the operation when yellow-colored ammonium uranate makes its appearance. Cool to about 40° C and filter into a 2-liter beaker. Boil filtrate and add sufficient 1 + 1 ammonia to precipitate all the uranium as ammonium uranate. Collect the bulky precipitate on several large ashless filter papers which have been prewashed with hot dilute hydrochloric acid and distilled water.

The yellow uranium precipitates are now ready for the final purification steps. Dissolve the compound in about 100 ml of 1 + 1 nitric acid redistilled in the presence of lead and barium nitrates. Receive filtrate of uranyl and ammonium nitrates in a 400-ml beaker whose surface has been extracted with hot nitric acid. Evaporate to a syrupy consistency on a steam bath, wash down sides of beaker with distilled water, and repeat evaporation until excess nitric acid is expelled. Cool the thick syrup, add 200 ml of redistilled ether, and filter the extract through a dry ashless filter paper. Catch the ethereal solution in a nitric-acid-extracted 1500-ml beaker, evaporate the solvent *near* a steam bath, and redissolve the uranyl nitrate in 1 liter of water. Boil, and precipitate ammonium uranate by the addition of 1 + 1 ammonia distilled from barium hydroxide. Filter the bright yellow compound onto an ashless, lint-free paper, and dry in an oven at 110 °C. Separate the compact masses of ammonium

* Great Bear Lake pitchblende contains about 1 per cent of rare-earth oxides which serve as a natural carrier for the traces of thorium and ionium present in the mineral. Specimens from Katanga or Joachimstahl usually contain a much lower rare-earth content, and it is advisable to add about 100 mg of Ce^{+++} ion as a carrier.

Pitchblendes contain variable quantities of calcium. In order to avoid a bulky precipitate of calcium fluoride at this stage, a specimen should be selected with less than 2 per cent CaO.

uranate, crush in an uncontaminated mortar, and transfer to a new porcelain crucible. Roast the powder and ignite at 800° C for 1 hour with the crucible in an inclined position.

Thin films of this uranium preparation are prepared by the methods described in Chapter 3. Clean glass or aluminum plates provide satisfactory supports.* The reliability of the track-counting technique has been investigated by Yagoda and Kaplan [Y14] using thin films of purified U_3O_8 as standards of alpha-particle activity. Their preliminary results, summarized in Table 19, indicate that the emulsion counting technique yields results in good agreement with determinations by other methods. The measurements with films weighing less than 1 mg per cm² are in particularly good agreement with values established by modern alpha pulse counting methods.

TABLE 19. DISINTEGRATION RATE IN U_3O_8 FILMS

Film	Weight, mg/cm²	k_w	Tracks Counted	Alphas per g U per sec
A	0.61	2.12	6,604	2.51×10^4
B	0.75	2.14	11,600	2.48
C	1.43	2.23	13,500	2.37
D	2.32	2.36	13,874	2.34
		Average		2.43×10^4
		Scintillation method		2.37×10^4
		Alpha pulses		$(2.48\text{–}2.53)10^4$

The alpha disintegration of UI leads to the formation of UX_1 and UX_2, both of which are beta emitters. The beta particles from UX_2 have a maximum energy of 2.3 Mev and can pene-

* The contaminants in the backing are of moment only in measuring very low activities as those of rocks. Investigations by Evans and Goodman [E14] show that aluminum produces a lower background count (about 4 alpha particles per cm² per day) than brass, copper, iron, or silver. The activity contributed by the backing can be estimated by covering one half of its surface with a layer of powdered dunite weighing about 5 mg per cm² and exposing the unit against a background-eradicated emulsion for about 1 month. Dunite is a basic igneous rock of unusually low radioactivity. Samples of dunite from Webster, North Carolina, showed on analysis by Evans and Goodman [E12] $0.03 \pm 0.01 \times 10^{-6}$ g of U, $0.00 \pm 0.03 \times 10^{-6}$ g of Th, and $(0.008 \text{ to } 0.016) \times 10^{-12}$ g of Ra per g of rock. Its potassium content of 0.0005 per cent is also exceptionally low. A thick layer of dunite has a T_α of about 5×10^{-6} per sec per cm² and provides an essentially non-radioactive test surface.

trate thin foils of aluminum weighing 30 mg per cm^2. These foils stop the alpha particles and the less penetrating beta rays from UX_1. Covered films of U_3O_8 are also serviceable as beta-ray standards. Kamen[K3] recommends a deposit of 350 mg of U_3O_8 per 10 cm^2 on a 1-mm-thick aluminum backing. The oxide may be deposited by suspension in acetone to which a small amount of Duco cement is added as a fixative. When the solvent evaporates, the aluminum foil is cemented over the oxide layer.

The activity of UX_2 is computed on the basis of complete equilibrium with the uranium. In recently purified samples of U_3O_8 the UX_1 is not in radioactive equilibrium, having been removed together with the thorium and ionium during the precipitation of the rare-earth fluorides. It is regenerated by the continuous decay of UI, but the source is not serviceable as a beta-ray standard until the preparation has aged for about 6 months. The thick layer of U_3O_8 absorbs beta radiation equivalent to 20 mg per cm^2. The effective disintegration rate corresponds to 15 mg of U_3O_8 per cm^2 or 159 beta particles per cm^2 per sec. When exposed against optical-type emulsions 7×10^6 beta particles are incident per square centimeter at the end of 24 hours. This suffices for the activation of emulsions of moderate grain size such as Lantern-Slide plates.

SERIES DISINTEGRATION

During the decay of uranium, actinouranium, and thorium to their stable end products, each parent atom passes through a complex series of intermediary bodies accompanied by the emission of alpha and beta particles. The particular stages of decay in which an alpha particle is emitted can be recorded photographically by introducing ions of the parent elements into the emulsion and observing the multiplicity of track formation at the end of a suitable exposure period. When the daughter elements in the chain are short-lived, multiple events, composed of 2 to 6 alpha-ray tracks, originating from a common center, can be observed microscopically. Typical multiple events or "alpha stars" are illustrated in Fig. 26. In the thorium series all the decay products from RdTh to ThC″ are short-lived; and their successive disintegration gives rise to numerous

stars. Even the traces of thorium normally present in the emulsion as impurity give rise to a small star population if the plates are allowed to age for several months between manufacture and development.
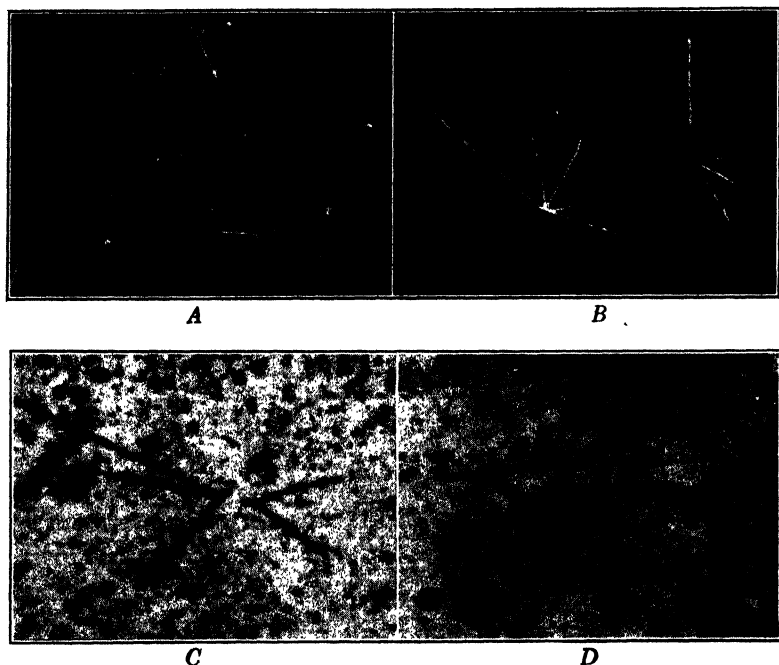
FIG. 26. Alpha stars.

A. Field of alpha stars from a thorium-loaded emulsion at 310×.
B. Field showing one of the alpha stars originating from decay processes in the glass backing.
C and *D*. Examples of alpha stars recorded in blank emulsions with displacements attributed to the diffusion of the radioactive parent atom between stages of decay. Magnification 630×, bright-field illumination.

The probability of disintegration with multiple-event formation is markedly different for uranium and thorium. The principles of star formation in the emulsion are made evident by considering the simpler cases where these elements are initially freed from their accumulated equilibrium products. Emulsions loaded by evaporation with 1 microgram of radiochemically purified uranium and thorium per cm^2 and developed about 100 hours later exhibit the single track and star populations

TABLE 20. ALPHA STAR FORMATION IN LOADED EMULSIONS *

Incorporated Atoms	Multiplicity I	II	III	IV	V	VI
A: UI + UII + AcU	7,590	0	0	0	0	0
B: Th + RdTh purified	1,260	12	30	94	60	0.4
C: Th + RdTh 6 days later	780	45	117	140	16	0
D: Th and its equilibrium products	2,200	133	405	204	21	4
E: U + Ra series †	12,500	152	410	517	21	0.4

* All populations reduced to events per cm^2 per 10^{-6} g of parent element per 100 hours of exposure.

† Plate loaded with a solution of analyzed pitchblende adjusted to a uranium concentration equal to that in exposure *A*.

summarized in Table 20. The uranium-impregnated emulsion exhibits a population of single tracks only, whereas the thorium plate contains a multitude of II-, III-, IV-, and V-branched stars. The distinctly different behavior of the two elements has its origin in the magnitude of the disintegration rates of the isotopes of uranium and thorium:

During the exposure of plate *A*, of the 2×10^{15} atoms initially incorporated, 4500 atoms of UI decayed to UX_1, 4500 atoms of UII decayed to Io, and 200 atoms of AcU decayed to UY. A dual event can be recorded only when one of these daughter atoms decays with the emission of an alpha particle. The most favorable route for this occurrence is the decay of one of the 4500 Io atoms to Ra. During the exposure period the average population of Io is 2250 atoms per cm^2, and since this element has a half-life of 83,000 years only 0.0002 disintegration per unit area is to be expected. The likelihood of observing a dual uranium star is thus very small. In exploring 5 cm^2 of emulsion only one II-branched star was observed, and this cannot be attributed with certainty to the dual decay of UI as the population of single tracks is high and coincidental overlapping of individual alpha tracks is probable.

The radiochemically purified thorium nitrate solution contains initially isotopic atoms of Th and RdTh. Neglecting the small quantity of ionium also present,* multiple events may

* All thorium compounds are derived from minerals which contain appreciable quantities of uranium, and hence the equilibrium amount of ionium. Since this decay product is isotopic with thorium, some ionium is present in all thorium compounds.

stem from the series decay of the two principal isotopes. Two long-lived beta-ray transitions between Th and RdTh greatly reduce the probability of star formation from this source. However, stars can form in considerable number from the primary RdTh isotope, as it decays rapidly and all its succeeding daughter atoms are short-lived. This chain is the primary cause of the large number of multiple events recorded in plate *B* of Table 20. As the initially purified thorium solution ages, the concentration of RdTh diminishes because its immediate progenitors, MsTh 1 and 2, were removed during the purification of the initial thorium nitrate. In an exposure made 6 days after purification (plate *C*) the population of multiple events increased owing to the presence of a third chain, initiated by the accumulated ThX atoms. This is indicated by the smaller number of V-branched stars and the pronounced increase in the population of the III- and IV-branched events. When the emulsion is loaded with a thorium solution containing the accumulated equilibrium products, as in plate *D*, the ratio of multiple to single events reaches its maximum.

These experiments show that a high star population is recorded whenever the emulsion is loaded with a radioelement whose daughter products are short-lived and disintegrate by alpha-particle emission. Multiple events occur frequently when the emulsion contains radium or its isotopes, AcX and ThX. Radium gives rise to IV- or V-branched stars depending on its final decay to either RaC′ or RaF prior to fixation of the emulsion.

As the uranium isotopes record single tracks only, the formation of stars in a uranium-impregnated emulsion can be employed as a criterion for the successful radiochemical purification of uranium preparations. Plate *E* was loaded with the same quantity of uranium as plate *A*, but the solution was freshly prepared from a sample of pitchblende. Plate *E* therefore also contained all the equilibrium products with the exception of the gaseous radon which escaped during the solution of the mineral. In this exposure about 9 per cent of the total track population consisted of multiple events. The majority of the stars were formed from the disintegration of the 3.5×10^{-13} g of Ra in equilibrium with the uranium loaded into the emulsion. As the number of stars in blank plates is

very small, a lower observational limit of 5 stars per unit area permits the detection of 10^{-15} g of Ra in a 1-mg sample.

The characteristics of the alpha-particle tracks in stars originating from the decay of radium has been investigated by Wilkins.[W18] His stereoscopic measurements of the angle between branches suggests that the relative directions of emission are not entirely random, and that characteristic angles of 110° and others of 170° occur frequently.

It has been demonstrated that radiothorium is a prolific begetter of stars even when the solution is freshly purified from other rapidly decaying radioelements. Because accumulated radium is readily separable from radiothorium by coprecipitation with barium sulfate, and the growth of new radium from ionium is inappreciable during short exposures, the multiple-decay mechanism offers the possibility of estimating traces of thorium using star populations as an index. This potentiality is worthy of further investigation, as the method would be applicable in the presence of rare-earth oxides and without appreciable interference from radioactive elements other than high concentrations of actinium.

The pronounced star population in thorium-loaded emulsions has also been observed in the early work of Taylor and Dabholkar.[T11,12] They likewise conclude that the multiple events stem from the decay of the RdTh isotope. Powell and coworkers[P34] have made comparative measurements of the alpha-particle tracks of ThC′ recorded in wet and dry emulsions. Using the Ilford Nuclear Research emulsions they find that the tracks are recorded during impregnation, but that their grain spacing is increased by the presence of the imbibed water. Exposure periods of loaded emulsions must therefore be reckoned from the moment of immersion in the loading back to the time of transfer into the fixing solution.

The synthesis of U^{233} by neutron bombardment of thorium has led to the discovery of the missing $4n + 1$ series of radioactive elements by both the American[H1] and the Canadian[E6] investigators. The chain of disintegrations is shown in Fig. 14, and the properties of the alpha-ray-emitting elements are recorded in Table 3. In this new series Ac^{225}, Fr^{221}, At^{217}, and Po^{213} are short-lived and decay with the emission of alpha particles. Evidence for the existence of this chain was first

provided [E6] by the observation of IV-branched stars in a nuclear-type emulsion which had been impregnated with a solution of Ra^{225} isolated from the decay of a few milligrams of U^{238}.

Actinium decays by alpha emission, and all the daughter products are short-lived. Guillot and Percy [G30] demonstrated the chain of succeeding disintegrations by loading plates for about 10 sec from a preparation of actinium freshly purified from its decay products. A plate developed 48 hours later revealed numerous stars comprised of tracks with a range corresponding to Ac, AcX, An, AcA, and AcC alpha particles.

The tracks constituting most stars originate from a common center within the limitations of microscopic measurements. This is to be expected, as the recoil of the daughter atoms is too small to produce a noticeable displacement in the emulsion. Nevertheless, stars are occasionally observed in which a single track or a component double branch is displaced by several microns from the other components of the event as shown in Fig. 26*C* and *D*. This phenomenon has been reported by Taylor and Dabholkar,[T11] and more recently by Demers.[D8] Demers has observed a splitting of V-branched thorium stars, such that the alpha tracks from RdTh and ThX radiate from one point, and those emitted in the decay of Tn, ThA, and ThC′ from another point several microns distant from the site of the initial decay.

The displacement phenomenon has also been observed [Y18] both in thorium-loaded plates and in stars occurring in blank emulsions. The occurrence of displaced stars in emulsions of very low single-track population seems to eliminate the possibility that the brecciated V-branched event is simply a random combination of two multiple events. Demers attributes the migration to the heterogeneous structure of the emulsion which provides in places paths of lesser resistance. Taylor is of the opinion that the displacement represents an actual diffusion of the ion in the gelatin during the intermediary stages of its stable existence.

The traces of radium and radiothorium present as impurities in the glass backing produce clusters of alpha-particle tracks owing to the rapid decay of their daughter products. When the parent atom is located several microns below the emulsion layer, the family of alpha tracks can often be recognized when

recorded at favorable angles. These glass stars differ from those located entirely within the emulsion only by the absence of the connecting center, as exhibited in Fig. 26*B*.

Huntley,[H39] who first observed the phenomenon in plates exposed at 11,000 ft, attributed the glass stars to cosmic-ray-induced nuclear evaporations in the glass backing. Spontaneous decay processes is a more probable explanation, as the extrapolated track lengths of the recorded portions almost invariably correspond to the ranges of the alpha particles emitted by members of the three radioactive series. True cosmic-ray disruptions originate in the glass of plates exposed at high altitudes, but at an exceedingly low rate. In these rare instances (Chapter 12, p. 302) one or more of the tracks belonging to the cluster has a range in considerable excess of the ThC′ alpha particle, and certain members have a grain density indicative of a proton trajectory.

The glass alpha-track clusters are readily differentiated from individual alpha-particle tracks originating from samples exposed above the emulsion by noting the direction and position of the terminal grains with reference to the emulsion boundaries. These observations are made with a sharply focusing objective of high numerical aperture. Poole and Bremner[P38] show in their investigations on the activity of granites that the impurities in the glass backing give rise to a population of 2.4 tracks per cm^2 per day.

Studies on star formation represent a unique tool in radioactive measurements. Most methods of studying radioactive transformations provide only statistical information on the average behavior of a large number of atoms. In contrast, star formation in the emulsion may record the entire life history of a single radioactive atom.

RADIOCOLLOID AGGREGATION

The first intimation of atomic aggregation of radioactive ions in solution was obtained by Paneth. He observed that during the dialysis of an aqueous solution of RaD and RaE nitrates admixed with common lead, all lead ions passed through the membrane, whereas the RaE was retained. Paneth attributed this behavior to the hydrolysis of RaE, as the stable isotopes of bismuth are known to form insoluble compounds as a result of their hydrolysis in neutral aqueous solutions.

Under conditions of high acidity, where hydrolysis is suppressed, RaE behaves as though it were dispersed ionically.

Evidence of aggregation is also indicated in the behavior of the solutions to electrolysis at different hydrogen-ion concentrations. The radioactive elements dispersed as ions in acid media migrate electrolytically whereas the colloidal units present in neutral solution move by cataphoresis. Soddy [S31] noted the phenomenon at an earlier date but failed to recognize its significance. He found that UX_1 can be separated by adsorption on filter paper by simply filtering a dilute solution of uranyl nitrate.

The presence of clusters of radioactive atoms in certain radioactive solutions is readily demonstrated by the emulsion technique. Using photographic plates as recording media, Chamie [C4,5,6] observed that a large number of radioactive substances, whether dispersed in gases, in the form of amalgams, or present in aqueous solutions, did not blacken the plate uniformly, as they would if dispersed as single atoms, but did show marked discontinuities with points of very intense photographic activity. Chamie attributed these points of high activity to the presence of clusters of radioactive atoms which she designated as *radiocolloids*.

The presence of radiocolloids can be demonstrated by immersing an emulsion in a neutral solution of a short-lived alpha-emitting element. When the solution is strongly acid, the exposure can be conducted by interposing a thin cleavage of mica between the emulsion and the drop of solution. An alternative technique devised by Chamie [C9] is to centrifuge the solution onto the surface of a paraffined slide which is subsequently exposed against an emulsion. Another simple means for demonstrating radiocolloid aggregation [Y11] is to rotate a polished copper disk in a slightly acid solution of polonium, which is then contacted with an emulsion. Following any one of these methods, microscopic examination of the processed plates shows that, besides the anticipated background of individual tracks, units composed of from 10 to several hundred tracks which radiate from a common center are also present. The microscopic appearance of the patterns recorded by these radiocolloids is exhibited in Fig. 27. The aggregation of radioactive atoms in the gaseous state has

been observed by Harrington [H14] by examining centrifuged radon tubes with an ultramicroscope.

The radiocolloids have been the subject of numerous investigations, all of which confirm the existence of the phenomenon, but
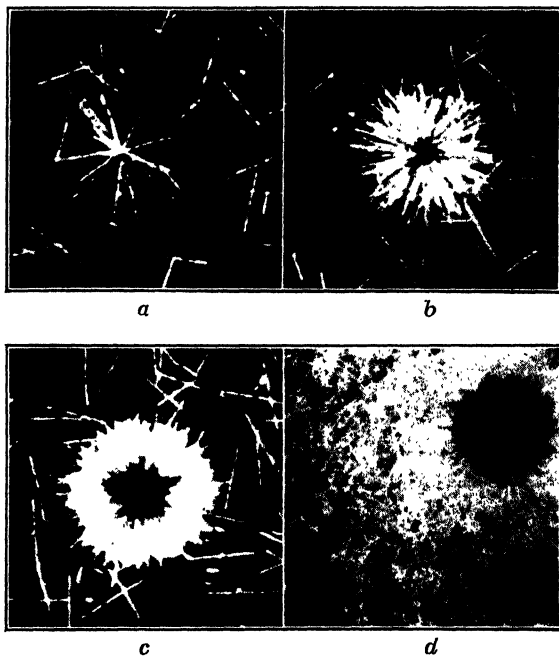
FIG. 27. Radiocolloid aggregates of polonium.

a, b, and *c*. Track formations produced by radiocolloids with increasing numbers of aggregated Po atoms. Dark-field illumination; magnification 420×.

d. Localized concentration of adsorbed Po in emulsion. Dark-field illumination; magnification 152×.

very few of which agree as to the mechanism of their formation. Werner [W6, 7] attributes radiocolloid aggregation to the invariable presence of inoculating nuclei of dust and silica originating from the air and glassware. These impurities, which cannot be excluded completely even under the most painstaking experimental conditions, serve as adsorption centers for the radioactive ions. According to Hahn [H3] the deciding factor in the formation of radiocolloid aggregates is the degree of hydrolyzability of the

radioactive solute. In his experiments, radiocolloids were not formed from compounds that are readily soluble in water, and the population of radiocolloids increased with the ease of hydrolysis of the salts in neutral solutions. The tendency for aggregation is reduced by increasing the acidity of the solution. It is also diminished by the addition of organic compounds such as citric acid and mannitol which form molecularly dispersed complexes with the radioactive aggregates.

Studies by Bouissieres, Chastel, and Vigneron [B38] employing nuclear-type emulsions as detecting media for the radiocolloids show that the character of the solute and the age of the solution are important factors in their growth. At an acidity of 0.3 *N* HCl radiocolloids were observed in aqueous solutions of polonium containing 5×10^9 RaF atoms per ml. When alcohol or acetone was employed as the solvent, radiocolloids were not observed, and the emulsions loaded from these solutions recorded randomly dispersed single tracks only.

This observation is of interest in the loading of emulsions with carrier fractions for purposes of their quantitative assay. The presence of radiocolloid aggregates complicates the estimation of the track population. In loading by evaporation the presence of a large volume of alcohol not only facilitates rapid drying but also minimizes radiocolloid aggregation.

In aqueous media the studies of Bouissieres [B38] show that the proportion of radiocolloid aggregates to single tracks increases markedly after the solution ages for several hours. This confirms the earlier work of Chamie and Haissinsky,[C8] who found that the proportion centrifuged down increased with the age of the polonium solution. Sedimentation studies indicate that the aggregates have a radius of about 10^{-6} cm. Measurements by Chamie [C7] based on the dimensions of the images recorded in the emulsion indicate that the aggregates have a diameter below 1 micron. However, the activity of the aggregates indicates that the entire unit cannot be composed of radioactive atoms, and that part of the mass must be attributed to an inert core.

Hahn agrees that impurities must be present in order for radiocolloids to form, and that the aggregates are an adsorption of radioactive atoms on a more massive inert condensation nucleus. Studies by Starik [S87] and Haissinsky [H6,7,8] are not in complete harmony with an exclusive adsorption mechanism. Their experi-

ments show that large quantities of variably charged adsorbents, such as silica, silver chloride, or titanium dioxide, can be introduced into a solution of polonium adjusted to a *p*H most favorable to adsorption, and, nevertheless, the adsorbents do not interfere with the electrochemical behavior of the RaF ions towards deposition on metallic foils.

The high resolving power of nuclear-type emulsions facilitates the study of radiocolloid aggregates.[Y17] A plate loaded with polonium by adsorption from a solution containing about 10^{-5} millicurie of RaF and developed 18 hours later carried a population of 50 radiocolloids per cm^2. The images of the radiocolloids were dispersed on a dense background of single tracks estimated at 3×10^5 per cm^2. Symmetrical clusters of 10 to 100 tracks directed from a common center were fairly common. The spherical track clusters indicate a point conglomeration of from 3000 to 300,000 polonium atoms. Several units of greater activity, exhibiting more than 1000 tracks, were also recorded. Of these, some contained a minute transparent grain embedded in the gelatin coincident with the center of the tracks. The grains probably originated as grindings from the glass-stoppered bottle in which the original polonium solution was stored. The activity of these glassy fragments can be attributed to an adsorption film of polonium.

A unit of extremely high activity is reproduced in Fig. 27*d*. This rare event may owe its origin to an electrochemical deposition of polonium atoms from the loading bath onto a speck of metal embedded in the emulsion.

Radiocolloid aggregates can be detected photographically only when the constituent radioelements decay rapidly. Thus, the presence of a cluster of uranium atoms in solutions of its compounds cannot be established by an exposure of reasonable duration. Because of the long life of the uranium isotopes a cluster of 10^6 atoms would yield only one disintegration during an exposure period of 7000 years. The technique has been applied successfully in the study of solutions of the less stable elements. The effect of acidity on the aggregation of ThC has been studied by Hahn and Werner.[H3] They find that radiocolloids are abundant in neutral solution, diminish with increasing acidity, but are still persistent in 0.1 *N* HCl. Wilkins[W24] has observed radiocolloid formation in emulsions carrying traces of radium. He sug-

gests that the size of the central dark kernel, as observed microscopically under dark-field illumination (Fig. 28), is a measure of the number of alpha particles emitted from the radiocolloid into the emulsion.
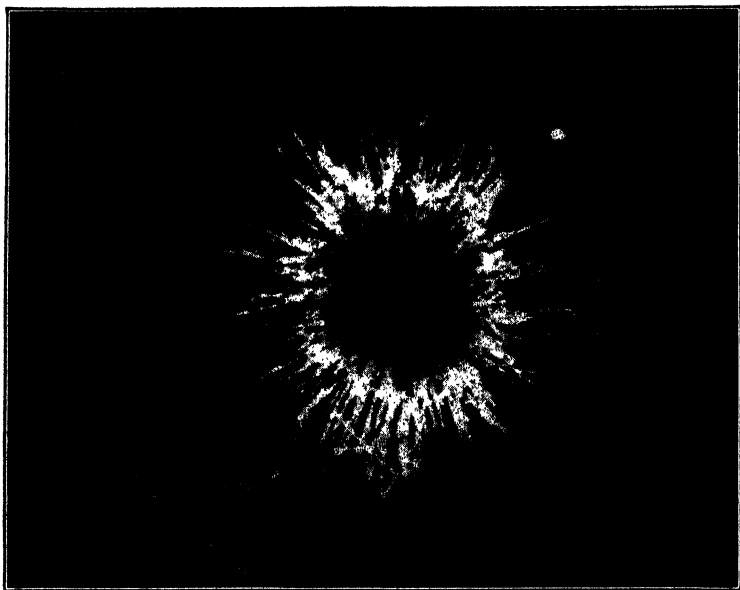
FIG. 28. Radiocolloid in a radium-loaded emulsion. Dark-field illumination, magnification 570×. The alpha particles ejected from the common center cause the development of an opaque film of silver. Under dark-field illumination this dense core appears black. The intermediary white halo represents the termination of the short-range alpha particles originating from the decay of Ra, Rn, and RaA. The thin outermost zone represents the terminal portions of the long-range alpha particles ejected in the decay of RaC′. The complex structure results from the series decay of a submicroscopic aggregate of radium atoms. Several alpha stars are recorded in the background. These originate from the series decay of individual radium atoms.

The radiocolloid aggregates exhibit a marked tendency to precipitate on cellular structures when the dispersion comes in contact with porous media. This property is exhibited strikingly by dilute solutions of radium sulfate. According to Hahn,[113] after the passage of the solution through a filter paper, over 98 per cent of the radium is retained by the cellulose fibers. As noted earlier

by Soddy, UX_1 deposits quantitatively on passage of the solution through filter paper, and the element undoubtedly exists in the uranium solution as a dispersion of radiocolloids.

The ready adsorption of certain radiocolloids by cellulose fibers has been utilized in the separation of synthetic radioactive isotopes from bombarded targets. Radioyttrium forms radiocolloids in aqueous solutions, a property which permitted Kurbatov [K21] to separate the element from a solution of a deuteron-bombarded strontium oxide target without the aid of a carrier. The solution was adjusted to *p*H 9 by addition of ammonium hydroxide. No visible precipitate of yttrium hydroxide formed, but on filtration aggregates of $Y^{86}(OH)_3$ separated on the filter paper. The successful separation of rare-earth fission products by means of chromatographic adsorption columns suggests that radiocolloid phenomena play an important role in the separation mechanism.

The phenomena associated with radiocolloid aggregation are important factors in the evaluation of activity measurements of both isolated carrier films and powdered-rock samples. As detailed in subsequent chapters, radiocolloids are formed during alteration processes of primary uranium minerals and are likely to be present in adjoining and more distant gangue materials. Because of their deposition on the walls of capillary structures, radiocolloids are frequently encountered in the autoradiography of plant and animal tissues and tend to concentrate in excretory organs.

Chapter 7 · ALPHA-PARTICLE PATTERNS OF URANIUM AND THORIUM MINERALS

Nay, if I understand anything, greater wealth now lies hidden beneath the ground of Freiberg, Annaberg, Schneeberg and in the other mountainous parts of your territory than is visible and apparent above ground.—Georgius Agricola, 1556

The minerals of the earth's crust containing uranium or thorium as major constituents are hotbeds of complex systems of alpha-particle activity. The radioactive minerals therefore provide practical subject matter for study by the emulsion techniques. These studies are of interest in conjunction with compositional variations in polished sections and in demonstrating alteration and diffusion processes in the radioactive minerals. These considerations enter as important factors in deductions on the age and thermal history of the earth. The diffusion of radioactive gases is also of importance in the geology of petroleum bed formations and natural-gas deposits associated with helium.

With the development of nuclear chain reactors the geochemistry and metallurgy of uranium have become subjects of major importance. Unless other extensive deposits of pitchblende or carnotite are discovered it will be necessary to extract the metal from the more abundant minerals containing only small percentages of uranium. The practical use of low-grade ores is limited by the state of dispersion of the radioactive elements in the matrix. The alpha-ray pattern of a potential ore not only is a measure of the combined uranium and thorium contents, but it also delineates the mode of segregation of the elements giving rise to the activity. The nuclear emulsion permits the recognition of radioactive segregates measuring in excess of several microns and thus offers a valuable criterion in determining whether the active matter can be concentrated economically by flotation methods.

URANIUM AND THORIUM CONTENTS OF MINERALS

Most radioactive minerals contain variable quantities of both uranium and thorium, and it is not possible to translate a single

activity measurement into a percentage estimate of either element. However, the two most common ores of uranium, pitchblende and carnotite, are substantially devoid of thorium. Likewise, monazite sand, the most important source of thorium, contains only a relatively small amount of uranium. If the identity of the ore is known, a rapid estimate of the principal radioactive constituent can be made from alpha-particle-activity measurements. Since the early days of the radium industry, approximate measurements of this character by rapid electroscopic measurements have preceded more accurate chemical analysis of the ore:

As described by Ellsworth[E1] a brass disk is fitted with a circular frame so as to provide a cup about 2 mm deep and 5 cm^2 in cross-sectional area. This is filled with a sufficient quantity of powder to cover the depression uniformly, and the activity is determined by measuring the leakage in a charged electroscope. By comparing the rate of discharge with that produced by a standard powder of known composition, correcting for the natural leak of the instrument, the radioactive metal content of the sample can be computed. The activity of ores containing both uranium and thorium is expressed arbitrarily in terms of equivalent uranium activity.

The method is subject to error by the ionization originating from beta and gamma radiations, variations in particle size and density between standard and sample, and the erratic behavior of the electroscope whose natural leak is dependent on the moisture and conductivity of the air. Nuclear emulsions can be substituted advantageously, as they are not subject to certain of these variables and their use extends the number of samples that can be assayed at one time. One needs an adequate supply of sampling trays, as each plate serves as an independent recording instrument.

Pitchblende and carnotite ores, after 24 hours' exposure, produce a blackening whose photographic density can be measured accurately. Samples of low uranium or thorium content can be assayed by counting individual tracks in the emulsions exposed above the cups for about 1 or 2 hours. Since the samples are finely divided the escape of emanation is appreciable. Results of improved accuracy are obtained by employing minerals of comparable emanating power as standards. Thus, in estimating the uranium content of ores the cup is filled with a 100- to 200-mesh fraction of the sample and the alpha-particle activity is compared with a similarly prepared sample of pitchblende of known uranium content. Samples predominating in carnotite or mona-

zite are compared with standards of the respective species. Preliminary studies on a series of analyzed pitchblendes show that under these crude conditions of exposure the photographic density serves as an index of the uranium content with an accuracy of about 15 per cent.

The same methods can be applied in the estimation of the uranium or thorium content of compact radioactive minerals occurring in polished section. The photographic density produced by the inclusion is compared with one produced by a similarly polished sample of known composition. The error introduced by attributing the total activity to one principal radioelement is indicated by the following example:

An unidentified mineral has found by chemical analysis to contain 30.6 per cent ThO_2 and 3.9 per cent U_3O_8. By comparing the photographic density of several polished chips with a section of monazite containing 12.7 per cent ThO_2, an emulsion assay of 33.9 per cent ThO_2 resulted. The small discrepancy between the chemical and photographic methods can be attributed in part to sampling error, as the photographic density of individual chips varied by 10 per cent.

Activities of Systems in Radioactive Equilibrium. The composite rate of alpha-particle emission from the polished surface of a radioactive mineral can be approximated from the basic relationship:

$$T_\alpha = 7.985 \times 10^{-5} \psi M(\bar{R} - \rho)$$

by evaluating M in terms of the uranium and thorium contents. The rate of disintegration of uranium in equilibrium with its daughter products has been determined experimentally by Rutherford and Geiger.[R18] By counting scintillations from thin weighed films of analyzed pitchblende, they observed the emission of 9.7×10^4 alpha particles per sec per g of U. This value is probably low, and a more exact one can be computed from the more accurate value of the rate of disintegration observed in pure films of U_3O_8. Modern measurements indicate that 1 g of uranium composed of 0.9928 part of UI + UII and 0.0072 part of AcU emits a total of 2.515×10^4 alpha particles per sec. The decay of AcU contributes 574 alpha particles, and 24,580 are produced by the decay of UI and UII.

Under conditions of complete radioactive equilibrium 1 g of UI emits a total of 9.90×10^4 alpha rays per sec, and 1 g of AcU

furnishes 5.58×10^5 alpha rays per sec. This corresponds to a total activity of 10.21×10^4 alpha disintegrations per sec per g of U in equilibrium, and is about 5 per cent higher than Rutherford's experimental value.

If the symbols U, Th, and Sm represent the fractional abundance of the respective elements in 1 g of mineral, the respective contributions to the track count recorded by an emulsion in contact with the polished surface are expressed by:

$$T_{UI} = 7.985 \times 10^{-5} \times 0.9928U \times 9.90 \times 10^4(3.96 - 0.84)\psi$$
$$= 24.49U\psi$$

$$T_{AcU} = 7.985 \times 10^{-5} \times 0.0072U \times 5.58 \times 10^5(4.71 - 0.84)\psi$$
$$= 1.24U\psi$$

The total activity $T_U = T_{UI} + T_{AcU} = 25.73U\psi$.

Similar considerations show that the number of alpha particles escaping per second from 1 cm^2 of a thorium mineral is expressed by:

$$T_{Th} = 7.985 \times 10^{-5} \times 2.46 \times 10^4 Th(4.81 - 0.84)\psi = 7.80Th\psi.$$

Estimates of the disintegration rate of samarium range between 67 and 150 alpha particles per sec per g. A value of 89 ± 5 is consistent with most determinations, yielding for the samarium contribution: $T_{Sm} = 7.985 \times 10^{-5} \times 89Sm(1.13 - 0.84)\psi = 0.0021Sm\psi$. The combined alpha-ray activity of each unit area of polished mineral surface is therefore: $T_\alpha = T_U + T_{Th} + T_{Sm} = (25.73U + 7.80Th + 0.0021Sm)\psi$. Since the samarium content of radioactive rare-earth minerals is well below 5 per cent, the track contribution of the samarium is in general negligible, and the activity simplifies to:

$$T_\alpha = \psi(25.73U + 7.80Th) \qquad (22)$$

The validity of this equation was tested with the aid of several polished sections of radioactive minerals whose uranium and thorium contents were determined by chemical analyses of adjacent portions of the same specimens. The observed track count is compared with the computed T_α values for these specimens in Table 21. It is evident that equation 22 coordinates the alpha-ray activity over a wide range of uranium and thorium contents, present in minerals of extreme composition, with a fair degree

of accuracy. The computed values are, however, invariably higher than the observed track counts.

TABLE 21. ALPHA-RAY ACTIVITIES OF POLISHED RADIOACTIVE MINERALS

Specimen	Percentage Uranium	Percentage Thorium	ψ *	Surface Activity, T_α Calc.	Surface Activity, T_α Obs.	% Diff.
Pitchblende, Katanga, Belgian Congo	76.7	.....	13.5	266	215	19
Pitchblende, Shinkolobwe, Belgian Congo	75.5	.....	13.2	256	186	27
Pitchblende, Joachimsthal	64.4	.....	11.8	196	141	23
Pitchblende, Great Bear Lake, Canada	57.7	.....	10.6	157	125	20
Thorianite, Ceylon	8.1	74.8	13.0	103	76	26
Samarskite, North Carolina	9.6	0.7	9.0	23	15	34
Monazite, South Africa	.....	11.2	9.2	8.0	6.7	13
Allanite, † Greenwich, Massachusetts	0.098	1.55	6.3	0.93	0.76	18
Kolm, Sweden	0.3	.....	4.0	0.31	0.27	13
Shale	Traces	.....	4.7	.....	0.03	..

* The permeability was computed from complete chemical analyses of the particular specimens.[Y17]

† The analysis of the allanite sample was made by Dr. J. P. Marble.

The deviation results partly from the use of the Bragg-Kleeman stopping-power law in evaluating the effective range of the alpha particles in the mineral. This relationship, as observed in Chapter 4, yields high values compared with experimental measurements of the range in heavy metals. The track count is also rendered low by the escape of emanation from the polished surface and the presence of minute non-radioactive inclusions in the specimens. The relationship expressed by equation 22 does not consider back-scattering of the alpha particles, which is probably an appreciable factor in solids composed of a large percentage of heavy atoms.

Activities of Isolated Systems. Equations correlating the alpha-ray activity of solids containing uranium or thorium purified from their radioactive equilibrium products are readily derived from the specific disintegration rates of the metals. Systems containing the three naturally occurring uranium isotopes have a surface alpha-ray activity expressed by:

$$T_\alpha = 7.985 \times 10^{-5} \times 2.515 \times 10^4 U(2.93 - 0.84)\psi$$
$$= 4.20 U\psi \qquad (23)$$

Equation 23 is applicable to alloy systems containing uranium as a component and to crystals such as uranyl sulfate or nitrate prepared from purified uranium oxide. For a thick slab of uranium metal, equation 23 yields a T_α value of 64.8 per sec per cm^2. In exposures with a polished specimen of the pure metal a track count of 59.4 $\pm$ 0.5 per sec per cm^2 was observed. The difference between the computed and observed T_α of 8.3 per cent is attributable to the uncertainty in the exact range of the alpha particles in uranium metal.

A similar expression can be derived for thorium composed of Th^{232} and RdTh. It has little practical utility, however, owing to the presence of variable quantities of ionium, and to the rapid growth of other alpha-ray-emitting isotopes originating from the decay of RdTh. Solids containing only the plutonium isotope Pu^{239} as the radioactive component have a surface alpha-ray activity expressed by:

$$T_\alpha = 7.985 \times 10^{-5} \times 2.3 \times 10^9 Pu(3.68 - 0.84)\psi$$
$$= 5.21 \times 10^5 Pu\psi \qquad (24)$$

Although equations 22 to 24 are serviceable in estimating the alpha-ray activity of infinitely thick solids on the basis of their chemical composition, the uncertainty in the coefficients does not permit the precise evaluation of the metal content from a track count. In quantitative work the exposure must be made on a thin film of known weight per unit area.

DETECTION OF RADIOACTIVE EMANATIONS

In the successive decay of uranium, actinouranium, and thorium to their stable end products the intermediary daughter elements are, at one stage, homologous to the rare gases of the periodic system. The isotopes of element 86, radon, actinon, and thoron are gases, and are capable of diffusing through porous media during their transitory stable existence. The emanating power of different radioactive solids is a function of exposed surface area, crystal-lattice packing, and temperature. Certain minerals can retain the emanation better than others,

and this was recognized by Starik [S38] as an important factor in determining the suitability of the specimen as a geologic age indicator.

Because of its long half-life radon has opportunity to diffuse from the interior of a uranium mineral and to decay in other surroundings, thereby diminishing the Pb^{206} and the helium contents of the solid in which it was generated.* The continuous weathering of surface rocks also causes the liberation of emanations which contribute to the minute radon content of the atmosphere, estimated at about 10^{-13} curie per liter of air. In pitchblende mines or radium factories the radon concentration increases markedly. Measurements by Evans and Goodman [E13] show that in gas-mantle factories the thoron content may run as high as 23 to 400×10^{-11} curie per liter.

Emanation studies by Israël-Köhler [I6] on ground air indicate that part of the radon may be adsorbed on aerosol particles. The horizontal distribution of emanations in the atmosphere has been investigated by Baranov and Grachova.[B3] This work indicates the possibility of exploring uranium deposits by measurements of the radon content of the atmosphere at distant points of observation.

When an atom of radium decays an alpha particle is emitted and a recoil atom of radon results. When the event occurs on or near the face of a crystal, a fracture, or a polished surface, and if the alpha particle is directed into the solid, the radon atom will be ejected into the surrounding space. As a result, every radioactive solid has an emanating layer whose volume is equal to the product of the surface area by one-quarter of the maximum range of the recoil atom within the solid. At a given temperature, assuming homogeneous distribution of the radioactive substances and no diffusion of the radioactive gases, the emanating power of a substance may be defined as the ratio of the volume of the emanating layer to the total volume of the solid.

* Běhounek and Klumpar [B13] have questioned the existence of thoron in the atmosphere. Their measurements indicate that thoron does not escape even from open containers of ThX. Experiments with the emanation methods described in this section show that thoron escapes from thorium nitrate and that the gas is readily detected even after diffusing through a thick sheet of filter paper. ThC′ tracks are recorded by the emulsion; hence the activity of the gas cannot be attributed to radon originating from the decay of associated ionium.

By increasing the surface area, either by mechanical grinding or chemical precipitation processes, the escape of emanation from a substance is greatly augmented. Experiments by Hahn [H8] show that at ordinary temperatures almost no diffusion of emanations occurs within closely packed inorganic crystal lattices or in compact structureless glasses. In compounds of this character the emanations escape entirely by the recoil mechanism. Processes which loosen the crystal structure, like the desiccation of a hydrated compound, tend to augment the emanating power. When a crystal of $BaCl_2 \cdot 2H_2O$ containing admixed radium is dehydrated, radon escapes with the water of crystallization. The process also increases the emanating power of the residual $BaCl_2$. Pulverulent hydrated minerals, such as carnotite, will tend to exhibit a higher emanating power than uranium minerals which occur in the form of compact crystals.

The electric charge carried by the recoil atoms is probably an important factor in emanation processes. The escape of radioactive atoms from a surface is not limited to gaseous daughter atoms as the recoil mechanism will also cause the ejection of "solid" atoms when the event occurs near the surface boundary. In general, recoil atoms behave like positively charged ions in a gas and are attracted to a surface of opposite charge. Studies on the radioactive gases indicate that when liberated by recoil the radon and thoron carry no charge and hence are free to diffuse until they are transformed by spontaneous decay into charged atoms of other elements.

Since the emanations decay with the emission of alpha particles their presence in a gas is readily detected by tracks recorded in nuclear emulsions.* The escape of radon and thoron is readily detected by passing a slow current of dry air over the solid and conducting the stream between two emulsions supported as described in the emanation camera in Fig. 29. Almost every atom of emanation that decays in the camera records an alpha-

* The first intimation of the possibilities of the emanation method was obtained inadvertently while testing the sensitivity of the emulsions to gamma radiation. About 100 g of uncrushed thorianite crystals enclosed in a sealed heavy cardboard box was employed as the source, and the emulsion exposed above it for 2 days. On development the plate appeared fogged, but microscopic examination showed the presence of a high population of long-ranged alpha-particle tracks.

particle track on one of the two plates. The track population is further augmented by the subsequent decay of RaA, AcA, and ThA, as all three are short-lived. If a potential in excess of 135 volts is applied between the two emulsions the positively charged recoil atoms of RaB, AcB, and ThB collect on the negatively charged emulsion, together with the remaining undecayed atoms of the A-bodies. Of the latter RaA is the most abundant as it has a half-life of about 3 min.
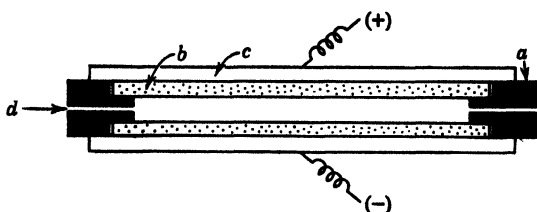
FIG. 29. Emanation camera.

a. Machined Bakelite form accommodating two 3 × 1¼-in. plates with emulsion faces separated about 1 mm.

b. Nuclear-type emulsions.

c. Brass or aluminum electrodes making contact with glass backing with the aid of lead foil. The potential is supplied by three or four 45-volt dry cells connected in series.

d. Small-bore glass tube connecting camera with the air flowing over the source.

If, after termination of the gas flow, development is delayed for about 2 days to permit the collected recoil atoms to decay through the C-body stage, a series of II-branched events will be recorded on the negatively charged emulsion that permits the differentiation of radon and thoron. The track population on the positively charged emulsion is an approximate measure of the number of emanation atoms that decayed in the camera during the gas flow. The negatively charged emulsion has a population of single tracks which exceeds that on the opposite plate as a result of subsequent decay of the collected recoil atoms.

When radon is present in the gas stream a large number of II-branched events are recorded on the collector plate owing to the decay of atoms of RaA through the RaB and RaC′ stages. These multiple events have branches of 4.66 and 6.91 air-cm and provide distinctive evidence for the presence of radon in the gas

stream. When thoron decays in the camera, the active deposit is composed almost entirely of ThB. On delayed development, the ThB decays by beta emission and single alpha-particle tracks are recorded from the almost immediate decay of either ThC or ThC′. The branching ratio favors the formation of the very long ThC′ alpha-particle tracks, and these serve as an indicator for thoron.

This simple technique will demonstrate the escape of emanations from a few grams of crushed mineral. Dry air is passed through a tube containing the sample at room temperature at a flow of about 2 ml per min. The flow is prolonged in accordance with the size of the sample and its radioactive metal content. A 1-hour period suffices for the detection of radon escaping from 10 g of carnotite containing about 5 per cent uranium. The escape of thoron from the natural crystal faces of thorianite is also readily demonstrated. The sensitivity of the method can be increased by powdering the mineral and conducting warm dry air through it. The detection of minor quantities of radon in the emanations from an essentially thorium-bearing mineral is facilitated by increasing the length of the tubing connecting the source with the camera. Because thoron is short-lived, the bulk of the atoms will decay during transit, and thus the gas entering the camera will be enriched in radon.

EMANATING POWER OF POLISHED SURFACES

The emanations have a recoil range of about 0.01 air-cm. By assuming a stopping-power relationship similar in form to the Bragg-Kleeman rule, it is possible to approximate the effective range of the heavy recoil atoms in radioactive solids of diverse atomic composition. Under conditions of radioactive equilibrium, and in the absence of internal diffusion, it is then possible to estimate the number of emanation atoms G ejected per sec per cm^2 of polished surface. On this basis the range of a recoil atom in a solid of density d and permeability ψ is $3.2 \times 10^{-6}\psi/d$, and the number of atoms of radon ejected by recoil G_{Rn} is:

$$G_{\mathrm{Rn}} = \frac{3.2 \times 10^{-6}}{4} \times \frac{\psi}{d} \times \frac{9.9 \times 10^{4}}{8} \times 0.9928Ud = 0.01U\psi \quad (25)$$

The rate for actinon and thoron is, likewise, $G_{An} = 0.00046U\psi$ and $G_{Tn} = 0.0033Th\psi$.

Since chemical analyses of the minerals are usually not available it is more convenient to express the recoil rate in terms of T_α which can be established experimentally for the identical polished specimen. For minerals containing uranium as the chief radioactive constituent the combined rate of radon and actinon ejection is $0.000397T_\alpha$ atoms per cm^2 per sec. Likewise, in thorian
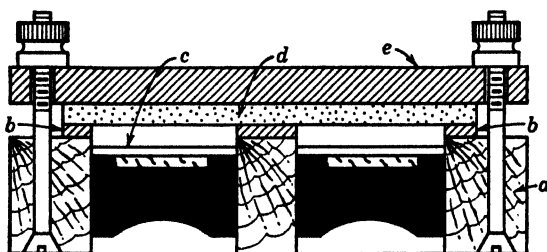
FIG. 30. Camera for measuring emanating power of polished surfaces.

a. Paraffin-impregnated wood block accommodating two Bakelite-mounted specimens.
b. Rubber gasket about 1 mm thick.
c. Filter-paper barrier for alpha particles emitted from surface.
d. Nuclear-type recording emulsion.
e. Clamping plate.

minerals thoron is ejected at a rate of $0.00042T_\alpha$ atoms per cm^2 per sec. These rates are minima applicable only to compact radioactive minerals. In general, the total rate of emission will be appreciably higher because of the absolute surface exceeding the geometric area and the escape of emanation from fissures within the solid.

The number of emanation atoms ejected from a surface can be determined from the population of alpha-particle tracks recorded on a nuclear-type emulsion which is exposed only to the radioactive gases. The exposure is conducted at room temperature in the block described in Fig. 30. A disk of filter paper about 0.2 mm thick stops the alpha particles originating from the surface but permits the emanations to diffuse through it. Atoms of radon or thoron which decay in the 2-mm air gap between the emulsion and the filter record tracks, and the popu-

lation is further augmented by the subsequent decay of the A- and C-bodies.* During a long exposure the decay of each emanation atom results in the ejection of three alpha particles, and geometric considerations indicate that approximately ⅓ of these will record tracks in the emulsion. Therefore each recorded track corresponds to the disintegration of one atom of primary emanation.

On the basis of these simplifying assumptions the total number of emanation atoms that escaped from the mineral as a result of both diffusion and recoil processes, n_e, can be computed from the track count P recorded per unit area and the disintegration rates of the respective gases. If recoil atoms are produced at the continuous rate of G atoms per sec per cm², and the exposure is conducted for t sec, the total number of emanation atoms escaping per square centimeter is given by:

$$n_e = P + \frac{G(1 - e^{-\lambda t})}{\lambda} \tag{26}$$

Actinon and thoron have very brief half-lives, making the second term in equation 26 negligible in exposures of long duration. For the long-lived radon, the number of undecayed atoms is appreciable, and after the standard experimental exposure period of 48 hours the total number of ejected radon atoms is $P + 1.44 \times 10^5 G$ atoms per cm².

This is a true measure only when the gas accumulates exclusively by recoil from the emanating layer. In highly porous materials the concentration is augmented by diffusion from the interior of the specimen. Since the second term in equation 26 applies only to those radon atoms originating from surface recoil, n_e will be low when diffusion is rapid. This uncertainty is a weakness in the method, which is reduced by preparing all test samples in the form of thin slabs of nearly equal thickness. The geometric surface area of the radioactive components is deter-

* Actinon and thoron decay rapidly, and an appreciable fraction probably disintegrates within the filter. Experiments with compact thorian minerals and thorium nitrate crystals show that thoron reaches the air gap as proved by the appearance of Tn and ThC′ alpha-particle tracks on the emulsion.

mined by projecting an alpha-ray pattern of the polished section and tracing the enlarged outlines on a sheet of paper. The weights of these irregular cutouts is a measure of the radioactive surface area.

TABLE 22. EMANATING POWERS OF URANIUM AND THORIUM MINERALS

Mineral	Obs. T_α	P	G	n_e	n_e/G
Pitchblende, Great Bear Lake, Canada	186	0.018	0.074	0.071	0.96
Pitchblende, Joachimsthal	141	0.0041	0.056	0.051	0.91
Carnotite, Colorado	29	0.29	0.012	0.30	25
Carnotite, Utah	48	0.490	0.019	0.51	27
Autunite, Mt. Painter	55	0.121	0.022	0.14	6.3
Monazite, South Africa	6.7	0.004	0.0028	0.004	1.4
Thorianite, Ceylon	76	0.050	0.032	0.050	1.6

The ratio n_e/G of the total number of emanation atoms to those ejected by recoil from the polished surface is recorded in Table 22. When the radioactive gases escape only by recoil the ratio has a value of unity. A large departure from unity is indicative of diffusion of emanation from the interior of the sample. Compact samples of pitchblende yield ratios close to unity indicating that the radon escaped essentially by recoil from the polished surface. In the case of carnotite the high n_e/G ratio demonstrates diffusion of radon from within the mineral.

These results are in harmony with available data on the relative emanating powers of powdered minerals of similar composition. Boltwood [B31] observed a 1.4 per cent loss of available radon during grinding of a dense uraninite crystal, whereas carnotite lost 33.6 per cent of its emanation. More recent studies by Keevil [K6] on the radioactivity of wall rock surrounding carnotite ores are also in conformity with a rapid diffusion rate.

These preliminary studies [Y17] indicate that the nuclear-type emulsion provides a semiquantitative tool for the measurement of radioactive emanations. The method should prove serviceable in studies of the relative emanating powers of powdered materials containing radium isotopes. The method is one of extraordinary delicacy. The recoil rate in the specimens investigated is only about 3 atoms per min per cm^2. Nevertheless, by prolonging the exposure for 2 days, an adequate track population is provided by specimens with a surface area less than 5 cm^2.

RADIOCOLLOIDS IN GEOCHEMISTRY

The surface alpha-ray activity of unaltered uranium and thorium minerals is usually less than 200 tracks per cm² per sec. Microscopic examination of the alpha-ray patterns of altered minerals reveals the presence of occasional minute points or lines of much higher activity. These areas may have a photographic density exceeding that of the matrix mineral by a factor of 100.

Fig. 31. Radiocolloid deposition in fissures of pitchblende. Alpha-ray pattern, bright-field illumination, magnification 10×. Pitchblende sample from Central City, Colorado.

The active points exhibit structural features in common with the more active radiocolloids observed in loaded emulsions. Typical formations recorded in the autoradiography of polished mineral sections are shown in Fig. 31.

The native radiocolloids are often deposited in quartz or other finely interdispersed gangue apparently unassociated with any parent uranium mineral. A mechanism for the formation of radiocolloids in altered minerals has been suggested by Yagoda:[Y11] Oxidation of associated sulfides produces traces of sulfuric acid which are carried by surface waters into the more porous portions of the deposit. The dilute acid attacks the altered minerals and effects solution of uranyl, lead, and radium ions. In this solution the traces of radium are probably dispersed as radiocolloids composed of radium and lead sulfates.

In percolating through the interface of adjoining pitchblende layers, or fissures in surrounding gangue minerals, the radiocolloids precipitate in the capillary structures. This process results in the formation of a localized concentration of radium and a uranium-bearing filtrate deprived of its equilibrium amount of radium. The radium concentrated by this mechanism, devoid of parent uranium or ionium, decays rapidly to Pb^{206}. The present-day activity of the native radiocolloids is due primarily to traces of undecayed radium, their chemical composition being essentially lead sulfate.

The presence of lead coincident with the particular points on the polished surface that furnish radiocolloid images has been demonstrated by chemical printing methods.[Y11] The polished section is contacted with a gelatin-coated paper moistened with 2 *N* ammonium acetate solution. This reagent dissolves lead sulfate but does not extract the lead held in solid solution in the unaltered portions of the primary uranium mineral. On developing the contact print with a 0.1 per cent solution of dithizone in 10 per cent KCN, a red-colored lead derivative precipitates in the gelatin. Comparative microscopic examination of the lead prints and the alpha-ray patterns shows a close correlation between the points of abnormal alpha-ray activity and extractable lead.

The activity of the native radiocolloid bodies can be measured with the aid of the dual-exposure technique described in Chapter 3. The size of the black core, as recorded in the long exposure, is a linear function of the number of radial tracks counted in the brief exposure. The radiocolloid cores, Fig. 24*A* (p. 125), as observed under dark-field illumination range between 30 and 100 microns in diameter. Structures of comparable dimensions are usually not evident on corresponding points of the polished surface. This indicates that the capillaries containing the $(Pb, Ra)SO_4$ are of much smaller dimensions. Measurements on a sample of Cornwall, England, pitchblende, particularly rich in radiocolloids, indicate that they possess a T_α value of about 3000. Since the dimensions of the radiographic cores originate from obliquely incident alpha particles, this estimate may be low by a factor of 5.

The separation of certain radioactive constituents from their parent elements as a result of weathering and radiocolloid deposition probably also takes place in exposed rocks. Surface coatings of secondary uranium minerals, such as autunite, occur fre-

quently with abnormally low alpha-ray activities. Age determinations, described by Holmes,[H33] indicate that these minerals are of comparatively recent origin, some being perhaps no more than 50,000 years old. Secondary minerals of this sort were probably formed by the crystallization of uranium solutions leached from primary ore bodies. These solutions, depleted of their equilibrium radium content by radiocolloid deposition, produce secondary minerals with an alpha-ray activity only slightly higher than that of purified uranium compounds.

The radiocolloids concentrate in localized spots or capillaries of the adjoining rocks and impart to the mass an alpha-ray activity in excess of the true uranium or thorium content held in solid solution. The difficulties encountered in sampling rocks for radioactivity measurements, discussed by Evans and Goodman,[E12] are attributable to the presence of radiocolloids. As shown in the section on activity in rocks, the radiocolloids are not distributed uniformly, and the deviation between duplicate check analyses of powdered-rock samples may originate from uneven dissemination of the intensely active specks.

Available data on the content of radioelements in sea and lake waters also indicate a large-scale geochemical separation of uranium and radium during alteration processes. Sea water is deficient in radium as compared with its uranium content. Under conditions of radioactive equilibrium the Ra/U ratio has a constant value of 3.4×10^{-7}. Measurements by Rona[R9] show that in sea water this ratio ranges between 0.24 and 1.64×10^{-7}. In allied studies on the concentration of radium in marine organisms Rona[R10] concludes that the lower radium content of ocean water cannot be accounted for by concentration processes in the bodies of algae and plankton.

Piggot and Urry[P22] likewise find that there is much less radium in the ocean water and much more in the bottom sediment than is appropriate to the uranium present in each place. The higher uranium content of sea water may possibly result from the continuous addition of uranium solutions depleted of their radium by surface adsorption of the radiocolloids. Variations in the radium content of lake water in the Great Bear Lake pitchblende region are explicable, according to Senftle,[S21] on the basis of the formation of radiocolloids near weathered and leached pitchblende deposits.

DETECTION OF RADIOACTIVE GRAINS

In the microscopic identification of minerals it is common practice to orient grains for refractive-index determination on a gelatin-coated slide. The identical technique can be employed advantageously in testing individual grains for alpha activity by substituting a nuclear-type emulsion as the embedding medium.
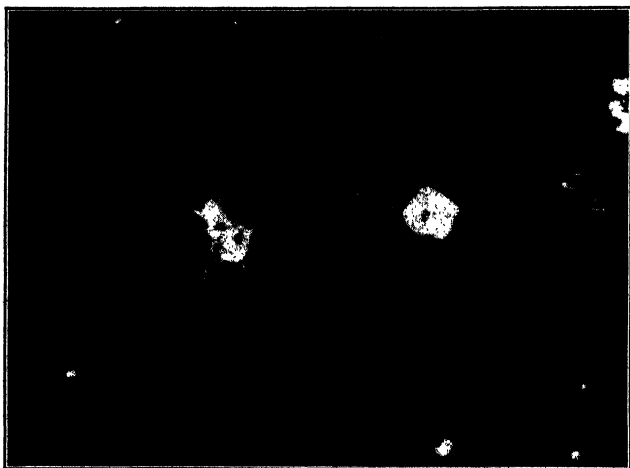
FIG. 32. Differentiation of radioactive and inert mineral grains. Dark-field illumination; magnification 310×. Showing a fragment of curite surrounded by alpha-particle tracks and an adjacent fragment of nonradioactive gangue associated with the mineral. Note minute grain in lower-right corner measuring about 3 microns, indicating its radioactivity by two emergent alpha-particle tracks.

The emulsion is softened by a brief immersion in distilled water, and the mineral grains are sprinkled over the moist surface. When on drying the gelatin resets the grains become embedded superficially and are not readily dislodged by subsequent photographic processing. After several days' exposure grains containing appreciable quantities of uranium or thorium are differentiated from the non-radioactive fragments by the development of a halo of radiating alpha-ray tracks, as illustrated in Fig. 32.

The number of tracks recorded about a grain is a complex function of its size, shape, activity, and the period of exposure. It is difficult to evaluate the uranium or thorium content from

the surrounding track count. As a qualitative test, however, the method is both sensitive and selective. A fragment measuring 10 microns in average diameter, containing about 50 per cent uranium, will record about 20 tracks per day of exposure. The isolated grain contains less than 10^{-8} g of uranium, and its activity would be difficult, if not impossible, to measure by electrical counting instruments.

By extending the exposure to 10 days, grains containing more than 1 per cent uranium, or equivalent thorium, can be detected readily in the presence of preponderant numbers of non-radioactive fragments. When the sample is composed of minerals of both low and high activity, the plate may record some random tracks originating from the decay of emanations. Non-radial tracks may also originate from alpha particles ejected from the upper portions of the larger grains and directed at small angles with the plane of the emulsion. As a lower limit, a grain is judged to be radioactive when at least two radial tracks are recorded around it.

The method is of practical application in the study of core drillings. The crushed sample is screened and a 80-on-100-mesh fraction is isolated for exposure. In order to facilitate microscopic examination, the sample can be concentrated by flotation methods. The heavy radioactive minerals sink in methylene iodide and are thus concentrated along with other heavy minerals. The heavy fraction is transferred to a filter and washed with successive portions of ether and methyl alcohol until freed from residual suspension fluid. A uniform grain dispersion on the emulsion surface is secured by the following procedure:

Support the plate in a petri dish half filled with distilled water. Shake about 20 mg of the mineral grains in about 3 ml of 50 per cent alcohol, and pour the mixture into the dish. Rock the vessel momentarily, and allow the grains to settle for about 1 min. Remove the plate, dry thoroughly, and expose for several days. It is good practice to prepare two slides, developing one after an overnight exposure and the other about 10 days later.

The slides are explored at low magnification so as to encompass an appreciable sample per field. Under dark-field illumination, alpha tracks are readily evident at 200$\times$ magnification. By focusing on translucent grains, colors and fracture can be noted, and these characteristics are of occasional aid in the identifica-

tion of species. Likewise, the grains can be observed in immersion fluids of known refractive index. In determining optical characteristics, it must be cautioned that secondary minerals of appreciable solubility become superficially altered during photographic processing. Refractive-index determinations must therefore be made on a separate slide. Other applications of nuclear-type emulsions in prospecting for uranium ores are described by Cüer [C32] and by Joliot-Curie.[J5]

STRUCTURE OF ALTERED MINERALS

The autoradiograph of a mineral surface serves as a representative measure of the distribution of the radioactive con-
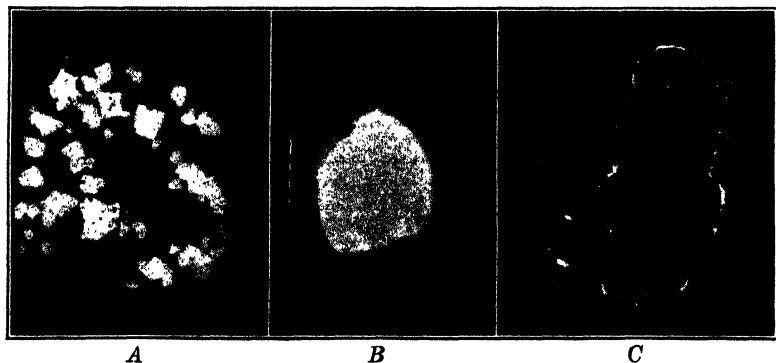
FIG. 33. Alpha-ray patterns of uraninite specimens. Reproduced as positive prints, about 1×.

A. Unaltered uraninite crystals in a feldspar matrix. Spruce Pine, North Carolina.

B. External alteration exhibited by a single crystal of uraninite from Morogoro, East Africa.

C. Highly altered uraninite nodule from English Knob Mine, Spruce Pine, North Carolina.

stituents within the mass. The pattern of unaltered specimens is one of essentially uniform photographic density. Altered minerals yield an image of variable blackness whose localized intensity is dependent on the composition of the hydrated or oxidized components. Typical patterns produced by unaltered and geochemically altered specimens of uraninite are compared in Fig. 33.

Radiocolloids are occasionally deposited along fine fissures of an altered mineral, and these produce an abnormally high photographic density along corresponding lines of the autoradiograph. The alpha-ray pattern reveals non-radioactive inclusions that are difficult to detect by visual inspection of the polished surface when they possess a color and luster similar to those of the matrix. These factors are of importance in the selection and sampling of specimens for their lead, uranium, and thorium contents when the data are to be employed in the estimation of the age of the mineral. The importance of autoradiography in this field of investigation is discussed in the work of Kovarik [K19] and Marble.[M6]

The nuclear emulsions are particularly suited for autoradiographic studies as their high resolving power permits detailed microscopic study of the resultant pattern.[Y10] The entire pattern can be enlarged 10-fold by the usual methods of projection printing. Also, small details of the primary alpha-ray pattern can be enlarged 200-fold by photomicrography.

Large polished slabs representing complete cross sections of the specimen are best employed, when ample material is available, as such sampling yields a complete pictorial representation of the surface variations in alpha-ray activity. Small chips selected at random during the preliminary stages of crushing are also satisfactory but require mounting in Bakelite. The duration of exposure varies with the activity of the minerals. Specimens containing 60 to 20 per cent uranium yield patterns of adequate contrast after 2 to 6 days' exposure.

ACTIVITY OF ROCKS

The distribution of radioactive components in specimens containing less than 1 per cent uranium is best determined by microscopic examination of the track population. The production of a visually discernible image on fine-grained emulsions necessitates impractically long exposure periods. Minerals with a T_α of 1 record over 86,000 tracks per cm^2 after a 24-hour exposure, and this population is ample for microscopic examination. By prolonging the exposure for 10 days, specimens containing only 0.1 per cent uranium provide a track population sufficiently dense for microscopic differentiation between solid solutions and states

of segregation. Clusters of alpha-particle tracks are readily evident at magnifications as low as 100×, and this permits a rapid survey of moderate-sized samples.

Visual impressions of the relative track abundance often suffice for the detection of marked variations in surface activity. A more satisfactory method is to plot the track count per field, at each 1-mm setting of the stage, on a suitably enlarged coordi-

(*a*) (*b*)
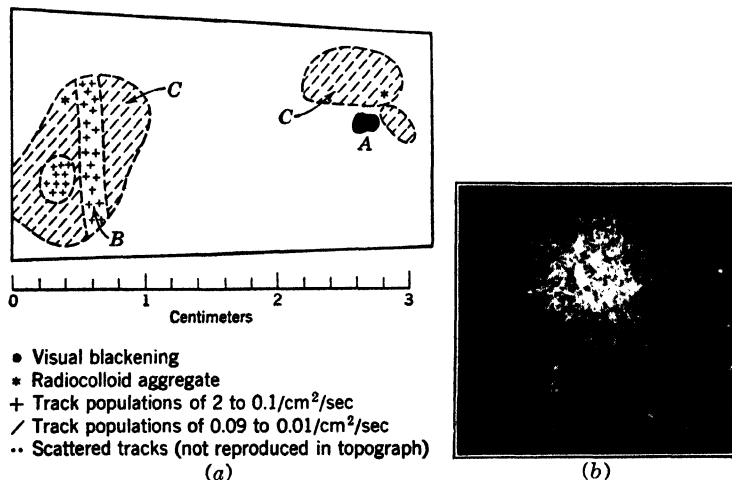
FIG. 34. Study of radioactive segregation in a beryl crystal.

a. Graphical distribution of segregates as observed microscopically in the alpha-ray pattern of a polished crystal face exposed for 858 hours.

b. Photomicrographic detail of a segregate in zone *B* of topograph. Dark-field illumination; magnification 58×. This inclusion measured 150 microns in diameter and possessed an activity of 2 tracks per cm^2 per sec.

nate scale. A topograph showing the track distribution in an emulsion exposed to one face of a beryl crystal is reproduced in Fig. 34. This study is of particular interest in revealing the presence of a minute grain of a radioactive mineral and zones of abnormally high alpha-ray activity within the beryl. Their presence probably contributes to the high helium content observed in many specimens of this mineral.*

* Beryl is composed of a large proportion of beryllium nuclei, and specimens containing localized alpha-ray-emitting elements constitute a natural neutron source of low activity. The formation of neutrons in certain beryllium minerals, such as gadolinite, from the $Be^9(\alpha n)C^{12}$ reaction has been considered probable by von Hevesy [V18] and Hahn.[H4]

By prolonging the exposure to 1000 hours the distribution of activity in normal rocks can be approximated. The interpretation of low track populations is rendered difficult by the simultaneous growth of background tracks. Rocks containing 10^{-12} g of Ra per g have nearly the same activity as the background, and the count is significant only when distinctive segregates are encountered. In an experiment with a cleavage plane of feldspar exposed for 858 hours, the track distribution was essentially uniform over the entire surface. After correction for background, the T_α of the crystal was 4×10^{-4}. In a low-power exploration of the plate several localized points of high activity were encountered. The pattern of the most pronounced point segregate is reproduced in Fig. 35. The tracks originate from an area less than 1 micron in diameter, and the event is indicative of radiocolloid deposition. These scattered points of high activity are probably responsible for the difficulties encountered in the sampling of powdered rocks for radium analyses.

FIG. 35. Radioactive point segregate in feldspar. Dark-field illumination; 110× magnification.

The track-counting technique has also been employed by Baranov and Kretschmer [B2] in the study of the activity of granites. The method has been extended by Baranov, Zhdanov, and Deizenrot-Mysovskaya [B4] to the localization of radium in sedimentary rocks and in plant tissues. The application of nuclear-type emulsions in radioactive studies of rocks has also been investigated by Joliot-Curie.[J5] In all these studies the activity of the polished slab of rock is computed by treating the specimen as an infinitely thick radioactive source with ¼ effective recording geometry. All investigators conclude that long exposures of several months' duration are essential and that the method is of primary utility for indicating uniform distribution or segregation within the sample.

An ingenious modification of the technique has been described by Hee [H41] which facilitates the correlation of track counts with specific min-

eral inclusions in the rock. A polished thin section about 30 microns thick is contacted with the emulsion for about three weeks. Just before development the unit is briefly exposed to white light. This causes the development of a superficial layer of fog beneath the transparent inclusions such as quartz, feldspar, and zircon and differentiates areas exposed beneath translucent or opaque components as biotite or hornblende. When the emulsion is examined with a sharply focusing objective the alpha-particle tracks can be discerned beneath the layer of optical fog. In a sample of granite studied by this method the alpha activity was found to be associated chiefly with the zircon inclusions.

CLASSIFICATION OF URANIUM AND THORIUM MINERALS IN POLISHED SECTION

Since the photographic density and the track count are quantitative measures of the uranium and thorium content, the emulsion technique permits a classification of the radioactive minerals based on their surface alpha activities. Though the track count provides an accurate activity measurement, its magnitude is only of limited application as a definitive index for species identification. The radioactive minerals are rarely of a fixed chemical composition but more often represent substitution systems of several elements of equal valence or similar ionic radius. The composition of an ideal unaltered crystal of uraninite is essentially UO_2 associated with variable quantities of radiogenic lead, depending on the age of the specimen. During its crystallization part of the UO_2 can be replaced by isomorphous ThO_2, as in the variety bröggerite. The alpha-ray activity of such crystals will be reduced owing to the slower decay rate of thorium. An even greater reduction in activity results from the substitution of CeO_2 and other rare-earth oxides, as in the varieties cleveite and nivenite.

The absence of radioactive equilibrium is a further factor limiting the utility of T_α as a species index. Complete equilibrium conditions are attained when the mineral has remained unaltered for 1,000,000 years. Minerals of recent geological origin exhibit activities intermediate between that of the pure parent elements and the total system of radioelements. As an example, radiochemically pure calcium uranyl phosphate has a T_α of 22, which increases to 136 when complete equilibrium with all members of the radium series is finally attained. The mineral autunite,

of identical chemical composition, usually exhibits T_α values ranging between 30 and 55, depending on age of the locality. Because of these limiting factors the method is serviceable only in allocating the primary radioactive minerals among several widely separated activity groups.

As all rocks contain minute quantities of radioactive elements it is difficult to draw a sharp dividing line between the radioactive and stable minerals. From an economic point of view the ore may be considered radioactive when the radioelements can be extracted profitably. This is dependent on the mode of distribution of the uranium and thorium. If held in solid solution within a refractory host these elements can be extracted only by costly chemical operations. When segregated, the radioactive grains can be concentrated by inexpensive flotation methods. In this respect, the emulsion is a unique tool for the determination of the state of dispersion of the radioactive components.

When radium was the element of primary interest, carnotite beds containing about 0.2 per cent U_3O_8 were considered workable ores, before the discovery of the pitchblende deposits in Belgian Congo and Canada. In seeking sources of uranium for atomic piles, shales containing only 0.02 per cent uranium may be considered as potential ores. Minerals containing about 1 per cent uranium (T_α = 1.3) or thorium (T_α = 0.4) may thus be considered as distinctly radioactive and of economic importance if the grains can be concentrated readily from extensive deposits. The alpha-ray pattern is made by the dual exposure technique. In low-grade ores the radioactive mineral grains are of small dimensions, but the activities of individual grains can be estimated from the track count when their diameter exceeds 0.3 mm.

About 150 radioactive mineral species have been described in the mineralogical literature. Extensive tabulations of these minerals have been compiled by Szilard,[S47] Holmes,[H133] and more recently by Yagoda.[Y10] Most species are of extreme rarity and have seldom been found in more than one locality. The more common minerals are listed in Table 23, with activity ranges measured in samples from different geologic localities. The surface activities are serviceable in identification of the species in polished section when employed in conjunction with chemical and optical tests.

TABLE 23. CLASSIFICATION OF COMMON RADIOACTIVE MINERALS

Mineral	Ideal Composition	Color	Hardness	Measured T_α*
Uraninite	UO_2 + var. Pb	Black	5–6	215–160
Bröggerite	$UO_2 + ThO_2$ + var. Pb	Black	5–6	170–160
Cleveite	UO_2 + rare earths	Black	5–6	176
Pitchblende	U_3O_8 + var. Pb	Black	5–6	186–140
Gummite	$UO_3 \cdot nH_2O$	Orange	2–5	135
Clarkeite	Sodian gummite	Brown	4	155
Curite	$2PbO \cdot 5UO_3 \cdot 4H_2O$	Orange	4–5	134
Soddyite	$12UO_3 \cdot 5SiO_2 \cdot 14H_2O$	Yellow	~4	115
Vandenbrandite	$CuO \cdot UO_3 \cdot 2H_2O$	Dark green	3–4	115
Thorianite	ThO_2 + var. Pb	Black	6	111–76
Uranophane	$CaO \cdot 2UO_3 \cdot 2SiO_2 \cdot 6H_2O$	Yellow	2–3	97–50
Torbernite	$CuO \cdot 2UO_3 \cdot P_2O_5 \cdot 8H_2O$	Green	2	97–82
Carnotite	Vanadate of U + K	Yellow	Soft	48–29
Autunite	$CaO \cdot 2UO_3 \cdot P_2O_5 \cdot 8H_2O$	Pale yellow	2	55–40
Betafite	Multiple oxide †	Brown	4–5	29
Uranothorite	Silicate of Th + U	Orange	5	25–15
Ferrothorite	Ferrian thorite	Reddish brown	4½	18
Samarskite	Multiple oxide	Dark brown	5–6	21–15
Euxenite	Multiple oxide	Brown	5–6	24–16
Priorite	Multiple oxide	Black	5–6	20–8
Polycrase	Multiple oxide	Brown	5–6	12
Fergusonite	Multiple oxide	Brown	5–6	12
Eschynite	Multiple oxide	Black	5–6	10
Monazite	Rare-earth phosphate	Brown	5	7–4
Microlite	Multiple oxide	Brown	5	1.6
Allanite	Cerian epidote	Black	5–6	0.8–0.2
Kolm	Hydrocarbon	Black	Soft	0.3

* Ranges indicate extreme values observed in specimens from two or more localities.

† Multiple oxides are composed of Cb, Ta, and Ti with variable quantities of UO_2, ThO_2, rare earths, and other metallic oxides.

The morphology of the alpha-ray pattern is occasionally of aid in the differentiation of pitchblende from uraninite. This mineral appears to have been deposited from colloidal dispersions of uranium oxides. As a consequence, specimens of pitchblende frequently exhibit botryoidal, colloform, cellular, and spherulitic forms typical of the slow solidification of solids from a gel state. These structures differentiate pitchblende from the crystalline radioactive minerals found in pegmatites. The structures are usually visible when the polished section is examined

by vertical illumination, but they are revealed in greater contrast and more specifically in the autoradiograph. Iron and manganese ores, occasionally associated with pitchblende, also exhibit colloform structures. Typical colloform structures revealed by the alpha-ray patterns of pitchblende are reproduced
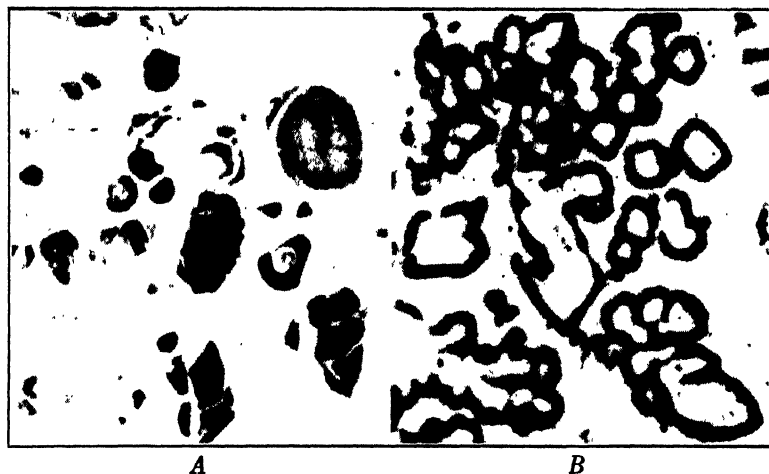
Fig. 36. Colloform structures in pitchblende. Enlargement prints (10×) of details from the alpha-ray pattern.

A. Colloform fragments dispersed in hematite in a sample from Hottah Lake, Canada.

B. Spherical shell deposition (ring cross sections) in a dolomitic pitchblende from the Great Bear Lake, Canada, deposit.

in Fig. 36. The type structures are not always present in small-sized polished sections. They are more conspicuous in samples from the Canadian and Joachimsthal deposits than in those from the Belgian Congo.

Chapter 8 · ALPHA TRACERS IN CRYSTALLOGRAPHY AND METALLURGY

It is possible that the nuclei of radioactive atoms composing a crystal may be oriented in space under their mutual forces. If this be the case, some asymmetry in the emission of alpha particles might be expected.—Rutherford, 1930

SPATIAL ORIENTATION OF RADIO IONS IN CRYSTALS

The visualization methods described in the study of radioactive minerals are also applicable to synthetic crystals isolated from solutions or melts. Crystals are grown by mixing a nearly saturated solution of the matrix compound with minute amounts of radioactive ions and allowing the solvent to evaporate slowly in order to favor the growth of a few large crystals. The concentration of the radioactive components is adjusted in accord with their disintegration rates. A suitable ratio of active to inert atoms can be approximated by assuming a uniform distribution in the crystals and adjusting the concentration of the tracer atoms so that the final preparation has a T_α of about 200.

Crystals are removed from the mother liquor, at successive stages of growth, with the aid of thin paraffined slats, and are freed from adhering liquid by being rolled over filter paper. Autoradiographs of flat crystal faces can be made by direct contact with the emulsion. The crystals can also be embedded in paraffin wax, as described in Chapter 3, and a pattern secured of the oriented polished cross section.

The surface activity may be perfectly uniform, as in a homogeneous crystal of uranyl sulfate, or when the admixed radio ion enters into solid solution with the host, as occurs when lead nitrate separates from solutions containing RaD. More often, however, the activity will be discontinuous and a series of symmetric depositions outlining growth zones will be observed. The character of the pattern is dependent on the nature of the tracer ion, matrix composition, and rate of crystal growth, and it is

probably further influenced by the presence of traces of other non-radioactive ions in the solution.

The technique of crystal autoradiography has been employed extensively by Hahn and his collaborators [H2,3] in the elucidation of coprecipitation mechanisms. By incorporating several radioactive species into the same salt solution it is possible to study the orientation of each one by making successive exposures of
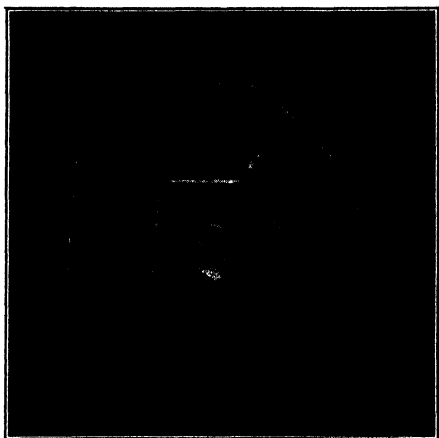
FIG. 37. Deposition of polonium in a crystal of ammonium bichromate. Positive print of alpha-ray pattern, enlarged about 3×.

the crystals at intervals commensurate with the disintegration rates of the tracers. Crystals of potassium sulfate grown in the presence of ThB-lead, ThX-radium, and RaF-polonium exhibit markedly different depositions of the respective tracer ions. The lead isotope is distributed uniformly throughout the crystal lattice, whereas the radium and polonium concentrate in the crystal core. The identical behavior is exhibited when these three radioelements are incorporated in other crystals, such as rubidium sulfate, which are isomorphous with potassium sulfate.

Crystals of ammonium bichromate grown in the presence of polonium usually exhibit marked variations in cross-sectional surface activity, as indicated by the alpha-ray pattern in Fig. 37. The nuclear-type emulsions permit detailed microscopic study of the crystal autoradiographs.[Y18] An enlarged detail from the alpha-ray pattern, reproduced in Fig. 38, shows that some polo-

nium was incorporated in the lattice throughout the growth of the ammonium bichromate, but that a preferential deposition of the tracer occurred periodically.

Similar studies can be made on crystals isolated from cooling melts and in investigations of ion exchange between a preformed crystal and a solution carrying radioactive isotopic ions. Studies have been reported by Schwab and Pietsch [S12] on the adsorption
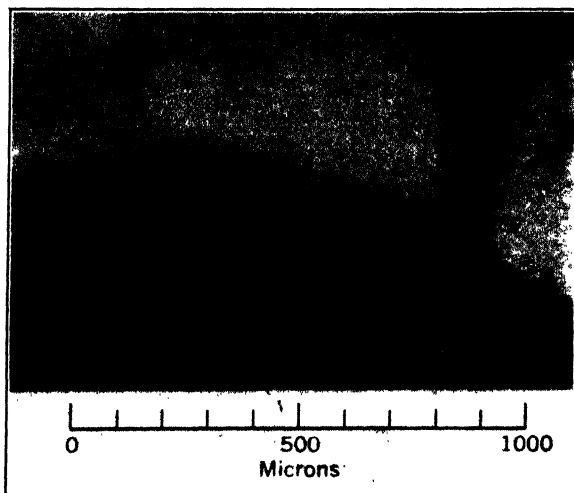
FIG. 38. Detail from alpha-ray pattern of ammonium bichromate crystal. Transmitted light; magnification 58×. Note segregation of polonium in fine bands 50 to 80 microns wide.

of active lead by crystals of lead chromate. The ThB ions employed as tracers were found to concentrate selectively on the corners of the crystals. That kinetic exchange occurs only at privileged positions on the outer face of the crystal was also observed by von Hevesy and Paneth.[V14] Activity measurements revealed that the number of molecules taking part in the exchange was distinctly smaller than the number of molecules present on the outside layer of the crystals. Autoradiographs of the crystals demonstrated that the exchanged radioactive atoms were situated almost entirely at certain crystal edges.

Hahn, Käding, and Mumbrauer [H2] have conducted extensive studies on mixed crystal formation. They studied the separation of barium and radium bromides, barium and lead chlorides, and

the adsorption of lead by silver and alkali halides. From the autoradiographic patterns produced by the crystals Hahn [H8] distinguishes between (*A*) normal and anomalous mixed crystals and (*B*) accidental adsorption inclusions. Members of class *A*, such as barium and radium bromides, produce patterns indicating that the ions form mixed crystals or systems resembling mixed crystals. In class *B* the radioelement is occluded by the host erratically, chiefly in the form of radiocolloid aggregates. This type of accidental inclusion is exhibited by barium bromide grown in the presence of ThB, and by hydrated crystals of copper sulfate isolated from solutions containing polonium.

The patterns produced by members of class *A* vary with the rate of crystallization. When small crystals separate rapidly from supersaturated solutions, the trace constituent is distributed uniformly. Slow crystallization promotes the formation of heterogeneous mixed crystals exhibiting zonal growths. Large crystals of $BaBr_2 \cdot 2H_2O$ grown by Marques [M11] from a slowly evaporating solution of barium and radium bromides exhibit very pronounced variations in the zonal deposition of the radium.

SPATIAL ORIENTATION IN MINERALS

Radioactive minerals of the columbium-tantalum group occasionally produce alpha-ray patterns simulating the characteristics of synthetic heterogeneous mixed crystals. The mineral crystals have a more complex composition than the laboratory preparations and differ in that the uranium and thorium serving as indicators are principal and not trace components of the lattice. Examples of selective concentration of the radioactive constituents within particular form loci in crystals of blomstrandine, polycrase, and fergusonite are described by Frondel.[F17] The compositional variations are usually not visible in the oriented polished section, but are revealed clearly in the autoradiographs.

Striking examples of spatial orientation in crystals of samarskite have been described by Yagoda.[Y15] A typical autoradiographic pattern is exhibited in Fig. 39. A chemical analysis of the specimen revealed an average content of 11.3 per cent U_3O_8 and 0.8 per cent ThO_2. The polished surface of the samarskite, exceeding 25 per cent between extreme zones, was essentially homogeneous and showed no visual evidence of the activity

variations. Since the uranian columbium-tantalum minerals are almost invariably in the metamict state,* the evidence of crystallinity revealed by the alpha-ray pattern indicates that

FIG. 39. Alpha-ray pattern of samarskite from Mitchell County, North Carolina. Positive print; reproduced approximately full size. Specimen loaned for study from Brush Mineral Collection, Yale University.

the mineral developed initially as an anisotropic crystal and has since become amorphous, possibly as a result of prolonged bom-

* Metamict is a term ascribed to certain minerals that possess external crystalline form but which prove to be amorphous when examined by x-ray diffraction or optical methods. These minerals usually have a complex composition, with tantalum, columbium, titanium, and members of the rare earths as the chief constituents. Minerals in the metamict state frequently contain uranium and thorium in tangible quantities or are found associated with strongly radioactive minerals. The metamict minerals have been studied extensively by Goldschmidt,[G14] who concludes that the presence of radioactive constituents is not the primary cause of the crystal-structure destruction, but that a rearrangement of the outer electrons takes place in crystals composed of weak acid and weak basic

bardment of the lattice and the recoil of atoms from the decay of uranium and thorium.

ACTIVITY OF CRYSTAL FACES

Experiments have been instigated to determine whether the rate of alpha-particle emission is the same from different faces of homogeneous radioactive crystals. Merton [M24] measured the ionization produced by the alpha and beta radiations from three faces of a large crystal of uranyl nitrate but was unable to observe any certain difference in activity. Using the scintillation method which avoids interference by beta particles originating from the interior of the crystal, Mühlestein [M34] observed different rates of alpha-particle emission from the three faces in the ratio of 1.00:1.09:0.68. This observation has not been confirmed by modern alpha-track-counting methods:

The rate of emission of alpha particles from different faces of radioactive crystals has been investigated by Mather and Kurie.[M45] Using a parallelepiped crystal of thorium sulfate about 2 mm along the edges, the activity of three crystallographically different sides was measured by counting alpha-particle tracks. The sides of the crystal were exposed against an Ilford C2 plate, avoiding direct contact with the emulsion by means of a thin layer of plastic drilled with an opening 0.04 in. in diameter. The difference in tracks per unit area among the faces was found to be within the statistical fluctuations of the number of tracks counted (about 800 per surface).

Poole and Bremner [P38a] also failed to observe a significant variation in the track count using a crystal of uranyl nitrate. They are of the opinion, however, that nuclei possessing nuclear spin and magnetic moment are not spherically symmetrical but have definite axes of symmetry. Because elements of even atomic number and mass as U^{238} and Th^{232} have zero spin and magnetic moment these nuclei should have no effect on the rate of disintegration in oriented media. On the other hand, nuclei such as U^{235}, U^{233}, and Pu^{239} possess a spin greater than zero, and crystals enriched in these isotopes might show an asymmetry in the rate of alpha-particle emission from crystallographically different faces.

---

constituents. Thus, bröggerite, thorianite, and monazite remain crystalline owing to their strong lattice binding despite the high uranium or thorium contents. When the structure is initially weak, as in minerals containing the $Y^{+++}CbO_4^{\equiv}$ grouping, they become amorphous because of degeneration into a solid solution of $Y_2O_3 \cdot Cb_2O_5$. Though weakness of the chemical bonds is a prerequisite, the change to the metamict state is probably accelerated by radioactive radiations.

APPLICATIONS IN METALLURGY

Shortly after the discovery of radioactivity Moissan [M27] prepared uranium metal in a pure form by electrolysis of fused uranium and sodium chlorides. The activity of this preparation was studied by Becquerel,[B11] who observed that the metal, like all its compounds, blackened photographic plates and concluded that the phenomenon was therefore an atomic property.

Polished sections of metallic uranium and thorium have T_α values of 59 and 25, respectively. On nuclear-type emulsions visual images are recorded after exposures of 2 or 3 days. Microscopic survey of the pattern produced by uranium metal revealed occasional minute areas devoid of tracks.[Y17] Corresponding areas of the metal, examined under vertical illumination, showed the presence of non-metallic inclusions which probably originated from the crucible from which the molten metal was poured.

Autoradiography of Alloys. Tammann and coworkers [T2,3] have studied methods for the introduction of traces of highly active radioelements into alloy systems. They found that an electrolytic deposit of polonium on a thin metallic foil can be incorporated into molten metals without marked loss due to volatilization if heating is not prolonged after the liquefaction of the foil. Tammann has studied alloy systems composed of copper, silver, antimony, bismuth, zinc, cadmium, tin, and tellurium admixed with polonium. The polonium exhibits only a very small solubility in these metals. The saturated solid solutions contain between 2.31×10^{-13} and 5.28×10^{-12} g of Po per g of alloy, necessitating exposures of about 3 days for the formation of visually discernible images.

The method has found practical application in the incorporation of polonium in nickel alloys intended for use as sparkplug electrodes. Dillon and Street [D10] found that 94 per cent of the polonium introduced into a molten nickel-manganese alloy remained in the metal after its solidification. Their procedure is to deposit the polonium on nickel foil attached to a nickel stirring rod and to plunge the deposit into the center of the melt. The resultant mix is poured about 1 min after the immersion of the foils. Comparative alpha-ray patterns of the casting and of the

wires drawn from it show that the polonium is distributed uniformly in both.

Tammann and Bandel [T5] have studied primary crystallization, segregation, and grain growth in several metals using ThB as a tracer. This isotope is introduced into the alloy system by exposing one of the metallic components to thoron and collecting the active deposit on the surface.* The metallic foil is charged negatively to a potential of 220 volts and exposed for about 2 days to the thoron emanating from about 1 mg of RdTh. This foil is melted together with other components of the system in an atmosphere of hydrogen. The castings are polished, without prior etching, and exposed photographically. ThB decays with the emission of beta particles, but the daughter elements are short-lived and eject alpha particles. This permits the use of high-resolution nuclear-type emulsions as recording media. As ThB is comparatively short-lived the sections must be exposed within 24 hours after the melt is cast.

ThB is not miscible with iron and is forced into the grain boundaries when the alloy solidifies and remains there owing to its low diffusibility. Autoradiographs of the polished surface, examined at about 60×, reveal the outlines of austinite grain boundaries. At the completion of the photographic exposure, the specimen can be etched in order to reveal the ferrite and pearlite structures. Although the austinite grain size can also be revealed microscopically, Tammann finds the radiographic method more reliable as etching and staining reactions are very sensitive to localized metallic couples, which fact renders the test uncertain.

Tammann and Bandel [T4] have also applied this method in studying the recrystallization of cadmium, tin, and zinc, and found that the initial grain structure is revealed autoradiographically by the ThB concentrated between grain boundaries. Grain growth at temperatures below the melting point can be investigated by making successive exposures after each thermal treatment. Similar studies have been made by Werner,[W8] employing ThX as indicator, in the recrystallization induced in zinc, alumi-

* In a series of investigations on the emanating power of metals Werner [W9,10] incorporated minute amounts of radioactive material into metals by evaporating neutral radium salt solutions on the metallic chips and heating them in a current of hydrogen at 750° to 1000° C.

num, and thallium as a result of cold working of the metals. Werner observed a change in the relative rate of alpha-particle emission following cold working which parallels the change in density effected in the alloy.

When ThB is alloyed with pure lead the composite solid produces a uniform autoradiographic pattern. Perfect solid solution also results when ThB is alloyed with thallium. In magnesium, however, the tracer is distributed discontinuously, but the aggregates of ThB disappear when the section is annealed. Segregation also occurs when ThB is incorporated in molten bismuth, tin, antimony, silver, copper, or gold. In each of these alloys the radiographic pattern is characterized by dendritic structures. Cadmium likewise exhibits a dendritic pattern, which disappears after annealing, thereby proving that lead is slightly soluble in cadmium.

In a series of investigations on the distribution of ThB in several metals Seith and Keil [S20] found that an alloy composed of Cd + Pb + ThB prepared by electrolysis of the mixed chloride salts also furnished a melt that exhibited a concentration of ThB along grain boundaries. This occurred even when the total amount of ThB + Pb was less than the saturation solubility of lead in cadmium. In complex alloys such as steel the ThB tends to dissolve preferentially in oxide, sulfide, and phosphide liquid inclusions. On solidification these compounds segregate between dendrites and grain boundaries and thereby produce an autoradiographic pattern depicting the primary casting structure.

Diffusion Processes in Metals. The self-diffusion of a layer of molten radiolead into a column of stable lead at 340° C was first demonstrated by von Hevesy. Diffusion processes in metals at room temperature can also be studied by employing scintillation screens or fine-grained emulsions as counters. The diminution in the number of alpha particles, as the superimposed layer of active material penetrates into the solid, serves as a measure of the diffusion. By depositing a thin layer of RaD on lead foil the self-diffusion can be traced by the polonium alpha particles associated with the chain of disintegrations from RaD to RaG.

Seith and Keil [S19] have measured self-diffusion coefficients of only 10^{-7} cm^2 per day using ThB as indicator and measuring the diminution of the alpha-ray activity from ThC + ThC′ as the

lead isotope diffused into its support. In single crystals of lead warmed to 182° C the coefficient of self-diffusion was found to be 4.12×10^{-8} cm² per day. The sinking of ThB into lead has also been measured by von Hevesy and Obrutscheva [V11] by observing the diminution in the scintillation count from the ThC + ThC′ in equilibrium with the tracer.

The emulsion technique is particularly effective in studying the penetration of surface deposits of alpha radiators into metallic foils. Montel [M28] has observed that, when polonium is deposited electrolytically on the upper surface of a lead foil, successive photographic exposures against the lower surface reveal the gradual penetration of the element through the thickness of the sheet. The pattern produced by the surface opposite the deposit is discontinuous, the blackening being composed of a network outlining crystal grains. The thickness of the lead foils employed by Montel measured between 40 and 100 microns, in considerable excess over the effective range of alpha particles originating from the upper polonium deposit. The penetration of the thinner foils is evident within 24 hours after the initial deposition. The results cannot be attributed either to normal diffusion or to contamination by creeping. Montel's foils were opaque to light, and supported a vacuum of 0.01 cm of Hg. Montel attributes the localized penetration of the polonium to an etching effect on the grain boundaries by the hydrochloric acid present in the electrolyte at the time of polonium deposition. The rapid penetration of the foil is not produced when the polonium is deposited on the lead by sublimation.

Creeping of Radioactive Sources. The rapid surface migration of polonium and several other radioactive elements from their site of deposition cannot be attributed readily to the dragging of source atoms by ejected alpha particles or recoil atoms. The migration is readily revealed by exposing an emulsion against surfaces adjacent to the source. The pattern usually exhibits multiple-track formations indicative of the mass movement and point aggregation of very large numbers of polonium atoms.

A potential explanation of this puzzling behavior is offered by experiments on the lateral surface diffusion of radioelements over metallic foils. Seith and Aten [S18] deposited ThB on a confined area of a platinum foil. A radiograph of the initial deposit exhibited homogeneous distribution over a sharply defined area.

After heating the platinum to 550° C, radiographs of the foil showed partial aggregation in the initial deposit and intense black spots on the platinum surface where no ThB was originally present. On heating to 700° C the initial uniform background disappeared, and the ThB was detected as scattered aggregates on the remote portions of the foil. It appears therefore that during the heating the volatilized atoms agglomerated while in the gaseous state and condensed on the cooler portions of the platinum surface. Schwarz [S13] has studied the lateral and depth penetration of polonium deposited at one end of a silver foil. At temperatures between 100° and 300° C surface diffusion is detected photographically by comparing the patterns made after initial deposition and after 2 days' warming. During this period no depth penetration of the polonium was observed unless the silver was heated to about 500° C.

These experiments indicate that the "creeping" of polonium sources may have its origin in an appreciable vapor pressure of the metal at room temperature.* Seith and Aten [S18] have observed that when ThB is deposited on quartz glass the heating process does not cause aggregation or migration and suggest the formation of a non-volatile lead silicate.

DIFFUSION IN POROUS MEDIA

The autoradiographic technique has also been applied successfully in the study of the diffusion of radioactive ions dispersed in gelatin. The method was initiated by Veil [V2] in the investiga-

* Polonium is homologous with sulfur, selenium, and tellurium. The vapor pressure of sulfur at 50° C is 0.0002 mm of Hg. At room temperature it is even lower; nevertheless, the escape of sulfur vapor can be demonstrated by delicate chemical reactions. By exposing a clean copper foil at a distance of 1 mm for 24 hours above the polished surface of a sulfur crystal, a visible stain of copper sulfide is produced. The diffuse image on the copper outlines the shape of the sulfur surface, and is proven to be copper sulfide by its solubility in potassium cyanide solution. Certain minerals containing excess sulfur, like pyrrhotite $Fe_{1-x}S$, also exhibit an appreciable volatilization of sulfur. These delicate chemical reactions indicate the volatilization of 10^{16} sulfur atoms per cm^2 per day.[Y17] Since 10^6 polonium atoms per cm^2 can be detected photographically, the creeping of polonium is explicable on the basis of volatility even if its vapor pressure is many magnitudes lower than that of sulfur.

tion of ionic diffusion from the site of chemical precipitation and also in the visualization of the flow of radioactive ions during electrolysis. The method is essentially a chromatographic adsorption process, in which the several zones of adsorbates are rendered visible by their photographic action on superimposed photographic emulsions.

As an example of the procedure, if a drop of barium and radium chlorides is deposited on a gelatin-coated paper impregnated with oxalic acid, a precipitate of barium oxalate forms at the point of contact, and the soluble components diffuse in circular rings in the lateral plane of the gelatin. A contact autoradiograph of the dried paper reveals the relative distribution and fractionation of the radium in the precipitate and in the migratory zones.

Migration of ions during electrolysis is likewise studied by coating a glass slide with a solution of barium and radium chlorides in gelatin and allowing it to gel. A potential of 10 volts is applied across opposite platinum electrodes causing the electrolytic migration of the metallic ions toward the cathode. Comparative autoradiographs made before and after the electrolysis show that the initial uniform distribution of the traces of radium is altered, and that zones of high activity accumulate towards the negative electrode.

These methods can also be employed in conjunction with beta-ray-emitting isotopes as the autoradiographic tracers. The method has been investigated by Fink and Dent [F9] as a means of differentiating inorganic iodide and organically combined derivatives such as diiodotyrosine and thyroxine. A drop of the test solution is extracted from an animal organ following injection and equilibration of the radioisotope. This is allowed to diffuse slowly over the surface of a filter paper. Owing to preferential adsorption by the cellulose fibers the components of the solution separate along individual circular zones. Contact autoradiography of the dried sheet reveals the location of the bands containing the active compounds.

The method is essentially a chromatographic adsorption process utilizing a paper sheet instead of the more common column of finely divided aluminum oxide.* When using stable isotopes

* Two-dimensional chromatographic analyses can also be made with the aid of thin plane castings of plaster of Paris. Methods for the preparation

the position of the bands is revealed either by color reactions or by differential fluorescent response to ultraviolet light. The use of radioactive isotopes extends the method to the separation of colorless compounds that do not fluoresce or form colored derivatives with analytical reagents.

of sheets free from air bubbles and ones containing special adsorbents such as calcium carbonate and aluminum oxide have been described by Yagoda.[Y7]

Chapter 9 · BIOLOGICAL APPLICATIONS OF ALPHA-PARTICLE TRACERS

Nucleonics, the science of the atomic nucleus, is only in its infancy. The more it is pursued, the more chance there is for accidents and the more need therefore of a better understanding of the bio-medico-physical problems.—R. S. Stone, 1946

The localization of ingested radioactive elements by autoradiographic study of the tissue has been applied extensively since the conception of the technique * by Lacassagne.[L1] A suitable dose, varying with the activity of the radioelement, its toxicity, and the weight of the animal, is injected intravenously. After a suitable period of equilibration tissue blocks of the several organs are prepared. The autoradiographs are made by exposing the surfaced paraffin blocks or thin sections thereof with fine-grained emulsions. The thin sections can also be mounted as an integral part of the emulsion and stained after development. Technical details of these methods are described in Chapter 3.

Sections having a T_α of about 100 produce visually discernible images on nuclear-type emulsions after an exposure of 2 or 3 days. This surface alpha-ray activity corresponds to a concentration of 5 microcuries per cm^3 of tissue. The dosage is readily achieved without loading the tissue excessively when the tracer atoms are short-lived. Thus, tissue containing 10^{-9} g of Po per cm^3 will produce a black image after an exposure of 1 day. The more stable elements, such as uranium or thorium, cannot be employed as tracers for visual autoradiography, as the necessary dosage would prove fatal to the animal.

The localization of the more stable elements can be studied, however, by prolonging the exposure and preparing a topograph

* Shortly after the discovery and isolation of radium, photographic emulsions were employed to detect radioactivity in intact animal organs. These images were necessarily diffuse and served only as a qualitative test for the presence of the ingested material. London [L37] and Kotzareff [K18] published crude autoradiographs showing the activation of tissue by radon and radium.

of track disposition. Also, the sensitivity can be increased by the microincineration of thick tissue sections (25 microns) and by exposing the resulting spodogram. This process removes the organic matter and in soft tissues effects a marked increase in the specific activity of the residual ash. The inorganic matter coalesces to a thin film without appreciable lateral distortion, and the emergent alpha particles record tracks of very nearly full energy.

Alpha particles produce intense localized ionization in traversing the tissue. According to Lea [L24] the ionization effects on certain cell structures can be observed microscopically. If the particular structures traversed are sufficiently vital for changes in them to affect the cell as an entity, a biological change will be produced by the passage of even a single densely ionizing particle. When elements emitting alpha particles are employed as tracers, a destructive action on the tissue may occur, particularly at the site of radiocolloid aggregation.

In his studies on the localization of polonium, Lacassagne has observed that the alpha particles exert a destructive action on lymph nodes and bone marrow. With increasing alpha activity cell formation is temporarily inhibited in the red and white hematopoietic series, and lymphocytes are destroyed by the localized radiation in the stroma cells. The destruction of the germinal elements in seminal tubules is also attributable to alpha-particle bombardment.

LOCALIZATION OF LEAD

There are no isotopes of lead which decay with the emission of alpha particles. Tracer studies are made with ThB or RaD which, by successive beta decay, lead to the formation of ThC and RaF respectively. These daughter products emit alpha particles and serve as secondary recording agents of the site of lead deposition. The range of the recoil atoms in tissue is about 0.1 micron. Hence the alpha tracks are not displaced appreciably from the position of the original lead isotopes. ThB has a half-life of only 10.6 hours, and the exposure of the tissue cannot be delayed for more than about 1 day. The longer life of RaD makes its application practical in studies of the accumulation of traces of lead over extended periods of ingestion.

ThB is prepared by collecting the active deposit of thoron on a thin lead foil charged negatively with respect to a metal disk carrying an emanating RdTh preparation. At the end of 2 days the foil is dissolved in nitric acid, excess acid is removed by evaporation, and the lead nitrate is diluted with water to a 0.5 per cent concentration.

A weak preparation of RaD, with admixed stable lead isotopes, can be prepared by separating lead sulfide from solutions of pitchblende. The sulfides are dissolved in dilute nitric acid and purified from polonium by the rotation of a silver disk in the solution for about an hour. Silver ions are removed by precipitation as silver chloride, and the lead is finally converted to lead chloride by repeated evaporation with concentrated hydrochloric acid. A more active preparation is obtained by extracting old radon needles with nitric acid. The accompanying RaE and RaF are separated by electrolytic deposition on plates of nickel and silver.

The distribution of lead in animal tissue has been studied by Behrens and Baumann,[B14] employing ThB as indicator. The lead solution was injected intravenously and autopsy performed about 1 hour later. In order to retain the activity a hurried fixation procedure was employed:

Dehydrate the tissue in three changes of alcohol at 60° C, employing concentrations of 70, 96, and 100 per cent ethyl alcohol and an immersion period of 30 min in each bath. Rinse tissues for 5 min in a mixture of absolute alcohol and acetone at 30° C, then for an equal period in pure acetone, and finally clear in xylol for 15 min. Infiltrate with paraffin and prepare sections 20 microns thick.

The autoradiographs produced by 2 days' exposure revealed that the greater part of a tracer dose of lead accumulated in the kidney, liver, and spleen. The patterns showed some deposition in bone, but no lead accumulation in skin, muscle, fatty tissue, or brain. Experiments on young animals showed a deposit of radiolead in newly formed bone, but none in compact bone or cartilage. In animals kept on a rachitic diet the lead replaced the calcium phosphate compound present in the subepiphyseal and subperiosteal areas.

Cittmar[C16] has investigated the distribution of lead in tumorous mice with the aid of the ThB isotope. The lead was absorbed chiefly in the kidney, liver, spleen, and bones. Autoradiographs of the tumorous tissue revealed a very low concentration of lead as compared with the normal tissue. A comparative study of the distribution of ThB and the radium isotope ThX has been made by Wolf and Born.[W25] The autoradiographs of the rat

organs revealed a markedly different distribution of the lead and the radium.

Lomholt[L36] has investigated the distribution of lead in rats, using RaD as the indicator. The animals were injected with 0.05 ml of a 0.33 per cent solution of Pb + RaD chlorides per 10 g of body weight. Sections of the viscera 20 microns thick were prepared 24 hours after the lead administration and exposed for 3 weeks. As in the earlier work with the ThB isotope, the resultant patterns showed pronounced accumulations of lead in liver, spleen, and kidney, and to a lesser extent in pancreas and muscle. Lead was also observed in the bones, particularly in the bone layer adjacent to the periosteum.

LOCALIZATION OF BISMUTH

Bismuth is represented by one alpha-emitting isotope ThC. Its use as a tracer is impractical because of its short life. Biological studies on the ingestion of bismuth have been made with RaE which decays by beta emission to polonium. The alpha particles from this disintegration product are serviceable in the photographic localization of the parent atoms.

The RaE is isolated from the active deposit in old radon tubes. The nitric acid extract contains RaE together with RaD and some RaF. About 50 mg each of lead and bismuth ions is added as carriers. The accumulated polonium is removed electrolytically on copper foil. The lead is removed by precipitation as lead sulfate. The acid filtrate is made strongly ammoniacal, and the washed bismuth hydroxide is redissolved in an organic acid for purposes of injection.

The absorption of bismuth by cancerous and normal tissues has been investigated by Kahn,[K2] Lacassagne and Loiseleur,[L9] and Lacassagne and Nyka.[L10] Mice with spontaneous tumors and rabbits grafted with Brown-Pearce tumor were injected with solutions of bismuth containing RaE. Lacassagne found that the bismuth distributed itself in essentially the same way as in animals injected with polonium. The kidney and spleen collect the largest amount of bismuth. Of the remaining organs, liver shows the greatest activity.

Malignant tumors retain a variable amount of RaE, depending on the histological group to which they belong, but always in smaller amounts than the normal organs. Lacassagne ob-

served that the retention of the bismuth isotope in the kidneys and hematopoietic organs produced a change in the general health of the animal accompanied by an important decrease in the number of formed elements in the blood and eventually caused nephritis. The toxic doses of Bi + RaE failed to bring about any regression of the malignant tumors.

LOCALIZATION OF POLONIUM

The ready isolation of polonium from other radioactive elements coupled with its moderate half-life has made RaF the subject of numerous autohistoradiographic studies. There are no stable isotopes of this element and the tracer experiments with RaF do not furnish information on the mode of segregation of any familiar heavy metal. The element is homologous to selenium and tellurium, and the results obtained with RaF may be indicative of the type of distribution of these elements in animal systems.*

In order to minimize radiocolloid deposition on the walls of the storage vessel, polonium solutions are usually strongly acid. A solution suitable for injection into animals is prepared by diluting 0.5 ml of a RaF stock solution (1 millicurie per ml of 1 + 1 HCl) with 1 ml of water. The solution is neutralized by the addition of solid sodium bicarbonate, until in excess, and is then diluted to a total volume of 2.5 ml. Intravenous injection of 0.25 ml per 10 g of body weight provides a dosage satisfactory for autoradiography.

The localization of polonium in animal organs has been studied extensively by Lacassagne and collaborators[L1,2,4,5] and by Lattes.[L18,19] After administration some polonium is found in all the organs but is deposited in greatest abundance in the kidney, liver, and spleen. Cotelle[C22] found that the polonium when injected into pregnant mice is adsorbed by the placenta, the fetus exhibiting very little activity. Lacassagne[L3,7] has studied the

* The excretion and distribution of radiotellurium has recently been investigated by De Meio and Henriques.[D3] The deposition of tellurium is in many respects similar to that of polonium. The greatest concentration of tellurium was found in the kidney. Autoradiographs of this organ showed, as with polonium, an uneven distribution with a large concentration in the cortex.

distribution of polonium after its injection into cancerous rats. In animals with syphilitic chancres the element is found in relatively large amounts in the site of the lesion, but always in distinctly less quantity than in the principal organs of elimination.

Fig. 40. Localization of polonium in kidney.

A. Stained thin section, 8×.
B. Corresponding alpha-ray pattern, 8×.

The influence of polonium on the formation of antibodies [L6] and its tolerance dosage [L8] have also been determined with the aid of autoradiographic methods. Microscopic examination of the alpha-ray patterns shows that polonium is not distributed uniformly throughout a particular organ but that it tends to segregate within fine capillary structures of the reticulo-endothelial system. The localized segregation of polonium in kidney is exhibited by the macro prints in Fig. 40. At higher magnifications, as shown in Fig. 41A (p. 209), radiocolloid aggregates of the element are observed in the fine capillary structures. The

studies of Leblond and Lacassagne [L25] indicate that polonium exerts a specific action on the lymphatic system and accumulates in the reticular cells.

LOCALIZATION OF ASTATINE

The element of atomic number 85 is represented by isotopes of mass 211, 216, 217, and 218, all of which decay with the ejection of alpha particles. At^{211} has a half-life of 7.5 hours. It has been prepared by the bombardment of bismuth with high-energy alpha particles accelerated to 32 Mev. Astatine is separated from the metallic target by vacuum distillation.

Studies by Hamilton [H11,12] on the comparative localization of astatine and radioiodine show that the two elements exhibit a similar behavior in accumulating in the thyroid gland. The proportional uptake of astatine, however, is considerably less than that of its lighter homolog. In the tissues examined, the iodine and astatine contents were found to be less than 1 per cent of their concentration in the thyroid. Hamilton's studies suggest that astatine is absorbed in the tissue as an organo complex with a benzene-ring structure.

RADIOACTIVE EMANATIONS

All the isotopes of element 86 are gases under ambient conditions and are not directly amenable to localization by autoradiographic methods. However, the emanations can be adsorbed on activated charcoal and their presence established in the adsorbent by the methods of contact autoradiography. By embedding the finely divided charcoal on the surface of the emulsion, as described in Chapter 7, in the section on detection of radioactive grains, the presence of the emanation is revealed by the alpha tracks originating from the decay of the adsorbed gas and its successive disintegration products.*

The decay of the radioactive gases causes the deposition of an active deposit on adjacent surfaces. The A- and C-bodies are alpha emitters, and the presence of the active deposits can be

* Käding and Riehl [K1] have employed charcoal adsorption columns for the separation of radioactive ions from solutions. The location of the radioactive zones is effected autoradiographically.

established by contacting the surfaces with nuclear-type emulsions. By exposing animals to radon, the distribution of the active deposit on the alveolar walls can be studied by autohistoradiographic techniques. In a report on the manipulation of radium concentrates Boden [B29] warns that minute amounts of RaD are deposited in the lungs as a result of radon inhalation and the decay of the active deposit.

A method for studying the surface structure of irregular objects has been described by Jech,[J7] utilizing films of active deposit. The material under study is first exposed to radon gas and subsequently contacted with a photographic emulsion. Although the active deposit is presumably distributed uniformly over the surface, the autoradiograph is not of uniform density but depicts clearly variations in surface structure. The photographic contrast results from variations in absorption of the short-ranged alpha particles by surface ridges differing in thickness or composition. The method has been applied successfully in the study of insect wings and in the delineation of the grain structure of wood.

LOCALIZATION OF RADIUM

Radium is represented by three alpha-particle-emitting isotopes. The long-lived Ra^{226} has been the subject of several autohistoradiographic investigations both in laboratory animals and on the exhumed bodies of radium and mesothorium factory workers. Investigations by St. George, Gettler, and Muller [S35] revealed the presence of 48 micrograms of radium in the skeleton. The element was deposited chiefly in the jawbone, vertebrae, femur, tibia, and metacarpal bone. Small quantities were also found in remnants of the soft tissues such as liver, brain, lung, and spleen. In a similar study, Martland and Humphries [M14,15] demonstrated the accumulation in the human cortex of mesothorium and its equilibrium products having an activity equivalent to 50 micrograms of radium. The bone was found to be sufficiently active for autoradiographs of thin sections to show visual segregates of the active matter after 2 or 3 weeks' exposure.

Experimental studies on radium metabolism in rats have been reported by Evans, Harris, and Bunker.[E15] As in the human autopsies, the radium was found to be absorbed preferentially in

the bone. These structures had an activity 100 times greater than lung, which proved to be the richest of the soft tissues. Autoradiographs of whole bone cross sections showed non-uniform distribution of the radium.

The distribution of radium in animals has also been studied with the aid of the short-lived isotope ThX. Daels, Fajerman, and Van Hove [D1] observed the localization of the element in the bones and the excretory organs. Comparatively little radium deposited in the muscle or brain. Investigations by Wolf and Born [W25] likewise show that the ThX concentrates chiefly in the skeletal parts, kidneys, and the intestines. The concentration of the element in the blood was observed to decrease very rapidly after intravenous injection of isotonic ThX solutions.

Like almost all objects that are part of the earth's crust, the normal human body also contains minute amounts of radium. The average radium content in the body has been estimated at 10^{-14} g per g by Vernadsky, and a value of similar magnitude, 5×10^{-15}, has been evaluated by Evans. In an adult weighing 80 kg this corresponds to a total accumulation of about 6×10^{-10} g of Ra. According to Lorenz [L38] about 90 per cent of the radium content is localized in the bones. The role of traces of radium in nature has received extensive study by the school of Russian geochemists directed by Vernadsky.[V3,4] In the study of vital phenomena, Vernadsky formulates the interesting concept that an organism, unlike a mineral, does not show a passive attitude towards its geochemical growth medium but actively selects, either consciously or unconsciously, the trace ions essential to its development.

Radium has been found in sea water to the extent of $(0.2 \text{ to } 3.0) \times 10^{-12}$ g per liter and is adsorbed by aquatic plants and organisms. The distribution of radium in aquatic plants grown in pond water with additions of 3×10^{-7} g of Ra per liter has been studied by Baranov.[B4] Photographic track counts resulting from exposure of different parts of the plants show that the growing leaves concentrate the radium by a factor of 10.

Mallet [M5] has observed that algae and bacteria accumulate ThX from activated culture media. On the basis of his autoradiographic studies Mallet is of the opinion that the technique might prove applicable to the visualization of viruses rendered photographically active by adsorption of radium. An *in situ* staining technique has been applied by Demers and Fredette [D7] as a means of studying microbe cells containing ingested

radium compounds. The individual tracks recorded by the emulsion designate the deposition of radium in or on the cell within 0.1 to 0.2 micron.

LOCALIZATION OF THORIUM

There are four isotopes of thorium which decay with the emission of alpha particles. Th^{232} and Io^{230} are very long-lived and are not suitable for tracer-visualization studies in biological systems. The metabolism of thorium can be studied with the aid of $RdTh^{228}$, which has a half-life of 1.9 years. RdTh accumulates from the decay of $MsTh_1$, and as these are not isotopic they can be separated chemically:

About 100 microcuries of an old mesothorium compound is dissolved in 0.3 N HCl, and 10 mg each of Pb^{++}, Th^{++++}, and La^{+++} is added as carriers. Precipitation of the lead with hydrogen sulfide effects the removal of the A-, B-, and C-bodies. The filtrate is boiled until free from excess hydrogen sulfide, diluted to about 250 ml, and precipitated with freshly distilled ammonium hydroxide free from carbon dioxide. The RdTh and the $MsTh_2$ are carried by the precipitate of thorium and lanthanum hydroxides, the $MsTh_1$ remaining in the filtrate. The hydroxides are dissolved in dilute nitric acid, evaporated to dryness on the steam bath, and redissolved in 100 ml of 10 per cent ammonium nitrate. The RdTh is separated on the thorium carrier as peroxynitrate by the addition of 5 ml of 30 per cent hydrogen peroxide. The peroxynitrate precipitate is washed with 2 per cent ammonium nitrate and is dissolved in dilute hydrochloric acid. After removal of excess acid by evaporation the resultant purified solution of Th + RdTh chlorides is concentrated to about 5 ml for purposes of injection.

Thorium dioxide of normal isotopic ratio is employed in a diagnostic test during x-ray visualization of certain soft-tissue organs. The colloidal dispersion of thorium dioxide, commonly known as "Thorotrast," has a low alpha-ray activity, but because of its retention in the organs it tends to produce a delayed hypoplastic anemia. In a study of aplastic anemia following the administration of Thorotrast, Urry [U3] observed the presence of 5 per cent ThO_2 in bone marrow and 0.27 per cent in spleen. Despite these large concentrations by weight, the tissue did not possess sufficient activity to produce a visual pattern on fast emulsions after 10-day exposure. The Thorotrast could be localized, however, by the observation of clusters of alpha-particle tracks recorded by long exposure of the tissue sections against

A *B*

C
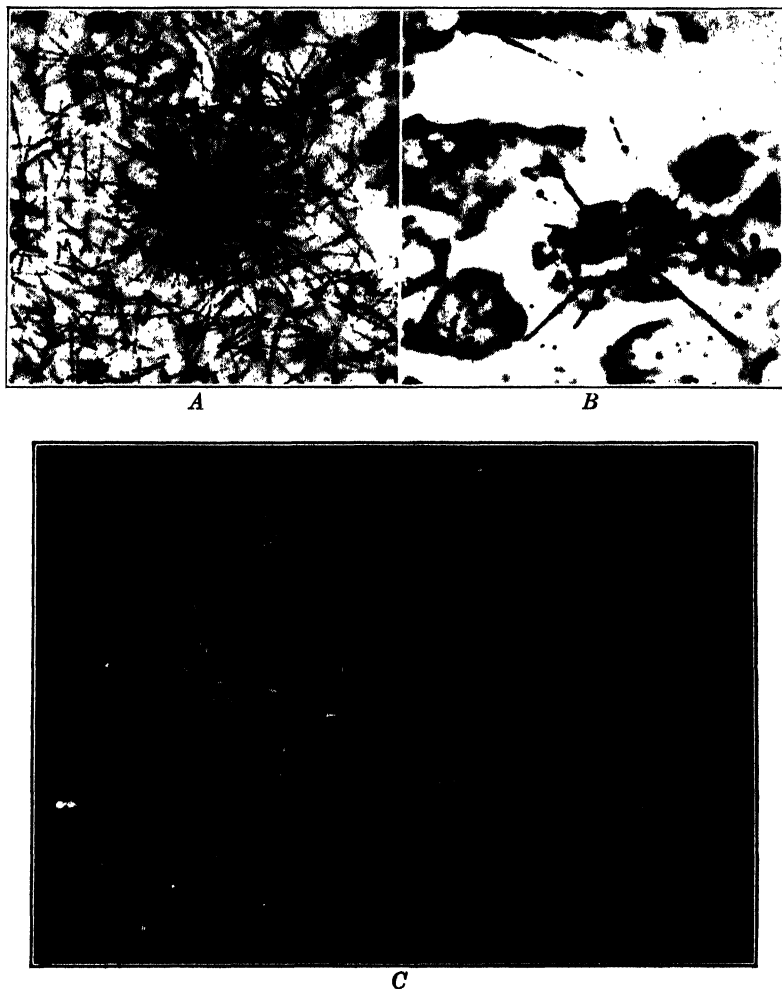
Fig. 41. Localization of alpha-emitting radioisotopes in tissue.

A. Deposition of a polonium radiocolloid in kidney tissue. Integral tissue-emulsion technique. Exposure 24 hours. Oil-immersion 62× objective, total magnification 500×. The superimposed stained section resides in a separate focal plane and is very diffuse when the tracks are in focus.

B. Localization of a Thorotrast grain in liver tissue. Integral tissue-emulsion technique. Exposure 40 days. Oil-immersion 62× objective, total magnification 900×. Intermediary focus, showing stained tissue and alpha-particle tracks emerging from a grain of Thorotrast.

C. Detail from alpha-ray pattern of microincinerated liver tissue containing Thorotrast. Exposure 21 days. Dark-field illumination, 150×.

nuclear-type emulsions.[Y17] Photomicrographs showing the track distribution from thin sections of liver are reproduced in Fig. 41.

LOCALIZATION OF URANIUM

Purified uranium compounds containing only the three natural alpha-ray-emitting isotopes have an activity of 2.5×10^4 alpha particles per sec per g of U. Like thorium, the slow rate of decay does not permit visual autohistoradiographic studies on tissues containing subtoxic quantities of this element. Studies by Neuman [N5] show that 2.5 mg of U per kg of body weight is a toxic dose which is sometimes lethal. After repeated injections of dilute uranyl nitrate over a period of 6 weeks analyses of the ash of the animals showed the presence of 2.1 micrograms of U per g of wet bone. A polished thick section of bone would thus have a surface activity of about 4×10^{-5} alpha particle per cm^2 per sec, and even after an exposure of 1000 hours the accumulated track population would be of the order 150 tracks per cm^2.

Radioactive-tracer studies on the metabolism and deposition of uranium are facilitated by the availability of more active uranium isotopes. U^{233} with a half-life of 1.63×10^5 years has a specific disintegration rate of 3.5×10^8 alpha particles per sec per g of U^{233}. Tissue containing 2×10^{-6} g of this isotope per unit of weight will eject about 2×10^6 alpha particles per cm^2 of emulsion during an exposure of 1000 hours. This flux is adequate for the production of a visual autoradiographic image, particularly if the distribution is uneven and segregation takes place along tissue boundaries. The localization can also be effected with a much smaller exposure period by the individual track counting methods described on p. 213.

The deposition of uranium in bone has been investigated autoradiographically by Neuman.[N6] Rats were injected intraperitoneally with toxic doses of uranyl acetate (1.5 to 3 mg U per kg) fortified by the addition of 1.5 microcuries of U^{233}. The bones were fixed in equal volumes of chloroform and methanol (these liquids do not displace adsorbed uranium), and ground into thin slabs of about 125 to 500 microns thickness. These sections gave visual images of the areas in which uranium concentrated after 4 weeks' exposure on Eastman Fine-Grain Alpha plates. Uranium was observed only in the calcified portion of the bone on surfaces readily available to the circulation. The pickup was particularly marked in areas where active calcification was taking place. The

studies showed that, once the metal became fixed in the tissue, little redistribution occurred from the initial site of deposition during a period of 40 days.

The toxicology of uranium has also been investigated by Tannenbaum and coworkers [T25,26] using uranium salts enriched with the U^{233} isotope. Autoradiographs revealed large concentrations of uranium in the kidney and bone structures. In the kidneys of mice and rats the concentration is highest in the cortex, principally towards the cortico-medullary junction. In bone the element deposits mainly in spongy cancellous areas and in the endosteum. The accumulation in the compact bone or in epiphyseal cartilage is relatively low. While bone and kidney are the principal sites of accumulation, small amounts are also found in the other organs, particularly the liver, which may contain 1 per cent of the total uranium deposited in the body.

LOCALIZATION OF PLUTONIUM AND OTHER TRANSURANIUM ELEMENTS

The transuranium elements, neptunium, plutonium, americium, and curium, are represented by one or more isotopes that decay with the emission of alpha particles. The properties of these isotopes are summarized in Table 3. In general, their disintegration rate is high as compared with that of uranium or thorium, and the elements should present no special difficulties in localization by photographic methods.

In a brief statement concerning autoradiographic techniques as applied in the health-protection activities of the plutonium project, Stone [S43] states that 1 microgram of plutonium is about as dangerous to the body as the ingestion of an equal weight of radium. This dosage could not be anticipated on the basis of the decay constants of these elements, as the alpha-particle radiation from radium is 65 times greater than that from an equal weight of plutonium, and the decay of radium is also accompanied by beta and gamma radiation.

Autoradiographic studies show that the plutonium deposits in the liver and may cause severe damage to the organ because of localized segregates. The accumulation of the element over long periods causes atrophy of the bone and the growth of bone sarcomas. Once plutonium enters the tissue it is not readily excreted. Because of this behavior, a maximum permissible dose of 1 microgram Pu^{239} was set as a limit not to be exceeded by humans.

The comparative deposition of plutonium, strontium, yttrium, and cerium in bone has been investigated by Copp, Axelrod, and Hamilton.[C21] Autoradiographs of thin bone sections reveal that plutonium is deposited in the uncalcified organic bone matrix below the epiphyseal cartilage and in the endosteum and periosteum. Plutonium does not appear to be incorporated in the cartilage itself. In this respect it differs markedly from radiostrontium, which is localized in a thin shell of bone salt in the shaft.

The comparatively high toxicity of plutonium is attributed to its concentration on the surface of the bone and the bone trabeculae. The densely ionizing alpha particles are thus concentrated on the cells of the endosteum, periosteum, and bone marrow. Attempts at the elimination of plutonium by low-calcium diets, or by means of parathormone or complexing salts, had no significant effect on the excretion of the metal. Experiments on animals suggest that the destructive action of the alpha radiation can be minimized by laying down new non-radioactive bone on the surface of the plutonium layer and thus preventing the short-ranged alpha particles from reaching the living cells.

Extensive investigations of plutonium metabolism in bone have been reported by Van Middlesworth.[V18] These studies show that the element localizes superficially in the endosteal and periosteal surfaces of the bone with no apparent concentration in the zone of bone growth and calcification. As noted by other workers in this field, this behavior is markedly different from that exhibited by fission products which deposit throughout the bone, particularly in the region of new bone growth. The deposition of plutonium is essentially independent of the oxidation state of the ions injected. Van Middlesworth [V18] found that, after intravenous injections, the plutonyl ion PuO_2^{++} disappears from the blood stream more rapidly than the tetravalent Pu^{++++} ion. There is also a much larger proportion of Pu^{++++} deposited in the liver, indicating that tetravalent plutonium may exist in solution as a colloidal dispersion (see section on radiocolloids, p. 154). Scott and coworkers [S57] likewise observed no significant variation in the metabolism of plutonium following injection of the element as Pu^{+++}, Pu^{++++}, and PuO_2^{++} ions. In all instances the skeleton is the chief organ of deposition. Of the soft tissues liver, kidney, and spleen exhibit the greatest concentrations. Plutonium is eliminated very slowly through the digestive track. The half-life of retention is estimated by Scott to be greater than 2 years.

When plutonium is injected into pregnant mice the element is transmitted to the offspring. Experiments reported by Finkel [F24] show that the young animals contain higher equivalent amounts of plutonium per body weight than those retained by the mothers. In mice living more than 200 days cases of osteogenic sarcoma developed, probably induced by the radiation localized in the bones. Studies on osteogenic sarcomas developed in rabbits, rats, and mice following the administration of plutonium or fission products are also described by Lisco.[L52]

Autoradiographs of lung tissue from animals exposed to an aerosol of plutonium oxide described by Hamilton[H13] reveal the deposition of the compound on the walls of the bronchi and bronchioles and throughout the alveolar structure. The oxide does not accumulate in the blood vessels. In an animal examined 1 day after the exposure, the plutonium oxide disappeared from the bronchiole surfaces but was still retained by the alveolar structures.

The plutonium isotope of mass 238 has a half-life of 50 years and can be employed advantageously in tracing the course of the more stable Pu^{239} atoms in biological systems. The nuclear-type emulsions are particularly useful in detecting and localizing plutonium when in admixture with its fission products. The fission products decay by beta-particle emission, and this concomitant radiation does not interfere seriously with the microscopic examination of alpha-particle tracks, as shown by the study in Fig. 42.

The metabolism of neptunium, americium, and curium have been investigated by Hamilton and coworkers.[H13] Am^{241} and Cm^{242} accumulate chiefly in the liver and bone structures, the activity in the liver representing 70 per cent of the total quantity ingested. Like plutonium, neptunium segregates chiefly in the bone structures. Autoradiographic studies of compact animal bones described by Axelrod[A7] and Scott[S58] show that americium tends to accumulate in the region of trabecular bone below the epiphyses, at the endosteal and periosteal surfaces of the shaft and throughout the cortical bone in the region of small blood vessels. One day after intramuscular injection of Am^{241} as $AmCl_3$ in normal saline, about 43.5 per cent of the element remained unabsorbed at the site of injection. Of the absorbed material 55 per cent concentrated in the liver and 20 per cent in the bone. Americium, like plutonium, is slowly excreted, and at the end of 256 days 19 per cent remained in the bone and 0.53 per cent in the liver.

QUANTITATIVE AUTOHISTORADIOGRAPHY

The number of alpha-particle tracks directed into the emulsion from a micro structure in the tissue is a quantitative measure of the amount of the radioelement ingested. For many purposes the relative numbers of tracks originating from different parts of the same tissue section suffice as a simple activity
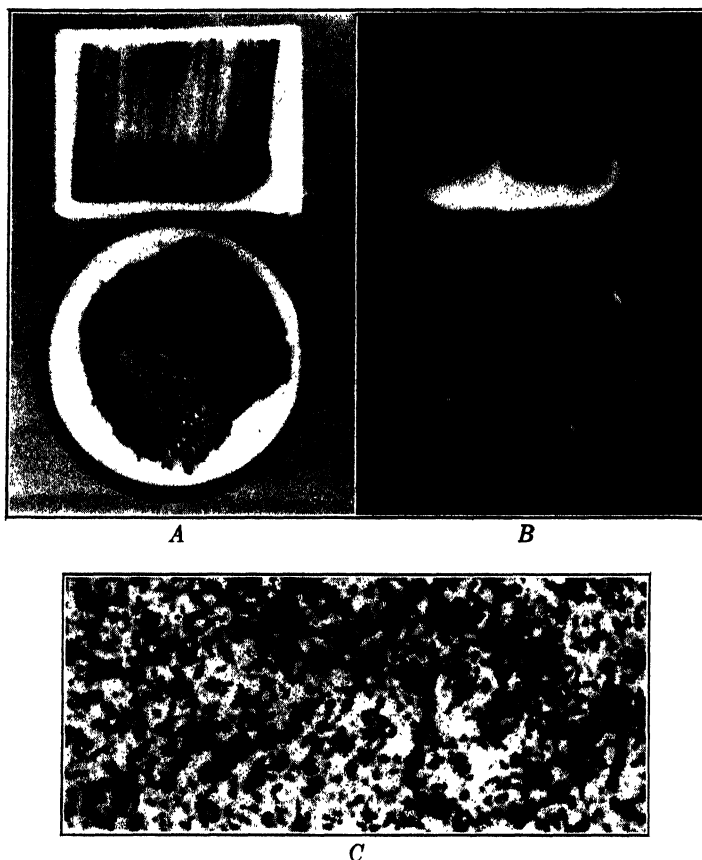
FIG. 42. Localization of traces of plutonium in the presence of its fission products.

A. Polished sections of wood contaminated by radioactive detonation products.

B. Corresponding autoradiographs on x-ray film showing concentration of activity in the bark and fissures.

C. Microscopic detail (800×) from an exposure on a nuclear emulsion showing plutonium alpha tracks in the presence of enhanced fog caused by beta radiation from fission products.

The visual contrast between the tracks and the fog is greater than indicated in the static photomicrograph, as the steep tracks can be followed through the gelatin layer by altering the focal plane.

index. However, the absolute weight of the element ingested can be computed from the structural dimensions, the disintegration constant, and the period of exposure. In view of the small dimensions of the source and the fact that each alpha-particle track represents the decay of a single atom, it is readily seen that the method permits a quantitative assay many orders of magnitude lower than the most sensitive microchemical techniques.*

In exposures with tissue sections whose thickness does not exceed 10 microns the number of disintegrations is very nearly twice the observed track count, C. The number of atoms of the radioelement n present in the point source at the time of development t is then expressed by:

$$n = \frac{2C}{\lambda t}$$

When the tracer element is short-lived, it is necessary to correct for the decay of atoms in the interval p between autopsy and the moment of contact with the emulsion. In general the total number of tracer atoms N originally present in the tissue is equal to:

$$N = \frac{2C}{\lambda t} e^{\lambda p} \tag{27}$$

For elements whose half-life is long compared with the interval p, the exponential term is negligibly small. The correction is significant only for short-lived tracers such as ThB and ThX.

In the pattern of tissue containing polonium 500 tracks were observed below a tissue volume of 420 cubic microns. Since the decay constant of RaF is 2.78×10^{-4} per hour and the exposure time was 72 hours, n evaluates to 5.00×10^4 atoms. A period of 24 hours elapsed between autopsy and initial exposure. Allowing for this unrecorded decay by means of equation 27 shows that the total number of atoms ingested is 5.04×10^4. If the short-lived ThB was the tracer, with the same experimental data n would evaluate to 212 atoms, and the corrected total N would amount to 1000 atoms.

* Chemical operations on microgram quantities necessitate the presence of 10^{16} atoms of the constituent. Lithium can be estimated spectrographically when 10^{15} atoms are present in the flame. By means of catalytic reactions, 10^{13} atoms of palladium can be detected. Helium can be determined spectrographically, after concentration by micro gas techniques, when the sample contains only 10^9 helium atoms.

Microscopic examination of the alpha-ray pattern usually reveals a considerable variation in the number of tracks per field. As an example, in the Thorotrast tissue described in the section on localization of thorium, the greater area was substantially devoid of tracks. At several points, however, about 450 tracks were recorded after 31 days' exposure. These tracks originated from a tissue volume estimated at 0.00041 mm^3. As 1 g of Th in equilibrium emits a total of 2.61×10^4 alpha particles per sec, it is readily seen that the track count corresponds to the localized deposition of 1.3×10^{-8} g of Th. In these particular areas the concentration is high and is equivalent to about 3 per cent ThO_2. In this analysis long tracks predominated, many with the characteristic length of ThC′ alpha particles, which also provided a qualitative identification of the parent element.

Organic tissues containing traces of alpha-particle-emitting elements can also be assayed, on a representative sample basis, by ashing a weighed quantity of the tissue and measuring the activity of a thin film prepared from the ash. Certain elements that volatilize readily, as polonium and to a lesser extent ThB, will be lost during ashing. When the element is non-volatile a portion of the ash can be dissolved in an appropriate solvent and loaded into an emulsion. This procedure often permits the identification of the radioelements present in the sample from measurements of the track lengths or from observation of the multiplicity of recorded alpha stars.

Chapter 10 · PRINCIPLES OF BETA-PARTICLE AUTORADIOGRAPHY

The photographic technique, first introduced for natural radioactivity, here comes into its own. It gives the story of detailed distribution, taking place simultaneously, in a very direct way, with relatively little trouble—at least, very little trouble that is not already overcome by known techniques.

—Pollard and Davidson, 1942

HISTORICAL INTRODUCTION

Unlike the naturally occurring radioelements which frequently reach stability by successive emission of alpha particles, the synthetic isotopes decay almost invariably by beta-particle, positron, gamma-ray, or x-ray emission. These radiations are not densely ionizing and do not produce distinctive tracks in photographic emulsions. The radiations activate optical-type photographic media of suitable sensitivity, and the blackening on development serves as a measure of the relative concentration of the radioisotopes in plant and animal tissue, metals, crystals, or other systems in which they were incorporated.

Autoradiography with the radiations from artificial radioelements had its historical origin in the work of Groven, Govaerts, and Guében,[G27] who demonstrated that the beta particles emitted by radiophosphorus and neutron-activated iridium metal produced a "neat blackening" on photographic film. The visualization technique has since been applied in numerous other investigations, the majority of which have been concerned with the distribution of the tracer elements in biological systems.

The general procedure is to introduce the tracer isotope into the system in the form of a readily ionizable compound. On solution, the radioactive ions have opportunity to interchange with non-radioactive ions of the same element and thus become incorporated in molecules of more complex composition. In their subsequent migration through the system, the assumption is made that the isotopic ions remain inseparable and that the rela-

tive distribution of the tracer and inactive atoms remains unaltered during their migration to the site of final deposition. The tracer and the more numerous isotopic atoms differ in mass only. A minute fractionation might occur when the atoms are of low atomic mass, such as C^{14} and C^{12}, as a result of the more rapid diffusion of the lighter isotope through cell membranes. In general, however, the difference in mass between tracer and stable atoms is less than 1 per cent, and appreciable fractionation cannot be anticipated.

PROPERTIES OF BETA PARTICLES

The beta particles are high-speed negatively charged electrons ejected from the nucleus of atoms in the process of radioactive decay. The positron is a positively charged particle having a rest mass equal to that of the electron. These light positively charged particles were first observed as components of the cosmic radiation but have since been identified with the radiation emitted in the decay of particular synthetic radioactive isotopes. The properties of the positron are in general identical with those of the beta particle, particularly with reference to range in solids.

The particles ejected by a given radioelement are rarely monoenergetic but are usually emitted with varying velocities. This gives rise to a continuous beta-ray (or positron) energy spectrum which is characterized by a maximum energy E_{max} and an average energy $\bar{E}$. The average energy of the beta particles is roughly one-third that of the maximum energy. The continuous variation in energy also results in a similar variation in the range of the beta particles.

The range of beta particles in solids is an important factor governing the resolution of autoradiographic patterns. The average range in cm $\bar{R}$ within a solid of density d is related approximately to E_{max} in Mev by a relationship deduced by Feather:[F4]

$$\bar{R} = \frac{0.543E_{max} - 0.16}{d}$$

Thus the beta particles emitted by P^{32} have an average range of about 0.28 cm in aluminum or 0.77 cm in tissue of unit density.

The properties of the more common radioactive isotopes employed in tracer studies are summarized in Table 24.

TABLE 24. PROPERTIES OF BETA-RAY-EMITTING ISOTOPES *

Element	A	Half-Life	E_{max}	$\bar{E}_\beta$	Range in Water, cm †	Radiations
Carbon	14	4700y	0.154			β^-
Sodium	24	0.61d	1.39	0.540	0.64	β^-, γ
Phosphorus	32	14.5d	1.712	0.695	0.82	β^-
Chlorine	38	0.62h		1.39	2.70	β^-, γ
Potassium	42	12.4h	3.5			β^-
Calcium	45	180d	0.3			β^-
Manganese	52	6.5d	0.58	0.24	0.25	β^+, K, γ
Cobalt	55	0.75d		0.515	0.70	β^+, K
Iron	59	47d	0.46	0.120	0.25	β^-, γ
Copper	61	3.42h		0.555	0.54	β^+
Zinc	63	0.65h		0.985	1.19	β^+
Bromine	82	1.5d	0.465	0.150	0.25	β^-, γ
Strontium	89	55d	1.5			β^-
Iodine	131	8d	0.595	0.205	0.25	β^-, γ
Lanthanum	140	1.67d		0.495	1.05	β^-, γ
Gold	198	2.7d	0.78			β^-
Pb (RaD)	210	22y	0.0255			β^-
Bi (RaE)	210	4.85d	1.17	0.33	1.51	β^-
Pa (UX_2)	234	1.14m	2.32	0.865	1.17	β^-, γ
Pa (UZ)	234	6.7h	0.45	0.15	0.25	$\beta,^- \gamma$

* This partial list includes only the isotopes commonly employed as tracers. A complete listing of the isotopes is available in the work of Mattauch and Fluegge [M17] and Seaborg.[S16]

† Range computed by Marinelli.[M9]

Because of their small mass, beta particles are readily scattered by the atoms in their path, and, unlike the essentially linear trajectory of the alpha particle, the locus of a beta particle is composed of a series of irregular movements somewhat analogous to the Brownian motion of colloidal particles. The marked scattering coupled with the long range places severe limitations on the resolution attainable by autoradiographic imprints. The diffuseness of the image is minimized by exposing thin sections in close proximity with the emulsion. In the decay of certain radioisotopes gamma as well as beta radiation is emitted. This penetrating radiation also exerts some photographic action, particularly on coarse-grained emulsions, and is a further cause of poor definition.

PHOTOGRAPHIC ACTION OF BETA PARTICLES

In the optical-type emulsions of moderate grain size a 4.8-Mev alpha particle will activate about 20 silver halide grains. The response to beta radiation is considerably less. Data cited by von Hevesy [V14] indicate that about 7 beta-particle impacts are required for the activation of a single grain. More recent experiments [Y18] on the comparative blackening produced by equal numbers of RaF alpha particles and P^{32} beta rays indicate that the response to beta particles diminishes rapidly with the grain size of the emulsion, as tabulated.

Emulsion Type	Lantern Slides	NTA	548-O
Beta:Alpha flux	20	30	60

In extremely fine-grained emulsions, such as Eastman 548, exposures up to 2×10^9 beta particles per cm^2 failed to produce any perceptible blackening. On the same emulsion, using a polonium source of identical geometry, 4×10^7 alpha particles produced a faint image, and a flux of 4×10^8 yielded an image with a photographic density of 0.19.

Cobb and Solomon [C39] compute the sensitivity of a film as the $\log_{10}$ of the number of beta particles per cm^2 required to produce a photographic density of 0.6 above the background fog. This criterion was selected as representing the minimal density required for the accurate measurement of very small images such as those of stars in astronomical photography. The contrast of different films is likewise expressed in terms of the slope of the characteristic curve at the point of 0.6 density above background fog. The approximate diameter of the clumps of silver grains measured microscopically on images developed to an approximate density of 0.6 serves as a measure of the film granularity.

Using a calibrated thin source of C^{14} and a carefully controlled development procedure Cobb and Solomon studied the properties of different emulsions having potential application as beta-ray recording media. Their results are summarized in Table 25. They conclude that Eastman No-Screen x-ray film is best suited for the detection of beta rays, and that slower media such as Ansco Reprolith and Eastman Type M x-ray stripping films are more suitable for autoradiographic patterns. In the microscopic

examination of Ilford B2 and Eastman NTB emulsions exposed to C^{14} radiation Cobb and Solomon were able to resolve individual beta tracks (see p. 227).

TABLE 25. CHARACTERISTICS OF BETA-SENSITIVE EMULSIONS *

Emulsion	Background, density	Sensitivity, $\log_{10}$ (β/cm^2)	Contrast, slope	Granularity, microns
Eastman No-Screen x-ray film	0.20	7.2	2.3	9
Eastman Spectroscopic I-O	0.30	7.2	1.0	9
Eastman Spectroscopic 103a-O	0.25	7.3	2.4	7
Eastman Tri X pan. cut film	0.14	7.6	0.9	6
Ilford Nuclear-Research B2	0.06	7.9	1.3	4
Cramer Hi-Speed	0.10	7.8	1.0	6
Eastman Contrast Lantern-Slide	0.06	8.1	1.4	5
Eastman Type-M stripping film	0.06	8.1	1.8	4
Ansco Reprolith Ortho stripping film	0.25	8.9	1.6	3
Eastman Kodalith Ortho stripping film	0.24	9.2	2.0	2
Eastman Nuclear-Track NTB	0.06	9.2	2.0	∼1
Ilford Nuclear-Research D1	0.03	>10	...	1

* All the test strips were developed in separate 50-ml portions of freshly prepared Eastman D19 developer. The 2.5 × 7.5 cm strips were supported vertically in stoppered test tubes and agitated 10 times during the 5-min period of development at 68°F.

In plates of fixed composition the beta-particle blackening increases with the number and average energy of the incident particles. With a constant flux of beta radiation the blackening increases with the grain size and the emulsion thickness. Information on the stability of the latent beta-ray image is not available. Some fading can be anticipated, as there is evidence that beta particles decompose water with the formation of hydrogen peroxide. Hence, in long exposures to weak sources a departure from reciprocity is probable.

In the application of commercially available optical emulsions to beta-ray autoradiography the choice is limited to types sensitive to blue light. Hypersensitive and panchromatic types cannot be employed conveniently as adequate illumination is essential to proper tissue or polished-section alignment. Sensitivity is an important criterion as it is often difficult to secure tracer preparations of high activity. Also, the introduction of large

doses of radioactive ions is undesirable because of possible damage to the living tissue by the intense radiation.

Since the tracer isotope is often short-lived, it is not always practicable to augment photographic blackening by prolonging the exposure. As an example, consider a tissue block activated by 1 microcurie of Co^{55} per gram. Since this isotope has a half-life of 18 hours, 3.36×10^6 cobalt atoms will be present initially in a ribbon cut 10 microns thick. At the termination of a 100-hour exposure period, 3.30×10^6 Co^{55} atoms will have disintegrated. This represents 98 per cent of all the tracer atoms originally present, and further prolongation of the exposure will not increase the photographic density materially.

The total number of tracer atoms present in a section of tissue having initially an activity of q microcuries is $N_0 = 3.7 \times 10^4 q/\lambda$. These decay in entirety only after an infinitely long exposure. During a finite exposure t the number of atoms which undergo decay is expressed by:

$$\delta = N_0 (1 - e^{-\lambda t})$$

In general, when t is about 5 times the half-life δ is practically identical with N_0.

Emulsions intended for the registration of x-rays will, in general, produce the most rapid response to beta radiation. The No-Screen x-ray type film has been employed successfully in the autoradiography of tissues carrying soft beta-ray-emitting elements. Using tissue sections 3 microns thick containing 0.3 microcurie of I^{131} Hamilton [H10] found that an exposure of 5 to 8 days provided satisfactory contrast. A flux of about 2×10^6 beta particles of 0.6 Mev initial energy per unit area is therefore indicated for the production of a satisfactory image.

X-ray film owes its sensitivity to very large grain size, and to the presence of an emulsion coating on both sides of the backing. The sensitivity is offset by a loss in definition, as beta particles entering the emulsion layers obliquely activate grains in the lower layer that are displaced laterally with reference to the point of origin of the radiation. A plate with a single heavy coating would improve definition without loss in sensitivity.

Better resolving power is secured by the use of emulsions of moderate grain size. Bartelstone [B7] reports that Lantern Slides provide better definition than x-ray film, but that the exposure must be prolonged about threefold. Spinks [S34] has employed Eastman process plates in autoradiographic studies of the uptake of P^{32} by wheat plants. These emulsions give a satisfactory image after exposure to 10^7 beta particles per cm^2. Studies by Kaplan [K4] on the response of several optical-type emulsions to the beta radiation emitted by a thin film of $Na_2HP^{32}O_4$ are summarized by the sensitometry curves in Fig. 43. Among the emulsions of moderate sensitivity, Lantern-Slide plates have the advantage of exhibiting a nearly linear response over a wide range of excitation.

The effect of sensitizers on the recording properties of emulsions activated by beta particles appears worthy of investigation. As is well known, plates designed for visual photography can be sensitized to light of short wavelength by the incorporation of fluorescent materials which absorb impinging ultraviolet light and reemit light of longer wave-
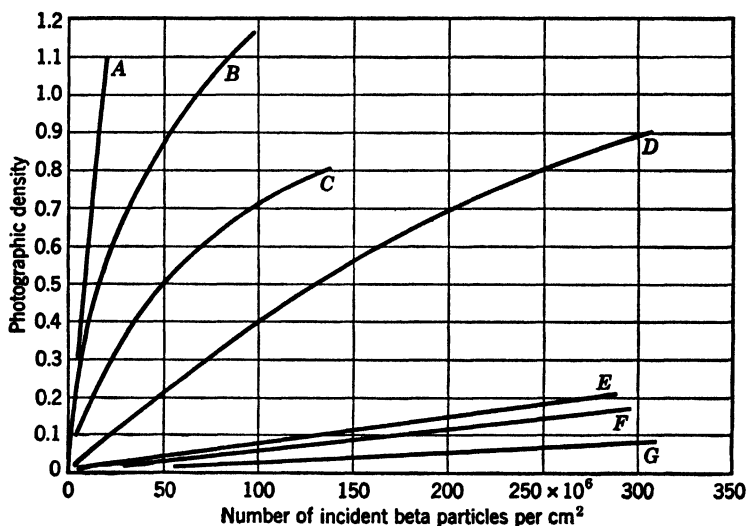
FIG. 43. Relationship between the number of incident beta particles and the photographic density.

Source: beta particles from P^{32}.
Development: 3 min in D19 at 20° C.
Emulsions: Eastman Kodak Co.

A. No-Screen x-ray film.
B. Type I-O plate.
C. Commercial Ortho film.
D. Lantern-Slide plate.
E. Type V-O plate.
F. Nuclear-Type NTA.
G. Nuclear-Type Fine-Grain Alpha.

lengths. As shown by Beese,[B12] petroleum mineral oil is a satisfactory sensitizer of the fluorescent type. A thin film of oil is incorporated on the surface by immersing the plate in a 5 per cent solution of mineral oil dissolved in petroleum ether. The oil film is removed before development by bathing in fresh solvent.

Cole [C18] has likewise demonstrated that the threshold sensitivity to slow-speed electrons is increased by application of a thin film of lubricating oil on the surface of the emulsion. Cole is of the opinion that the photographic action, on both oiled and unoiled emulsions, is due chiefly to

fluorescence excited at the surface by electron impact. Similar sensitizing action to slow electrons has been reported by Whiddington and Taylor,[W13] who recommend the use of Vaseline as the phosphor. These borderline investigations suggest that the sensitivity of emulsions to beta particles may be augmented by the incorporation of fluorescent dyes or other phosphors in the gelatin medium.*

RESOLVING POWER OF BETA-RAY PATTERNS

Contact Autoradiography. In studies on the localization of ingested radioactive isotopes in tissues the blackening in the autoradiograph must be sufficiently sharp to permit exact correlation with corresponding points in the tissue. It is also desirable to differentiate adjacent points in the section of appreciably different activity by corresponding variations in photographic density. Attempts at improved resolution have centered chiefly in the use of extra-thin tissue sections (1 to 3 microns) and in the perfection of contact by permanent adhesion of the tissue to the emulsion.

The total resolving power is dependent on emulsion characteristics, radiation energy, tissue thickness, and perfection in cutting and mounting. Investigations by Pelc [P7] show that perfection of contact between tissue and emulsion is an important factor governing resolving power. A gap of even 2 or 3 microns will impair resolution materially. Neither the slides nor the photographic plates are geometrically plane, and to secure good contact one of these should be flexible. Wrinkles in the tissue ribbon produce a wedge effect, and exceptional care must be taken during mounting when aiming at maximum resolution. Depending on grain size of the emulsion, a resolution of 100 to 20 microns can be secured by careful attention to detail.

The autoradiography of single cells is of considerable importance in problems related to the action of localized radiations on tissue. Some progress has been made, within the limitations of

* Investigations by Schopper [S8] show that plates treated with pinakryptol yellow yield an increased density of developed grains along the vague tracks of beta particles. This dye is unstable in the presence of oxygen and necessitates exposures either in an atmosphere of nitrogen or in vacuum. Dyes of analogous structure but of greater stability to atmospheric oxidation appear worthy of investigation as potential sensitizers for fine-grained emulsions.

the technique, in the study of large algal cells such as Nitella and Chara. Mullins[M35] demonstrated that the uptake of P^{32} is confined to cellular areas in which initially a high concentration of phosphate ion resides and which is available for exchange with the radiophosphorus.

The problem of the localization of radioelements in cells of smaller dimensions, such as those occurring in root tips, has been considered by Bayley.[B9] To secure adequate definition an emulsion capable of resolving 100 lines per mm must be employed. This necessitates long exposures even when the 10-micron tissue section has an activity of 0.04 microcurie per cm^2.

The back-scattering of beta particles by the glass slide carrying the tissue section is another factor which limits the resolution of fine detail. Experiments by Pelc[P7] show that the back-scatter can be reduced by mounting the tissue on thin cleavages of mica about 20 microns thick. The increased resolution is not sufficient to warrant the routine application of the method.

Focusing Methods. Efforts to increase the resolving power of autoradiographs by conducting the exposure in a strong magnetic field have not proved successful. According to Lawrence,[L23] available magnetic fields are not intense enough to produce deflections of the beta particles for improvement of cell definition.

Marton and Abelson[M16] have described a method of tracer micrography in which the soft radiation emitted from the source is focused by electron optical lenses onto the photographic recording medium. This focusing method is practical only when the energy spectrum of the radiation is essentially monoenergetic and soft. This critical requirement is met by Cb^{93}, Y^{87}, Sr^{85}, Sr^{87}, Pa^{233}, and Ga^{67}. The tissue section must be extra thin in order to avoid appreciable self-absorption. In a preliminary study of the method Marton and Abelson achieved a resolution of 30 microns using magnetic lenses producing a linear amplification of $1.6\times$.

With Process Plates as the recording media and a source of Ga^{67} having an activity of 1 microcurie per mm^2, an image of satisfactory photographic density resulted after an exposure of 1 hour. The radioisotopes to which the method is applicable decay by special radioactive processes such as *K*-capture and by internal conversion of gamma radiation. The electrons liberated

during internal conversion are perfectly homogeneous in energy and can be focused successfully by magnetic lenses.

Scott and Packer [S15] have developed an electron focusing method for the localization of stable calcium and magnesium isotopes in biological tissues. Certain features of this method of analysis can be incorporated effectively in focusing techniques in samples containing radioisotopes:

A polished nickel cathode surface is coated with a uniform film of barium and strontium carbonates over which a 10-micron-thick tissue section is deposited. The temperature is increased slowly until organic matter is destroyed and the sodium and potassium chlorides present in the tissue are volatilized. Areas in the residual ash containing calcium or magnesium cause the emission of electrons from the hot alkaline-earth subscreen. The electrons are focused onto a fluorescent screen with the aid of low-magnifying-power magnetic solenoids, and when a sharply defined image is secured it is recorded photographically.

By applying this technique to tissue containing elements that decay with electron emission it should be possible to localize the predominating quantities of calcium and magnesium in the microincinerated ash while the cathode is hot. A second pattern, recorded at room temperature by prolonged exposure to the electrons resulting from radioactive decay, would then reveal the mode of deposition of the radioisotope.

Resolution Testing. The resolving power of optical-type emulsions is commonly measured by photographing a miniature standard parallel-line test object, either by contact printing or optical projection. After development the image is examined microscopically for the minimum separation observable between the reproduced lines. In testing autoradiographic resolution it has been the practice to employ thin tissue sections carrying small adjacent radioactive segregates as test objects. The biological structures, however, are rarely of reproducible dimensions even when the sections are removed from the same part of the tissue block. Stevens [S50] has devised a radioactive test object of minute reproducible dimensions:

An image of a parallel-line test chart is photographed onto a high-resolution emulsion. After the usual processing the developed miniature silver image is converted to silver bromide, and this compound is then transformed into the iodide using a droplet of solution carrying I^{131}. After washing and drying a radioactive test object results which has a line separation of 0.5 micron. These units may be exposed against different emulsions either by temporary contact or stripping film adhesion techniques. After development the resultant radiographic images can be compared with the dimensions of the test object and the resolution evaluated in terms of a minimum line separation. In the fine-grain emul-

sions tested by Stevens, useful radiographic resolution could be obtained when the lines of AgI^{131} were separated by 2.5 microns.

ELECTRON TRACKS

Kodak, Ltd., at Harrow, England, has recently developed an especially sensitive nuclear-type emulsion, designated as NT2a plates, which are activated by slow-speed electrons. In a study by Berriman [B57] the emulsion was exposed to gamma radiation filtered through 17 cm of lead and on microscopic examination showed "numerous fairly short, highly curved chains of developed grains." These are attributed to the low-energy end of tracks due to photoelectrons and recoil electrons liberated by the gamma rays.

In an independent investigation with the NT2a emulsion Herz [H40] found that electron tracks were recorded by exposure to heavily filtered x-rays. The track characteristics produced at increasing x-ray voltage are as tabulated.

X-ray Voltage, Kev	Range of Curved Path, microns	Maximum Number of Grains	Mean Grain Spacing, microns
35	8	13	0.67
50	14	18	0.82
130	35	28	1.30

Herz has also found that by loading these emulsions with thorium or uranium nitrates electron tracks were recorded at the origin of the alpha-particle trajectories. These thin curved tracks were probably produced by beta particles from UX_1 and ThB as these elements emit soft beta radiation.

The Kodak Research Laboratories at Rochester have also devised an electron-sensitive emulsion (type NTB) which exhibits scattered tracks of electrons with energies below 50 Kev. This emulsion is identical in composition and general grain size with their NTA plates. The increased sensitivity is probably due to the presence of a dye. In a trial exposure to a radium $D + E + F$ source the NTB emulsion recorded exceptionally robust alpha tracks from the decay of RaF, and also short curved tracks of low grain density attributable to the beta particles from RaD or the softer components of the RaE spectrum. Figure 44 exhibits a polonium alpha-particle track at one end of

which an electron track is also recorded. Studies by Spence, Castle, and Webb [S54] indicate that the sensitivity of the NTB emulsion suffices for the detection of ionization effects as low as
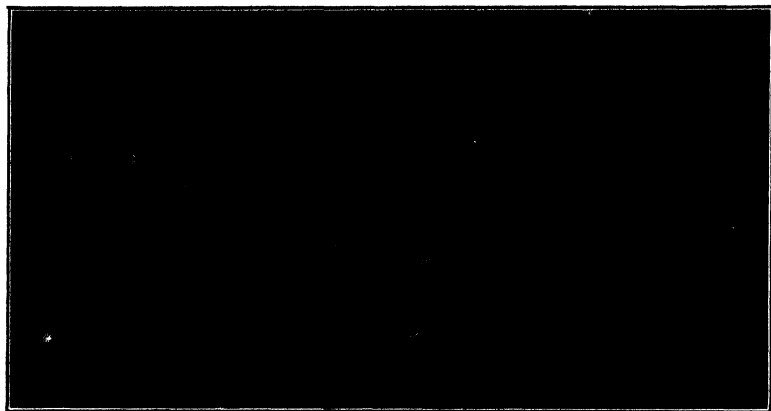
FIG. 44. Comparative grain density in electron and alpha-particle tracks. Eastman NTB emulsion developed by Method II. Dark-field illumination; 2500$\times$ magnification. The curved electron tracks are more conspicuous when the emulsion is examined visually with a sharply focusing objective. The photomicrograph, taken with a deeply focusing objective in order to depict both events, also includes all the fog grains developed throughout the entire emulsion thickness.

0.005 Mev per air-cm. This is very close to maximum sensitivity, as the minimum of the energy loss curve for charged particles in air is 0.0022 Mev per cm of path.*

* A fast charged particle produces about 70 ion pairs per cm of standard air. Since each ion pair requires the expenditure of 32 ev, the minimum energy loss per air-cm is $32 \times 70 \times 10^{-6} = 0.0022$ Mev.

Chapter 11 · APPLICATIONS OF BETA-RAY PATTERNS

If there is one thing that is needed in histochemistry, and there can be no doubt of the need, it is a new method of attack. This is most emphatically true of the localization of inorganic salts.

—Scott and Packer, 1939

LOCALIZATION OF RADIOISOTOPES IN TISSUE

Localization of Carbon. von Grosse and Snyder[V8] have recorded autoradiographs of the soft beta radiations from C^{14} by employing samples of high specific activity in conjunction with fast emulsions. Using a barium acetate compound with a specific activity of 266,000 disintegrations per minute, appreciable blackening on Eastman "Super XX" film was secured after an exposure of 1 hour. The photographic density was approximately proportional to the time of exposure. A minimum of 20×10^6 disintegrations produced a barely discernible image, and about 330×10^6 disintegrations were found necessary for adequate contrast.

By employing x-ray film as the recording medium von Grosse and Snyder were able to follow the migration of sodium acetate in a sweet-potato leaf into which the solution was introduced by absorption through the stem. An exposure of 42 hours provided the best contrast, indicating that a total beta-particle flux of 4×10^6 per cm^2 was necessary for the production of an autoradiograph. In another experiment, a leaf grown in an atmosphere containing $C^{14}O_2$ had a total activity of 225 disintegrations per minute and produced an autoradiograph after an exposure of 20 days. The pattern showed a uniform distribution of radiocarbon throughout the body of cells, but very little was found in the capillaries.

The deposition of C^{14} in bone has been investigated by Bloom, Curtis, and McLean.[B28] Rats were injected intraperitoneally with barium carbonate or sodium bicarbonate in which 75 to 150 microcuries of C^{14} were present. The deposition of radiocarbon as exhibited in the autoradiographs was compared with similar prints of the bones of animals to which Sr^{89} and P^{32} were ad-

ministered. The bones of rats injected with C^{14} show that this element deposits differently from Sr^{89}. Shortly after injection the C^{14} compound concentrates in the shaft of the bones and the deposit produces black lines on the beta-ray pattern. In animals studied over a period of 16 weeks, essentially the same type of radiocarbon deposition was observed, except that the images increase successively in length and width. The animals injected with Sr^{89} exhibit heavy deposition of the active compound in the metaphysis which extends into the calcified cartilage. A similar pattern of deposition is observed in the bones of animals injected with radiophosphorus preparations.

Sections of the liver and kidney of animals exposed to C^{14} gave fairly intense autoradiographs at the 3-day and 2-week stages but were negative after longer intervals. Because of the retention of C^{14} in bone, Bloom is of the opinion that health hazards are involved in working with this isotope and that bone tumors might develop from its ingestion.

Localization of Phosphorus. Radiophosphorus is usually administered in the form of a water-soluble salt that furnishes $P^{32}O_4^{\equiv}$ ions on solution. Gross and Leblond[G26] have observed that the uptake of radiophosphorus is extremely rapid. The tissues reach maximum activity a few hours after injection, and the deposition extends to all bone formations.

Autoradiographic studies revealing the distribution of phosphorus in the leg bones of chickens were made by Dols, Jansen, Sizoo, and van der Maas.[D11] The prints of bone sections showed that the epiphysis accumulated a larger quantity of P^{32} than the diaphysis. Comparative chemical analysis of the total phosphorus content in the same structures checked with the autoradiographic observations. These investigators found that phosphorus metabolism is more intense in the bone of rachitic than in that of normal animals. Phosphorus is a substantial constituent in almost all tissues, either as inorganic phosphate ion or as a component of complex organic compounds. The retention of ionic phosphate varies in different tissues and decreases in the following order: bone, muscle, liver, blood, kidneys, heart, lungs, and brain.

Radiophosphorus tends to accumulate in leukemic lymph nodes, and these regions are thus subject to a greater degree of beta radiation than normal tissue, which accumulates this element to a

lesser extent. Lawrence [L22] demonstrated the selective deposition of Sr^{89} in bone and P^{32} in the neoplastic cells by autoradiographs of the tissue of mice carrying subcutaneous bilateral lymphosarcomata. The animals to which radiophosphorus was administered showed a marked concentration of the tracer atoms in the subcutaneous tumors, and some deposition in other soft tissues and in the skeleton. The radiostrontium was observed to segregate almost completely in the skeletal structure, without deposition in the tumors or other soft tissues.

The therapeutic use of P^{32} has been investigated by Low-Beer, Lawrence, and Stone.[L41] They demonstrated variations in activity in different parts of a lymph node removed from a patient with generalized lymphosarcoma. The autoradiograph was made of a frozen section maintained under refrigeration during the exposure.

The autoradiographic technique has also been applied by Shimotori and Morgan [S27] in studying the effect of vitamin D on the accumulation of ingested radiophosphorus. The distribution of this element in teeth has been studied by Erbacher and Wannenmacher,[E9] and more recently by Berggren.[B17] These autoradiographic investigations show that the P^{32} uptake is highest in young teeth and is higher in those parts of adult teeth that have not matured. Detailed studies on the distribution of phosphorus in bone and teeth have been made by Bélanger and Leblond,[B15] employing their integral emulsion-tissue-staining technique.

The absorption of phosphates by plants has been investigated by Arnon, Stout, and Sipos.[A4] Tomato plants were grown in a nutrient solution having an activity of 28.5 microcuries of P^{32} per liter, containing 1 *M* $NH_4H_2PO_4$ as the inactive phosphate. The distribution in the leaves was studied by direct contact against x-ray film. Autoradiographs of the moist tomato fruit were made by interposing a paraffined paper between the emulsion and the thin slices.* The studies showed that the assimilated phosphorus accumulated in the capillary conduction system of the leaves and in the seeds of the green fruit.

The autoradiographic method is particularly advantageous in the study of the metabolism of radioactive isotopes in insects or other small organisms in which the minute size of the individual organs makes radioactive measurements by counting techniques difficult.

Posin [P29] has reported studies on bacteria rendered radioactive by growth in a medium containing $Na_2HP^{32}O_4$. Lindsay and Craig [L34] have investigated the distribution of P^{32} in whole sections of insects fed with sodium dihydrogen phosphate solutions having an activity of 193 microcuries per ml. After several days of this diet about 2 microcuries

*The cutting of extra-thin slices of tomatoes and other foodstuffs is a highly perfected art as practiced by restauranteurs. Details of these guild techniques have not been published.

per gram of body weight was consumed. Sections cut 10 microns thick were exposed against x-ray film until the beta-particle impact totaled 5.5×10^6 per cm^2. The patterns produced by whole insect cross sections could be enlarged tenfold. The prints revealed that the radiophosphorus was least concentrated in the fat body, and accumulated chiefly in the epithelium of the midintestine, in the reproductive ducts, and in the gonads.

Localization of Sulfur. Axelrod and Hamilton [A5] have investigated the deposition of sulfur compounds in skin and eye tissues after exposure to mustard gas. The exposures were made with dichloroethyl sulfide labeled with radiosulfur containing 5 microcuries of S^{35} per mg. Samples of skin were washed with petroleum ether to remove superficial deposits of the compound and were fixed in formalin. Cross sections of the skin were cut 10 microns thick, the paraffin was removed by xylol, and the sections were reimpregnated with a thin solution of celloidin. The sections were exposed for 1 to 3 weeks against x-ray film, and the image was developed by means of Eastman x-ray developer diluted 1:4, developing for 2.5 min at 21° C.

Comparison of the autoradiographs with the stained tissue sections revealed that the sulfur compound was fixed primarily in epidermis, dermis, and hair follicles. The mustard compound also accumulated around blood vessels, forming an annulus about 30 microns wide. The concentration in these minute structures was estimated by comparing the photographic density with the blackening produced by thin films of $BaS^{35}O_4$ of known activity. These measurements indicated the deposition of 0.1 microgram of mustard compound in a volume of 7×10^{-5} mm^3. In the eye, fixation of the mustard compound occurred chiefly in the cornea, and smaller amounts in the conjunctiva, iris, and lens.

Radiosulfur has also been applied in studies of the distribution of this element in plants. Experiments by Harrison, Thomas, and Hill [H43] show that wheat plants grown in an atmosphere containing $S^{35}O_2$, or in soil containing $S^{35}O_4^{=}$ ions, pick up the radiosulfur and show a transmigration into the kernels. Autoradiographs of the wheat kernels reveal a heavy concentration of sulfur in the embryo, the aleurone layer, with smaller quantities in the inner part of the endosperm. In general, their work shows that the sulfur distribution coincides with concentrations of proteins in the kernel, suggesting that the inorganic radiosulfur enters into combination with protein in the seed.

Localization of Iodine. The iodine content of most tissue is very low. An unusually high concentration of iodine, which ranges between 0.25 and 1 mg per gram of organ, is present in the

normal human thyroid. The extraordinary selective accumulation of this element in thyroid has been the subject of numerous investigations using I^{131} as the tracer for its localization both in normal and pathologic tissue. A typical example of a stained section of thyroid and its corresponding autoradiograph is shown in Fig. 45.

The deposition of radioiodine in various types of human thyroid tissue was first studied by Hamilton, Soley, and Eichorn.[H10, 12] In normal thyroid the radioiodine is evenly distributed throughout the section. Although the autoradiographic resolution is not sufficient to distinguish the pattern of individual cells, no great difference can be observed between the amount of tracer iodine in the cells and that in the surrounding colloid.

In sections of cancerous thyroid, Hamilton found that most of the accumulated radioiodine segregates in the colloid. In a non-toxic goiter it was found that the cells and small acini surrounding the large colloid deposits accumulated the greater part of the iodine. Leblond[L27] has observed that the colloid in thyroids stimulated with pituitary extract contains more radioiodine than the colloid of normal animals.

Hamilton and collaborators[H12a] have studied the accumulation of iodine in the thyroids of children with hypothyroidism. The organ concentrates only small amounts of orally administered inorganic iodide, and the autoradiographs show a greater accumulation of radioiodine in the cells than in the colloid. Leblond[L28] has investigated the distribution of iodine in human goitrous thyroid glands. Autoradiographs revealed that only true thyroid tissue absorbed the tracer. The radioiodine was not found in associated blood vessels, nerves, or connective tissue.

Refinements in technique designed to minimize loss of water-soluble inorganic iodides during the preparation of the sections have been described by Leblond.[L26] The tissue is frozen rapidly with the aid of acetone-Dry Ice mixtures, dehydrated under vacuum at temperatures between −25 and −30° C, and infiltrated with paraffin under reduced pressure. A notable advance in exposure technique was introduced by Bélanger and Leblond[B15] by uniting the tissue with the emulsion as an integral permanent preparation. Considerable detail concerning tissue preparation, exposure, and the examination of the radiographic pattern at high magnification is described in the work of Evans[E17] and Gross.[G25]

The storage of radioiodine in a metastasis from thyroid carcinoma is described by Keston.[K9] An extensive study of the retention of I^{131} in thyroid carcinomas has been reported by Marinelli, Foote, Hill, and Hocker.[M10] Their work shows that thyroid carcinomas of high-grade malignancy do not retain the radioiodine. About 15 per cent of thyroid
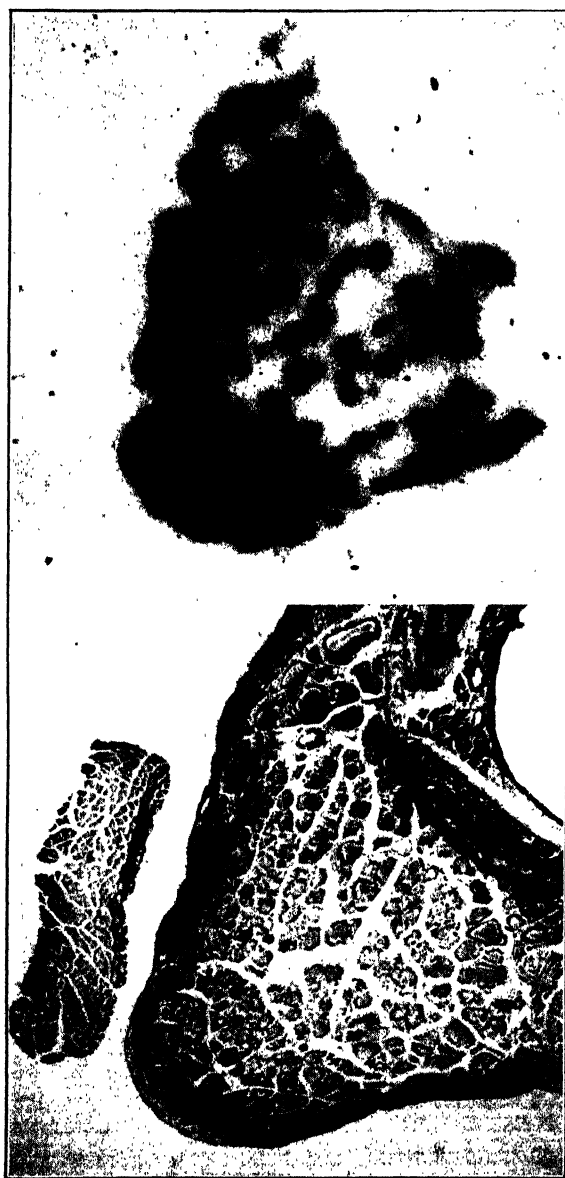
FIG. 45. Segregation of radioiodine in thyroid.

A. Stained section.
B. Contact autoradiograph.
Detail enlarged 35× from pattern developed on Ilford Line film by Pelc.[PS]

cancers may be expected to accumulate this isotope in some degree. The ability to pick up tracer iodine is a function of structural properties. An orderly cell arrangement in follicular pattern and the presence of colloid-like material appear to favor iodine accumulation.

Radioiodine has also been applied in the study of iodine metabolism in tissues other than thyroid. Gorbman [G18] has investigated the distribution of iodine in *Perophora annectens* Ritter, an ascidian that does not contain a thyroid gland. After 2 days' absorption in sea water containing 150 microcuries of I^{131} per 100 ml, autoradiographs of the prepared sections revealed the accumulation of iodine in the stolonic septum. Gorbman and Evans,[G19] who repeated these absorption experiments using tadpoles, found that the iodine uptake increased with the size and amount of colloid in the thyroid gland.

The tracer technique has also been applied in the isolation of iodine metabolites in animals in which the thyroid was removed prior to inorganic radioiodine administration. Morton, Chaikoff, Reinhardt, and Anderson [M31] demonstrated the absence of thyroid tissue in neck and mediastinal regions by means of autoradiographs and found organically combined iodine in the small intestine and the liver.

Reinhardt [R4] utilized radioiodine to determine the degree of completion of thyroidectomies. A tracer dose was injected before the operation, and the tissue about the operative site was studied autoradiographically. Thyroid remains escaping gross observation are readily detected in the beta-ray pattern. The effect of thiourea-type drugs on the conversion of inorganic iodide into organically bound iodine has been studied by Couceiro.[C24] The process is inhibited by thiouracil, as indicated by radiographs of the thyroids of treated and control animals.

Bartelstone and collaborators [B7] have employed radioiodine as a tracer in the study of the physiology of teeth. Animals were injected intraperitoneally with NaI^{131} in physiologic saline, employing a dose of 0.5 millicurie per kg of body weight. After 12 hours, the teeth were extracted and ground down into sections 100 to 150 microns thick. The radiographs of these thin sections revealed the accumulation of tracer iodine in the enamel, dentine, and cementum. This accumulation indicates that a dynamic fluid medium exists in the calcified structures.

Localization of Calcium and Strontium. Calcium is an important constituent of bone structures. The element also serves as an activator for enzymes governing muscle metabolism. Ca^{45}, half-life 180 days, is serviceable as a biological tracer. This isotope decays with the emission of soft beta particles having an upper energy limit of 0.3 Mev. Strontium does not occur in appreciable amounts in normal tissues. Tracer experiments with Sr^{89} indicate that it follows the same metabolic route as calcium. The beta radiation from Sr^{89} is more penetrating than the radia-

tion emitted by Ca^{45} and is therefore more convenient for activity measurements.

Pecher[P4] compared the distribution of calcium and strontium in the tissue of mice injected with the lactate salts of Ca^{45} and Sr^{89}. The segregation of these alkaline-earth metals was revealed by autoradiographs of whole animal cross sections. The uptake of calcium was found to be greater than that of strontium, but the relative distribution among different tissues was almost the same for both elements. Pecher also compared the distribution of the alkaline-earth metals with the deposition of phosphate, using P^{32} as the indicator. Intercomparison of the patterns showed that almost all the assimilated Sr^{89} segregated in the bone structures, whereas moderate amounts of P^{32} accumulated both in the skeleton and throughout the soft tissues.

The selective migration of radiostrontium to bone structures has suggested its use in the clinical therapy of bone tumors. The penetrating beta radiation from the accumulated Sr^{89} is thereby localized chiefly at and near the site of the tumor. Metabolic studies on the neoplasm of bone have been reported by de Treadwell and collaborators[T15] employing the localized radiations of Sr^{89} deposits. The deposition of the element after injection, as revealed by autoradiographs and x-ray pictures, was primarily in the tumor and along the epiphyseal line.

That strontium follows the path of calcium metabolism and is deposited chiefly in the bone salt has been substantiated in the investigations of Bloom,[B28] Posin,[P28] and Copp.[C21] Bloom found that Sr^{89} deposits most heavily in the metaphysis and is present in smaller amounts in the bone structures of diaphysis and epiphysis. The differences in the relative amounts of the element at different points in the bone is attributed by Bloom to the formation of a fresh deposit of bone salt in the zone of recent growth. Radioactive strontium ions replace existing calcium atoms from the crystal lattice by the ion-exchange mechanism.

Localization of Trace Constituents. Biochemical studies in conjunction with microchemical methods of analysis have demonstrated that certain elements, existing only in very small concentration, are essential to plant and animal growth. These trace elements include boron, molybdenum, manganese, zinc, copper, cobalt, and gallium. Although these constituents occur only to the extent of a few parts per million of tissue, their sig-

nificant metabolic role may result from their concentration in particular enzymes, or segregation along cell walls.

Studies of the function of copper on plant development indicate that the metal enters the composition of an enzyme catalyzing oxidation processes. In the potato and mushroom plants the enzyme is a protein compound containing 0.30 per cent of copper. It should be possible to study the role of micro nutrient elements with greater facility by means of radioactive tracers. The approximate points of concentration may, in select instances, be determined by present-day autoradiographic techniques.

Smith and Gray [S56] have shown that on injection of radiocopper into the egg white of chick embryos the metal migrates throughout the structures with marked accumulation in the early central nervous system. The autoradiographs of entire cross sections show heavy concentrations in the anterior brain structures. Smith and Gray note that the distribution of copper ion runs parallel with the oxygen uptake and cytochrome oxidase concentration, lending support to the view that traces of copper play an important part in the metabolic activities of the embryo.

Molybdenum is another trace constituent whose presence is essential to the growth of healthy plants. Stout and Meagher [S59] have demonstrated that molybdenum is rapidly absorbed by tomato plants grown in a nutrient medium containing the radioactive isotope Mo^{99}. Autoradiographs revealed that the element concentrated in the interveinal areas of the leaves, in contrast with macronutrient elements such as potassium which were observed to accumulate chiefly in the stem tissue. It is noteworthy that in plants deprived of the essential traces of molybdenum loss of chlorophyll takes place in the same interveinal regions in which this metal concentrates.

Investigations on the absorption and retention of zinc and its occurrence in crystallized insulin are described by Kamen.[K3] The uptake of zinc by tomato plants grown in nutrient media containing Zn^{65} has been investigated by Stout and reported by Pollard and Davidson.[P27] Autoradiographs of the fruit show a pronounced concentration of radiozinc in the seeds.

The migration and reaction of lewisite gas into skin have been studied autoradiographically by Axelrod and Hamilton.[A5] The compound was synthesized from radioarsenic and possessed an activity of 10 microcuries of As^{74} per mg of lewisite gas. Beta-ray patterns of the exposed tissue showed that the compound was concentrated chiefly in epidermis. The exposure produced a massive necrosis of the greater part of the epidermal layer, and the radioactivity was confined almost entirely to dead cells.

Certain members of the rare-earth group of elements such as yttrium. cerium, and lanthanum have a beneficial effect on plants grown in nutrient media containing between 100 and 500 ppm of these ions.[S42] It has

also been shown by Milton, Murata, and Knechtel[M44] that certain rare-earth mineral deposits originate from the decay of plants whose leaves concentrated the traces of rare earths present in the soil. Members of the rare-earth group are included among the principal end products of uranium fission, and their mode of deposition in tissue has become a matter of considerable interest.

The concentration of rare earths by vegetation is a matter of concern in the disposal of fission products. Disposal by dilution into streams may be offset by subsequent reconcentration by plants along the embankments. The average abundance of yttrium in the earth's crust is about 0.003 per cent. Analyses of dried hickory leaves show the presence of 0.17 to 0.8 per cent rare-earth oxides.

The investigations of Copp, Axelrod, and Hamilton[C21] show that the rare-earth metals behave biologically like plutonium and are deposited in the uncalcified organic matrix of the bone. This mode of deposition appears to be unrelated to calcium content and differs from the segregation of other heavy metals in the skeleton.

APPLICATIONS IN METALLURGY

The results which may be gained by the aid of microscopic or other metallographic investigations are therefore to a great extent of a pathological character. To diagnose different kinds of slag inclusions, to determine their quantity and mode of occurrence, must of course be questions of great importance as a guide in carrying out metallurgical processes on which the quality of the metal ultimately depends.—Benedicks and Löfquist, 1931

Study of Segregates. Shoupp[S29] has investigated the segregation of phosphides in steel by incorporating P^{32} into a small melt of metal heated in an induction furnace. The metal was cast into a 2-in. disk, which was exposed against photographic film after polishing. The pattern suggested that the phosphorus concentrated along minute blowholes in the cast alloy. This interpretation does not appear to be justified in view of subsequent experiments by Nelson.[N2] He drilled holes of varying depth into the polished surface of a P^{32} steel alloy. The autoradiograph produced by this test specimen showed that the blackening increased progressively with the depth of the artificial blowholes. Since beta particles are not absorbed appreciably in traversing a few millimeters of air, greater blackening results because of the incidence of rays originating from the walls of the cavities.

It is difficult to avoid the formation of blowholes in small experimental castings. Samples selected for autoradiography must therefore be impregnated with low-melting-point alloys of high stopping power in order to avoid spurious effects from air pockets. Better resolving power can be secured by employing thin polished sections of the type commonly employed in x-ray microradiography. With proper attention to detail the beta-ray patterns should prove invaluable in checking conclusions based on etch reactions, printing methods, and microradiographic studies.

Chemical and electrographic printing methods [Y7] are employed extensively in the identification of segregates. In these methods a surface film of the alloy is transferred to a gelatin-coated paper. By developing the ionic surface replica with suitable chemical reagents the identity and distribution of the segregates are revealed by specific colorations. Owing to preferential solubilities of different phases or marked variations in conductivity the stripping of the surface film is apt to be non-uniform. Points of this nature can be elucidated by comparative chemical and autoradiographic tests on alloy specimens containing radioactive isotopes. Thus, it is not known whether in sulfur printing (p. 7) all metallic sulfides produce the reaction, and it is not established whether liquations of MnS, FeS, or (Mn,Fe)S print with equal facility.

Stanley [S36] has suggested that the distribution and identification of certain inclusions might be facilitated by adding active isotopes of calcium and titanium to a molten slag-metal system and testing the resultant ingots autoradiographically. It should also prove practical to follow the mechanism and depth of case hardening by heating the polished surface of steels with $KC^{14}N$.

Friction Processes. Radioactive tracers have proved serviceable in the study of friction between metallic surfaces. If the moving slider carries a radioactive metal, an autoradiograph of the traversed surface will reveal the extent and location of the indicator metal transferred from the slide to the test surface. Studies of this sort have been made by Gregory [G24] employing radioactive lead as the slider.

The adhesion component in friction processes has also been studied with the aid of a Cu-Be base plate rendered radioactive by deuteron bombardment. Metallic transfers to the rider as small as 10^{-10} g could be detected by radioactive measurements. The investigations of Sakmann, Burwell, and Irvine [S2] show that

riders of all materials tested removed some bulk metal from the radioactive base, and that even at the smallest loads matter was transferred under lubricated as well as dry conditions.

The quantity of metal transferred in friction processes is very minute and difficult to estimate even with the increased sensitivity made possible by the use of radioactive indicators. Burwell [B49] has described several techniques for the measurement of the activity of the minute samples. As an example of the autoradiographic technique he describes a series of friction tracks made by rubbing a neutron-activated mild steel on the surface of the same non-radioactive alloy. The patterns showed an adherence of the transferred material in discrete spots suggesting the formation of local welds with the test surface.

With soft metals, such as lead, crossing over copper, the friction patterns indicate a continuous smudging of the active metal. Fast x-ray film is employed as the recording medium for the beta-ray pattern as the activity of the transferred metallic film is usually low. The pliable photographic film can be wrapped around the surface of cylindrical test blocks.

APPLICATIONS IN CRYSTALLOGRAPHY

The crystal habit is often altered by traces of minor constituents in the mother liquor. Habit modifications of ammonium dihydrogen phosphate crystals grown from solutions containing minute quantities of added metallic ions have been described by Kolb and Comer.[K17] These investigations indicate that adsorption of trace constituents occurs on the growing crystal surface. The use of radioactive cations would permit the visualization of the traces of adsorbed metals, particularly if inclusion takes place along select crystal loci.

Since beta-ray-emitting isotopes representative of nearly all elements are now readily available, it should be possible to extend the crystal tracer studies initiated by Hahn to systems of fundamental importance in analytical precipitation reactions, and in the growth of special crystals suitable for radiofrequency control purposes.

Tracer techniques are also serviceable in studying self-diffusion and replacement phenomena in minerals. Gaudin and Vincent [G5] have observed that when chalcocite, native Cu_2S, is im-

mersed in a solution of radioactive copper ions the mineral acquires activity. The depth replacement of copper from the Cu_2S lattice by Cu^{63} was demonstrated as follows: The section was coated with paraffin, except for one face which was immersed in the solution. The face subject to replacement was then ground at a slight bevel, thereby exposing parts of the mineral that were at different depths during the diffusion experiment. The gradation in the blackening of the beta-ray pattern from one end of the piece to the other is a measure of the depth of penetration of the radioactive atoms.

AUTORADIOGRAPHY OF NEUTRON-ACTIVATED SOLIDS

The number of neutrons captured by a target varies over a wide range depending on the nuclear components and the neutron energy. In almost all the elements slow neutron capture results in the formation of an unstable compound nucleus which eventually reaches stability by the delayed emission of beta particles, positrons, or gamma radiation. Solids exposed to a stream of neutrons thus become radioactive. The activity is dependent chiefly on the cross section of the nuclei for neutron capture and the rate of decay of the isotopes produced in the capture process.

The capture cross section for slow neutrons ranges between a maximum of $79{,}000 \times 10^{-24}$ cm^2 for dysprosium and 0.01×10^{-24} cm^2 for carbon. The wide range of capture cross sections coupled with the distinctive half-lives of the induced activities offers many possibilities for the identification and localization of elements in polished section.

Studies by Hoffman and Bacher [H30] on the photographic effects produced by neutron bombardment of thin metallic foils show that every element causes an enhanced blackening as compared with the emulsion background. The photographic density increases with the atomic number of the element when the thickness of the foils is adjusted to equal numbers of atoms per unit area. Certain elements, such as cadmium, produce exceptionally pronounced blackening owing to resonance neutron capture and electron emission from the compound nucleus reaching equilibrium by internal conversion.

Part of the blackening produced by irradiated cadmium probably originates from pseudophotographic effects. Direct contact of freshly cast cadmium produces an image on x-ray film with a photographic density of 0.3 after 48 hours' exposure.[Y17] Freshly abraded cadmium metal and alloys in which cadmium is a major constituent activate coarse-grained photographic emulsions. Kallmann[K24] has also observed that the gamma radiation emitted by cadmium under neutron bombardment has a high photographic efficiency and produces a stronger blackening than is to be anticipated from external gamma-ray sources of equal intensity.

The activities induced in metallic foils of indium, rhodium, or copper are employed extensively in the estimation of neutron flux. In alloys of elements of markedly different cross section for slow neutron capture, segregates can be localized by means of autoradiographs of the neutron-irradiated section. The method has been applied by Stephens and Lewis[S40] in the study of Al-Si alloys employed in the manufacture of crystal rectifiers.

Autoradiographic methods for the localization of minerals in polished section after their exposure to neutrons have been investigated by Goodman.[G16] During irradiation by slow neutrons certain isotopes, as for example Au^{197}, are transformed into radioactive species, Au^{198}. If a sufficiently large number of atoms become radioactive, the beta particles emitted in their subsequent decay serve as a means for their identification by half-life measurements and localization by autoradiography.

Preliminary experiments showed that the radioisotopes formed by Mn, Au, W, As, Na, K, and P during slow neutron bombardment were particularly suited for studies of this type. Goodman and Picton[G15] have applied the method to manganese minerals by *in situ* neutron formation of Mn^{56} which decays by beta-particle emission with a half-life of 2.6 hours.

In a more detailed study, Goodman and Thompson[G17] list the elements in the order of their suitability for autoradiography. The classification is based on capture cross section of the target nuclei and the disintegration rates of the radioisotopes formed by neutron capture. Elements with half-lives between 1 and 10 hours are most convenient from the viewpoint of activity measurements. In the order of decreasing suitability for autoradiographic study, Goodman and Thompson list the elementary constituents of segregates as follows:

Excellent: Dy, Eu, Ba, In, Mn
Good: As, Cu, Ir, La, W, Au
Fair: I, Pt, K, Na, Ca, Ni, Si, Y
Poor: Cl, Zn, Bi, P, Se, Ta, V, Mg, Al

Silver, cadmium, and rhodium, not included in this tabulation, are also suitable for beta-ray-pattern studies after slow neutron irradiation.[Y17]

The selectivity of the beta-ray pattern is confused by the presence of minerals in the section which become persistently photoluminescent as a result of neutron bombardment. The phosphorescence induced in samples of scheelite is sufficiently intense for the activation of color film. On contact with Kodachrome film the irradiated minerals record a blue image, indicating that the emitted light resides chiefly in the near ultraviolet.[Y17] The enhanced blackening resulting from luminous effects can be recognized by separating the activated specimen from the emulsion by a composite filter one half of which is black paper and the other half Cellophane. These materials absorb beta radiation to about the same extent, but the Cellophane is transparent to the visible and the near ultraviolet light. Concomitant luminescent effects are thus revealed by a greater blackening beneath the Cellophane portion of the filter.

The polished sections are enclosed in a container assembled from slabs of paraffin about 3-in. thick and are exposed with the polished surface facing the cyclotron target. The time of irradiation is dependent on the neutron flux and the half-life of the induced activity and may vary from a few minutes to several hours. The induced activity is visualized by exposing the specimens against emulsions of moderate grain size, such as Lantern-Slide plates.

Bakelite is not activated appreciably by slow neutron bombardment. Polished specimens of the type commonly employed in mineralographic studies yield induced beta-ray patterns of fairly good definition. The resolution is improved by thinning the section to about 100 microns. The thin sections cannot be mounted on glass slides, as the backing becomes radioactive during neutron exposure. Plastics free from inorganic fillers or slabs of pure graphite provide satisfactory supports.

The magnitude of the initial autoradiographic exposure can be approximated with the aid of an average activity measurement of the individual sections. However, if the activity is localized in select components constituting a small fraction of the total

surface, the initial trial is apt to be overexposed. Several trial exposures are usually necessary to secure a pattern showing detailed structure of the segregates. Examples of this technique, using sections irradiated by neutrons from the Carnegie cyclotron, are shown in Fig. 46.

With but few exceptions the elements best adapted to this method of study occur in minerals which are readily identified
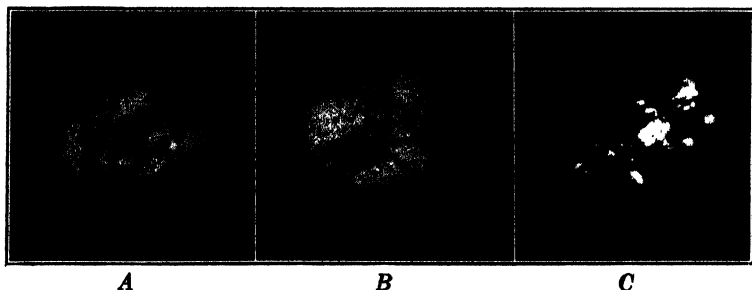
FIG. 46. Autoradiographs of mineral sections activated by neutron bombardment. Positive prints 1×: white, highly active; gray, moderate activity; black, no activity. Neutron bombardment: $Be^9(d, n)B^{10}$, 7 hours at 150 microamperes, 3-in. paraffin filter. Autoradiographic exposure: 5 hours on Eastman Process Ortho film.

A. Copper ore (gray) containing inclusions of pyrite (black).
B. Cuprite (light gray) and intergrowths of malachite (dark gray).
C. Cerussite (dark gray) enclosing native gold (white) and showing external replacement film of malachite (gray).

by simple petrographic techniques. Neutron irradiation, however, presents a new approach to the study of the distribution of minor constituents in natural and synthetic crystals. The trace constituents responsible for the fluorescence of certain crystals under ultraviolet light are often elements such as europium, samarium, and other rare earths of large cross section for neutron capture. When the matrix atoms are not rendered active by the bombardment, the orientation of the minor constituents can be revealed by means of autoradiographs.

The method should likewise prove serviceable in detecting minute grains of minerals of the rare-earth group. Euxenite, samarskite, and monazite also contain appreciable amounts of uranium or thorium, but the spontaneous activity is comparatively small as compared with the neutron-induced activity in

the rare-earth nuclei. The interference of the spontaneous activity is further reduced by interposing a thin black paper between the section and the emulsion. This absorbs the alpha particles responsible for the major part of the photographic action contributed by uranium and thorium. Under these conditions, the method should prove applicable in studying the distribution of rare earths in altered radioactive minerals.

The application of the method is limited to investigators having access to cyclotrons or atomic piles. Radium-beryllium neutron sources generate a total of 2×10^7 neutrons per sec per curie of radium. To secure slow neutrons this source must be surrounded by about 10 cm of paraffin, which reduces the emergent flux to a point where it is inadequate for sample activation. A 60-in. cyclotron generates a neutron flux equivalent to about 10^6 curies of Ra + Be. According to Fermi [F10] the pile at the Argonne Laboratory generates a thermal neutron flux of about 4×10^{10} per cm^2 per sec when operated at 100 kw.

NEUTRON ABSORPTION PATTERNS

By interposing a thin section in a beam of neutrons, the attenuation resulting from capture in segregates offers another approach for the localization of certain nuclei. Thus, if a silver foil is irradiated with slow neutrons, it becomes uniformly radioactive. When a thin section is placed in front of the detector foil, areas composed of atoms with large cross sections for neutron capture stop a fraction of the incident neutrons, and the activity of the silver foil is reduced correspondingly. The variation in activity is visualized by placing the detector foil in contact with a fast optical-type emulsion. Peter [P37] has designated this process as "neutron photography." The patterns resemble x-ray photographs of the same objects but differ in showing strong shadows where hydrogenous materials are concentrated. Unlike microradiography with x-rays, which produces greatest contrast with heavy metals like iron or lead, neutron radiography offers the prospect of securing patterns of structures composed of light elements which are transparent to x-rays.

Kallmann [K24] has investigated several mechanisms for enhancing the photographic action of neutrons. The capture of slow neutrons by Li^6 or B^{10} produces densely ionizing particles.

The photographic action of these secondaries can be increased 100-fold by including a phosphor in the system and recording the fluorescent light on fast emulsions:

A photographic system of high neutron sensitivity is prepared by sandwiching a double-coated photographic film between two layers of phosphor, which in turn are covered by very thin films of lithium or boron compounds. The thickness of the neutron capture layers is adjusted to the range of the ionizing particles in the respective compounds. Kallmann found that the efficiency could be further increased by interposing a 0.5-micron aluminum foil between the capture layer and the phosphor, thereby reflecting fluorescent light back into the photographic emulsion.

Kallmann also observed that the intensity distribution of a beam of fast neutrons can be recorded photographically by interposing thin layers of a phosphor and paraffin between the source and the emulsion. The recoil protons ejected from the hydrogenous layer transfer their energy to the phosphor with a high yield of light for photographic activation.

By employing an intense collimated beam of thermal neutrons Shull [S29a] was able to photograph the Laue pattern produced by neutron diffraction in single crystals. Indium foil was employed as the detector for the diffracted neutrons. The position of the Laue spots was visualized by making autoradiographs of the beta activity induced in the indium.

MASS ASSIGNMENT OF RADIOISOTOPES

The photographic technique has found an important application in establishing the atomic mass number of the radioactive isotopes formed in nuclear reactions. The reaction products are separated from solution and deposited on the source filament of a mass spectrograph. The ion beams of different mass are thus collected in separate lines on a photographic plate. Like all other charged particles, the heavy ions form a developable latent image. To distinguish the radioactive isotopes, the collector plate is contacted with a second photographic emulsion sensitive to beta radiation, thereby producing an autoradiographic replica of those line deposits which are radioactive. In the Eastman Type III-O plates employed as recording media Hayden [H18a] notes that about 10^{10} positive ions of mass 100 to 150 accelerated to 8 kev produce a developable line measuring 0.2×10 mm. On the same area of emulsion 10^5 beta particles emitted from the radioactive isotopes produce a comparable blackening on the indicator plate.

The method has been employed by Hayden and Inghram [H18] in establishing the mass numbers of the isotopes responsible for the 46-hour

activity induced in samarium and the 9.2-hour activity of europium when these rare earths are bombarded by neutrons. Comparison of the indicator and collector plates showed that the active isotopes were Sm^{153} and Eu^{152}. Inghram [I3] has applied the technique in the determination of the masses and half-lives of the radioactive isotopes of element 61 formed in the fission of uranium. After the deposition of the separated ions, the collector plate was placed successively against different portions of the indicator plate for periods calculated to give equal intensity at the mass 149 position if the half-life was 49 hours. The photographic densities from a series of five exposures showed that 61^{149} decays with a half-life of slightly more than 49 hours, although the isotope of mass 147 showed no detectable decay. The latter, 61^{147}, has a half-life of about 4 years, and since the weight deposited on the collector plate is extremely small the number of beta particles was not adequate to blacken the indicator. The method has also been employed by Hess, Hayden, and Inghram [H25] in assigning mass numbers to the active isotopes of rhenium, Re^{186} and Re^{188}. The neutron-induced activities in lutecium, ytterbium, and dysprosium have likewise been studied by Inghram, Hayden, and Hess.[I4]

Efforts have been made to establish the mass of the isotope responsible for the feeble spontaneous alpha activity of samarium. In 1938 Wilkins and Dempster [W22] prepared a mass spectrograph film of the separated isotopes of the element on an Eastman Fine-Grain Alpha-Particle plate. After an exposure of three and one-half months 10 tracks were observed at the position corresponding to the deposit of Sm^{148}. On the basis of this preliminary experiment the activity has since been assigned to this isotope with a half-life of 1.4×10^{11} years.

The recent extensive investigations on the details of the technique revealed that in depositing the film large clusters of ions may be detached from the electrodes and may settle at the collector plate at random. With sources of low activity more tracks may thus be emitted from the stray specks than from the lines of separated isotopes. With this possibility in view Dempster [D14] has reinvestigated the problem, vaporizing the samarium from a hot anode ion source and collecting the separated isotopes on metal plates coated with graphite. In one experiment a total quantity of about 0.19 microgram of the element was collected, and this source recorded 117 alpha-particle tracks when exposed against a nuclear emulsion for 170 days. Only short tracks of 7-micron range were ascribed to samarium. Of these, 48 tracks were located in the region between mass 150 and mass 154, and no concentration was found in any other region. From the track

distribution it is concluded provisionally that the activity is associated with the Sm^{152} isotope.

MEASUREMENT OF GAMMA RADIATION

The gamma rays accompanying alpha- or beta-disintegration processes are penetrating electromagnetic radiations emitted from the nuclei undergoing radioactive transformation. Like all other divergent radiation the gamma rays are emitted with the velocity of light and have a specific wavelength λ and an energy E related by $\lambda E = 1.238 \times 10^{-10}$ cm. The nuclear gamma rays have energies residing between 0.05 and 3 Mev as indicated in Table 26, are very penetrating, and lose their energy very slowly. Hence, a flux of gamma-ray photons produces comparatively small blackening on photographic emulsions compared with an equal flux of alpha or beta particles. The gamma radiations interact with matter chiefly by the following three mechanisms:

TABLE 26. GAMMA RADIATION FROM RADIOISOTOPES

Isotope	Primary Decay Mechanism	Associated Gamma-Ray Energy, Mev *
Na^{24}	β^-	2.76
Ca^{45}	β^-	0.7
Mn^{56}	β^-	2.7
Co^{60}	β^-	1.3
Ga^{65}	K	0.05–0.12
Y^{88}	K	2.0
La^{140}	β^-	2.5
RaC	α, β^-	1.75
ThC″	β^-	2.62
Ra^{226}	α	0.19
UX_2	β^-	0.8

* The gamma rays are usually emitted over a wide-line spectrum of varying intensity. Thus, the gamma rays from Th(C + C′) have components of:

Energy, Mev	1.35	1.50	1.60	1.80	2.20	2.62	3.20
Relative intensity	1	0.65	1.1	0.65	0.6	10	0.25

1. Photoelectric Effect. When a gamma-ray photon interacts with an atom an electron may be ejected from either a K or an L orbit, and this electron receives all of the energy of the ab-

sorbed gamma ray. The residual atom emits x-rays and Auger electrons capable of photographic action. When the source emits low-energy gamma rays the fast photoelectrons tend to emerge at right angles to the beam of gamma radiation. When the flux is directed at right angles to the emulsion the fast photoelectrons have some opportunity to expend part of their energy in ionizing the silver halide grains. In general, the absorption is most effective when the medium is composed of heavy atoms, and screens of lead foil or lead tungstate are often interposed between the source and the emulsion in order to enhance the photographic blackening by the photoelectrons scattered into the emulsion.

2. Compton Effect. Instead of reacting with the atom as a whole the incident gamma ray may react with one of the outer electrons, accelerating it but moderately, and at the same time the initial photon becomes converted into a gamma ray of lesser energy. This process of elastic scattering, discovered by Compton, is particularly effective when the medium is composed of lighter elements such as aluminum or carbon. The gelatin of the emulsion and the cellulose film base are therefore serviceable in reducing the intensity of an incident gamma-ray beam as a result of processes of Compton scattering by the nitrogen and carbon atoms. The attendant low-energy electrons form a latent image on traversing the silver halide grains.

3. Pair Production. Gamma rays with energies in excess of 1.022 Mev can interact with heavy nuclei in such manner that the incident photon is completely absorbed at a point near the nucleus of the atom. This annihilation process materializes the energy of the photon and results in the production of a pair of + and − electrons. Pair production plays a significant role only for high gamma-ray energies incident on heavy-metal absorbers. When lead foils are irradiated by ThC″ gamma rays in a Wilson cloud chamber the resultant positrons and electrons can be visualized as thin tracks. These particles also cause latent-image formation in coarse-grained emulsions.

These considerations show that the photographic action of gamma radiation is caused entirely by the production of secondary electrons in the sensitive film or its immediate surroundings. The efficiency of the process is low. Thus, Type K film exposed for 4 min at a distance of 29 cm from 300 mg of radium enclosed in a platinum tube with walls 0.5 mm thick produces

on standard development a photographic density of 0.7. Because 1 gram of radium in equilibrium emits 7.28×10^{10} gamma rays per sec, the exposure is equivalent to 500×10^{6} photons per cm^2 of film. Under conditions of direct incidence the same photographic blackening would be produced by only 10^6 alpha particles or 10^7 beta rays. Although the instantaneous effect is small, the action is additive with time, and with sufficiently long exposures very small gamma-ray intensities can be measured.

The principal application of gamma-ray patterns resides in the detection of flaws and macro inclusions in large metallic castings. The gamma rays from radium can penetrate through 10 in. of steel without being completely absorbed. By placing a fast emulsion behind the thick metal it is thus possible to demonstrate the presence in the interior materials of low density, such as voids, cracks, and inclusions of slag and sand. These absorb fewer of the impinging rays than the matrix, and the emergent gamma rays will register as dark spots on the processed emulsion. Methods of radiographic testing by means of radium gamma rays are described by Barrett,[B6] Doan,[D15] and Johnson.[J9]

The photographic method has also been applied in the estimation of the radium content of sealed plaques. By comparing the photographic density with that produced by a standard radium preparation Meyer [M46] has shown that the method is applicable in the assay of small amounts of radium over a range of 0.01 to 100 mg. The uniformity of the distribution of the radium sulfate within the plaque can also be demonstrated autoradiographically by contacting the container briefly against photographic film. Experiments reported by Perry [P40] indicate that a contact period of about 20 sec provides a suitable exposure for sealed preparations containing 5 mg of radium.

Emulsions are employed extensively as gamma-ray dosimeters in the health monitoring of personnel employed in the radium industry, and in the large scale concentration of U^{235} and plutonium. Owing to dangers of excessive radiation exposure all laboratory workers using radioactive isotopes should be monitored in order to determine whether the shielding facilities are adequate to reduce the stray radiation below the tolerance level. The tolerance dose of penetrating radiation is frequently taken at 0.1 roentgen per day. The roentgen (r) is a measure of energy absorption per unit volume. It is defined as the amount of x- or gamma radiation which produces as a result of ionization 1 electrostatic unit of electric charge in 1 ml of standard air. Fast x-ray-type emulsions, abetted by the action of intensifying

screens, can register as little as 0.03 r by a measurable increase in photographic density above the background fog.

The penetrating radiation dosimeters consist of one or more photographic films wrapped in black lighttight paper enclosed in a moisture-proof envelope. The wrappings stop all alpha particles and soft-beta radiation, and the recording media are thus activated by gamma rays, fast beta particles, and x-rays. By superimposing a cross of lead foil about 1 mm thick, even the more energetic beta rays are stopped and the blackening beneath the shielded portion is attributable to gamma radiation. The lead also serves as an intensifying screen because of the larger number of electrons generated within the metal by photoelectric and pair-production processes.

Emulsions of varying sensitivity are available (Table 27) and

TABLE 27. SENSITIVITY RANGE OF EMULSIONS FOR PENETRATING RADIATIONS

Emulsion	Dose in Roentgens
Type K x-ray film	0.05–2.0
Type A x-ray film	1.0–10
Ciné Positive 5301	5–80
Ciné Positive 5302	40–400
Kodalith 6567	70–700
Kodabromide paper G3 *	400–8,000
Eastman Type 548-O	2,000–20,000
Defender Adlux film	50–15,000

* Slow-speed contact and enlarging papers can also be employed advantageously in the photographic visualization of intense alpha- and beta-ray sources. The slow media require long exposures thereby giving the operator ample opportunity for assemblage of the contact camera, and at times avoid the use of an evacuated pinhole camera (see p. 25). Autoradiographs of polished sections of moderate activity can also be made directly on paper media by extending the exposure. Pitchblende samples furnish sharply defined patterns of the radioactive matter after 7 to 10 days' exposure on Kodabromide enlarging paper.

by proper selection a range of 0.05 to 20,000 r can be measured. The largest exposure is limited by the maximum density measururable, which is of the order of about 3 units. The Adlux film described by Whipple [W30] is particularly useful in monitoring personnel subject to high dosages of radiation because of its unusually extensive scale. The characteristic curves of Type K and Adlux film are compared in Fig. 47. The latter preparation consists of a transparent safety base 150 microns thick doubly

coated with a slow-speed bromide emulsion, each layer averaging 15 microns in thickness. Whipple[W30] recommends a development in Eastman Formula D72 diluted with 2 parts of water at 20° C for 3 min using constant agitation. After the usual fixation and washing the developed aggregates of silver vary between 0.5 and 0.7 micron in diameter.
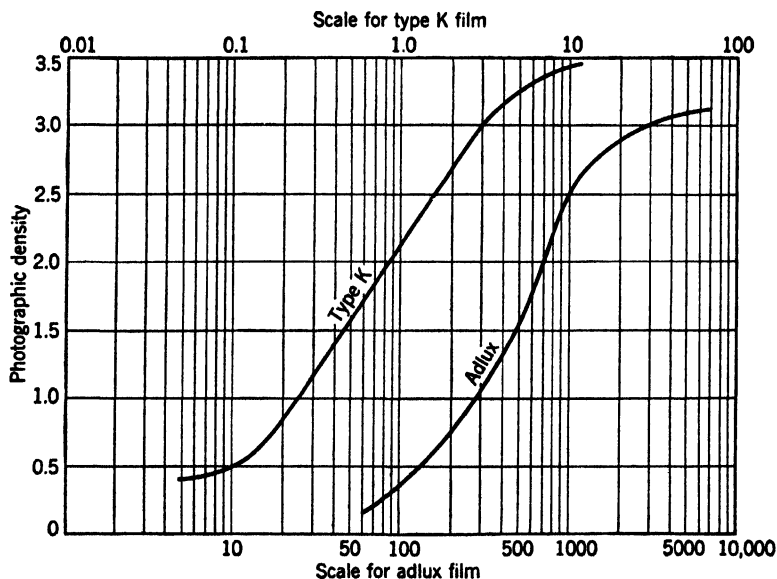
FIG. 47. Characteristics of fast (Type K) and slow (Adlux) gamma-ray recording media.

All film intended for radiation dosimetry should be stored at low temperature and low humidity in a room free from stray radiation. Each batch of new film must be calibrated against radiation doses of known intensity. This is effected by enclosing the emulsion in the same type holder as carried by the personnel and exposing at a measured distance, exceeding 25 cm, from a known weight of radium for a time commensurate with the range of dosage to be measured. The calibration is best made with a minimum of matter in the vicinity in order to reduce scattering of the radiation.

The dosage varies inversely as the square of the distance (d in cm) between source and film and is related to the exposure (t in min) and the weight of radium (w in mg) by $r = 0.14\ tw/d^2$. The standards and a blank are developed in the same bath with the monitor films, and their densities are compared either visually or by means of a densitometer. When very low intensities are compared the films are best viewed on a support of

white paper. Incident light thus passes through the film once on its downward course and again when it is reflected by the paper to the eye, thereby accentuating the contrast between the image and the fog background. Densities above 0.5 unit can be measured more accurately by means of transmission-type photoelectric or visual-matching densitometers.

The characteristic curve produced by gamma radiation is similar in shape to that produced by beta particles on emulsions of moderate grain size. The greatest accuracy in the gamma-ray measurement results when the exposure falls on the nearly linear portion of the S-shaped curve, as then a small variation in intensity causes a large change in photographic density. Emulsions differing in speed exhibit the linear response at different levels of radiation intensity, as is evident from Fig. 47. By proper choice of film quantitative measurements are possible over a range of about 0.05 to 20,000 r. When a wide range of radiation dosage is apt to be encountered the monitoring unit should contain two or more films of different sensitivities. By incorporating a nuclear-type emulsion along with the x-ray films it is also possible to evaluate the exposure to fast neutrons by a microscopic count of the number of recoil proton tracks (see p. 286).

A survey of photographic film as a radiation dosimeter by Pardue, Goldstein, and Wollan [P41] shows that the reliability of film meters does not change with duration of exposure and that blackening will almost certainly be the result of radiation exposure. Possible pseudophotographic effects, however, must not be overlooked, and may occur when films are stored in freshly machined aluminum holders (see p. 12). In this respect, it is noteworthy that Morrison [M47] has observed that film stored for a few hours in direct contact with lead intensifying screens under conditions of elevated temperature and high humidity shows considerable irregular blackening. By proper consideration of conditions of film storage and care in development gamma-ray exposures of 0.1 r can be measured with an accuracy of about 10 per cent, and at the lower limit of 0.05 r an accuracy of about 20 per cent is attainable.

Chapter 12 · APPLICATIONS IN NUCLEAR PHYSICS

When we consider the wonderful advances made by Rutherford and his collaborators in nuclear physics with sources separated out of the minerals of the earth, and then note that for ultranucleonic research also this globe is supplied with particles of the necessary energy, we marvel at the richness of nature.—J. A. Wheeler, 1946

The early chapters of this work have been confined almost exclusively to alpha particles and the tracks left by them in photographic emulsions. The alpha particle is the only densely ionizing fragment ejected in the spontaneous disintegration of the naturally occurring radioactive elements. In nuclear reactions with artificially accelerated particles the disintegration of the compound nucleus is accompanied by the emission of other types of heavy charged particles, as the proton, deuteron, triton, light recoil atoms, and heavy fission fragments. These particles also record tracks in the emulsion, often with a grain spacing sufficiently characteristic to permit their differentiation and identification.

The ability to differentiate the tracks of different particles makes the emulsion a valuable tool in modern nuclear physics research on a level of importance equal to that of the cloud chamber. A complete exposition of the applications of the nuclear emulsion covers almost the entire field of experimental and theoretical nuclear physics. A comprehensive survey is beyond the confines of this work. The description will be limited to the purely laboratory aspects of the problem, such as range measurement and particle identification from the grain characteristics of its trajectory.

The exposition is not of exclusive interest to the nuclear physicist. It may be read profitably by other experimentalists even though the only source of densely ionizing radiation available to them may be the alpha-emitting uranium and thorium minerals. The earth and everything on its surface is a gigantic target under constant bombardment by a thin rain of particles origi-

nating from the cosmic radiation. Almost any nuclear emulsion is thus likely to carry a record of incident cosmic-ray particles included among the population of alpha-particle tracks recorded from the experimental exposure. An example of this concurrent process is illustrated in Fig. 60*B* on p. 292. It is desirable to have an understanding of the origin of these rare events and to keep a systematic record of their occurrence in terms of period of exposure and area of plate surveyed.

RANGE MEASUREMENTS

The nuclear emulsion consists of a concentrated dispersion of silver halide granules of roughly spherical shape in a matrix of gelatin. The size of the grains ranges between 0.1 and 0.6 micron in diameter, and the grains are distributed at random, separated by thin layers of water-permeable gelatin. In traversing the heterogeneous medium the ionizing particle intersects the grains in its path along chords of varying length, as indicated at *A* in Fig. 48. If sufficient energy is spent in the intersected grains they become reduced to metallic silver during photographic development. Grains which are not activated are removed during fixation, leaving voids of comparable volume in the wet gelatin. On drying, the gelatin layer contracts in thickness, as shown in *B*, owing to the coalescence of the voids left by the extracted grains.

The residual row of silver grains outlining the path of the particle is a measure of its range in the original emulsion. Since the medium is discontinuous the particle may originate and terminate its trajectory in gelatin, and its recorded range, as defined by the terminating grains of silver, will tend to be somewhat smaller than the actual distance traversed. In the modern nuclear-type emulsions the grains per unit of path are numerous, and the blind spots about the terminations do not introduce appreciable uncertainty in the range estimate.

In microscopic examination of the plate on a fixed stage only the horizontal component L_h of the complete track length L is observed. In order to reconstruct the full length of the track in the original emulsion from its measurement L_h in the contracted gelatin film it is necessary to measure the depth of the track z in the gelatin and to establish the shrinkage factor f resulting

from the processing. The latter is determined by making depth measurements on the terminal grains of the track with the aid of a sharply focusing objective. The readings are taken off the
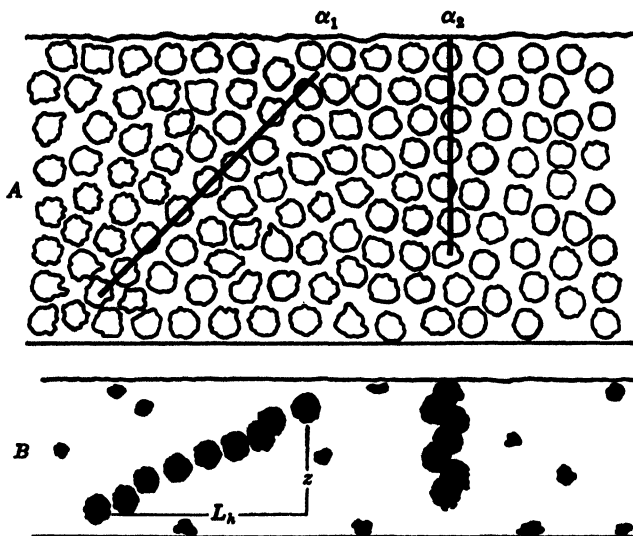
FIG. 48. Diagrammatic representation of track-recording mechanism.

A. The lines represent the trajectories of alpha particles α_1 and α_2 in a thick-layered fine-grain emulsion.

B. Corresponding tracks delineated by grains of developed silver, as oriented in the dry gelatin layer after photographic processing. The trajectory of particle α_1 can be reconstructed by microscopic measurements of L_h and z. The accuracy of these measurements is in general about 5 per cent. A perpendicularly incident particle, such as α_2, produces a visible track owing to the compression and slight distortion of the column of silver grains, but its length is subject to considerable uncertainty owing to the large correction in converting the depth measurement z to its original length Z.

Note that at high magnification the upper emulsion surface is not a true mathematical plane.

scale of the fine adjustment, taking care to avoid backlash of the micrometer screw. The presence of scattered fog grains is of material aid in locating the upper and lower surfaces of the gelatin layer.

In employing the fine adjustment for depth measurements, it is important to make all movements for final readings in the same direction.

Lag of the mechanism is reduced by starting all readings from the lower limit of the range of the movement. If the value of the depth divisions is not marked on the microscope it can be obtained by placing a cover glass of known thickness on a slide and recording the settings at which the lower and upper surfaces are brought into sharp focus. In making absolute measurements of the depth of a grain the immersion oil should have the same refractive index as the gelatin. Since the value of z is obtained by difference, a correction for the difference in refractive index of oil and gelatin is unnecessary. A more precise measurement of z can be made with the aid of a depth gauge attached to the microscope tube, as described by Powell and Champion.[P33]

Owing to gelatin shrinkage the inclination of the track is altered, and the angle of dip as measured in the gelatin must be corrected before the track length is computed. The nature of the shrinkage has been studied by Powell [P34] by exposing plates to a precisely defined beam of protons at a known angle of incidence and comparing the obliquity of the recorded tracks. No appreciable change occurs in the length or width of the emulsion, but the removal of the silver bromide causes a 10 to 50 per cent reduction in the emulsion thickness depending on its initial composition. The shrinkage is dependent on the volume of soluble material removed during processing, and its value can be approximated from the volume of the silver halides on the assumption that the fixing process leaves no voids after the gelatin dries. The vertical component of the trajectory

$$Z = z\left(1 + \frac{\text{volume of extractables}}{\text{volume of gelatin}}\right)$$

and the complete track length is expressed by $L = \sqrt{L_h^2 + Z^2}$.

In the Eastman NTA or NTB emulsions containing 83 per cent by weight of silver halides, $Z = 1.99z$. It is noteworthy that certain emulsions contain water-soluble plasticizers, such as glycerine, and that these are also removed during fixation and washing. Their presence introduces a significant change in the value of the shrinkage factor. As an example, an emulsion composed of 82.0 AgBr + 2.5 AgI + 13.5 gelatin and 2.0 per cent of glycerine by weight has a shrinkage factor of 2.41. If the presence of the glycerine was not known a factor of 2.11 would be computed on the basis of the silver halide content.

DIFFERENTIATION OF IONIZING PARTICLES

The tracks produced by nuclear fragments differing in mass, charge, or velocity are differentiated by variations in the number of developed grains along the trajectory. The mean grain spacing Δ is defined as $L/(n-1)$, where n is the total number of grains in the track L microns long. The track characteristics can also be expressed in terms of average grain density $G = n/L$. When the grain densities at the fast and slow ends of the trajectory are appreciably different, the quantity serves as an indicator for the direction of motion of the particle. In long proton tracks the terminal grain densities, G_f and G_s, are determined by grain counts on 50-micron portions of the track adjoining the initial and terminal grain.

The mean grain spacing Δ is a function of the average grain diameter d and the concentration c of the silver bromide in the emulsion. By assuming that the track is linear, the grains spherical, and that each grain traversed is rendered developable, Zhdanov[Z1] derived from geometric considerations that $\Delta = 2gd/3c$, in which g is the density of the silver halides. For essentially pure silver bromide emulsions, $\Delta = 4.31d/c$. The nuclear-type emulsions contain about 3.3 g of AgBr per ml, and the developed grains have a diameter of about 0.3 micron. If all the grains are activated, then the mean grain spacing would be 0.39 micron. Measurements of Δ in the tracks of low-energy alpha particles show an average value of about 0.55 micron, indicating that about 80 per cent of the grains traversed are rendered developable.

Since all grains are not of equal sensitivity and require different degrees of energy expenditure for latent image formation, the observation of the mean grain spacing along the developed track permits the differentiation of nuclear particles. The quantitative aspects of the problem have been considered by Wilkins and St. Helens.[W28] They visualize the trajectory of a nuclear particle as being surrounded by a cone of action which is smaller when its speed is large and increases in radius as the particle slows down. Hence the grain density increases as the projectile slows down. This is particularly noticeable in the tracks produced by energetic protons, and the points of entry and termi-

nation can be readily recognized by the low and high grain densities near these points.

To render a grain developable an amount of energy in excess of a minimum threshold value must be communicated to it. Under conditions of equal sensitivity grains crossed through a major diameter will have more energy imparted to them than those traversed along a minor chord and hence will have a greater probability of eventual development. Emulsions can be prepared with a sufficient variation in grain size, concentration, and sensitivity so that a fairly selective response is exhibited towards one or more nuclear particles.

The investigations of both Richards and Speck [R6] and Demers [D9] show that the extremely fine-grained Eastman 548-O emulsion is essentially insensitive to proton and alpha particles but is activated by fission fragments. The fission-fragment tracks are almost continuous lines, which according to Demers [D9] are of maximum width at their points of origin and taper down towards the termination. The greater grain spacing in proton tracks permits their ready differentiation from the tracks produced by alpha particles of comparable energy. Light particles, such as protons and mesons, are easily deflected from their linear course by close approach to nuclei in the emulsion, and the tracks produced by these particles frequently exhibit scattering.

The mean grain spacing in the tracks of particles of moderate energy is in general below 1 micron, and the counting of individual grains necessitates the use of an optical system of maximum resolving power. An oil-immersion objective of high numerical aperture and oculars providing a total magnification of about 1250× are essential. In visual grain counting Köhler illumination with pale green light (Corning green-glass filter 4010, 4 mm thick) is more effective than dark-field illumination. Under dark-field lighting adjacent small grains tend to coalesce and present the appearance of a single large grain.

The quantitative aspects of the variation in grain spacing as a function of the ionizing power of charged nuclear particles are described in publications by Pignedoli,[P23] Lovera,[L40] Demers,[D9] and Feld.[F19] The more recent investigations of the Bristol group [L16] show that log n is a linear function of log L, the experimental data for alpha particles, tritons, protons, and mesons falling on nearly parallel lines. The relationship among the total number of grains in a track n is related to the mass of the particle M and its recorded range L by $n = Kz^{(2k - 2/3)}M^{(1 - k)}L^k$, where z is the particle charge, k is a constant for a particular particle, and the

coefficient K is dependent on emulsion characteristics and mode of development.

In the practical application of these considerations to the identification of the particles producing the tracks, the grains are counted, starting from the terminal end of the trajectory, along 50 micron lengths until the last grain is tallied at the fast end. These data are tabulated in terms of the sum of grains for each 50, 100, 150— of residual range L. For a given track the plot of log L against log n is essentially a straight line, particularly in the region where L exceeds 50 microns. Within the limitations of straggling the curve is independent of the energy of the particle, both long and short tracks falling on essentially the same locus, provided the slow end terminates in the emulsion. The curves for alpha particles, deuterons, protons, and mesons are approximately parallel, and are displaced from each other in accordance with the discriminating power of the emulsion. A 45° line will intersect the several loci at points of equal grain density. At these intersections the residual ranges are proportional to the masses of the particles when they are of the same charge. Thus, if grain counts on proton tracks are available, the tracks of tritons, deuterons, and mesons recorded in the same emulsion can be identified by the position of their log L vs log n curves with reference to the locus of the proton standard. A typical plot for an Eastman NTA emulsion exposed in the stratosphere is exhibited in Fig. 49.

The method is applicable only if the tracks are recorded in emulsions of equal sensitivity, given the same development, and in which fading of the latent image between exposure and development has not occurred. According to Webb [W20] the sensitivity of different batches of the same emulsion is essentially constant for protons of moderate energy, but the tracks may exhibit large fluctuations in grain spacing at higher energies where latent-image formation is critically dependent on the threshold sensitivity of individual grains.

The problem of nuclear-particle identification arises chiefly in the study of emulsions exposed to cosmic radiation. In such exposures the best practice is to depend on internal standards recorded in the same plate as the event under study. The back-

ground alpha stars provide data for the grain spacing characteristics of low-energy alpha particles. Among the tracks arising from nuclear disruptions a large proportion are recorded by protons and these can often be sorted out from the tracks of more densely ionizing particles on the basis of Δ vs L plots. The
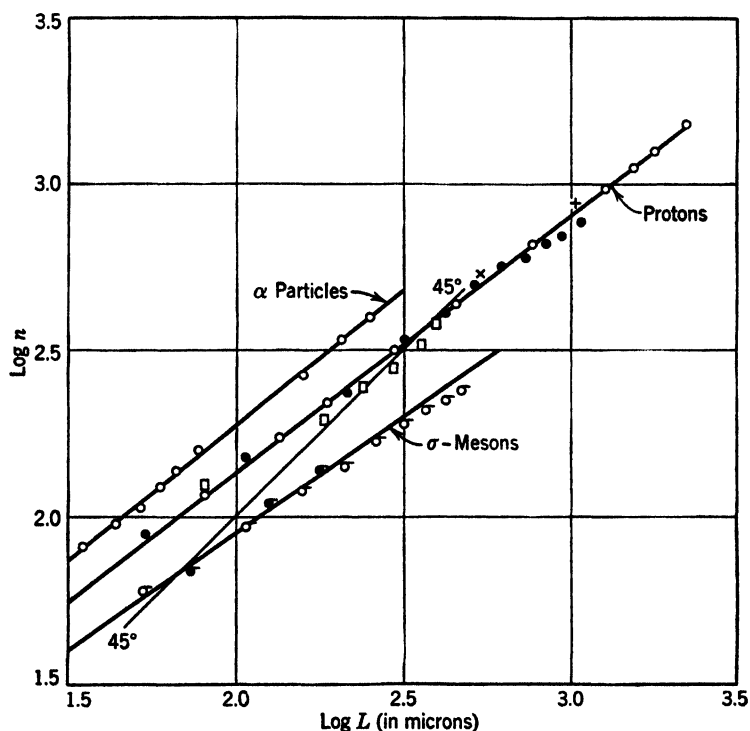
FIG. 49. Relationship between residual range L and grain count n. Eastman NTA emulsion 100 microns thick exposed in the stratosphere and developed by Method III.

tracks of σ mesons are readily recognized by the star at the end of their highly scattered trajectory and these provide calibration data for a particle of 313 electron masses. The tracks produced by Li^8 fragments are characterized by a hammer structure (see Fig. 65). Further details on the determination of the masses of charged particles are described in the work of the Bristol investigators [L17a, G32] on the grain structure and scatter of π-, μ-, ρ-, and σ-meson tracks.

RANGE-ENERGY RELATIONSHIPS

The deceleration of fast charged particles is caused by their interaction with the orbital electrons of the matter traversed. When the velocity of the incident particle is large compared with that of the electrons the rate of energy loss per centimeter of path is expressed by:

$$-\frac{dE}{dL} = \frac{4\pi e^4 z^2}{mv^2} NZ \log\left(\frac{2mv^2}{I}\right)$$

In this formulation ez is the charge on the incident particle, N is the number of atoms per cubic centimeter of emulsion, and Z and I are the average nuclear charge and average excitation potentials of the atoms constituting the emulsion, and m is the electron mass. The range L traversed by a charged particle of mass M until it is slowed down from its initial velocity v_0 to zero has the form

$$L = \frac{M}{e^2} f(v_0)$$

Choudhuri [C13] has investigated the applicability of this basic relationship to the tracks of alpha particles and protons recorded in the Ilford Halftone emulsion. The theory on which the relationship is based is valid only in media, such as air, composed essentially of light atoms. In the emulsion, however, a 30 per cent deviation is observed between calculated and observed proton ranges owing to the presence of a large number of heavy silver and bromine atoms whose inner K and L shells cannot be excited by incident particles of low energy.

Although this relationship is not directly applicable to the translation of range measurements in the emulsion into energy of the incident particle it permits useful deductions of a general nature:

1. Alpha particles and protons of identical velocity exhibit the same range, because their ratio of M/e^2 is the same.

2. A proton of energy E will have the same range as an alpha particle of energy $4E$.

3. A deuteron has twice as large a range as a proton of the same velocity.

4. The range of a deuteron of energy E is twice that of a proton of energy $E/2$.

5. When two different kinds of particles of identical charge, but differing in mass, produce tracks with equal mean grain spacing their kinetic energies are directly proportional to their masses.

The curves constructed by Livingstone and Bethe [L35] relating the energies of alpha particles and protons to their respective air ranges are immediately applicable when the stopping power of the emulsion relative to air is known. The mean stopping power of an emulsion is defined as the ratio of the mean range in standard air to the mean range in the emulsion. The stopping power is
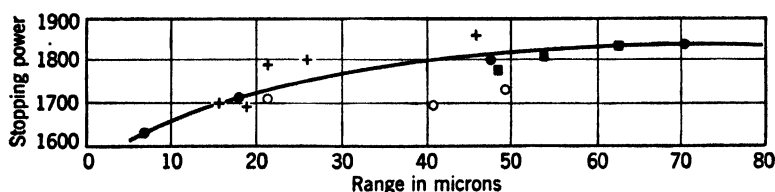
FIG. 50. Relationship between range of alpha particles and the stopping power of nuclear-type emulsions.

● Ilford B1, from data of Lattes, Fowler, and Cüer.[L17]
+ Ilford Halftone Concentrated, from data by Tsiang.[T16]
■ Ilford Concentrated, from data by Cotton.[C23]
⊙ Eastman NTA, from data by Yagoda.[Y17]

dependent on the identity and energy of the particle. The independent measurements of several investigators summarized in Fig. 50 indicate that the mean stopping power for alpha particles of 5 to 9 Mev is 1760 ± 50. For alpha particles of greater energy the stopping power increases slowly, and Cüer [C30, 33] has computed a value of 2070 for alpha particles of 75 Mev.

The stopping power for protons is of the same general order of magnitude as for alpha particles. The measurements of Peck [P6] on the Eastman NTB emulsion show that the stopping power for protons with energies in excess of 5 Mev is about 2030. Lattes, Fowler, and Cüer [L17] find that in the Ilford B1 emulsion the stopping power for protons ranges between 1800 and 2000 for particles of 2 to 13 Mev.

Certain nuclear emulsions, as the Eastman NTB, carry an inert top coating about 1 micron thick intended as a protective layer for the silver bromide grains. Mauer and Reynolds [M89] have reported that the presence of this T-coat introduces an ap-

preciable error in the measurement of stopping power by means of particles entering the emulsion at small angles. Thus, the track of a 2.5 Mev proton entering the emulsion at 15° is 9 microns longer than the recorded trajectory of the same particle when incident at 2°. The Eastman emulsions are now available both with and without the protective T-coat.

The most reliable estimate of energy from measured track lengths results when the plate is calibrated by means of particles of known charge and energy. Track-length measurements in plates loaded with purified solutions of the radioelements provide a satisfactory calibration for low-energy alpha particles. This method is limited to the range of 2.4 to 8.78 Mev provided by the alpha particles from the decay of samarium, thorium, and its equilibrium products.

As described in Chapter 5, while the gelatin is wet the loaded emulsion records tracks which are of greater length than those subsequently recorded in the normal dry state. When the length of all tracks is analyzed statistically the wet tracks produce a minor peak to the right of the principal peak. Variations in stopping power can be eliminated by collecting the active deposits of thoron or radon on negatively charged emulsions as described in Chapter 7. This records full energy tracks from the decay of the *A, C,* and *C′* bodies covering a range of 4.73 to 8.57 air-cm. Powdered pitchblende makes a convenient source of radon that is essentially devoid of thoron.

To secure calibration data for particles of higher energy or different mass and charge, it is necessary to expose plates to particles accelerated to known energy levels by the cyclotron or other high-voltage apparatus. Studies of this type have been reported by Lattes, Fowler, and Cüer [L17] on high-energy protons and alpha particles. Their experimental data are represented graphically in Fig. 51 together with functions computed for deuterons, tritons, and mesons with the aid of the basic range-energy relationships. Although the proton- and alpha-track measurements were made on the Ilford Nuclear Research plates the data are applicable also to emulsions of other types but of similar composition and grain size.

PROTON TRACKS

The proton is a singly charged hydrogen nucleus accelerated to velocities in excess of 10^9 cm per sec. When alpha particles collide with hydrogen atoms in hydrogenous materials "knock-on" protons are produced. Protons also originate from the alpha bom-

bardment of thin metallic foils, as for example in the $Al^{27} + He^{4} \rightarrow Si^{30} + H^{1}$ nuclear reaction. The proton tracks are recorded photographically by interposing target foils between the alpha-particle source and the emulsion which are sufficiently thick to stop the alpha particles. The protons, having greater
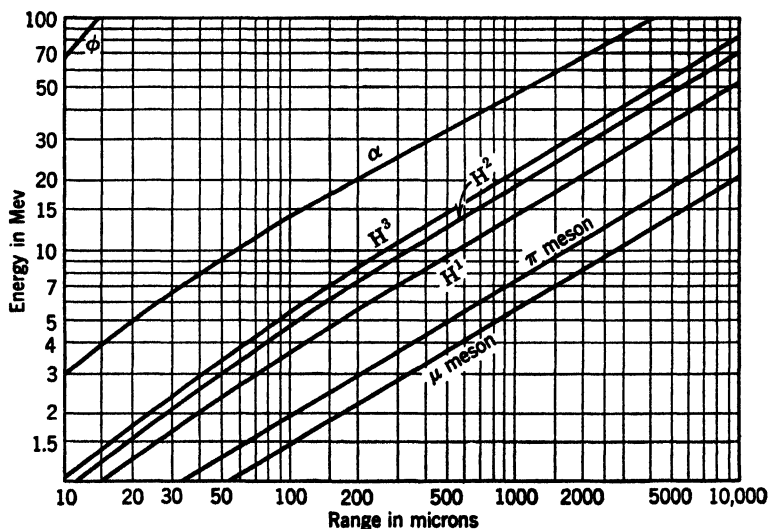
FIG. 51. Relationship between range and energy of ionizing particles in Ilford "Nuclear Research" emulsions.

The loci of the singly charged particles (H^3, H^2, H^1, π, and μ) are fitted by $E = 0.262\ M^{0.425}\ L^{0.575}$, where E is the energy in Mev, and L the range in microns of a particle of M mass units (proton = 1).[L17a] On the graph, the lines for the π- and μ-meson were constructed for particles of 400 and 200 electron masses, respectively.

ranges, penetrate the foil and record tracks of length proportional to their residual energies.

Tracks exhibiting the full energy of the proton are recorded by elastic collision of fast neutrons with hydrogen atoms within the emulsion layer. In collisions in which the hydrogen nucleus is projected at an angle less than 5° with the original direction of the neutron it has been demonstrated by Powell[P32] that the proton is accelerated with more than 99 per cent of the incident neutron energy. Under these conditions the range of the proton is a measure of the neutron energy.

A neutron source adequate for the study of knock-on proton tracks can be assembled as illustrated in Fig. 52. A beryllium disk carrying a deposit of about 20 millicuries of polonium provides an ample number of neutrons when the exposure is prolonged for about 2 days. The proton track popu-
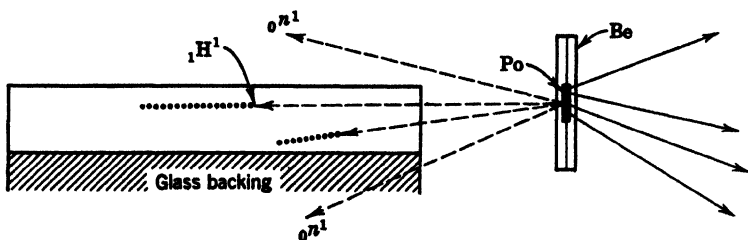
FIG. 52. Emulsion exposed to fast neutrons from a Be-Po source.

lation varies roughly as the inverse square of the distance between the source and the point of observation in the emulsion. To secure conditions of good geometry the center of the source should be about 10 cm from the nearer end of the emulsion. This necessitates an increased ex-
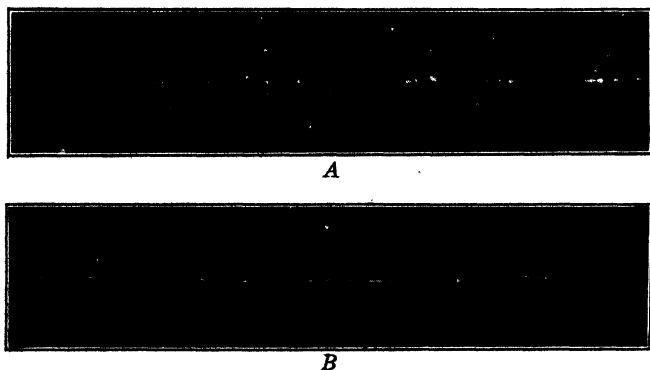
FIG. 53. Grain structure in a proton track. Terminal details from a 11.3-Mev proton track recorded in an Eastman NTA emulsion. Dark-field illumination; 620× magnification.

A. Fast end, grain density 0.42 per micron.
B. Slow end, grain density 1.65 per micron.

posure, and Demers,[D9a] using a 450-millicurie Po-Be source found a 10-day period essential for a good density of recoil tracks.

Demers' measurements on 1800 tracks show that this source emits neutrons with extreme energies residing between 0.4 and 11 Mev. A statistical study of the ranges in the emulsion indicates the presence of energy

groups producing proton tracks of 3.1, 7.1, 14.9, 23.2, and 33.1 air-cm. The emulsion method of detecting recoil protons has been investigated by Reines[R21] as a means of determining the neutron spectra emitted by nuclear chain reactors. The technique has also been applied by Peck[P6a] in the elucidation of the neutron spectra emitted in the bombardment of aluminum by alpha particles, and in the disruption of silicon by deuterons.

The track characteristics of protons have been studied by Choudhuri.[C13] In the Ilford Halftone plates the mean grain spacing is nearly constant at low energies and increases linearly with proton energies in excess of 4 Mev. Essentially the same conclusion was drawn by Schopper[S10] using Agfa K plates as the recording media. The tracks of energetic protons show a marked variation in grain density at the fast and slow ends of the track, as may be seen from the portions reproduced in Fig. 53. Statistical studies of grain density at track terminations show that, when the entire trajectory is recorded, G_s at the slow end is approximately a constant independent of track length, whereas G_f at the fast end diminishes linearly with the proton-track length. These observations are of utility in estimating the energy of a proton when only the initial portion of the trajectory is recorded, as often occurs in cosmic-ray stars.[Y16,20]

NUCLEAR-SCATTERING CAMERAS

When a beam of accelerated particles is directed on a target a small fraction of the projectiles is captured with the momentary formation of a compound nucleus. In its subsequent disintegration fragments such as protons, deuterons, and alpha particles are ejected. The number, nature, and angular orientation of these particles can be studied conveniently by recording the tracks of the ejected fragments in nuclear-type emulsions. These data are of importance in providing a measure of the energetics of nuclear reactions, in demonstrating the existence of nuclear-excitation states, and in serving as a check on the masses of the particular isotopes involved in the reaction.

The general experimental approach is illustrated by the camera (Fig. 54) employed by Talbott[T27] in his investigation of the angular distribution of the alpha particles produced by the interaction of protons with thin films of lithium. The brass chamber is fitted with three 1 × 3 in. plates supported by blocks at an angle of 45°. The windows in front of the plates are covered with 25-micron-thick aluminum foil which stops light and low-energy protons, but is permeable to the energetic alpha particles produced in the $Li^7(p, \alpha)\alpha$ reaction. The lid of the chamber

(not shown in the illustration) is made of Lucite and makes a vacuum-tight seal with the aid of a neoprene gasket. The unit is attached to the cyclotron or Van de Graaff generator by means of the sleeve on the right. After evacuation the target support is rotated to the lithium stove and a thin film of the metal is dis-
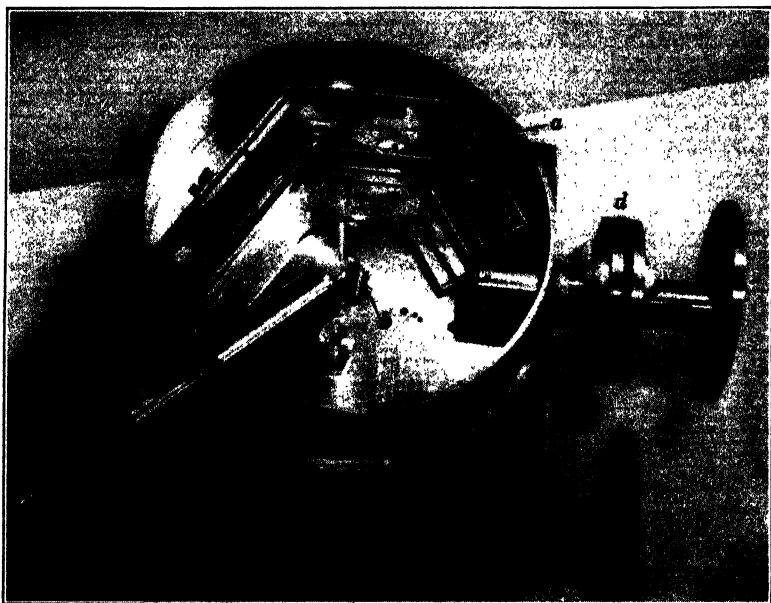
Courtesy of F. L. Talbott

FIG. 54. Triple-plate scattering camera. The emulsions are supported on the 45° blocks (*a*). The target support (*b*) is coated with lithium by distillation after the unit is evacuated by means of the lithium stove contained in the sylphon cylinder (*c*). The camera is attached to the proton accelerator by the coupling (*d*) which also contains a slit system for collimating the beam.

tilled onto its face. The collimated proton beam (about 0.1 microampere) is turned on and the plates are exposed to the alpha particles emerging in different directions from the target for about 2 to 10 min depending on the accelerating voltage. Microscopic examination of the developed plates reveals the number of alpha particles emerging from the target over a span of about 180°. From the known geometry of the camera it is possible to convert each point of observation on the plates to specific angles of emission with reference to the primary proton beam.

Since the inception of the technique by Wilkins,[W24] the method has been applied extensively in the study of the mechanism of diverse nuclear reactions. Details of experimental arrangements are described in the work of Chadwick,[C3] May,[M18] and Heitler[H29] in their studies of the scattering of protons by hydrogen, deuterium, helium, and thin foils of the lighter elements. A single-plate scattering camera with an angular range of 25° to 160° is described in the investigations of Rubin, Fowler, and Lauritsen [R12, 13] on the angular distribution of the alpha particles originating from the bombardment of lithium and fluorine with protons.

Dearnley [D13] has described another type of scattering camera utilizing two plates, one above and one below the collimated proton beam. To define oriented paths in the emulsion which facilitate subsequent track counting, the plates are exposed to ultraviolet light through a grating ruled with lines 0.25 mm apart. The light from an argon glow lamp, employed as the illuminant, is readily absorbed by the gelatin, and only the top grains of the emulsion carry the image of the grid. This permits microscopic examination of the scattered proton tracks without interference by the superimposed lines.

Buechner and coworkers [B53] have devised a camera in which the scattered particles are deflected onto the emulsion with the aid of a powerful annular magnet. When used in conjunction with thin targets of the light elements deflected particles differing in energy by 1 per cent are readily resolved by the position of the tracks on the oriented emulsion. This method has been applied by Strait [S49] in the study of the $Be^9(d\alpha)Li^7$ reaction. By accelerating the incident deuterons to 1.5 Mev, the ejected alpha particles escaped with a total of 5.2 Mev. This facilitated comparison of their magnetic deflection onto the emulsion with the tracks recorded from polonium alpha particles (5.30 Mev) employed as a calibration standard.

Chupp, Gardner, and Taylor [C36] have studied the energy distribution of the protons emitted from a target bombarded by 190-Mev deuterons. In the excitation of targets with high-energy deuterons either the neutron or proton component of the H^2 projectile may be stripped off when one of the component nucleids strikes the edge of a nucleus in the target. The ejected protons have a peak energy of about 90 Mev and are difficult to detect photographically owing to the very low grain density in the tracks. The difficulty of following the fast end of the track in the high fog background was obviated by slowing down the protons with suitable filters before they entered the emulsion. In the Ilford type B1 plates employed in this investigation, protons with energies below 20 Mev were found to record recognizable tracks. The method furnished a proton energy distribution curve in good agreement with theoretical predictions for the energy spectrum produced by the stripping process.

PHOTODISINTEGRATION PROCESSES

The fine-grained nuclear-type emulsions are not activated appreciably by gamma radiation. Tests by Demers[D9] revealed that the gamma-ray fogging is tolerable until the plate receives a total exposure of a few hundred roentgens. This property permits the study of photodisintegration processes in emulsions loaded with light nuclei. The products of the disintegration can be identified by grain counts, and the energy of the particles can be estimated from measurements of the track length. The method was applied initially by Powell[P31] in the disintegration of deuterium by gamma radiation. The heavy hydrogen was incorporated on the emulsion surface by the application of a thin layer of ammonium chloride containing substituted deuterium, ND_4Cl. After the irradiation, proton tracks of 2-Mev energy were observed in the developed emulsion layer.

The photodisintegration of deuterium has been reinvestigated more recently by Gibson, Green, and Livesey[G11] employing Ilford plates loaded during manufacture with calcium nitrate hydrated with heavy water, $Ca(NO_3)_2 \cdot nD_2O$. After bombardment with 6-Mev gamma rays, a group of protons' tracks with an average range of 36 microns was recorded. The energy of these protons (1.88 Mev) furnishes a measure of the quantum energy of the gamma radiation, as $h\nu = 2E_p + Q$, and the dissociation energy Q of the deuteron is known from its mass conversion. The reaction is endoergic and consumes 2.18 Mev of atomic mass equivalent. The kinetic energy of the particles corresponds to 2×1.88 Mev. The disintegration of a H^2 atom into a proton and a neutron was thus effected by the conversion of a total of 5.9 Mev gamma-ray energy.

The method has since been applied by Bosley, Craggs, and Nash[B54] in the determination of the energy spectrum of the x-radiation emitted from the Metropolitan-Vickers 20-Mev Betatron. A histogram of 75 proton recoil tracks measured in Ilford type C2 plates loaded with deuterium showed a sharp peak indicative of the presence of photons of 5 Mev with minor components with energies up to 17 Mev. Gamma-ray spectra can also be evaluated by loading heavy water into nuclear emulsions and exposing the wet plates, enclosed in a moisture-chamber,

to the source under investigation. Goldhaber [G33] reports that by this simple technique from 30 to 80 per cent D_2O by weight can be introduced into Ilford C2 emulsions coated 200 microns on a stripping base. The proton tracks recorded in the wet emulsion are elongated, and the stopping power of the medium must be determined by calibrating the moist plates by exposure to neutrons of known energy. Monoenergetic neutrons of 4.25 Mev are produced in the $H^2(H^2,He^3)n^1$ reaction. By comparing histograms of tracks recorded in plates loaded with D_2O and H_2O exposed to the radiations from the F^{19} $(p\alpha, \gamma)O^{16}$ reaction, Goldhaber was able to resolve two groups of photons with energy peaks at 6 and 7 Mev in the deuterium-loaded plate.

Similar methods are potentially applicable using emulsions loaded with other light atomic nuclei as Be^9. On exposure to gamma radiation beryllium is known to disintegrate with the emission of neutrons. Two mechanisms are possible:

$$Be^9 + h\nu \rightarrow Be^8 + n^1$$

or

$$Be^9 + h\nu \rightarrow 2He^4 + n^1$$
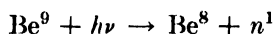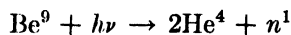
Glückauf and Paneth [G13] have demonstrated that the second mechanism is more probable by measuring the volume of the helium accumulated in samples of beryllium metal bombarded with the gamma radiation from radon. While the gamma rays from radon are capable of disrupting the Be^9 nucleus, the resultant alpha particles have too low a kinetic energy for the production of recognizable tracks. However, beryllium-loaded plates might prove serviceable in the estimation of exceptionally high gamma-ray energies associated with the decay spectrum of ThC″.

It is noteworthy that certain nuclei such as C^{12} are also susceptible of photodisintegration by high-energy gamma radiation:

$$C^{12} + h\nu \rightarrow 3He^4$$

and more rarely

$$C^{12} + h\nu \rightarrow Be^8 + He^4$$
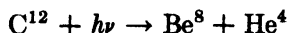
This reaction is endoergic and requires an energy expenditure of 7.16 Mev to initiate the disruption. In plates exposed to 17.5-Mev gamma rays Hänni, Telegdi, and Zünti [H44] observed III-pronged alpha stars which they attributed to photodisintegration of carbon nuclei in the gelatin. In these stars the component

alpha tracks are of small range and are readily differentiated from the alpha stars of radioactive origin.

In a plate exposed to cosmic radiation at 3500 meters' elevation a miniature star was observed [Y18] with alpha tracks of 10.9, 11.7, and 13.8 microns range, all terminating within the emulsion layer. The kinetic energy of the three alpha particles totals 10.4 Mev, and, if this event is attributed to a C^{12} photodisintegration, the energy of the initiating photon is about 17 Mev. In photodisintegration stars the orientation of the tracks indicates conservation of momentum, whereas in alpha stars of radioactive origin the tracks are generally ejected at random.

IDENTIFICATION OF ALPHA-EMITTERS BY TRACK LENGTHS

Emulsions loaded with ions of the radioactive elements permit the identification of the source material by track-length measurements. When the quantity adsorbed is known accurately, the half-life can also be evaluated from the track population and the known period of exposure. The distribution curves on track-length measurements described in the work of Powell,[P34] Demers,[D9] and Faraggi [F2] exhibit maxima sufficiently sharp for purposes of source identification. Owing to statistical fluctuations in the magnitude of the recorded track length caused by straggling of the range in heterogeneous media a large number of tracks must be measured in order that the mean range may be defined sharply. Typical track-length distributions for RaF, RaC′, and ThC′ alpha particles are shown in Fig. 55. By increasing the number of tracks measured the spread at half-maximum allows resolution of admixed alpha-particle emitters provided their ranges differ by 10 per cent.

Measurements reported by Demers [D9] show that the energy of alpha particles over the range of 4 to 8.5 Mev can be determined from microscopic range measurements with an accuracy better than 2 per cent. Groups of alpha particles of similar range, such as UI and UII, can be differentiated from track-length measurements in nuclear emulsions. By loading a plate with actinium, Guillot and Perey [G80] demonstrated that the principal group of alpha particles of 3.46 air-cm is accompanied by a 15 per cent group of fewer energetic particles with an air-range of 3.1 cm. Faraggi [F2] has measured the range of thorium alpha

particles in emulsions and arrives at an equivalent air-range of 2.43 ± 0.03 cm, in agreement with other recent measurements which indicate that the current value of 2.60 air-cm is probably high.

When the system contains several radioelements about 1000 tracks must be measured to provide adequate statistical data
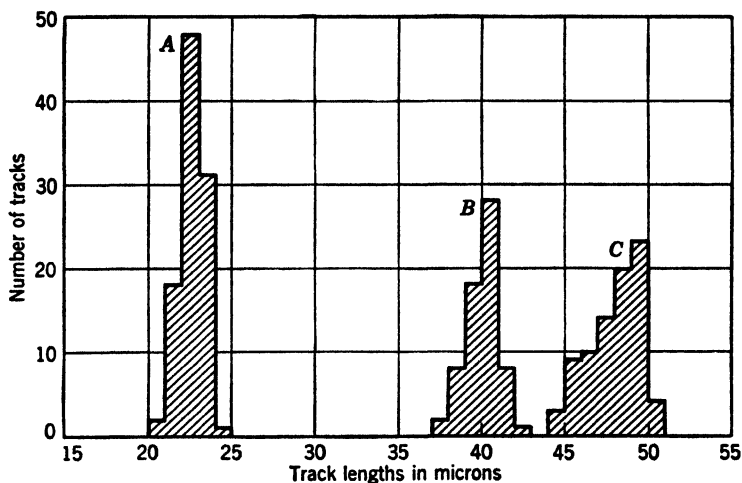
FIG. 55. Range distribution of alpha-particle emitters.

A. Emulsion loaded from an aqueous solution of polonium (RaF).
B. Emulsion exposed to radon emanation (carnotite).
C. Emulsion exposed to thoron emanation (thorianite).
In plates *B* and *C* only the long-ranged tracks formed by RaC′ and ThC′ decay respectively were selected for measurement.

for a sharp delineation of the several peaks. This is admittedly a laborious task, but the results achieved are comparable with those obtained by elaborate mechanical alpha-pulse analyzers of the type described by Freundlich.[F15] The emulsion technique has the advantage of inherent simplicity, freedom from mechanical breakdown, and ability to handle low concentrations of the more stable elements. The emulsion in addition portrays series disintegrations when the daughter products also decay by alpha-particle emission. This aspect of the technique aided in the discovery of the $4n + 1$ series and should prove serviceable in the study of collateral chains following the bombardment of heavy metal targets by accelerated particles.

RADIOACTIVITY OF SAMARIUM

Because of its continuous registration over long periods of time, track counting can be employed advantageously in measuring the disintegration rates of long-lived elements like samarium. The results obtained by investigators using electrical and emulsion counting methods are compared in Table 28. The agreement

TABLE 28. IONIZING PARTICLES ASSOCIATED WITH THE DECAY OF SAMARIUM

	Alpha Particle		Associated Particles		
Investigation	Range in air-cm	Disintegrations per sec/g Sm	Range in air-cm	Identity	Abundance
von Hevesy[V12]	1.13	75			
Lyford and Bearden[L45]	1.28	102			
Libby[L31]	1.28	150			
Herszfinkiel[H24]	1.5	67			
Mader[M1]	1.16	89	1.37	Proton	0.37
Ortner[O2]	1.10				
Pahl and Hosemann[P1]		88			
Schintlmeister[S5]	1.1		2.1	Alpha	
Hosemann[H35]	1.13	89		Proton?	<0.01
Lewin[L30]	1.13		0.13	Densely ionized	
Investigations by the Photographic Technique					
Taylor[T11]	1.13		3.5	Proton	0.01
Wilkins and Dempster[W22]	1.13				
Blau[B26]			1.8	Alpha	0.25
Cüer and Lattes[C31]	1.12	96	3.90	Alpha	0.014
Yagoda and Kaplan[Y18]	1.1	88-loading with Sm^{+++}; 114-Parlodion film of Sm_2O_3		None in samples analyzed	

is consistent in regard to the emission of an alpha particle of 1.13 air-cm range. Several independent studies suggest the presence of a minor group of ionizing particles possessing a longer range. Both Mader[M1] and Taylor and Dabholkar[T11] claim that the second group consists of protons rather than alpha particles.

It is difficult to evaluate the significance of the second group of particles owing to the difficulty of separating samarium from all other radio-

active elements, particularly the members of the actinium family, because the parent is isomorphous with the rare earths. The problem is further complicated in that the samarium preparations originated from different type minerals varying in uranium, and hence actinium, contents.

In view of present-day knowledge of the fading effect, the proton tracks observed by Taylor may be attributed to deterioration of the older background alpha-particle tracks. Exposures conducted on old plates exhibit a population of partially faded radium tracks which have a grain structure easily confused with that of proton tracks. This explanation, however, is not applicable to Mader's observations as his measurements showing proton emission were made in an ionization chamber. A minor group of associated alpha-particle tracks was also observed in the studies by Yagoda and Kaplan,[Y18] but an identical group appeared on the control plates, so that the long-range particles cannot be associated with decay processes in the samarium preparation.

Based on deductions from his theory of the nuclear-energy surface Feenberg[F23] has suggested that one of the isotopes of gadolinium, Gd^{152}, of relative abundance 0.2 per cent, may be a long-lived alpha-particle emitter. This hypothesis has been tested by Keller and Mather[K27] using Ilford C2 plates 100 microns thick in which about 2 mg of Gd_2O_3 per cm^2 was incorporated during emulsion manufacture. Plates developed at the end of 4, 9, and 14 weeks showed a small number of low-energy alpha-particle tracks with a range similar to those emitted by samarium. The track population was equivalent to a samarium content of less than 0.01 per cent, suggesting that the observed activity was probably caused by an associated samarium impurity in the gadolinium oxide preparation. This experiment indicates that if gadolinium has a radioactive isotope the half-life based on the abundance of Gd^{152} probably exceeds 10^{16} years.

The problem of the radioactivity of samarium and other adjoining members of the rare-earth group is worthy of further investigation. Element 61 is known to have long-lived beta-emitting isotopes, and the existence of a long-lived alpha-decaying isotope cannot be ruled out. Certain samarium preparations might contain traces of element 61, as the chemical fractionation methods employed in the isolation of samarium from other rare earths would not free it from element 61 if it were present in the original mineral.

Lutecium, Lu^{176}, is a spontaneous beta-ray emitter with a half-life of 2.4×10^{10} years. It is possible that other members of the rare-earth group may disintegrate at an even lower rate than

lutecium or samarium. There are indications that dysprosium emits alpha particles at 1/300 the rate of samarium as shown by the measurements of Gysae;[G31] and Yagoda[Y2] has suggested that thulium might have a natural radioactivity. If these elements decay with the emission of alpha particles, the decay rate can be estimated by carefully controlled exposures on background-eradicated emulsions. The technique should also prove applicable in establishing the feeble activities associated with zinc and platinum noted by several earlier investigators whose measurements are discussed by Rutherford.[R20]

TRACKS PRODUCED BY FISSION FRAGMENTS

Shortly after the discovery of the fission of uranium under neutron bombardment, tracks of the massive fission fragments were recorded in emulsions by Perfilov[P12] and Myssowsky and Zhdanov.[M37] In these investigations a thick film of uranium, separated from the emulsion by about 2 mm of air, was irradiated with slow neutrons from a RdTh-Be source.* The tracks were heavy and had an air range of about 1.6 cm. Data published by the Plutonium Project[P25] show that the masses of the fission fragments range between 72 and 158, with maxima at 96 for the light group and 139 for the heavy group. The average range of these massive densely ionizing fragments, as recorded in nuclear emulsions, is summarized in Table 29. These measurements correspond to a total air range of 4.2 cm, in good agreement with cloud-chamber measurements by Böggild[B30] ranging between 3.9 and 4.3 air-cm.

The fissionability of different nuclei can be determined by exposing suitably loaded emulsions to neutrons and observing the formation of fission tracks. Because of the importance of this technique, a considerable number of emulsions and processing methods have been studied, aiming at the selective registration of fission-fragment tracks.

The experimental approach can be classified into three main categories. In the first, an extremely slow emulsion which is

* The common practice of covering thin film sources with a layer of Scotch tape was in a large measure responsible for the delay in the discovery of the fission phenomenon. The coating, intended as a filter for the alpha particles, also stopped the fission fragments and prevented the observation of the intense ionization produced by them.

rendered developable only by intense localized ionization is employed. In the second class, a normal nuclear-type emulsion is utilized, and the tracks of the fission fragments are differentiated from other type tracks by variations in grain spacing. In the third category an effort is made to obliterate the latent image of alpha and proton tracks with the selective retention of the fission-fragment latent image.

TABLE 29. RANGE OF URANIUM FISSION FRAGMENTS IN EMULSIONS

Investigation	Range, microns		
	Long Track	Short Track	Total Range
Demers[D5]	14.4	11.2	25.5
Richards and Speck[R6]			23
Wollan, Moak, and Sawyer[W26]	14.5	10.5	
Green and Livesey[G22]	13	10	23–25
Tsien San-Tsiang[T20]			23
Yagoda[Y17]			24 ± 1 *

* Fission tracks recorded in the Eastman NTC emulsion loaded with 0.1 mg U per cm^2.

Special Fission Plates. In cooperation with the Eastman Research Laboratories, Borst and Floyd[B32] developed an emulsion type NTC which is insensitive to light, alpha, beta, gamma, x-ray, and neutron radiations but records the tracks of fission fragments. Exposure to large numbers of alpha particles causes eventual blackening, but the image is composed of a network of fog grains without track structures. When the ratio of alpha to fission disintegrations is not excessive, the fission-fragment tracks are observable on the fog background. The Ilford type D1 plate is of an analogous character, recording good fission tracks, and has a low sensitivity to alpha particles and protons. Borst and Floyd have employed these emulsions in measuring the fission cross section of uranium, lead, bismuth, and polonium.

Richards and Speck[R6] make similar use of the extremely fine-grained Eastman 548-O emulsion. When these plates are loaded from solutions of uranyl nitrate and exposed to slow neutrons, fission tracks are recorded without serious interference from the alpha particles emitted in the spontaneous decay of the uranium. Demers[D9] reports that the mean grain spacing of fission-fragment tracks in the Eastman 548 emulsion is 0.4 micron after development in D19 for 5 min.

Fission Tracks in Nuclear-Type Emulsions. The tracks of fission fragments can be differentiated from those of alpha particles and protons by their greater grain density. The method is practical only when short exposures can be made under high neutron flux in order to avoid the registration of a high population of alpha-particle tracks. According to Demers,[D9] loading from a 0.06 per cent solution of uranyl nitrate for 5 min yields an optimum concentration of uranium nuclei for exposures to slow neutrons from a chain-reacting pile. Larger concentrations tend to desensitize the emulsion, and the fission tracks develop with a low grain density.

The chief advantage of the nuclear-type emulsion resides in its ability to register the tracks of other ionizing particles which accompany the fission process. Demers,[D5] one of the earliest investigators of the phenomenon, observed the emission of long-ranged alpha particles accompanying the heavy tracks of the fission fragments, one of the recorded alpha tracks exceeding 28 air-cm in range. Subsequent measurements by Farwell, Segré, and Wiegand [F3] showed that 16-Mev alpha particles are emitted in the fission of U^{235} in the ratio of 1 alpha particle per 250 fissions, and that a fragment of similar energy is ejected in the fission of Pu^{239} with a frequency of 1 in 500. Marschall [M38] observes that in uranium-loaded NTB plates 1 per cent of the fissions show the track of an alpha particle directed nearly at right angles to the direction of the fission tracks.

Wollan, Moak, and Sawyer [W26] have made a systematic investigation of the alpha particles associated with the fission process, employing the Eastman Fine-Grain Alpha-Particle plates loaded from saturated solutions of uranyl acetate as the recording media. They observed alpha-like tracks with ranges between 9 and 39.7 air-cm, the maximum frequency residing between 20 and 25 air-cm. These tracks originate near the center of the fission track and thus serve as an indicator in measurements of individual fission-fragment ranges.

Along with the long-ranged group of alpha particles Green and Livesey [G22] have also observed the emission of charged particles with ranges of about 0.87 air-cm. According to Feather [F5] in about 1 per cent of all fissions an alpha particle is liberated at the moment of the separation of the massive fragments. These alpha particles are mostly of small energy below 2 Mev, but some are found with energies in excess of 20 Mev.

Tsein San-Tsiang and his collaborators [T17, 18, 21] have observed events in uranium-loaded emulsions indicative of ternary ϕ_3 and quaternary ϕ_4 splitting of the uranium atom, along with the more numerous instances of the binary fission process ϕ_2. These disintegrations are rare, and the relative frequency has been estimated at $\phi_3/\phi_2 = 0.003 \pm 0.001$ and $\phi_4/\phi_2 = 0.0003 \pm 0.0002$, respectively. In tripartition two of the fragments are heavy and the third one is light. The heavy fragments have ranges of 1.9 and 2.3 air-cm, and that of the light particle ranges between 2 and 44 air-cm.

In ternary fission the most frequent track length of the light particle corresponds to 25 air-cm and is emitted almost at right angles to the line of direction of the heavy fragments. These light particles appear to be identical with the alpha particles observed by Demers, Wollan, and others. Tsien San Tsiang also reports short-ranged fragments of 0.8 air-cm, probably identical with those observed by Green and Livesey. In the quaternary fission process, also studied by Ho Zah-Wei, San Tsiang, Vigneron, and Chastel,[H36] the compound nucleus of mass 236 splits into four fragments whose masses are estimated to be 84, 76, 72, and 4.

Tsien San Tsiang, Ho Zah-Wei, and Faraggi [T20] have estimated the energy liberated in the fission process from the range of the fragments in neutron-bombarded emulsions. When the compound nucleus of U^{235+1} splits into fragments with masses of 96 and 138, 150 ± 5 Mev kinetic energy is associated with the two particles. When the U^{238} isotope undergoes fission the energy of the fragments totals 160 ± 5 Mev.

In emulsions loaded with thorium and exposed to neutrons the fission fragments produce tracks of 21 microns total length. This corresponds to a kinetic energy of 135 ± 10 Mev for the Th^{233} compound nucleus. San Tsiang and Faraggi [T19] have also observed the tripartition of thorium in loaded emulsions exposed to fast neutrons. The third light fragment emitted at an angle of 70° to the line of direction of the heavy fragments has a range of 0.6 ± 0.2 air-cm. The ratio of ϕ_3/ϕ_2 is 0.014 ± 0.002 and appears to be more common than in the analogous tripartition of uranium.

In the investigations of San Tsiang and coworkers [T21a] the emulsion (Ilford C2, 40 microns thick) is loaded for 5 min in a 20 per cent uranyl nitrate solution, and is dried rapidly by dehydrating with 95 per cent ethyl alcohol for 3 min and exposing to a stream of air. Track discrimination is secured by altering the concentration of the developer or the time and temperature of development in accordance with the uranium pickup and the type of phenomenon under investigation. The tracks of fission fragments are differentiated from those of alpha particles and proton recoils by developing the plate for 40 min at 18° C in 1 part of D19 developer diluted with 19 parts of water.

Selective Processing for Fission Tracks. Studies on the action of oxidants on the latent image produced by ionizing particles led Perfilov [P13, 14] to the conclusion that the development of all silver bromide grains receiving only a single impact could be in-

hibited by oxidation before development. Since the specific ionization produced by fission fragments is greater than that of alpha particles traversing the same medium, Perfilov reasoned that a differential oxidation of the emulsion could be arranged such that only the grains traversed by fission fragments would subsequently develop.

Perfilov [P15, 16] observed that in plates exposed to external films of uranium under neutron bombardment the predominating population of alpha-particle tracks could be obliterated by bathing the emulsion in a solution containing about 0.15 mg of CrO_3 per ml before development. The exact concentration of the oxidizing solution and the period of immersion are dependent on emulsion characteristics, and the conditions are best determined by trial.

Concentrated solutions of uranium salts also have a destructive action on the alpha-particle latent image. Green and Livesey [G21] have observed that when the Ilford plates are loaded with increasing quantities of uranyl ions the tracks of alpha particles and protons are weakened whereas the grain structure of the fission-fragment tracks is not altered appreciably. Their studies show that the grain density in the fission tracks decreases with diminishing energy of the fission fragment. This behavior differs from the ionization functions of protons and alpha particles, which exhibit increased ionization towards the trajectory termination. It is therefore possible that the complete range of the fission fragments may not be recorded in uranium-loaded emulsions.

Green and Livesey [G22a] load Ilford C2 plates from uranyl acetate solutions acidified with 10 per cent acetic acid. In order to secure uniform distribution of the uranium throughout the emulsion thickness, a 1-hr immersion period is employed for 20-micron-thick emulsions, and the imbibition period is extended to 12 hr with plates coated 100 microns thick. After drying in a current of air and exposure to slow neutrons, the plates are developed for 40 to 50 min in 1 volume of D19 diluted with 10 parts of water. Development is terminated by immersing the plates for 5 min in a 1 per cent potassium metabisulfite stop bath, and the plates are fixed for 2 hr in a 30 per cent sodium thiosulfate solution, washed, and dried. Varying degrees of discrimination between proton, alpha particle, and fission fragment tracks can be secured by altering the concentration of the uranyl acetate bath as shown in the tabulation. The long-range alpha particles associated with the fission process record best in plates loaded from 0.5 to 1.0 per cent uranyl acetate.

Per Cent	Track Structure in Ilford C2 or B1 Plates		
Uranyl Acetate	Proton	Alpha	Fission
1.0	Faint	Distinct	Very dense
2.0	None	Light	Dense
4.0	None	Very weak	Dense

The investigations of Broda[B42] demonstrate that the Ilford plates can be desensitized to gamma rays and proton recoils from fast neutrons by bathing the plates for 5 min in 1 per cent chromic acid, rinsing with water, and drying prior to the neutron exposure. On loading the oxidized plates with uranium compounds the alpha-particle tracks are weakened, but fission tracks are clearly evident when the plate is examined at 1500$\times$ magnification. The method prevents the registration of proton tracks during neutron bombardment, and the plates can therefore be exposed to very high doses of fast neutrons, as is necessary in studying the fissionability of certain heavy nuclei such as lead and bismuth.

Spontaneous Fission. There is a small but finite probability that certain nuclei of mass greater than 220 may split spontaneously in the absence of external activating radiation. The effect was first observed in uranium by Flerov and Petrzhak,[F18] who measured a spontaneous neutron emission corresponding to a fission rate of (0.2 to 2) 10^{-24} sec^{-1}. This phenomenon has been confirmed by numerous other investigations, and the measurements of Pose[P39] and Scharff-Goldhaber[S48] indicate that the half-life for spontaneous fission is 3.1×10^{15} years. Khlopin[K26] has demonstrated the presence of occluded xenon in old samples of uraninite, the quantity being consistent with the age of the mineral and the magnitude of the spontaneous fission rate.

The rate of spontaneous fission in uranium and thorium has been investigated by Perfilov[P16a] utilizing emulsions as recording media for the tracks of the ejected fission fragments. The measurements are rendered difficult owing to the low magnitude of the fission process, the simultaneous high rate of alpha-particle emission, and the complication introduced by cosmic-ray neutrons. The heavy alpha-track background was eliminated by destroying their latent images by oxidation with $\frac{1}{7500}$ g CrO_3 per ml solution before development. Control exposures demonstrated that 10^8 alpha tracks per cm^2 emitted from UI and UII could be obliterated without destroying the latent image of slow-neutron-induced fission fragments. With thin films weighing about 1 mg U per cm^2 it is possible to extend the exposure for over a month and thereby to build up an appreciable population of fission tracks.

In his final experiments Perfilov employed radiochemically purified films weighing 0.924 mg of U_3O_8 and 1.23 mg of ThO_2 per cm^2. The thin films were separated from the emulsion by 1.5 mm of air at a pressure of 1 mm

of Hg. In order to exclude external neutrons the evacuated camera was enclosed by cadmium screens and stored in the Moscow subway 50 meters below ground level. After an exposure of 1684 hours, 96 fission tracks were counted over 5.67 cm^2 of the uranium film and 5 tracks over 4.95 cm^2 of the thorium dioxide.

Under the particular conditions of microscopy (100× apochromatic oil-immersion objective and Köhler illumination), tracks with a residual air range of 0.25 air-cm could be differentiated from the background fog. Most of the fission tracks had a range of 0.75 to 1.0 air-cm, the entire spectrum falling between 0.25 and 2 air-cm. Perfilov believes that the ranges of the individual fission fragments are somewhat longer than indicated by his observations as the oxidation process doubtlessly obliterates the thinly ionizing terminal portions of the fission tracks.

To compute the fission rate, the track count has to be corrected for internal absorption of fission fragments within the test film. This factor can be evaluated by assuming a stopping-power relationship similar in form to the Bragg-Kleeman rule for alpha particles (equation 16, p. 118). For the films in question $[(1 - \tau)/2(\bar{R} - \rho)]$ has a value of 0.83 for the uranium and 0.79 for the thorium preparation. With two oppositely directed fragments ejected per fission, Perfilov evaluated the half-life for spontaneous uranium fission at $1.3 \pm 0.2 \times 10^{16}$ years. This corresponds to a somewhat lower disintegration rate than that estimated from neutron counts on large masses of uranium. Owing to the extremely small magnitude of the effect it is difficult to evaluate the reliability of the two methods. The smaller value measured by Perfilov may possibly originate from a fading of the latent fission-track images during an exposure of 70 days. On the basis of the thorium fission-track count the half-life is estimated at $\sim 4 \times 10^{17}$ years, which is again somewhat longer than the value of 1.7×10^{17} years observed by Pose.[P39]

TRACKS OF HEAVY IONIZING PARTICLES

The track characteristics of deuterons have been described by Wilkins and St. Helens,[W23] Husizawa and Tajima,[H38] and Sagane.[S51] The Ilford emulsions have been employed in the study of the elastic scattering of deuterons by Guggenheimer, Heitler, and Powell.[G29] The mean grain spacing of deuteron tracks has been measured by Brock and Gardner [B41] using particles accelerated to high velocities in the 184-in. Berkeley cyclotron. In deuteron tracks of 950 microns' recorded length the mean grain spacing is about 2.4 microns, and the terminal grain densities are $G_f = 0.19$ and $G_s = 0.85$ grain per micron.

The mean grain spacing in the tracks produced by tritons has been studied by Lattes, Occhialini, and Powell [L15] and Lattes,

Fowler, and Cüer.[L17] Triton tracks are recorded in the neutron bombardment of lithium-loaded emulsions. The disintegration of the Li^{6+n} compound nucleus results in the formation of a triton and an alpha particle. With slow neutrons the tracks of the two particles are collinear as illustrated in Fig. 56. When the reaction is initiated by a fast neutron its momentum causes the particles to deviate, thereby defining the point of origin of the alpha and the triton tracks.

It is noteworthy that the tracks produced by the more lightly ionizing triton fragment tend to disappear first on delayed development, and in
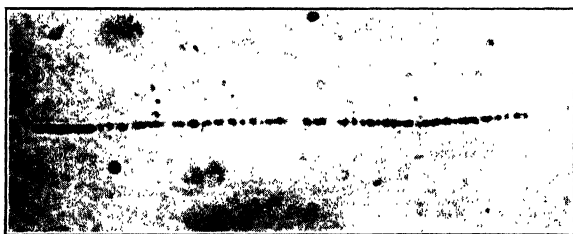
Fig. 56. Comparative grain densities in a collinear triton and alpha-particle track. Recorded in an Eastman NTA emulsion loaded with lithium borate.

certain experiments this fading effect can be employed to increase the discrimination between the triton and alpha trajectories.[L17] Experiments described by Faraggi[F2b] show that this effect can be accelerated by brief exposures above hydrogen peroxide vapor or moist air prior to development.

The tracks produced by accelerated helium ions of mass 3 have been investigated by Lukirsky, Mescheryakov, and Khrenina.[L43] The mean-grain spacing of He^3 particles is not appreciably different from that observed in the tracks of He^4 particles of comparable energy.

Comparatively few data have been reported on the track characteristics of particles intermediate in mass between He^4 and the fission fragments. The tracks of high-energy carbon nuclei accelerated to 96 Mev have been studied by Tobias and Segré.[T14] The tracks of Li^8 fragments are occasionally observed in cosmic-ray stars. More often these disruptions exhibit tracks of higher density designated as heavy splinters. In a rare event

reproduced in Fig. 57 all the ejected particles are massive.[Y18] Track A exhibits a feature characteristic of fission fragments in that the grain spacing increases as the particle slows down, suggesting a rapid loss of charge towards the end of its range.

The grain density along splinter tracks is rarely a true measure of the ionization, as the standard development renders the tracks
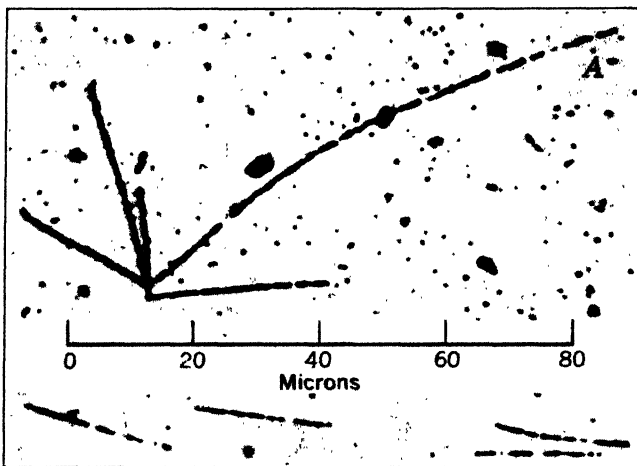
FIG. 57. Nuclear disruption with emission of heavy charged particles. Eastman NTA emulsion 100 microns thick exposed in the stratosphere, developed by Method III. All the tracks terminate in the emulsion and have a higher grain density than low-energy alpha-particle tracks.

The alpha tracks in the insert were recorded in the same plate from a polonium infection center (see p. 4).

of alpha particles very nearly continuous. Better differentiation can be secured by the use of less sensitive emulsions, or by giving the emulsion a weaker development. Stevens[S50a] has demonstrated that by means of low-energy para-aminophenol developers fission tracks can be recorded selectively even in emulsions that are electron sensitive when developed by the more energetic elon-hydroquinone reducing agents.

Freier and coworkers[F21] describe tracks exhibiting exceptionally heavy ionization which they attribute to primary cosmic-ray particles. These tracks are characterized by a solid pencil of developed silver surrounded by a halo of individual grains from

secondary electrons. The enormous ionizing power of these heavy particles as compared with low-energy alpha particles is
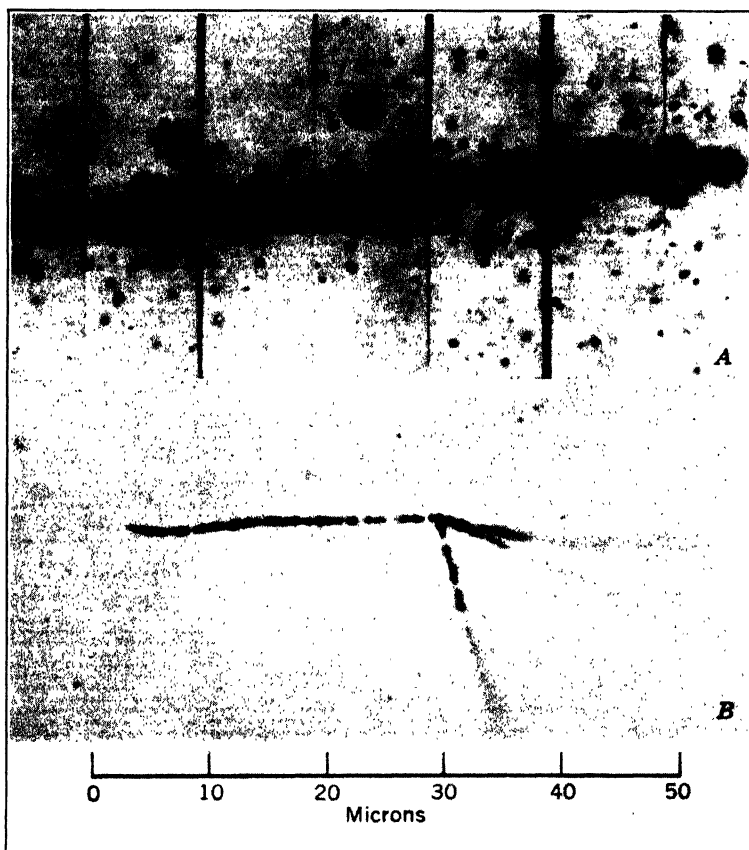
FIG. 58. Track of a heavy cosmic-ray primary *A* compared with trajectories of low-energy alpha particles *B* recorded in the same plate. Ilford C2 emulsion 200 microns thick exposed in the stratosphere at 104,000 ft, and developed for grain gradation. Track *A* entered the camera at an angle of 45° and could be followed through a series of three plate sandwiches without any appreciable loss in ionizing power after traversing more than 1 cm of glass and emulsion.

exhibited clearly in Fig. 58. The plate received grain-gradation development (p. 62) in order to increase its differentiating power.[Y18]

PHOTOGRAPHIC DETECTION OF FAST NEUTRONS

The observation of proton recoils in emulsions has been applied for many years in the detection of fast neutrons among the products of nuclear reactions. In one of the earliest applications of the method Richards and Hudspeth [R4a] showed that low-energy neutrons were emitted during the bombardment of deuterium with deuterons by observing the knock-on proton tracks. Geometric considerations pertinent to the evaluation of the energy of the incident neutrons from the recorded range of the proton recoils are described by Richards.[R5] The method has also been studied by Livesey and Wilkinson [L53] and by Gibson and Livesey.[G11a] Their reports provide further details on the measurement of stopping power and emphasize the importance of the residual moisture in the emulsion on the lengths of proton- and alpha-particle tracks.

The proton-recoil method of neutron detection has been applied by Cheka [C12] in the health monitoring of personnel working about cyclotrons and atomic piles. In a description of the special film packs Morgan [M30] states that the tolerance level to neutrons is represented by an accumulation of 10^4 proton tracks per cm^2 at the end of a 2-week exposure period. Studies of the method by Morgan and Cheka [M29] show that the latent proton image is also subject to fading on delayed development. More recent investigations by Cheka [C12a] indicate that partially faded latent images can be developed into recognizable proton tracks by employing fresh developer and extending the normal time of development.

When boron-loaded plates are exposed to fast neutrons Taylor [T7] observed III-branched stars whose origin is attributable to the following reaction:

$$B^{10} + n^1 \rightarrow He^4 + He^4 + H^3$$

This recording mechanism has been studied by Lattes and Occhialini [L18] as a means of estimating the energy and momentum of fast neutrons in the cosmic radiation. In a monitoring experiment they exposed boron-loaded plates to 13.4-Mev neutrons. Microscopic examination revealed many III-particle disintegrations. Grain counts showed that two of the tracks were produced

by alpha particles of 7.4 and 1.4 Mev, and the third by a 5-Mev triton. The total energy of the disintegration of 13.8 $\pm$ 0.5 Mev is in close agreement with the energy of the incident neutrons.

In identical plates exposed to cosmic radiation at 2800 meters' elevation Lattes and Occhialini observed a number of III-branched stars with individual tracks oriented in the same form as those on the neutron-irradiated control emulsions, differing only in a greater range. These investigations indicate that neutron energies up to 50 Mev can be evaluated from recorded alpha- and triton-track lengths, and that by using thicker emulsions neutron energies up to 100 Mev may be measured. The proton recoil tracks produced by neutrons of this energy would exceed 10 mm in length. Tracks of this magnitude can be recorded in nuclear emulsions only under a very limited near-grazing angle of incidence.

High neutron fluxes can be measured with the aid of uranium-loaded plates. The number of fission tracks serves as a measure of neutron capture. Lark-Horovitz and Miller [L20] have exposed uranium-loaded emulsions at 30-km altitude and recorded fission tracks initiated by cosmic-ray neutrons. More recently, Froman, Rosen, and Rossi [F16] have made quantitative estimates of neutron abundance at altitudes above 10 km. Eastman fission plates were exposed during 5-hour airplane flights against metallic foils of U^{235} weighing 1 mg per cm^2. The population of fission tracks corresponds to a neutron flux of 20 particles per cm^2 per min. When the exposures were conducted under paraffin the rate was augmented to 130 slow neutrons per cm^2 per min.

SLOW-NEUTRON REACTIONS

When fast neutrons are slowed down by elastic collision with light nuclei (hydrogen or carbon) they can be captured readily by atoms of N^{14}, B^{10}, or Li^6. The compound nucleus is unstable, and its rupture is attended by the formation of densely ionizing particles:

(*a*) $$N^{14} + n^1 \rightarrow H^1 + C^{14}$$

(*b*) $$B^{10} + n^1 \rightarrow Li^7 + He^4$$

(*c*) $$Li^6 + n^1 \rightarrow H^3 + He^4$$
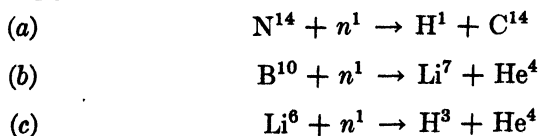
These nuclear reactions are utilized in the detection of slow neutrons as the tracks of the ionizing particles are readily identified in nuclear emulsions.

In irradiating plates with slow neutrons short proton tracks of about 6.8 microns' length originate from the $N^{14}(n, p)C^{14}$ reaction with nitrogen atoms of the gelatin. The cross section for this reaction is low, but the number of N^{14} nuclei can be augmented by loading the emulsion from sodium azide (NaN_3) solutions. This technique has been employed by Cüer [C33c] in a study of the range distribution of the low-energy protons. Cüer observed a peak range at 0.985 air-cm, in excellent agreement with recent cloud-chamber measurements by Cornog,[C37] who reports 1.00 air-cm, and Böggild,[B30a] who finds the mean range of the H^1 particle to be 1.00 air-cm and that of the accompanying C^{14} recoil 0.03 air-cm.

When the emulsion is loaded with lithium compounds slow neutrons produce characteristic tracks about 40 microns long composed of oppositely directed triton- and alpha-particle trajectories. The $Li^6(n, \alpha)H^3$ reaction has been investigated by Burcham and Goldhaber,[B47] Taylor and Dabholkar,[T11] and Demers.[D9] For a given flux of slow neutrons Shapiro and Barnes [S23a] report that the track population from this reaction is about 150 times more abundant than the proton tracks originating from interaction with N^{14} nuclei.

Emulsions loaded with boron compounds record short tracks from the $B^{10}(n, \alpha)Li^7$ reaction. The alpha particle carries the bulk of the energy and records a track about 7 microns long. Although these tracks are not as distinctive as those produced in lithium-loaded plates the mechanism is favored by the large cross section of the boron slow-neutron reaction. The individual advantages of the Li^6 and the B^{10} slow-neutron capture processes can be combined by loading the emulsion from a solution of lithium borate. This compound is readily soluble in water, and greater concentrations of borate ion can be introduced than are possible by the use of sodium tetraborate. The loading bath is prepared as follows:

Dissolve 60 g of boric acid crystals in 300 ml of hot water and slowly add about 19 g of lithium carbonate until in slight excess. Cool, filter, and dilute to 400 ml. The resultant solution contains about 10 per cent lithium borate. After a 15-min loading period a 30-micron Eastman NTA

plate picks up about 0.24 mg of $Li_2B_4O_7$ per cm^2. When loading thicker emulsions about 5 per cent glycerine should be added to the bath to avoid peeling of the emulsion during the last stages of drying. The loaded plates are developed by method I.

The loaded emulsion contains about 320×10^{19} atoms of N^{14}, 25×10^{19} atoms of B^{10}, and 5.3×10^{19} atoms of Li^6 per ml. However, owing to the exceptionally small cross section of N^{14} for slow-neutron capture, tracks from the interaction with boron or lithium nuclei predominate. A microscopic field from a lithium borate-loaded emulsion exposed to slow neutrons is exhibited in Fig. 59. At higher magnifications tracks favorably oriented in
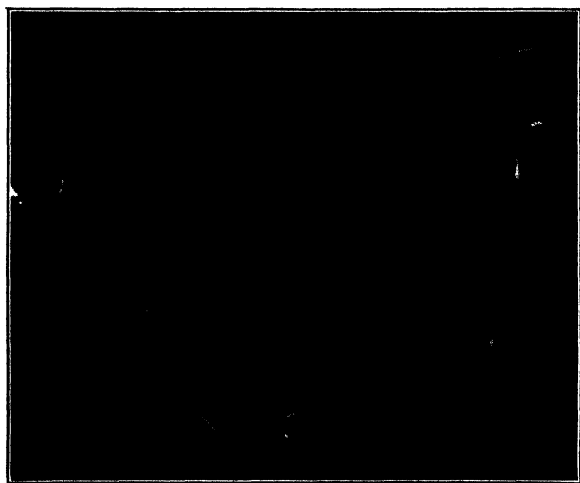
FIG. 59. Microscopic field from a slow-neutron-bombarded emulsion loaded with lithium borate. The short tracks represent alpha trajectories from the capture by B^{10} nuclei. The long tracks are collinear trajectories of the triton and alpha particle resulting from the splitting of the $(Li^6 + n)$ compound nucleus.

the plane of the emulsion show differential grain densities in the collinear triton- and alpha-particle components, as indicated in Fig. 56, p. 283.

COSMIC RADIATION

The cosmic ray group at the University of Bristol, led by Powell, has found a brand-new meson, or maybe two of them. The Bristol experiments are simple, powerful, and elegant. They use no com-

plicated series of coincidence circuits, no microsecond timing circuits, no magnets. They employ a photographic plate, a microscope, and plenty of insight, patience, and skill, always the best of apparatus.—P. Morrison, 1948

Introduction. The cosmic radiation directed towards this planet is of low intensity equal to about 20 primary particles per cm^2 per min at the top of the atmosphere. The charged primary particles, believed to be protons with energies in excess of 7000 Mev, interact with the atoms of the atmosphere producing positive and negative electrons, mesons, protons, neutrons, alpha particles, and gamma radiation. These secondaries reach a maximum intensity at an elevation of about 10 miles above sea level. The total ionization diminishes rapidly towards sea level as a result of absorption or capture. Among the latter reactions Libby [L32] has suggested that the neutrons are captured by nitrogen with the formation of C^{14}, evidence of which has been secured by von Grosse,[V9] who demonstrated the accumulation of the long-lived radiocarbon in methane of biological origin.

At sea level about 1 cosmic-ray particle crosses a horizontal square centimeter per minute in the ratio of 3 mesons to 1 electron. Mesons have been detected in mines at a depth of about 1 mile, indicating that an appreciable fraction of these particles possess energies of the order of 10^6 Mev. Unlike the penetrating mesons, the electrons and their accompanying gamma radiation are easily absorbed and are referred to collectively as the soft component of the cosmic radiation. The radiation is studied by the ionization produced by the charged components, the nuclear emulsion being a particularly effective recording device because of its ability to integrate the rarer type of phenomena associated with the generally feeble flux of cosmic radiation.

Excellent summaries on special phases of cosmic radiation are available in a symposium published in the *Reviews of Modern Physics,* No. 3–4, 1939. A review of more recent developments is edited by Heisenberg.[H27] In this work, Bagge and Flügge contribute sections on nuclear disruptions produced by cosmic radiation in photographic emulsions. Further applications of the emulsion technique are described by Powell and Occhialini.[P35] The applications of photographic emulsions in cosmic-ray research are also described in publications by Ortner,[O3] Schopper,[S7, 8, 9] Shapiro,[S22, 23] Lovera,[L39, 40] Brunetti and Ollano,[B46] Morrison,[M40] Feld,[F19] and Jánossy.[J8]

In 1937 Blau and Wambacher [B25] exposed a series of Ilford Halftone plates on Mt. Hafelekar at Innsbruck (2800 meters' elevation) for a period of 4 months and observed a total of 31 multi-branched stars whose component tracks represented an energy evolution in excess of 160 Mev. The formation of these cosmic-ray stars was confirmed by Schopper,[S10] Wilkins,[W23] and Filippov, Gurevich, and Zhdanov.[F8] Plates exposed at high altitudes also record long individual tracks indicative of charged particles with ranges equivalent to several meters of air. These unusually long trajectories have been reported by Wilkins [W17, 20, 21] and by Rumbaugh and Locher [R14] in plates exposed during stratosphere balloon ascents and have also been observed by Inai [I2] and Forster [F11] in plates exposed during airplane flights. In stratosphere exposures Freier and coworkers [F21] report densely ionizing tracks indicative of heavy nuclei of atomic number up to 40 with kinetic energies of about 500 Mev per nucleon as components of the primary cosmic radiation.

Owing to pronounced fading effects in low-concentration silver bromide emulsions exposed for long periods under variable conditions of temperature and humidity it is not possible to evaluate the significance of the recorded track populations in the older work or to place much credence on the identity of the particles deduced from grain counts. Most of the tracks observed in the early-type nuclear emulsions were attributed to protons, but it is probable that more densely ionizing particles escaped recognition because of partial fading of the track structures.

This fading is indicated by the results reported by Schopper [S10] on the events recorded in Agfa K plates which were developed shortly after several hours' exposure in the stratosphere. Under these favorable conditions for latent-image retention the recorded cosmic-ray stars contained tracks attributable to alpha particles. In contrast, similiar plates exposed for several months by Wambacher [W3] exhibited stars whose component tracks were attributed invariably to protons. Studies by Shapiro [S23] on the frequency of proton- and alpha-particle tracks in cosmic-ray stars show that more than 90 per cent of the tracks are produced by protons, the rest being probably formed by alpha particles with energies less than 9 Mev. In the more complex stars Perkins [P19] estimates that 25 per cent of the tracks are produced by alpha particles.

Under conditions of low humidity the latent image persists for several weeks, particularly in the emulsions of high silver bromide concentration. In the absence of marked fading, the grain densities in the component tracks of cosmic-ray stars may be compared with those in tracks produced by particles of known identity and energy. Cosmic-ray events recorded in the modern nuclear-type emulsions exhibit tracks attributable to protons, alpha particles, and more densely ionizing fragments. Long tracks
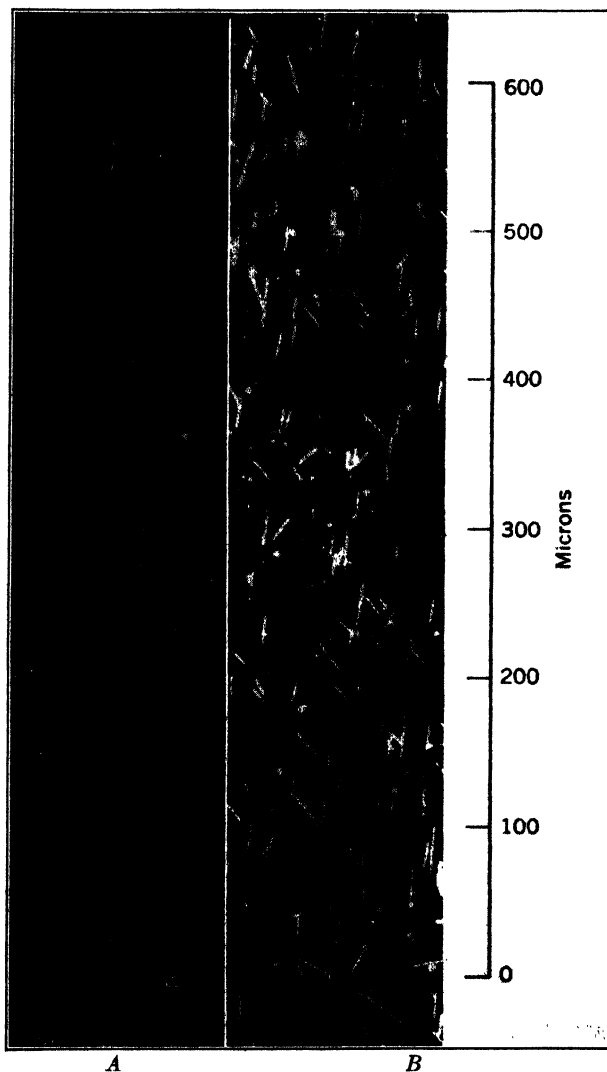
FIG. 60. Trajectories of light ionizing particles.

A. Track observed in an NTA plate exposed at 4530 meters. Its mean grain spacing of 1.5 microns together with the degree of scatter suggests the trajectory of a ρ-meson. In the same emulsion protons of equal range produce tracks with a mean grain spacing of 1.1 microns.

B. A dual event [L50] recorded in an emulsion at sea level during an experimental alpha-particle exposure. The long track has a mean grain spacing of

of lower grain density than that found in the tracks of protons and which exhibit frequent scattering have been attributed to mesons. Tracks of this character have been reported by Filippov,[F8] Bose,[B34, 36a] Perkins,[P18] and Lattes, Occhialini, and Powell.[L15, 16]

On the basis of the small-angle scatter along the trajectory Bose and Choudhuri [B35, 36] have estimated the mass of these particles to reside between 217 and 336 electron masses. Perkins [P18] was the first investigator to report and correctly interpret a cosmic-ray star showing the track of an entering meson particle. This process has since been observed by several other investigators, and Lattimore [L46] deduced a mean mass of these star-begetting mesons of $290 \pm 80\ m_e$. Meson tracks exhibiting a large-angle scatter have been interpreted by Bhabha and Daniel [B52] as possibly originating from the decay of the particle while in motion into a lighter particle and a neutral meson.

The extensive investigations of Powell and his coworkers on the tracks of light singly charged particles may be summarized by the following descriptive classification of meson tracks as observed in nuclear emulsions:

(*a*) Tracks differentiated from more densely ionizing particles by grain density and degree of Coulomb scatter which come to rest in the emulsion without any observable disintegration products are designated as those produced by ρ-mesons. An example of this type of trajectory is shown in Fig. 60*A*. When the track is observed under conditions of high resolution the terminal portion exhibits a pronounced increase in grain density.

(*b*) Certain meson particles which stop in the emulsion produce a star with a multiplicity of from I to V branches. The ionizing particles producing these evaporations are negatively charged, have a mass of about 300 m_e, and are designated σ-mesons (star-producing).

(*c*) A small number of meson tracks produce, at the end of their range, a second track of lower grain density than the parent particle. These events have been interpreted as originating from the spontaneous decay of a heavy π-meson into a lighter μ-meson. In order to conserve momentum a third neutral particle termed a

---

1.6 microns and was probably produced by a meson particle. The other member, also terminating in the emulsion layer, has a mean grain spacing of 0.6 micron and is identifiable with the trajectory of a 13-Mev alpha particle. The short tracks from the experimental exposure reside in the upper plane of the emulsion and do not interfere with grain counting with an oil-immersion objective.
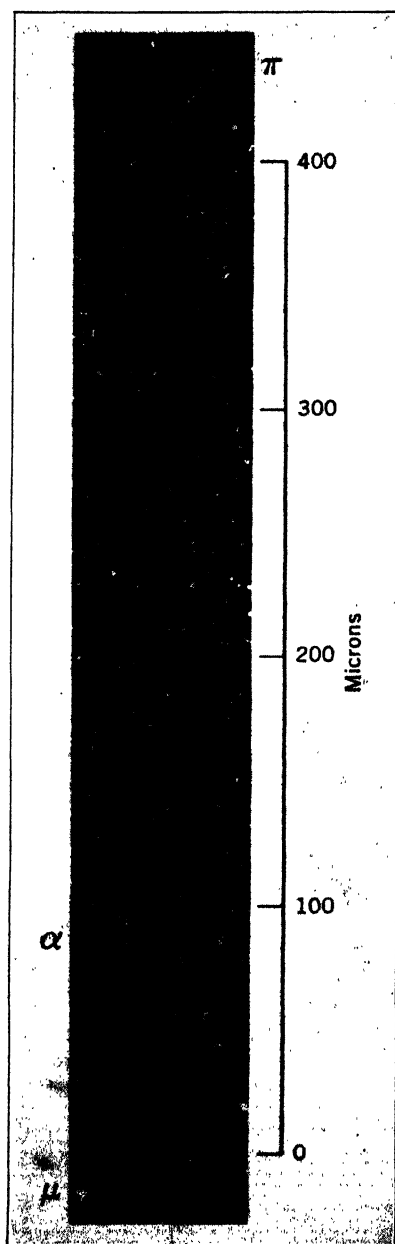
neutretto is probably emitted in the process which has a mass of $\sim 100\ m_e$. On the basis of grain counts in the tracks of π-μ events the mass ratio of the two charged mesons has been estimated at $\pi/\mu = 1.65 \pm 0.11\ m_e$. A π-μ decay process recorded in an Eastman NTA plate is reproduced in Fig. 61. In these processes whenever the track of the μ-meson terminates in the emulsion the particle appears to have a constant range of 614 ± 8 microns. On the basis of a mass of 200 m_e the average kinetic energy of the μ-meson is 4.09 ± 0.04 Mev. On this assumption the mass of the parent π-meson is 330 m_e, and that of the unrecorded neutral meson is computed at about 115 m_e.

(*d*) In certain nuclear evaporations a meson particle is ejected together with the proton and alpha particles. These processes are comparatively rare. In a study of

FIG. 61. Tracks of a π-μ meson interaction. Event recorded in an Eastman NTA emulsion exposed in the stratosphere. The plate was preeradicated by H_2O_2 vapor. The short background track (α) is serviceable in comparing relative grain densities. Dark-field mosaic.

1600 stars reported by Lattes [L14] only two events were observed exhibiting the track of an ejected meson. The process is probably somewhat more common than these statistics would indicate as the initial grain density of a meson track is low and that portion cannot be differentiated from that of a fast proton. Unless the track of the meson particle terminates in the emulsion it is likely to escape recognition. A process involving the ejection of
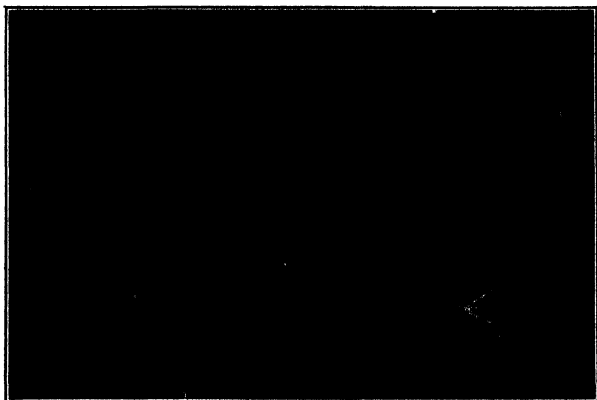
FIG. 62. Nuclear evaporation with asymmetric distribution of light and densely ionizing particles. Recorded in a preeradicated Eastman NTA plate exposed at high altitude and developed by Van der Grinten's method.

a meson, recorded in an Eastman NTA emulsion exposed at sea level, is exhibited in Fig. 60*B*.

Nuclear Evaporation Processes. The tracks constituting a cosmic-ray star or nuclear evaporation are in general distributed spatially in about equal abundance in all directions from the common center. The events are attributed to an intense thermal excitation of a nucleus in the emulsion layer in which either all or a limited number of the nucleids receive sufficient energy to penetrate the potential barrier. The energy for this evaporation process originates from the mass conversion of the captured cosmic-ray particle or photon. The stars produced by σ-meson capture are relatively simple, and the complex cosmic-ray stars of 15 or more tracks cannot be attributed to this process. Perkins [P20a] has suggested that the more complex nuclear evaporations may be due to inelastic scattering of very fast cosmic-ray

particles with energies in the relativistic region where the cross section for scattering on nucleons becomes large.

Perkins[P20a] has observed, in a statistical analysis of the angular distribution of the tracks ejected in the disruptions of heavy nuclei, that the proton tracks are spherically symmetrical but that the alpha particles show a directional trend. The tracks of the alpha particles appear to be oriented in a direction opposite to that of the recoil fragment from the initial partial evaporation. A star exhibiting marked directional orientation of the densely and lightly ionizing fragments is exhibited in Fig. 62.

Since the emulsion records the tracks of charged particles only over a limited energy range, the star is an incomplete picture of the evaporation process devoid of the trajectories of neutral particles or very fast singly charged particles.* In some of the simpler evaporation processes the number of tracks and their charge appear to be consistent with a complete disruption of the lighter nuclei if it is assumed that the number of neutrons accompanying the process is equal to the number of proton particles:

$$
\begin{aligned}
{}_6C^{12} + \sigma_0 &\rightarrow {}_2He^4 + 4\,{}_1H^1 + 4\,{}_0n^1 \\
{}_6C^{12} + \sigma_- &\rightarrow {}_2He^4 + {}_1H^3 + 2\,{}_1H^1 + 3\,{}_0n^1 \\
{}_7N^{14} + \sigma_0 &\rightarrow {}_2He^4 + 5\,{}_1H^1 + 5\,{}_0n^1 \\
{}_8O^{16} + \sigma_0 &\rightarrow 4\,{}_2He^4
\end{aligned}
$$
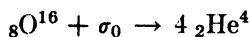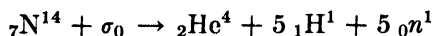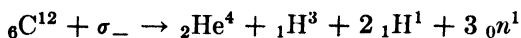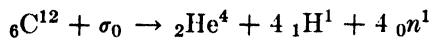
An evaporation attributed[Y16] to a $N^{14} + \sigma_0$ reaction is described in Fig. 63. In general it is not possible to make a unique identification of the target nucleus as the recorded number of tracks may have boiled off from a heavier atom, such as silver, bromine or iodine, with the production of a residual nucleus of intermediate mass. Short tracks of very high grain density which may represent the trajectory of the residual heavy particle are often observed. With sufficient excitation a heavy nucleus, as for example $Ag_{47}{}^{107}$, might conceivably yield a star with 47 proton tracks. In the greater proportion of evaporations the evidence recorded in the emulsion indicates a less complete breakdown into about 10 to 20 ionizing particles. Examples of complex but incomplete evaporations are shown in Figs. 62 and 69. Leprince-Ringuet and coworkers[L47] have described

* The Eastman NTA emulsion records the tracks of alpha particles up to 200 Mev. The tracks of protons with energies exceeding 20 Mev and those of deuterons exceeding 40 Mev have a grain density too low for microscopic differentiation from the fog background. The more sensitive NTB emulsion is suitable for recording alpha particles up to 400 Mev, protons to 50 Mev, deuterons to 100 Mev, mesons to 5 Mev, and also for recording the tracks of electrons with energies less than 0.05 Mev.

a star, reproduced in Fig. 64, consisting of 34 tracks which they attribute to the complete disintegration of a silver atom. All the trajectories could not be identified either because they leave the emulsion before terminating their range or because they have unfavorable angles of incidence for grain counting. Of the measurable tracks 17 were identified as protons, 4 as alpha, and 1 as a triton trajectory.
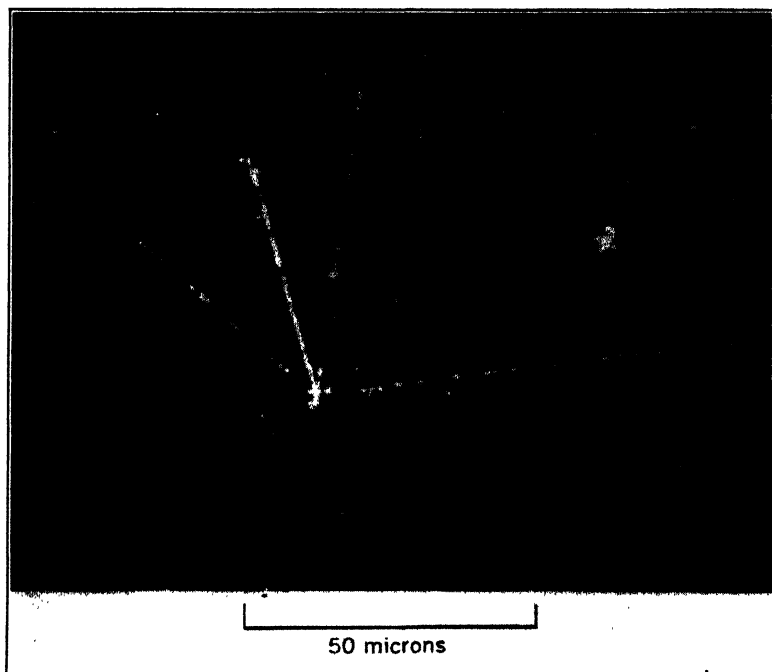
FIG. 63. Cosmic-ray star. In this event one alpha particle and five proton tracks are recorded. If five neutrons were also ejected, the star is consistent with the nuclear evaporation of a N^{14} atom into $1He^4 + 5H^1 + 5n^1$. The total kinetic energy of the fragments is 74 Mev, and, since the binding energy of N^{14} is 76 Mev, the event is consistent with the annihilation of an incident meson of about 300 electron masses.

Another type of complex star has been described in the work of Zhdanov [Z3, 6] in which the tracks originating from a common center are confined to a narrow solid angle with a pronounced unilateral direction. Zhdanov, Perfilov, and Deisenrod [Z5] have described two such events, designated as proton showers, comprised of 20 and 50 tracks.

The emission of a novel type of particle in nuclear evaporations has been observed by Tamburino,[T1] in which a short track of high grain density divides at its termination into two tracks of lower grain density. These events have since been observed by other investigators and the bifurcations
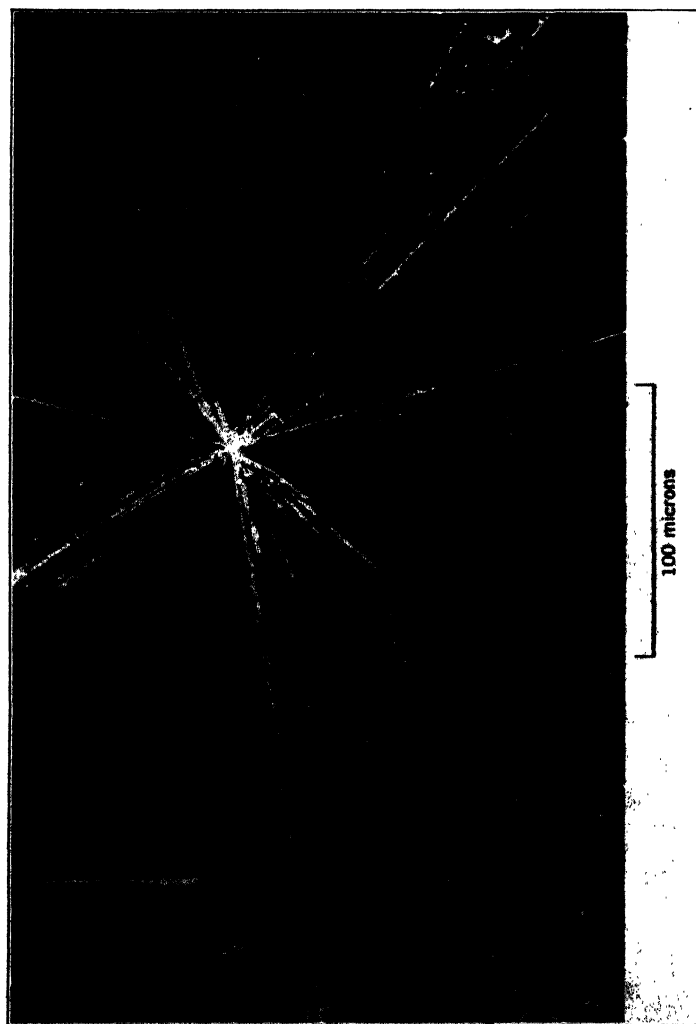
Courtesy of Leprince-Ringuet

FIG. 64. Nuclear disruption of a silver nucleus. Star observed in an Ilford B2 emulsion exposed at 4400 meters.

designated as "hammer tracks."[P35] Franzinetti and Payne[F20] have made a statistical analysis of 28 examples of this process and conclude that the heavy track is that of a Li^8 fragment which decays into 2 alpha particles. In 13 of the stars the hammer track is accompanied by an alpha particle
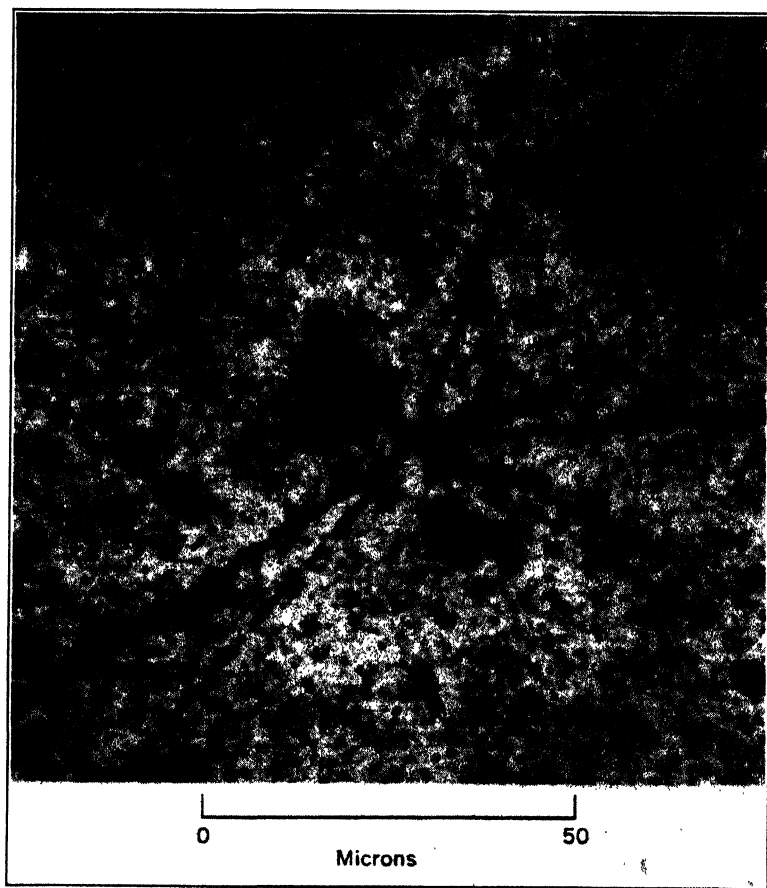
FIG. 65. Nuclear evaporation exhibiting "hammer track" of a Li^8 fragment.

and a proton trajectory which suggests the disintegration of a C^{12} nucleus by a fast neutron:

$$C^{12} + n^1 \rightarrow Li^8 + He^4 + H^1$$
$$\downarrow$$
$$2He^4 + \beta^- + \text{neutrino}$$
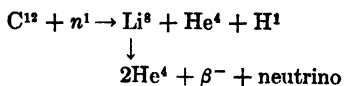
A nuclear evaporation exhibiting the track of a Li^8 fragment is shown in Fig. 65.

The hammer tracks of Li^8 particles are also recorded when boron-loaded emulsions are exposed to fast neutrons. Pickup [P42] attributes their formation to the following nuclear reaction:

$$B^{11} + n^1 \rightarrow Li^8 + He^4$$
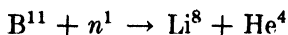
This mechanism provides another valuable index for detecting fast neutrons and evaluating their energy from the comparatively short ranges of the disintegration products. In an exposure of lithium borate-loaded plates to cosmic radiation in the stratosphere, among a total of 387 disruptions two events were observed attributable to a (B^{11}, n^1) capture process.[Y18]

Binary Evaporations. Lattes, Occhialini, and Powell [L16, O1a] describe a very rare type of nuclear evaporation process in which a meson ejected from one star engenders a second multiple disintegration at the end of its range. A similar double star in which the track of the initial σ-meson is also recorded has been observed by Leprince-Ringuet (see Fig. 66). This binary-star phenomenon, suggestive of a meson chain reaction, may have an appreciable rate of occurrence if it is assumed that the meson ejected in the primary evaporation is uncharged and leaves no track between two neighboring nuclear evaporations.

In a statistical study of the distribution of 2250 stars in plates exposed at a 3600-meter elevation Leprince-Ringuet and Heidmann [L48] find that 88 stars reside in close proximity, with distances of only 50 to 250 microns between centers. These observations are in marked excess over the number of coincidences to be anticipated from a random distribution of unrelated single stars. The same conclusions are drawn by Li and Perkins,[L49] who encountered 47 closely adjacent stars among a total of 1230 recorded evaporations.

Leprince-Ringuet and Heidmann suggest that one of the stars of the pair has produced the other through the medium of an "asterogen particle" which does not leave a track in the emulsion. The ejected intermediary may be a neutron, a neutral meson, photon, electron, very fast protons or mesons, or possibly some as yet unidentified particle.

Evaporations in the Glass Backing. The cosmic-ray-induced nuclear evaporations, evidence of which is recorded vividly in the emulsion layer, occur in all matter exposed to the radiation.
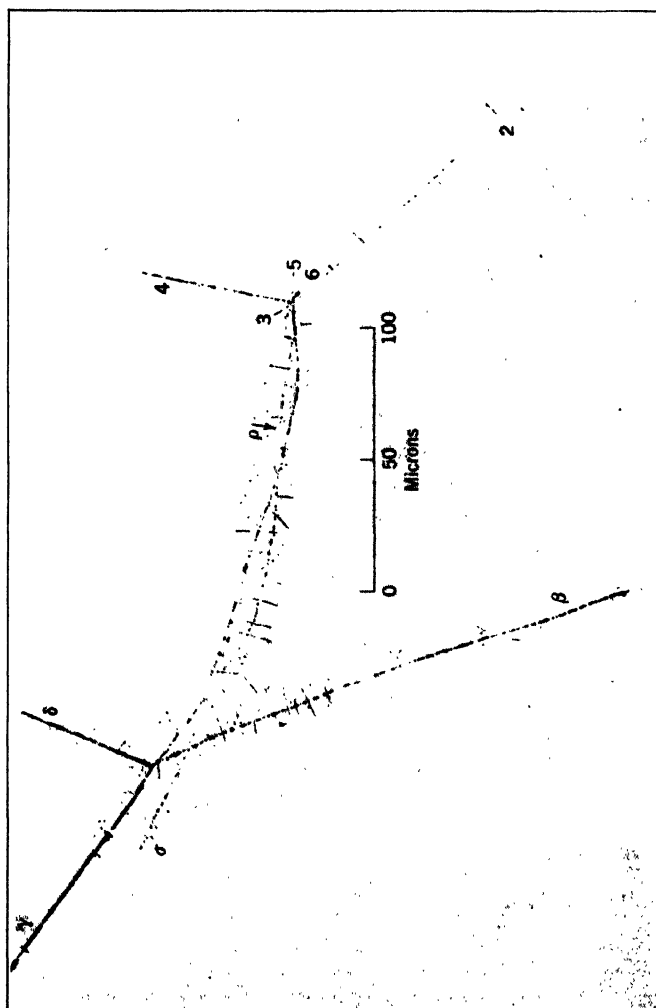
Courtesy of Leprince-Ringuet

Fig. 66. A binary cosmic-ray evaporation. Event observed in an Ilford C2 emulsion by Leprince-Ringuet and coworkers. A σ-meson stops in the emulsion and produces a disruption in which the tracks of six charged particles are recorded. One of the ejected particles (ρ) initiates a second evaporation recorded by tracks β, γ, and δ.

Fragmentary evidence of the process has been observed in cloud-chamber photographs in which several tracks leading to a common center emerge from one of the lead plates or the metallic walls of the chamber. The identical phenomenon can be observed in nuclear emulsions when an atom in the glass backing
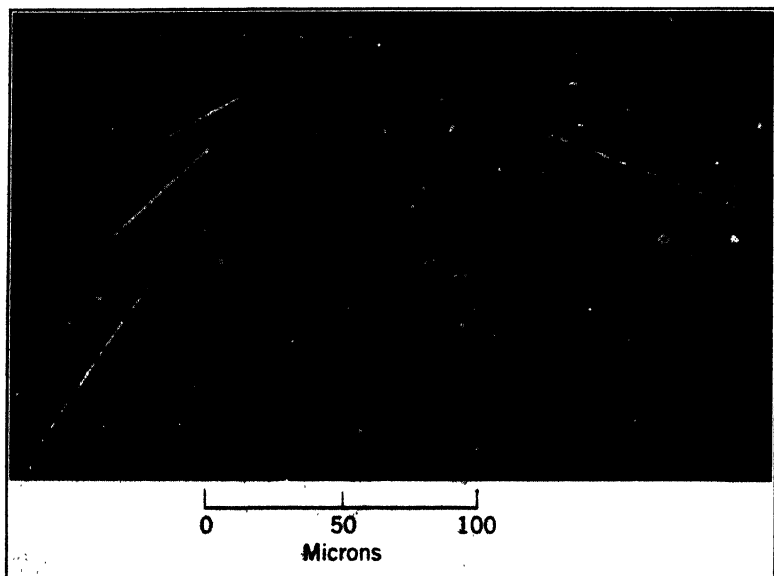
FIG. 67. Track cluster from a nuclear evaporation originating in the glass backing. The lines of extension of the four tracks meet at a common center in the plane of the horizontal projection. With the aid of this point, the spatial depth of the common origin can be computed from the obliquity of the tracks. In this particular event the disintegration occurred 35.3 ± 0.5 microns below the glass-emulsion interface.

is disrupted and several of the evaporated fragments are directed into the emulsion layer.

These partially recorded cosmic-ray stars can be differentiated from random tracks and from similarly oriented track clusters originating from radioactive impurities in the glass backing by the following considerations:

1. All the members of the event start at the glass-emulsion interface and are oriented so that the extensions of the tracks meet at a common center.

2. At least one of the tracks must be longer than 50 microns in order to exclude conically grouped tracks originating from series decay of radium or radiothorium present in the glass (see p. 152). The differentiation is

often facilitated by the observation of one or more tracks with a grain density or with scatter characteristic of proton trajectories.

An event indicative of the evaporation of a nucleus in the glass is reproduced in Fig. 67. The observation of cosmic stars with origins in the glass is of interest in conjunction with statistics on binary evaporations, as adjoining stars with centers in the two media may be related by a common asterogen particle. Alternatively, by exposing the emulsion against metallic foils, the number of track clusters originating from the metal may serve as a measure of the evaporation cross section for nuclei of known identity.[Y17]

TABLE 30. FREQUENCY OF COSMIC-RAY DISRUPTIONS AT DIFFERENT ALTITUDES *

Altitude, meters	Locality	Geo-magnetic Latitude	Stars, ml per day	Investigation
Sea level	Bethesda, Maryland	50° N	0.6	Yagoda [Y18]
Sea level	London, England	54° N	1.2	Perkins [P17]
Sea level	Lima, Peru	1° S	0.1	Yagoda [Y18]
670	Interlaken	48° N	2.0	Perkins [P17]
1,300	Wengen	48° N	2.9	Perkins [P17]
2,300	Eigergletscher	48° N	4.5	Perkins [P17]
3,500	Testa Grigia, Italy	48° N	15.3	Bernardini [B58]
3,500	Climax, Colorado	48° N	14	Yagoda [Y18]
3,600	Jungfraujoch	48° N	11	Perkins [P17]
3,650	Chamonix	48° N	9	Li [L49]
4,500	Vallot	48° N	19	Perkins [P17]
4,530	Morococha, Peru	1° S	3	Yagoda [Y18]
5,500	La Oroya, Peru	1° S	16.5	Perkins [P17]
18,300	Stratosphere above Illinois, U.S.A.	55° N	6,000	Schein [S52]
27,600	Stratosphere above Minnesota, U.S.A.		1,500	Yagoda [Y18]
30,600			2,000	Salant [S53]

* The tabulation includes only those investigations employing concentrated nuclear emulsions. The data of the earlier investigators are low owing to pronounced fading effects in emulsions of high gelatin content. Thus, Stetter and Wambacher[S41] observed populations of 1.4 and 2.9 stars per cc per day at altitudes of 2000 and 3400 meters in plates exposed at 48° N geomagnetic latitude.

Variation with Altitude. The population of cosmic-ray emulsion stars in plates exposed at different altitudes is summarized in Table 30. The data are not entirely comparable owing to the variation in sensitivity, thickness, and the duration of exposure

of the emulsions employed by different investigators. Also, the sea-level and high-altitude exposures were seldom compared at the same station, and, in view of the dependence of cosmic-ray intensities on geomagnetic latitude, a similar variation can be anticipated for the population of nuclear evaporations. In general, however, the data in Table 30 show that the number of stars per unit volume increases rapidly with elevation and that in the stratosphere an appreciable population is recorded after only a few hours' exposure.*

As suggested by Kupferberg [K22] another variable is introduced by the variation in height of the main meson-production region with geographic latitude and seasonal temperature. If, as is commonly assumed, the primary meson generation takes place in the first 100-millibar segment of the atmosphere, a change in altitude of this layer will in turn cause a change in the meson intensity as observed in a recording device situated at a lower fixed depth. Data of greater consistency can probably be obtained, following a suggestion by Arley,[A3] by exposing plates in captive balloons at different altitudes instead of on accessible but randomly situated mountain tops.

Exposures conducted by Bernardini [B58] at the Testa Grigia cosmic-ray station indicate the existence of an appreciable multiplicative effect when the plates are stored under 2 cm of lead, followed by a diminution in star population with greater thicknesses of lead absorber:

Cm of Pb	0	2	9	13
Stars/ml/day	15.3 ± 1	18.0 ± 0.9	13.1 ± 1.15	9.7 ± 1

* The charged primary components of the cosmic radiation are deflected by the earth's magnetic field. This deflection results in a smaller flux of secondaries in regions near the equator as compared with areas closer to the magnetic poles. At sea level the rate of ionization increases by about 10 per cent between the geomagnetic equator and 50° N geomagnetic latitude. The effect is more pronounced at higher elevations, and at 4360 meters the geomagnetic effect is about 33 per cent.

The geomagnetic latitude λ corresponding to a location of geographic latitude L and longitude ω (measured west of Greenwich, England) can be computed from the relationship:

$$\sin \lambda = \cos \psi \cos (\omega - \phi) \cos L + \sin \psi \sin L$$

In this expression $\psi = 78° 32'$ N and $\phi = 69° 8'$ W are the coordinates of the geomagnetic south pole.

Camerini and coworkers[C40] have likewise observed that the number of ρ- and σ-meson tracks are augmented by surrounding the plates with 5 cm of lead.

TABLE 31. MULTIPLICITY OF COSMIC-RAY STARS

Locality:	Austria	Testa Grigia	Italy	Minnesota
Elevation, km:	2.3	3.5	18–22	~27
Investigation:	Wambacher[W5a]	Bernardini[B58]		Yagoda[Y18]
Total cosmic star count:	109	523	443	327
Multiplicity	Percentage Abundance			
III	35.8	38.6	38.6	27.6
IV	32.1	28.0	22.6	24.8
V	15.6	14.9	13.8	10.7
VI	4.6	7.1	9.0	8.9
VII	3.7	2.9	1.1	4.9
VIII	3.7	2.3	4.7	6.4
IX	1.8	1.5	6.8	5.2
X	0	1.1	1.1	2.5
XI	0.9	1.0	1.0	1.8
XII	0.9	1.0	0	1.5
XIII	0	0.6	0	0.3
XIV	0.9	0.2	1.1	0.9
XV	0	0.2	0	0.9
XVI	0	0.6	0	1.8
XVII	0	0	0	0.6
XVIII	0	0	0	0
XIX	0	0	0	0.6
XX	0	0	0	0.3
XXI	0	0	0	0
XXII	0	0	0	0
XXIII	0	0	0	0
XXIV	0	0	0	0
XXV	0	0	0	0.3

Multiplicity of Cosmic Stars. The relative multiplicity of the disruptions recorded in plates exposed at different altitudes is compared in Table 31. In the mountain top exposures over 90 per cent of the stars consist of III to VII tracks of ionizing particles. With increasing altitude stars of greater complexity become more frequent and those of multiplicity VIII and higher constitute about 20 per cent of the total population. As a first approximation, the star frequency P_s is related to the multiplicity M by $P_s = Ae^{-M}$ in which A is a constant for a given altitude.

This relationship is not applicable when M is unity, and it also predicts a greater abundance of II-branched events than is commonly observed. The exponential relationship does fit the observed data for multiplicities residing between III and XII.

Single Trajectories. The long single tracks of cosmic-ray origin greatly outnumber the star population. In exposures not influenced by fading effects the ratio is approximately 100 tracks per star. A fraction of the single tracks originate from nuclear evaporations occurring in matter adjoining the emulsion layer. Part of the proton-track population may originate from collisions between neutrons and hydrogen atoms in the sensitive layer. A very small fraction of the single trajectories are produced by meson particles. Perkins [P17] has observed the following ratio of cosmic-ray events in plates 100 microns thick exposed at sea level:

Stars	Single Tracks	ρ-Mesons	σ-Mesons	π-μ Decay
135	16,000	33	7	1

Morand [M49] has identified 200 single trajectories in plates exposed at sea level. On the basis of grain counts along the tracks the particles giving rise to the tracks occur in the following relative proportions:

Protons	Tritons	Alpha Particles	Deuterons
75	15	9	1

Measurements by Forster [F11a] show that in emulsions exposed between 30,000 ft and sea level the single trajectory count decreases exponentially by a factor $e^{-0.77p}$ in which the atmospheric pressure p is expressed in meters of water equivalent.

Cosmic-Ray Camera. In a review of emulsion technique in cosmic-ray study Korff [K23] comments that, since all events are integrated between manufacture and development, it is not possible to ascribe an especially interesting event to a particular experiment whose duration is a small fraction of the total age of the emulsion. The hydrogen peroxide method of latent-image eradication, p. 110, provides a convenient means for initiating exposures on a clean background. After drying the plates it is advantageous to reassemble the emulsions face to face as illustrated in Fig. 68. This minimizes subsequent absorption of atmospheric moisture and permits the follow-up of tracks of particles that traversed both emulsion layers. The radioactive-ink

lines drawn on one of the plates record autoradiographic images on the surface of its mate. These internal markings facilitate intercomparison of the position of events recorded in the two layers. The continuous registration of short-ranged alpha tracks also provides internal standards for gauging the extent of latent-image fading.

Evaporations of high multiplicity have been reported by Evans,[E10] Roy,[R11] and Cüer[C33b] in plates exposed at sea level.
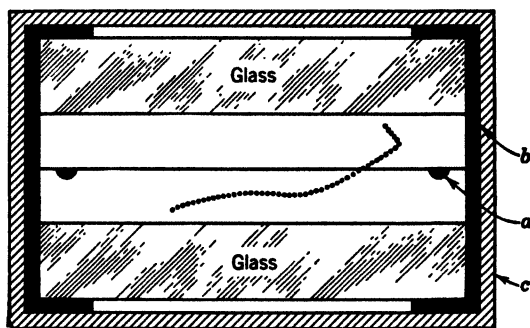
FIG. 68. Assembly of preeradicated plates for prolonged cosmic-ray exposures.

a. Uranium-ink line on lower emulsion (cross-sectional view); the ink, consisting of a 2 per cent solution of uranyl sulfate in equal volumes of alcohol and water, must be completely dry before sandwiching the emulsions.
b. Black-rubber-coated adhesive paper serving as a clamp.
c. Layer of paraffined black paper to exclude light and moisture.

A complex nuclear evaporation, Fig. 69, has been observed by Kaplan[K4] in an emulsion exposed at 82 meters following the eradication of its prior background. In this instance the entire history of the exposure between resensitization and development was known explicitly, and the 19-branch star cannot be attributed to some earlier high-altitude exposure, as incurred in shipment of the plates to the laboratory.

EVAPORATIONS PRODUCED BY ACCELERATED PARTICLES

Helium atoms and deuterons can be accelerated to about 400 and 200 Mev, energies approximating those of particles in the

cosmic radiation. Cloud-chamber studies with particles accelerated in the 184-in. Berkeley cyclotron show IV-pronged disintegrations which probably represent the evaporation of O^{16} atoms
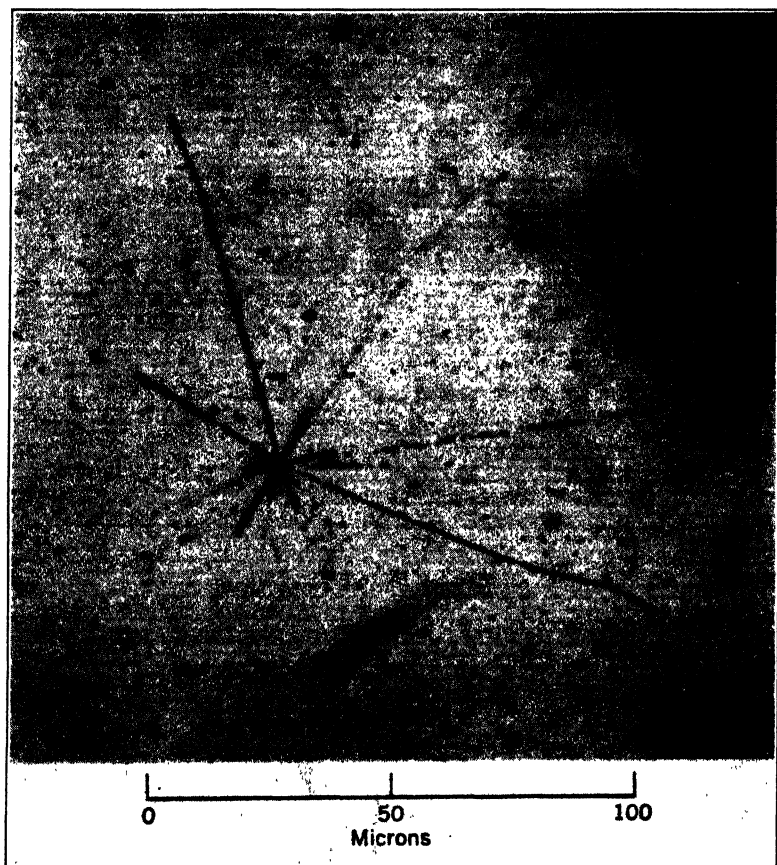
FIG. 69. Complex nuclear evaporation recorded at sea level. Eastman NTA emulsion preeradicated before exposure at Bethesda, Maryland. When examined in full depth the star consists of 19 recorded tracks. Only 10 tracks are evident at the particular focal setting at which the photomicrograph was taken.

into 4 alpha particles. Thornton and Powell [T13] have observed III-, IV-, and V-pronged stars in cloud-chamber exposures to 100-Mev neutrons. These induced disintegrations can also be studied by exposing nuclear-type emulsions for about 0.01 sec to the

cyclotron beam, orienting the emulsion plane parallel with the line of direction of the accelerated particles.

Fowler, Burrows, and Curry [F12] exposed Ilford plates to 9-Mev deuterons from the Liverpool cyclotron and observed numerous IV-branched stars which they attributed to the evaporation of nitrogen atoms:

$$N^{14} + H^2 \rightarrow 4He^4 + Q$$
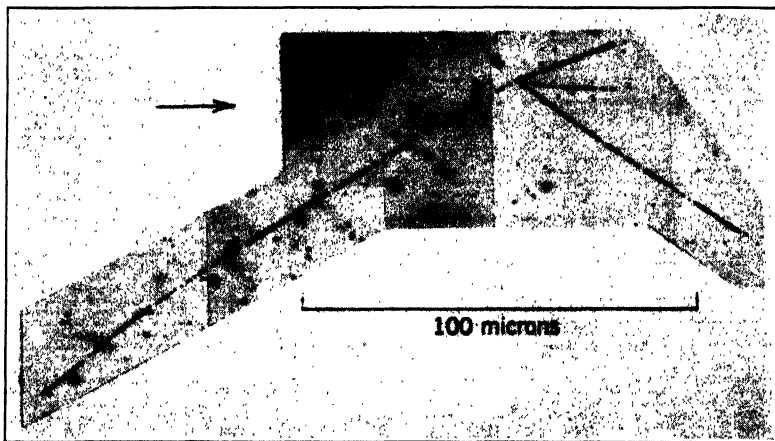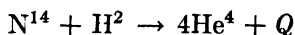
FIG. 70. Star initiated by a high-energy alpha particle. The arrow points to the direction of the incident beam of radiation. Reproduced by courtesy of E. Gardner, Radiation Laboratory, University of California, from work supported by the Atomic Energy Commission under contract W-7405-Eng-48.

This reaction is exoergic, and the mass conversion is equivalent to 6.09 Mev. The energy of the 4 alpha particles, as estimated from the recorded track lengths, tallied between 13.2 and 14.3 Mev. The experimental summation is in good agreement with the energy of the incident deuteron and the mass conversion, which may total 15 Mev. Two of the events observed by these investigators exhibit the path of the incident deuteron, whose track is readily differentiated from those of the ejected alpha particles by its lower grain density.

The stars produced in emulsions by artificially accelerated particles have been studied extensively by Gardner.[G1,2] In nuclear-type plates bombarded by high-energy deuterons, Gardner and Peterson [G3] have observed over 1200 stars with an aver-

age multiplicity of 3.0. Alpha-particle bombardment results in evaporations with a greater number of ejected charged particles. A V-branched event representative of Gardner's investigations is reproduced in Fig. 70. Horning[H34] has computed the excitation energy of nuclei for a given energy of the bombarding particle.
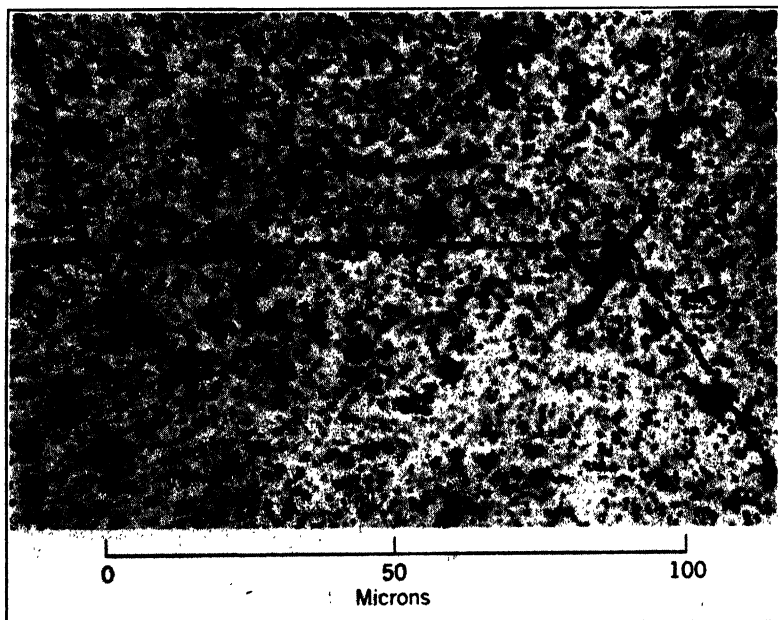
FIG. 71. Double star with the connecting track of a heavy charged particle. Event recorded in an Eastman NTB emulsion exposed to cosmic radiation in the stratosphere. The range of the connecting track is too short to indicate the direction of the particle by variation in grain density.

This can be employed as an approximate index to predict the number of particles that will be evaporated from the nucleus at each excitation level. For 35-Mev deuterons and 190-Mev alpha particles an average multiplicity of 3.0 and 3.9 is anticipated, which is in approximate agreement with the average number of tracks per event observed by Gardner.

The protons and alpha particles ejected from cosmic-ray disruptions often possess sufficient energy to penetrate the nuclear barrier of light elements, and the more energetic particles may on rare occasions initiate a secondary disruption process. An

event which appears to be explicable on this basis is shown in Fig. 71. The track connecting the two stars exhibits no small-angle scatter and possesses too high a grain density to be the initial portion of a σ-meson. The dual disruption probably was caused by a heavy charged particle (H^1, H^2, or He^4) emitted from one of the stars and captured by a constituent atom of the gelatin.

THE ARTIFICIAL MESONS

The measurements reported are admittedly preliminary, and much more work is to be done, but it seems certain that this marks the beginning of meson study under controllable laboratory conditions. The large intensities, approximately 10^8 times those available in cosmic rays, mean that the rate of progress in this field can be greatly accelerated.—Gardner and Lattes, 1948

Until very recently cosmic radiation was the only available source of meson particles. When the more powerful cyclo-

Courtesy of E. Gardner
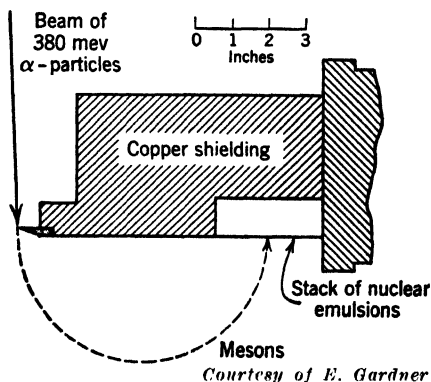
FIG. 72. Experimental arrangement for track recording of cyclotron-produced meson particles.

trons became available the theoreticians reasoned that sufficient energy was on hand in the interaction of 400-Mev alpha particles with nuclei for the creation of meson particles. Although the early work of Gardner and Peterson [G3] demonstrated that these projectiles were effective agents in producing nuclear disruptions in the emulsion, it was not possible to identify the tracks of any accompanying ejected mesons. Cosmic-ray exposures demon-

Courtesy of E. Gardner
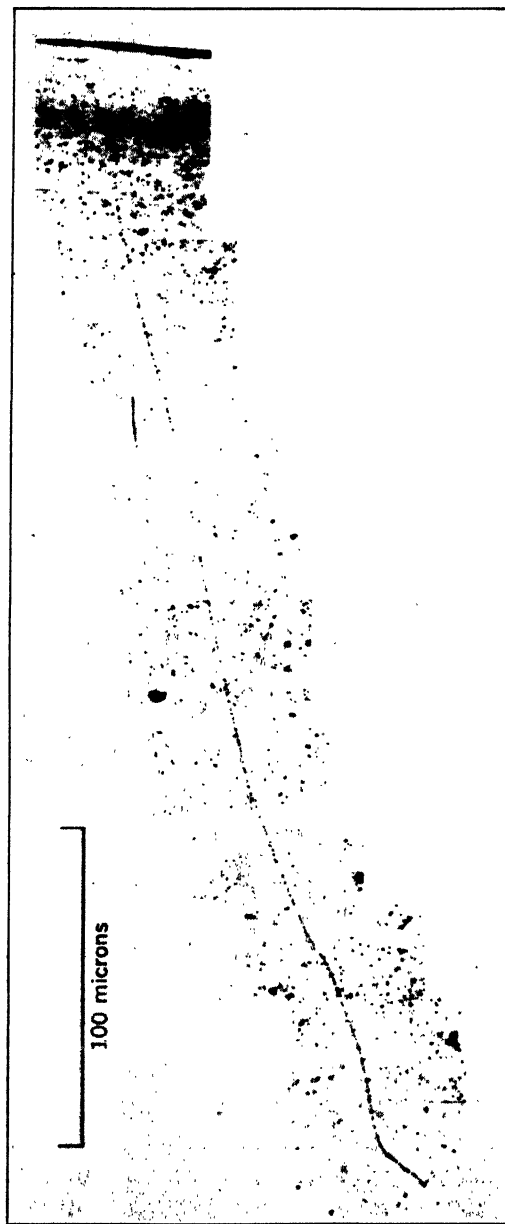
FIG. 73. Track of a negative meson terminating in the emulsion unaccompanied by visible disintegration products. The black band on the right is a mass of silver which commonly develops as a result of strains at the extreme edges of plates.

strate that these occurrences are rare, and while the greater flux from the cyclotron would favor the process the extremely high background track population rendered the detection of the low grain density meson tracks very difficult.
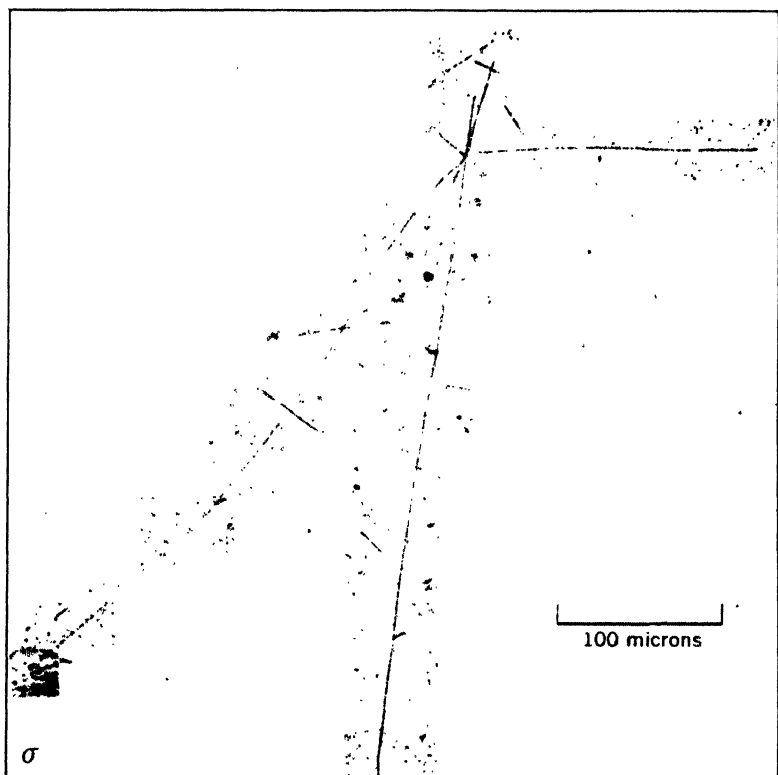
Courtesy of E. Gardner

Fig. 74. Track of a negative meson (σ) which produces a nuclear evaporation.

This situation was overcome by an ingenious experimental arrangement, Fig. 72, which avoided the direct bombardment of the emulsion by the primary alpha-particle beam. In the experimental disposition of Gardner and Lattes[G4a] the beam of 380-Mev alpha particles was directed on a thin target within which mesons and other particles were generated. By means of a magnetic field, the light negatively charged mesons were sorted out from the other particles and roughly focused on a stack of nuclear
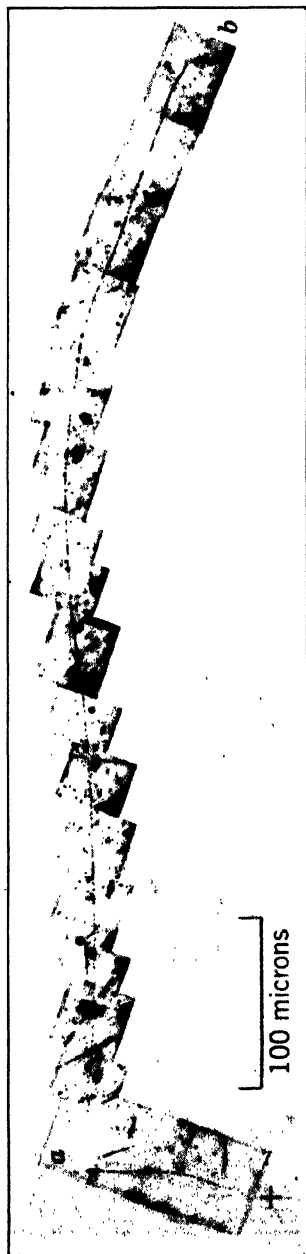
Courtesy of E. Gardner

Fig. 75. Track of a positive meson (+) terminating in the emulsion accompanied by a track *ab* of a secondary particle. The low grain density of track *ab* near point *a*, together with the increasing grain density towards *b*, proves that the secondary particle was moving in the direction $a \rightarrow b$.

emulsions. Microscopic examination of the plates revealed about 50 meson tracks concentrated chiefly along the exposed edge with a scatter and grain density similar to those observed occasionally in emulsions exposed to cosmic radiation. Some of the meson tracks on coming to rest in the emulsion produced a star, thereby eliminating all doubt as to the identity of the track. Examples of these processes, reproduced from the early plates of Gardner and Lattes, are exhibited in Figs. 73 and 74.

The mass of these laboratory-created mesons, as determined by measurements of their magnetic deflection and range in the emulsion, is $313 \pm 16\ m_e$ which indicates that they are probably identical with the heavy mesons observed in cosmic-ray exposures. These mesons were produced in the bombardment of carbon, beryllium, copper, and uranium targets by 380-Mev alpha particles. Reducing the energy of the incident projectiles to 300 Mev gave a greatly reduced yield of mesons from a bombarded carbon target.

By modifying the experimental arrangement for exposing the plates the Berkeley investigators have succeeded in the detection of positively charged mesons.[B56] The tracks of the positive mesons are identified by the registration of a second track produced by the decay product of the primary particle. The nuclear death and transfiguration of the positive meson are depicted clearly by the variation in grain density of the dual tracks reproduced in Fig. 75. Only about one-half of the positive mesons exhibit the track of the secondary particle, but the Berkeley investigators are of the opinion that all primary positive mesons decay into secondary charged mesons. Instances where the second track is not observed are attributed to unfavorable angle for registration in the emulsion layer or poor observational background caused by a high population of knock-on proton tracks or a combination of both detriments. Studies are in progress[B55] on the estimation of the mass of these mesons on the basis of grain counts along the trajectories. The tracks produced by the laboratory-created positive mesons suggest that they are similar to the particles responsible for the π-μ events in cosmic-ray plates.

BIBLIOGRAPHY

A1: S. P. ALEXANDROV, *Z. Krist.*, **65**, 141 (1927).
A2: J. M. ANSHELES, *Univ. Boubonov*, Ser. 10, No. 3, **2**, 1–14 (1936).
A3: N. ARLEY, *Phys. Rev.*, **72**, 1253 (1947).
A4: D. I. ARNON, P. R. STOUT, and F. SIPOS, *Am. J. Botany*, **27**, 791 (1940).
A5: D. AXELROD and J. HAMILTON, *Am. J. Path.*, **23**, 389 (1947).
A6: D. AXELROD, *Anat. Rec.*, **98**, 19–24 (1947).
A7: D. AXELROD and J. G. HAMILTON, *Supp. U. S. Naval Med. Bull.*, March 1948, pp. 122–141.

B1: H. BÄCKSTRÖM, C. A. BRUNO, and M. MILLER, *The Svedberg*, Uppsala, 1944.
B2: V. I. BARANOV and S. I. KRETSCHMER, *Compt. rend. acad. Sci. U.R.S.S.*, **1**, 543–549 (1935).
B3: V. I. BARANOV and E. G. GRACHOVA, *Proc. State Radium Inst. U.S.S.R.*, **3**, 111–116 (1937).
B4: V. I. BARANOV, A. P. ZHDANOV, and M. YU. DEIZENROT-MYSOVSKAYA, *Bull. acad. sci. U.R.S.S., Classe sci. chim.*, **1944**, 20.
B5: M. G. BARDET, *Bull. soc. min.*, **27**, 63 (1904).
B6: C. S. BARRETT, R. A. GEZELIUS, and R. F. MEHL, *Metals and Alloys*, **1**, 872 (1930).
B7: H. J. BARTELSTONE, I. D. MANDEL, E. OSHRY and S. M. SEIDLIN, *Science*, **106**, 132–133 (1947).
B8: R. BAUMANN, *Metallurgie*, **3**, 416 (1906).
B9: S. T. BAYLEY, *Nature*, **160**, 193 (1947).
B10: H. BECQUEREL, *Compt. rend.*, **122**, 420, 501, 698 (1896).
B11: H. BECQUEREL, *Compt. rend.*, **122**, 1086 (1896).
B12: N. C. BEESE, *Photo Tech.*, **2**, 50 (July, 1940).
B13: F. BĚHOUNEK and J. KLUMPAR, *Nature*, **160**, 640 (1947).
B14: B. BEHRENS and A. BAUMANN, *Z. ges. exptl. Med.*, **92**, 240, 251 (1933).
B15: L. F. BÉLANGER and C. P. LEBLOND, *Endocrinology*, **39**, No. 1, 8–13 (1946).
B16: C. BENEDICKS and H. LÖFQUIST, *Non-Metallic Inclusions in Iron and Steel*, John Wiley & Sons, New York, 1931.
B17: H. BERGGREN, *Acta Radiol.*, **27**, 248 (1946).
B18: M. BLAU, *Sitzber. Akad. Wiss. Wien*, Abt. 2*a*, **134**, 427 (1925).
B19: M. BLAU, *Z. Physik*, **34**, 285 (1925).
B20: M. BLAU, *Sitzber. Akad. Wiss. Wien*, Abt. 2*a*, **140**, 623–628 (1931).
B21: M. BLAU and H. WAMBACHER, *Sitzber. Akad. Wiss. Wien*, Abt. 2*a*, **141**, 617 (1932).
B22: M. BLAU and H. WAMBACHER, *Monatsh.*, **61**, 99–106 (1932).
B23: M. BLAU and H. WAMBACHER, *Z. wiss. Phot.*, **31**, 243 (1933).
B24: M. BLAU, *J. phys. radium*, **5**, 61 (1934).

B25: M. BLAU and H. WAMBACHER, *Sitzber. Akad. Wiss. Wien,* Abt. 2*a,* **146,** 259, 469, 623 (1937).

B26: M. BLAU, *Arch. Math. Naturvidenskab, B*42, No. 4 (1939), 10 pp.

B26*a*: M. BLAU and J. A. DE FELICE, *Phys. Rev.,* **74,** 1198 (1948).

B27: J. M. BLAIR and M. C. HYLAN, *J. Optical Soc. Am.,* **25,** 246 (1935).

B28: W. BLOOM, H. J. CURTIS, and F. C. MCLEAN, *Science,* **105,** 45 (1947).

B29: G. W. BODEN, *Sands, Clays and Minerals,* **2,** No. 4, 33–44 (1936).

B30: J. K. BÖGGILD, O. H. ARRÖE, and T. SIGURGEIRSSON, *Phys. Rev.,* **71,** 281 (1947).

B30*a*: J. K. BÖGGILD, *Nature,* **161,** 810 (1948).

B31: B. B. BOLTWOOD, *Am. J. Sci.,* **25,** 269 (1908).

B32: L. B. BORST and J. J. FLOYD, *Bull. Am. Phys. Soc.,* **21,** No. 3 (1946).

B33: H. BORUTTAU, *Über das Verhalten der Di- und Trihydroxylbenzole im Tierkörper,* Dissertation, Berlin, 1892.

B34: D. M. BOSE and B. CHOUDHURI, *Nature,* **145,** 894 (1940).

B35: D. M. BOSE and B. CHOUDHURI, *Nature,* **148,** 259 (1941); **149,** 302 (1942).

B36: D. M. BOSE, *Trans. Bose Research Inst. Calcutta,* **15,** 55–71 (1942–1943).

B36*a*: D. M. BOSE, B. CHOUDHURI, and M. SINHA, *Phys. Rev.,* **65,** 341–343, (1944).

B37: W. BOTHE, *Z. Physik,* **13,** 106 (1923).

B38: G. BOUISSIERES, R. CHASTEL, and L. VIGNERON, *Compt. rend.,* **224,** 43–45 (1947).

B39: W. H. BRAGG and R. KLEEMAN, *Phil. Mag.,* (6), **10,** 318 (1905).

B40: H. V. A. BRISCOE, *Science Progress,* **33,** 460 (1939).

B41: R. L. BROCK and E. GARDNER, *Rev. Sci. Instruments,* **19,** 299–303 (1948).

B42: E. BRODA, *Nature,* **158,** 872 (1946).

B43: E. BRODA, *Nature,* **160,** 231–232 (1947).

B44: E. BRODA, *J. Sci. Instruments,* **24,** 136–138 (1947).

B45: W. L. BROWN, *Univ. Toronto Studies,* Geol. Ser., No. 35 (1933); No. 32 (1932); No. 36 (1934).

B46: R. BRUNETTI and Z. OLLANO, *Ricerca sci.,* **13,** 106–111 (1942).

B47: W. E. BURCHAM and M. GOLDHABER, *Proc. Cambridge Phil. Soc.,* **32,** 632–636 (1936).

B48: I. P. C. BURTON, *Phot. J.,* **86B,** 62–70 (1946).

B49: J. T. BURWELL, JR., *Nucleonics,* **1,** No. 4, 38–50 (1947).

B50: C. R. BURCH, *Proc. Phys. Soc. London,* **59,** part 1, 41–47 (1947).

B51: W. J. BATES and G. P. S. OCCHIALINI, *Nature,* **161,** 473 (1948).

B52: H. J. BHABHA and R. R. DANIEL, *Nature,* **161,** 883 (1948).

B53: W. W. BUECHNER, R. J. VAN DE GRAAFF, E. N. STRAIT, C. G. STERGIOPOULOS, and A. SPERDUTO, *Bull. Am. Phys. Soc.,* **23,** No. 3, 30 (1948).

B54: W. BOSLEY, J. D. CRAGGS, and W. F. NASH, *Nature,* **161,** 1022 (1948).

B55: W. H. BARKAS, E. GARDNER, and C. M. G. LATTES, *Bull. Am. Phys. Soc.,* **23,** No. 5, 7 (1948).

B56: A. S. BISHOP, J. BURFENING, E. GARDNER, and C. M. G. LATTES, *Bull. Am. Phys. Soc.,* **23,** No. 5, 7 (1948).

B57: R. W. BERRIMAN, *Nature,* **161,** 432 (1948).

B58: G. BERNARDINI, G. CORTINI, and A. MANFREDINI, *Phys. Rev.,* **74,** 845 (1948).

B59: I. G. BARBOUR, *Phys. Rev.,* **74,** 507 (1948).

C1: N. R. CAMPBELL and A. WOOD, *Proc. Cambridge Phil. Soc.,* **14,** 15–21 (1906); **14,** 211 (1907).

C2: J. G. CAPSTAFF and N. B. GREEN, *Phot. J.,* **64,** 97 (1924).

C3: J. CHADWICK, A. N. MAY, C. F. POWELL, and T. C. PICKAVANCE, *Proc. Roy. Soc. London,* **183A,** 1 (1944).

C4: C. CHAMIE, *Compt. rend.,* **184,** 1243 (1927).

C5: C. CHAMIE, *Compt. rend.,* **185,** 770 (1927).

C6: C. CHAMIE, *Compt. rend.,* **185,** 1277 (1927).

C7: C. CHAMIE, *J. phys. radium,* **10,** 44 (1929).

C8: C. CHAMIE and M. HAISSINSKY, *Compt. rend.,* **198,** 1229 (1934).

C9: C. CHAMIE, *Compt. rend.,* **208,** 1300 (1939).

C10: W. Y. CHANG, *Phys. Rev.,* **69,** 60–77 (1946).

C11: A. CHARITON and D. E. LEA, *Proc. Roy. Soc. London,* **122A,** 304 (1929).

C12: J. S. CHEKA, *Phys. Rev.,* **71,** 836 (1947).

C12*a*: J. S. CHEKA, *Phys. Rev.,* **74,** 127 (1948).

C13: B. CHOUDHURI, *Trans. Bose Research Inst. Calcutta,* **15,** 29 (1942–1943).

C14: B. CHOUDHURI, *Indian J. Phys.,* **18,** 57 (1944).

C15: J. R. CHURCHILL, *Trans. Electrochem. Soc.,* **76,** 341–357 (1939).

C16: D. CITTMAR, *Z. Krebsforsch.,* **48,** 121–128 (1938).

C17: W. CLARK, *Brit. J. Phot.,* **69,** 462 (1922); **70,** 717 (1923).

C18: K. COLE, *Phys. Rev.,* **27,** 809 (1926).

C19: R. COLSON, *Compt. rend.,* **122,** 598 (1896); **123,** 49 (1896).

C20: J. W. COLTMAN and F. H. MARSCHALL, *Nucleonics,* **1,** No. 3, 58–64 (1947).

C21: D. H. COPP, D. AXELROD, and J .G. HAMILTON, *Am. J. Roentgenol.,* **58,** 10–16 (1947).

C22: S. COTELLE and A. LACASSAGNE, *Compt. rend. soc. biol.,* **129,** 248 (1938).

C23: E. COTTON, *Compt. rend.,* **224,** 823 (1947).

C24: A. COUCEIRO, G. LA VEIRA, and J. DE MORAES, *Rev. brasil. biol.,* **4,** 173 (1944).

C25: R. T. COX and C. T. CHASE, *Phys. Rev.,* **58,** 243–251 (1940).

C26: W. CROOKES, *Proc. Roy. Soc. London,* **66A,** 409–423 (1900).

C27: W. CROOKES, *Proc. Roy. Soc. London,* **71A,** 405 (1903).

C28: W. CROOKES, *Chem. News,* **87,** 241 (1903).

C29: P. CÜER and T. SAN TSIANG, *J. phys. radium,* (8), **4,** 231 (1943).

C30: P. CÜER, *Compt. rend.,* **223,** 1121 (1946).

C31: P. CÜER and C. M. G. LATTES, *Nature,* **158,** 197 (1946).

C32: P. CÜER, *Ann. géophys.,* **2,** 147–159 (1946).

C33: P. CÜER, *Compt. rend.,* **224,** 41 (1947).

C33*a*: P. CÜER and M. MORAND, *Compt. rend.,* **225,** 1146 (1947).

C33*b*: P. CÜER, M. MORAND, and H. MOUCHARAFYEH, *Compt. rend.*, **226**, 713 (1948).

C33*c*: P. CÜER, *J. phys. radium*, **8**, 83 (1947).

C34: S. CURIE, *Compt. rend.*, **126**, 1101 (1898).

C35: L. F. CURTIS and B. W. BROWN, *Phys. Rev.*, **72**, 643 (1947).

C36: W. W. CHUPP, E. GARDNER, and T. B. TAYLOR, *Phys. Rev.*, **73**, 742–749 (1948).

C37: I. C. CORNOG, W. FRANZEN, and W. E. STEPHENS, *Phys. Rev.*, **74**, 1 (1948).

C38: A. CHIORSO, W. W. MEINKE, and G. T. SEABORG, *Phys. Rev.*, **74**, 695 (1948).

C39: J. COBB and A. K. SOLOMAN, *Rev. Sci. Instruments*, **19**, 441 (1948).

C40: U. CAMERINI, H. MUIRHEAD, C. F. POWELL, and D. M. RITSON, *Nature*, **162**, 433–438 (1948).

D1: F. DAELS, H. FAJERMAN, and VAN DE PUTTE-VAN HOVE, *Strahlentherapie*, **63**, 545–555 (1938).

D2: T. DATCHANG, *J. Chinese Chem. Soc.*, **3**, 381–387 (1935).

D3: R. H. DE MEIO and F. C. HENRIQUES, JR., *J. Biol. Chem.*, **169**, 609–621 (1947).

D4: P. DEMERS, *Phys. Rev.*, **70**, 86 (1946).

D5: P. DEMERS, *Phys. Rev.*, **70**, 974 (1946).

D6: P. DEMERS, *Bull. Am. Phys. Soc.*, **22**, No. 1, 31 (1947).

D7: P. DEMERS and V. FREDETTE, *Phys. Rev.*, **72**, 538 (1947).

D8: P. DEMERS, *Bull. Am. Phys. Soc.*, **22**, No. 3, 17 (1947).

D9: P. DEMERS, *Can. J. Research*, **25A**, 223–251 (1947).

D9*a*: P. DEMERS, *Natl. Research Council Can.*, N.R.C. No. 1571 (1945).

D10: J. H. DILLON, and J. N. STREET, *J. Applied Phys.*, **13**, 189–198 (1942).

D11: M. J. L. DOLS, B. C. P. JANSEN, H. J. SIZOO, and G. J. VAN DER MAAS, *Nature*, **142**, 953 (1938).

D12: J. DE FELICE, *Bull. Am. Phys. Soc.*, **23**, No. 3, 52 (1948).

D13: I. H. DEARNLEY, C. L. OXLEY, and J. E. PERRY, *Phys. Rev.*, **73**, 1290 (1948).

D14: A. J. DEMPSTER, *Phys. Rev.*, **73**, 1125 (1948).

D15: G. E. DOAN, *J. Franklin Inst.*, **216**, 183–216, 351–385 (1933).

D16: C. C. DILWORTH, G. P. S. OCCHIALINI, and R. M. PAYNE, *Nature*, **162**, 102 (1948).

E1: H. V. ELLSWORTH, "Rare-Element Minerals of Canada," Econ. Geol. Ser., No. 11, Ottawa, Canada, 1932.

E2: J. ELSTER and H. GEITEL, reported in St. Meyer and Schweidler's *"Radioaktivität."* See M25.

E3: C. EMMERMANN, *Schweiz. Phot.-Ztg.*, **32**, 264 (1930).

E4: K. M. ENDICOTT and H. YAGODA, *Proc. Soc. Exptl. Biol. Med.*, **64**, 170 (1947).

E5: K. M. ENDICOTT and F. A. CLARK, personal communication.

E6: A. C. ENGLISH, T. E. CRANSHAW, P. DEMERS, J. A. HARVEY, E. P. HINCKS, J. V. JELLEY, and A. N. MAY, *Phys. Rev.*, **72**, 253 (1947).

E7: S. Epstein and J. P. Buckley, *Metals and Alloys,* **1,** No. 5, 226 (1929).
E8: O. Erbacher, *Z. physik. Chem.,* **163A,** 215 (1933).
E9: O. Erbacher and E. Wannenmacher, *Deut. Zahn-, Mund- u. Kiefer-heilk.,* **8,** 201 (1941).
E10: G. R. Evans and T. C. Griffiths, *Nature,* **159,** 879 (1947).
E11: R. D. Evans, *Phys. Rev.,* **45,** 29–37 (1934).
E12: R. D. Evans and C. Goodman, *Bull. Geol. Soc. Am.,* **52,** 459–490 (1941).
E13: R. D. Evans and C. Goodman, *J. Ind. Hyg. Toxicol.,* **22,** 89–99 (1941).
E14: R. D. Evans and C. Goodman, *Phys. Rev.,* **65,** 216–227 (1944).
E15: R. D. Evans, R. S. Harris, and J. W. M. Bunker, *Am. J. Roent-genol.,* **52,** 353–373 (1944).
E15*a*: R. D. Evans, *The Science and Engineering of Nuclear Power,* edited by C. Goodman, Addison-Wessley Press, Cambridge, 1947, p. 64.
E16: T. C. Evans, *Proc. Soc. Exptl. Biol. Med.,* **64,** 313 (1947).
E17: T. C. Evans, *Radiology,* **49,** 206–213 (1947).

F1: K. Fajans, *Radioelements and Isotopes,* McGraw-Hill Book Co., New York, 1931.
F2: H. Faraggi, *J. phys. radium,* **7,** 353 (1947).
F2*a*: H. Faraggi and G. Albouy, *Compt. rend.,* **226,** 717–719 (1948).
F2*b*: H. Faraggi, *Compt. rend.,* **227,** 527 (1948).
F3: G. Farwell, E. Segrè, and C. Wiegand, *Phys. Rev.,* **71,** 327 (1947).
F4: N. Feather, *Proc. Cambridge Phil. Soc.,* **34,** 599 (1938).
F5: N. Feather, *Nature,* **159,** 607 (1947).
F6: F. Feigl, *Laboratory Manual of Spot Tests,* Academic Press, New York, 1943.
F7: A. Filippov, J. Gurevich, and A. Zhdanov, *J. Exptl. Theoret. Phys. U.S.S.R.,* **8,** 623–638 (1938).
F8: A. Filippov, A. Zhdanov, and I. Gurevich, *J. Phys. U.S.S.R.,* **1,** 51 (1939).
F9: R. M. Fink, C. E. Dent, and K. Fink, *Nature,* **160,** 801 (1947).
F10: E. Fermi, *Science,* **105,** 27–32 (1947).
F11: H. H. Forster, *Bull. Am. Phys. Soc.,* **22,** No. 4, 8 (1947).
F11*a*: H. H. Forster, *Bull. Am. Phys. Soc.,* **23,** No. 5, 5 (1948).
F12: P. H. Fowler, H. B. Burrows, and W. J. J. Curry, *Nature,* **159,** 569 (1947).
F13: M. Francis, *Compt. rend.,* **201,** 473 (1935).
F14: M. Francis and T. Da Tchang, *Phil. Mag.,* **20,** 623 (1935).
F15: H. F. Freundlich, E. P. Hincks, and W. J. Ozeroff, *Rev. Sci. Instruments,* **18,** 90–100 (1947).
F15*a*: H. Friedman, L. S. Birks, and H. P. Gauvin, *Phys. Rev.,* **73,** 186 (1948).
F16: D. Froman, L. Rosen, and B. Rossi, *Bull. Am. Phys. Soc.,* **22,** No. 3, 5 (1947).
F17: C. Frondel, W. H. Newhouse, and R. F. Jarrell, *Am. Mineral,* **27,** 726–745 (1942).
F18: G. N. Flerov and K. A. Petrzhak, *Phys. Rev.,* **58,** 89 (1940).

F19: B. T. FELD, "The Photogenic Mesons," *Office of Naval Research Tech. Rept.* 8, T. O. VI, Cambridge, 1948.

F20: C. FRANZINETTI and R. M. PAYNE, *Nature,* **161,** 735 (1948).

F21: P. FREIER, E. J. LOFGREN, E. P. NEY, F. OPPENHEIMER, H. L. BRADT, and B. PETERS, *Phys. Rev.,* **74,** 213 (1948).

F22: G. FOURNIER, *Compt. rend.,* **184,** 878 (1927).

F23: E. FEENBERG, *Revs. Modern Phys.,* **19,** 239 (1947).

F24: M. P. FINKEL, *Physiol. Zoöl.,* **20,** 405 (1947).

G1: E. GARDNER, *Manhattan Eng. Dist. BP Rept.,* 71 PBL80593, June 1947.

G2: E. GARDNER, *Bull. Am. Phys. Soc.,* **22,** No. 4, 10 (1947).

G3: E. GARDNER and V. PETERSON, *Phys. Rev.,* **73,** 533 (1948).

G4: E. GARDNER, personal communication.

G4*a*: E. GARDNER and C. M. G. LATTES, *Science,* **107,** 270 (1948).

G5: A. M. GAUDIN and K. C. VINCENT, *Am. Inst. Mining Met. Engrs. Tech. Pub.,* 1663 (1944).

G6: H. GEIGER and J. M. NUTTALL, *Phil. Mag.,* **22,** 613 (1911); **23,** 439 (1912).

G7: H. GEIGER, *Z. Physik,* **8,** 191 (1921).

G8: H. GEIGER and A. WERNER, *Z. Physik,* **21,** 187–203 (1924).

G9: A. N. GERRITSEN, *Physica,* **12,** 311–320 (1946).

G10: I. GERSH, *Anat. Rec.,* **53,** 309 (1932).

G11: W. M. GIBSON, L. L. GREEN, and D. L. LIVESEY, *Nature,* **160,** 534 (1947).

G11*a*: W. M. GIBSON and D. L. LIVESEY, *Proc. Roy. Soc. London,* **60,** 523 (1948).

G12: J. L. GLASSON, *Phil. Mag.,* **43,** 477 (1922).

G13: E. GLÜCKAUF and F. A. PANETH, *Proc. Roy. Soc. London,* **165A,** 229 (1938).

G14: V. M. GOLDSCHMIDT, *Videnskapsselskapets-Skrifter I. Mat-naturv. Klasse Kristiania,* **5,** 51–58 (1924).

G15: C. GOODMAN and D. C. PICTON, *Phys. Rev.,* **60,** 688 (1941).

G16: C. GOODMAN, *J. Applied Phys.,* **13,** 276–289 (1942).

G17: C. GOODMAN and G. A. THOMPSON, *Am. Mineral.,* **28,** 456–467 (1943).

G18: A. GORBMAN, *Science,* **94,** 192 (1941).

G19: A. GORBMAN and H. M. EVANS, *Proc. Soc. Exptl. Biol. Med.,* **47,** 103 (1941).

G20: L. C. GRATON, *Am. Mineral.,* **22,** 491–516 (1937).

G21: L. L. GREEN and D. L. LIVESEY, *Nature,* **158,** 272 (1946).

G22: L. L. GREEN and D. L. LIVESEY, *Nature,* **159,** 332 (1947).

G22*a*: L. L. GREEN and D. L. LIVESEY, *Phil. Trans.,* **241A,** 323–343 (1948).

G23: R. GREGOIRE and M. PEREY, *Compt. rend.,* **225,** 733 (1947).

G24: J. N. GREGORY, *Nature,* **157,** 443 (1946).

G25: J. GROSS, C. P. LEBLOND, and W. L. PERCIVAL, *Proc. Soc. Exptl. Biol. Med.,* **67,** 74 (1948).

G26: J. GROSS and C. P. LEBLOND, *Canadian Med. Assoc. J.,* **57,** 102–122 (1947).

G27: C. GROVEN, J. GOVAERTS, and G. GUEBEN, *Nature,* **141,** 916 (1938).

G28: B. Gudden, *Z. Physik,* **26,** 110 (1924).
G29: K. M. Guggenheimer, H. Heitler, and C. F. Powell, *Proc. Roy. Soc. London,* **190,** 196 (1947).
G30: M. Guillot and M. Perey, *Compt. rend.,* **225,** 330 (1947).
G31: B. Gysae, *Naturw.,* **32,** 219 (1944).
G32: Y. Goldschmidt-Clermont, D. T. King, H. Muirhead, and D. M. Ritson, *Proc. Phys. Soc.,* **61,** part 2, 183–194 (1948).
G33: G. Goldhaber, *Phys. Rev.,* **74,** 1725 (1948).

H1: F. Hagemann, L. I. Katzin, M. H. Studier, A. Chiorso, and G. T. Seaborg, *Phys. Rev.,* **72,** 252 (1947).
H2: O. Hahn, H. Käding, and R. Mumbrauer, *Z. Krist.,* **87,** 387–416 (1934).
H3: O. Hahn, *Applied Radiochemistry,* Ithaca, New York, 1936.
H4: O. Hahn, cited as a personal communication by I. Oftedal, *Norsk Geol. Tids.,* **19,** 341 (1940).
H5: O. Hahn and F. Strassmann, *Abhandl. preuss. Akad. Wiss. Math-naturw. Klasse,* No. 12, 1944, 14 pp.
H6: M. Haissinsky, *Compt. rend.,* **198,** 580 (1934).
H7: M. Haissinsky, *Trans. Electrochem. Soc.,* preprint 70–1 (1936).
H8: M. Haissinsky, *Les radiocolloides,* Herman & Cie, Paris, 1937.
H9: M. Haissinsky, *Electrochimie des substances radioactives,* Herman & Cie, Paris, 1946.
H10: J. G. Hamilton, M. H. Soley, and K. B. Eichorn, *Univ. Calif. Berkeley Pub. Pharmacol.,* **1,** No. 28, 339–368 (1940).
H11: J. G. Hamilton and M. H. Soley, *Proc. Natl. Acad. Sci. U. S.,* **26,** 483–489 (1940).
H12: J. G. Hamilton, *J. Applied Phys.,* **12,** 440–460 (1941).
H12*a*: J. G. Hamilton, M. H. Soley, W. A. Reilly, and K. B. Eichorn, *Am. J. Diseases Children,* **66,** 495 (1943).
H13: J. G. Hamilton, *Radiology,* **49,** 325–343 (1947).
H14: E. L. Harrington, *Phil. Mag.,* **6,** 685–695 (1928).
H15: J. Hartmann, *Eder's Jahrb.,* **13,** 106 (1899).
H16: B. G. Harvey, *Ind. Eng. Chem. News Ed.,* **25,** 1585 (1947).
H17: B. G. Harvey, H. G. Heal, A. G. Maddock, and E. L. Rowley, *J. Chem. Soc.,* pp. 1010–1021 (August 1947).
H18: R. J. Hayden and M. G. Inghram, *Phys. Rev.,* **70,** 89 (1946).
H18*a*: R. J. Hayden, *Phys. Rev.,* **74,** 650 (1948).
H19: R. E. Head, *U. S. Bur. Mines Tech. Paper* 8, 1929, 29 pp.
H20: F. Hecht, *Sitzber. Akad. Wiss. Wien,* Abt. 2*a,* **144,** 213 (1935).
H21: F. Hecht and A. Grünwald, *Mikrochemie,* **30,** 279–296 (1942).
H22: G. H. Henderson and F. W. Sparks, *Proc. Roy. Soc. London,* **173A,** 239 (1939).
H23: K. Henney and B. Dudley, *Handbook of Photography,* McGraw-Hill Book Co., New York, 1939.
H24: M. Herszfinkiel and A. Wroncberg, *Compt. rend.,* **199,** 133 (1934).
H25: D. C. Hess, R. J. Hayden, and M. G. Inghram, *Phys. Rev.,* **72,** 730 (1947).

H26: F. L. HESS, *Am. J. Sci.*, **22**, 215 (1931); **25**, 426 (1933).

H27: W. HEISENBERG, *Cosmic Radiation*, translated by T. H. JOHNSON, Dover Publications, New York, 1946.

H28: W. HEITLER, C. F. POWELL, and G. E. F. FERTEL, *Nature*, **144**, 283 (1939).

H29: H. HEITLER, A. N. MAY, and C. F. POWELL, *Proc. Roy. Soc. London*, **190A**, 180–195 (1947).

H29*a*: W. HEITLER, C. F. POWELL, and H. HEITLER, *Nature*, **146**, 65 (1941).

H30: J. G. HOFFMAN and R. F. BACHER, *Phys. Rev.*, **54**, 644 (1938).

H31: R. HOFSTADTER, J. C. D. MILTON, and S. L. RIDGWAY, *Phys. Rev.*, **72**, 977 (1947).

H32: R. HOFSTADTER, *Phys. Rev.*, **72**, 1120 (1947).

H32*a*: R. HOFSTADTER, *Phys. Rev.*, **74**, 100 (1948).

H33: A. HOLMES, "Radioactivity and Geological Time," *Natl. Research Council U. S. Bull.* 80, Washington, D. C., 1931.

H34: W. HORNING, *Phys. Rev.*, **73**, 533 (1948).

H35: R. HOSEMANN, *Z. Physik*, **99**, 405–427 (1936).

H36: HO ZAH-WEI, T. SAN TSIANG, L. VIGNERON, and R. CHASTEL, *Compt. rend.*, **223**, 1119 (1946).

H37: W. HUME-ROTHERY, *Phil. Mag.* (7), **10**, 217 (1930).

H38: S. HUSIZAWA and E. TAJIMA, *Sci. Papers Inst. Phys. Chem. Research Tokyo*, **41**, 62–67 (1943).

H39: H. E. HUNTLEY, *Nature*, **161**, 356 (1948).

H40: R. H. HERZ, *Nature*, **161**, 928 (1948).

H41: A. HEE, *Compt. rend.*, **227**, 356 (1948).

H42: W. HÄLG and L. JENNY, *Helv. Phys. Acta*, **21**, 131–136 (1948).

H43: B. F. HARRISON, M. D. THOMAS, and G. R. HILL, *Plant Physiol.*, **19**, 245 (1944).

H44: H. HÄNNI, V. L. TELEGDI, and W. ZÜNTI, *Helv. Phys. Acta*, **21**, 203 (1948).

I1: S. IIMORI and E. IWASE, *Sci. Papers Inst. Phys. Chem. Research Tokyo*, **16**, 41–67 (1931).

I2: T. T. T. INAI, T. SAGITA, and M. HUSIZAWA, *Proc. Phys. Math. Soc. Japan*, **19**, 88 (1937).

I3: M. G. INGHRAM, D. C. HESS, R. J. HAYDEN, and G. W. PARKER, *Phys. Rev.*, **71**, 743 (1947).

I4: M. G. INGHRAM, R. J. HAYDEN, and D. C. HESS, *Phys. Rev.*, **71**, 270 (1947).

I5: A. M. ISMAIL and H. F. HARWOOD, *Analyst*, **62**, 185 (1937).

I6: H. ISRAËL-KÖHLER, *Gerlands Beitr. Geophys.*, **46**, 413–417 (1936); **48**, 13–58 (1936).

J1: E. A. JOHNSON and L. HARRIS, *Rev. Sci. Instruments*, **4**, 454 (1933).

J2: F. JOLIOT, *Compt. rend.*, **218**, 733–735 (1944).

J3: I. JOLIOT-CURIE and G. BOUISSIERES, *Cahiers phys.*, No. 26, 1–9 (1944).

J4: I. JOLIOT-CURIE and S. T. TSIEN, *J. phys. radium*, **6**, 162 (1945).

J5: I. JOLIOT-CURIE, *J. phys. radium*, **7**, 313–319 (1946).

J6: J. JOLY, *Brit. J. Phot.*, **52,** 551 (1905).
J7: Č. JECH, *Nature*, **161,** 314 (1948).
J8: L. JÁNOSSY, *Cosmic Rays*, Oxford Univ. Press, London, 1948.
J9: P. D. JOHNSON, *Ind. Radiography*, **1,** No. 1, 19–21 (1942).

K1: H. KÄDING and N. RIEHL, *Angew. Chem.*, **47,** 263 (1934).
K2: H. H. KAHN, *Strahlentherapie*, **37,** 751 (1930).
K3: M. D. KAMEN, *Radioactive Tracers in Biology*, Academic Press, New York, 1947.
K4: N. KAPLAN, unpublished investigations.
K5: G. L. KEENAN, *Chem. Revs.*, **3,** 95–111 (1926).
K6: N. B. KEEVIL, *Econ. Geol.*, **36,** 844 (1941).
K7: G. C. KENNEDY, *Econ. Geol.*, **40,** 353 (1945).
K8: G. L. KEHL, *The Principles of Metallographic Laboratory Practice*, 2nd ed., McGraw-Hill Book Co., New York, 1943.
K9: A. S. KESTON, R. P. BALL, V. K. FRANTZ, and W. W. PALMER, *Science*, **95,** 362 (1942).
K10: S. KINOSHITA, *Proc. Roy. Soc. London*, **83A,** 432 (1910).
K11: S. KINOSHITA and H. IKEUTI, *Phil. Mag.*, (6), **29,** 420 (1915).
K12: G. KIRSCH, *Geologie und Radioaktivität*, Springer, Berlin, 1928.
K13: G. KIRSCH and H. WAMBACHER, *Sitzber. Akad. Wiss. Wien*, Abt. 2*a*, **142,** 241 (1933).
K14: A. KNOPF, "The Age of the Earth," *Natl. Research Council U. S. Bull.* 80, Washington, D. C., 1931, p. 6.
K15: E. B. KNOPF and E. INGERSON, *Structural Petrology*, Geol. Soc. Am., Mem. 6, 1938.
K16: W. KNOWLES and P. DEMERS, *Phys. Rev.*, **72,** 535 (1947).
K17: H. J. KOLB and J. J. COMER, *J. Am. Chem. Soc.*, **67,** 894 (1945).
K18: A. KOTZAREFF, *J. élec. radiol.*, **6,** 131 (1922).
K19: A. F. KOVARIK and L. W. MCKEEHAN, "Radioactivity," *Natl. Research Council U. S. Bull.* 51, Washington, D. C., 1929.
K20: A. F. KOVARIK and N. I. ADAMS, JR., *Phys. Rev.*, **40,** 718 (1932).
K21: J. D. KURBATOV and M. H. KURBATOV, *J. Phys. Chem.*, **46,** 441–457 (1942).
K22: K. M. KUPFERBERG, *Phys. Rev.*, **73,** 804 (1948).
K23: S. A. KORFF, *Revs. Modern Phys.*, **20,** No. 1, 327 (1948).
K24: H. KALLMANN, *Research*, **1,** No. 6, 254–260 (1948).
K25: F. H. KRENZ, *Proc. Conf. Nuclear Chem.*, part 2, 192, Ottawa, Canada, 1947.
K26: V. G. KHLOPIN, E. K. GERLING, and N. V. BARANOVSKAYA, *Bull. acad. sci. U.R.S.S. Classe sci. chim.*, **1947,** 599–604.
K27: K. K. KELLER and K. B. MATHER, *Phys. Rev.*, **74,** 624 (1948).
K28: B. KARLIK and T. BERNERT, *Naturw.*, **31,** 492 (1943).

L1: A. LACASSAGNE and J. S. LATTES, *Compt. rend.*, **178,** 488 (1924).
L2: A. LACASSAGNE and J. S. LATTES, *Bull. histologie*, **1,** No. 6, 1–6 (1924).
L3: A. LACASSAGNE and J. S. LATTES, *Compt. rend. soc. biol.*, **90,** 352 (1924).
L4: A. LACASSAGNE and J. S. LATTES, *Compt. rend. soc. biol.*, **90,** 487 (1924).

L5: A. LACASSAGNE, J. S. LATTES, and J. LAVEDAN, *J. élect. radiol.*, **9**, 1–14, 67–82 (1925).

L6: A. LACASSAGNE and A. PAULIN, *Compt. rend. soc. biol.*, **94**, 327 (1926).

L7: A. LACASSAGNE, C. LEVADITI, J. S. LATTES, and S. NICOLAU, *Compt. rend. soc. biol.*, **94**, 1179 (1926).

L8: A. LACASSAGNE and J. S. LATTES, *Compt. rend. soc. biol.*, **97**, 697 (1927).

L9: A. LACASSAGNE and J. LOISELEUR, *Compt. rend. soc. biol.*, **107**, 462 (1931).

L10: A. LACASSAGNE and W. NYKA, *Radiophysiologie et radiothérapie*, **2**, No. 11, 595–613 (1932).

L11: E. H. LAND, *J. Optical Soc. Am.*, **37**, 61 (1947).

L12: J. LAPALME and P. DEMERS, *Bull. Am. Phys. Soc.*, **22**, No. 3, 17 (1947).

L13: C. M. G. LATTES and G. P. S. OCCHIALINI, *Nature*, **159**, 331 (1947).

L14: C. M. G. LATTES, H. MUIRHEAD, G. P. S. OCCHIALINI, and C. F. POWELL, *Nature*, **159**, 694 (1947).

L15: C. M. G. LATTES, G. P. S. OCCHIALINI, and C. F. POWELL, *Nature*, **160**, 453 (1947).

L16: C. M. G. LATTES, G. P. S. OCCHIALINI, and C. F. POWELL, *Nature*, **160**, 486 (1947).

L17: C. M. G. LATTES, P. H. FOWLER, and P. CÜER, *Proc. Phys. Soc. London*, **59**, 883 (1947).

L17*a*: C. M. G. LATTES, G. P. S. OCCHIALINI, and C. F. POWELL, *Proc. Phys. Soc. London*, **61**, part 2, 173 (1948).

L18: J. S. LATTES and A. LACASSAGNE, *Compt. rend.*, **178**, 488, 630, 771 (1924).

L19: J. S. LATTES and A. LACASSAGNE, *J. Radiol. Electrologie*, **12**, 1–4 (1928).

L20: K. LARK-HOROVITZ and W. A. MILLER, *Phys. Rev.*, **59**, 941 (1941).

L21: J. LAUDA, *Sitzber. Akad. Wiss. Wien*, Abt. 2*a*, **145**, 707 (1936).

L22: J. H. LAWRENCE, *Am. J. Roentgenol.*, **48**, 283 (1942).

L23: J. H. LAWRENCE, *Am. J. Roentgenol.*, **58**, 31 (1947).

L24: D. E. LEA, *Action of Radiations on Living Cells*, Cambridge, England, 1947.

L25: C. P. LEBLOND and A. LACASSAGNE, *Am. J. Roentgenol.*, **50**, 801 (1943).

L26: C. P. LEBLOND, *Stain Technol.*, **18**, 159 (1943).

L27: C. P. LEBLOND, *Anat. Rec.*, **88**, 285–289 (1944).

L28: C. P. LEBLOND, M. B. FERTMAN, I. D. PUPPEL, and G. M. CURTIS, *Arch. Path.*, **41**, 510 (1946).

L29: G. LE BON, *The Evolution of Forces*, London, 1908.

L30: L. LEWIN, *Nature*, **138**, 326 (1936).

L31: W. F. LIBBY, *Phys. Rev.*, **46**, 196–204 (1934).

L32: W. F. LIBBY, *Phys. Rev.*, **69**, 671 (1946).

L33: L. N. LIEBERMANN and H. H. BARSCHALL, *Rev. Sci. Instruments*, **14**, 89 (1943).

L34: E. LINDSAY and R. CRAIG, *Ann. Entomol. Soc. Am.*, **35**, 50 (1942).

L35: M. S. LIVINGSTONE and H. A. BETHE, *Revs. Modern Phys.*, **9**, 268 (1937).

L36: S. LOMHOLT, *J. Pharmacol. Exptl. Therap.*, **40**, 235 (1930).

L37: E. S. LONDON, *Arch. élect. méd. physiothérapie cancer*, **12**, 363 (1904).

L38: E. LORENZ, *J. Natl. Cancer Inst.*, **5**, No. 1, 1–15 (1944).

L39: G. LOVERA, *Ricerca Sci.*, **13**, 538–541 (1942).

L40: G. LOVERA, *Nuovo cimento*, **3**, 320–327 (1946).

L41: B. V. A. LOW-BEER, J. H. LAWRENCE, and R. S. STONE, *Radiology*, **39**, 573–597 (1942).

L42: S. S. LU and CHANG HUNG-CHI, *Chinese J. Phys.*, **4**, No. 1, 55–66 (1940).

L43: P. I. LUKIRSKY, M. G. MESCHERYAKOV, and T. I. KHRENINA, *Compt. rend., acad. sci. U.R.S.S.*, **55**, No. 2, 117 (1947).

L44: H. LÜPPO-CRAMER, *Kolloidchemie und Photographie*, 2nd ed., Dresden, 1921, p. 56.

L45: D. LYFORD and J. A. BEARDEN, *Bull. Am. Phys. Soc.*, **9**, No. 2, 10 (1934).

L46: S. LATTIMORE, *Nature*, **161**, 518 (1948).

L47: L. LEPRINCE-RINGUET, J. HEIDMANN, H. TCHANG-FONG, L. JAUNEAU, and J. STROUMSA, *Compt. rend.*, **225**, 1144 (1948).

L48: L. LEPRINCE-RINGUET and J. HEIDMANN, *Nature*, **161**, 844 (1948).

L49: T. T. LI and D. H. PERKINS, *Nature*, **161**, 844 (1948).

L50: R. M. LANGER and H. YAGODA, *Bull. Am. Phys. Soc.*, **23**, No. 3, 43 (1948).

L51: W. A. LAMB and F. W. BROWN III, *Phys. Rev.*, **74**, 104 (1948).

L52: H. LISCO, M. P. FINKEL, and A. M. BRUES, *Radiology*, **49**, 361 (1947).

L53: D. L. LIVESEY and D. H. WILKINSON, *British Report* 638, May 1945.

M1: M. MADER, *Z. Physik*, **88**, 601 (1934).

M2: W. MAKOWER and H. GEIGER, *Practical Measurements in Radioactivity*, Longmans, Green and Co., New York, 1912.

M3: W. MAKOWER and H. P. WALMSLEY, *Proc. Phys. Soc. London*, **26A**, 261 (1914).

M4: W. MAKOWER, *Nature*, **99**, 98 (1917).

M5: L. MALLET, *J. radiol. électrologie*, **26**, 4 (1944).

M6: J. P. MARBLE, *Repts. Comm. Meas. Geol. Time*, 1937, p. 65.

M7: J. P. MARBLE, *Am. Mineral.*, **25**, 169 (1940).

M8: J. P. MARBLE, *Am. J. Sci.*, **241**, 32–42 (1943).

M9: L. D. MARINELLI, R. F. BRINKERHOFF, and G. J. HINE, *Revs. Modern Phys.*, **19**, 25–28 (1947).

M10: L. D. MARINELLI, F. W. FOOTE, R. F. HILL, and A. F. HOCKER, *Am. J. Roentgenol.*, **58**, 17–30 (1947).

M11: B. E. MARQUES, *Compt. rend.*, **198**, 819 (1934).

M12: J. K. MARSH, *Nature*, **158**, 134 (1946).

M13: L. C. MARTIN and T. R. WILKINS, *J. Optical Soc. Am.*, **27**, 340–349 (1937).

M14: H. S. MARTLAND, *J. Am. Med. Assoc.*, **92**, 556 (1929).

M15: H. S. MARTLAND and R. E. HUMPHRIES, *Arch. Path.*, **7**, 406–417 (1929).

M16: L. MARTON and P. H. ABELSON, *Science*, **106**, 69 (1947).

M17: J. MATTAUCH and S. FLUEGGE, *Nuclear Physics Tables*, translated by P. GROSS and S. BARGMANN, Interscience Publishers, New York, 1946.

M18: A. N. May and C. F. Powell, *Proc. Roy. Soc. London,* **190A,** 170–180 (1947).

M19: H. N. McCoy, *J. Am. Chem. Soc.,* **27,** 391 (1905).

M20: C. E. McClung, *Handbook of Microscopical Technique,* 2nd ed., Hoeber, New York, 1937.

M21: D. M. McCutcheon, *Proc. Am. Soc. Testing Materials,* **42,** 1023–1044 (1942).

M22: H. E. McKinstry, *Econ. Geol.,* **22,** 669 (1927).

M23: C. E. K. Mees, *Theory of the Photographic Process,* Macmillan, New York, 1946.

M24: T. R. Merton, *Phil. Mag.,* **38,** 463 (1919).

M25: St. Meyer and E. von Schweidler, *Radioaktivität,* 2nd ed., Teubner, Berlin, 1927.

M26: W. Michl, *Sitzber. Akad. Wiss. Wien,* Abt. 2*a,* **121,** 1431 (1912).

M27: H. Moissan, *Compt. rend.,* **122,** 1088 (1906).

M28: E. Montel, *J. phys. radium,* **10,** 78 (1929).

M29: K. Z. Morgan and J. S. Cheka, personal communication.

M30: K. Z. Morgan, *Ind. Eng. Chem. News Ed.,* **25,** 3794 (1947).

M31: M. E. Morton, I. L. Chaikoff, W. O. Reinhardt, and E. Anderson, *J. Biol. Chem.,* **147,** 757 (1943).

M32: L. Moser, *Pogg. Ann.,* **56,** 177–234 (1842).

M33: O. Mügge, *Centr. Mineral.,* **71,** 114, 142 (1909).

M34: E. Mühlestein, *Arch. sci.,* (5), **2,** 240 (1920).

M35: L. J. Mullins, *Proc. Soc. Exptl. Biol. Med.,* **64,** 296 (1947).

M36: L. Myssowsky and P. Tschijow, *Z. Physik,* **44,** 408 (1927).

M37: L. Myssowsky and A. Zhdanov, *Nature,* **143,** 794 (1939).

M38: L. Marschall, *Bull. Am. Phys. Soc.,* **23,** No. 4, 10 (1948).

M39: P. B. Mauer and H. L. Reynolds, *Phys. Rev.,* **73,** 1131 (1948).

M40: P. Morrison, *J. App. Phys.,* **19,** 311 (1948).

M41: F. J. Morris and A. E. Lockenvitz, *Phys. Rev.,* **73,** 649 (1948).

M42: C. R. Maxwell, W. H. Beamer, and D. T. Vier, "Physical Properties and Crystal Structure of Polonium," LADC 284, declassified.

M43: R. J. Moon, *Phys. Rev.,* **73,** 1210 (1948).

M44: C. Milton, K. J. Murata, and M. M. Knechtel, *Am. Mineral.,* **29,** 92 (1944).

M45: K. B. Mather and F. N. D. Kurie, *Phys. Rev.,* **73,** 1474 (1948).

M46: H. Meyer, *Brit. J. Radiology,* **15,** 85 (1942).

M47: A. Morrison, *Nucleonics,* **3,** No. 3, 46 (1948).

M48: A. Morrison and E. Pickup, *Phys. Rev.,* **74,** 706 (1948).

M49: M. Morand, P. Cüer, J. Edmont, and H. Moucharafyeh, *Compt. rend.,* **226,** 1008 (1948).

N1: C. B. Neblette, *Photography,* 4th ed., D. Van Nostrand Co., New York, 1942.

N2: H. R. Nelson, *Metal Progress,* **42,** 391 (1942).

N3: Niepce de Saint-Victor, *Compt. rend.,* **65,** 505 (1867).

N4: A. A. Noyes and W. C. Bray, *A System of Qualitative Analysis for the Rare Elements,* Macmillan, New York, 1927.

N5: W. F. NEUMAN, M. W. NEUMAN, and B. J. MULRYAN, *J. Biol. Chem.*, **175**, 705–709 (1948).
N6: M. W. NEUMAN and W. F. NEUMAN, *J. Biol. Chem.*, **175**, 711–714 (1948).

O1: G. P. S. OCCHIALINI and C. F. POWELL, *Nature*, **159**, 189 (1947).
O1*a*: G. P. S. OCCHIALINI and C. F. POWELL, *Nature*, **162**, 168–173 (1948).
O2: G. ORTNER and J. SCHINTLMEISTER, *Sitzber. Akad. Wiss. Wien*, Abt. 2*a*, **143**, 411 (1934).
O3: G. ORTNER, *Sitzber. Akad. Wiss. Wien*, Abt. 2*a*, **149**, 259 (1940).

P1: M. PAHL and R. HOSEMANN, *Naturw.*, **23**, 318 (1935).
P2: F. PANETH, *Kolloid-Z.*, **13**, 297 (1913).
P3: F. PANETH, *Physik. Z.*, **15**, 924 (1914).
P4: C. PECHER, *Proc. Soc. Exptl. Biol. Med.*, **46**, 86 (1941).
P5: R. A. PECK, JR., *Bull. Am. Phys. Soc.*, **22**, No. 1, 7 (1947).
P6: R. A. PECK, JR., *Phys. Rev.*, **72**, 1121 (1947).
P6*a*: R. A. PECK, JR., *Bull. Am. Phys. Soc.*, **23**, No. 2, 36 (1948).
P6*b*: R. A. PECK, JR., *Phys. Rev.*, **73**, 947–955 (1948).
P7: S. R. PELC, personal communication.
P8: S. R. PELC, *Nature*, **160**, 749 (1947).
P9: H. S. PENN and J. KAPLAN, *Bull. Am. Phys. Soc.*, **22**, No. 2, 20 (1947).
P10: M. PEREY, *Compt. rend.*, **208**, 97 (1939).
P11: M. PEREY, *J. chim. phys.*, **43**, 269–278 (1946).
P12: N. A. PERFILOV, *Compt. rend. acad. sci. U.R.S.S.*, **23**, 896 (1939).
P13: N. A. PERFILOV, *Compt. rend. acad. sci. U.R.S.S.*, **42**, 258 (1944).
P14: N. A. PERFILOV, *Compt. rend. acad. sci. U.R.S.S.*, **43**, 14 (1944).
P15: N. A. PERFILOV, *Compt. rend. acad. sci. U.R.S.S.*, **47**, 623 (1945).
P16: N. A. PERFILOV, *J. Phys. U.S.S.R.*, **10**, 1–12 (1946).
P16*a*: N. A. PERFILOV, *J. Phys. U.S.S.R.*, **11**, No. 3 (1947).
P17: D. H. PERKINS, personal communication.
P18: D. H. PERKINS, *Nature*, **159**, 126 (1947).
P19: D. H. PERKINS, *Nature*, **160**, 299 (1947).
P20: D. H. PERKINS, *Nature*, **160**, 707 (1947).
P20*a*: D. H. PERKINS, *Nature*, **161**, 486 (1948).
P21: K. PHILIPP, *Z. Physik*, **17**, 23 (1923).
P22: C. S. PIGGOT and W. D. URRY, *Am. J. Sci.*, **239**, 81 (1941).
P23: A. PIGNEDOLI, *Atti soc. nat. e mat. Modena*, **72**, 77–88 (1941).
P24: M. F. PISANI, *Bull. soc. min.*, **27**, 58 (1904).
P25: PLUTONIUM PROJECT, *J. Am. Chem. Soc.*, **68**, 2411–2442 (1946).
P26: A. POLICARD and H. OKKELS, *Anat. Rec.*, **44**, 349 (1930).
P27: E. POLLARD and W. L. DAVIDSON, *Applied Nuclear Physics*, John Wiley & Sons, New York, 1942.
P28: D. Q. POSIN, *Proc. Montana Acad. Sci.*, **3** and **4**, 10–15 (1942–1943).
P29: D. Q. POSIN, *Phys. Rev.*, **69**, 702 (1946).
P30: C. F. POWELL and G. E. F. FERTEL, *Nature*, **144**, 115 (1939).
P31: C. F. POWELL, *Nature*, **145**, 155 (1940).

P32: C. F. Powell, *Endeavour,* **1,** 151–156 (1942).

P33: C. F. Powell and F. C. Champion, *Proc. Roy. Soc. London,* **183A,** 64 (1944).

P34: C. F. Powell, G. P. S. Occhialini, and D. L. Livesey, *J. Sci. Instruments,* **23,** 102–106 (1946).

P35: C. F. Powell and G. P. S. Occhialini, *Nuclear Physics in Photographs,* Oxford Univ. Press, London, 1947.

P36: C. F. Powell and S. Rosenblum, *Nature,* **161,** 473 (1948).

P37: O. Peter, *Z. Naturforsch.,* **1,** 557–559 (1946).

P38: J. H. J. Poole and J. W. Bremner, *Nature,* **161,** 884 (1948).

P38*a*: J. H. J. Poole and J. W. Bremner, *Phys. Rev.,* **74,** 836 (1948).

P39: H. Pose, *Z. Physik,* **121,** 293 (1943).

P40: W. E. T. Perry, *Radiography,* **6,** 7–11 (1940).

P41: L. A. Pardue, N. Goldstein, and E. O. Wollan, MDDC 1065 (Ch-1553; A-2223) declassified April 8, 1944.

P42: E. Pickup, *Phys. Rev.,* **74,** 495 (1948).

R1: C. V. Raman, *Proc. Indian Acad. Sci.,* Symposium on the Structure and Properties of Diamond, 1944, p. 189.

R2: W. M. Rayton and T. R. Wilkins, *Phys. Rev.,* **51,** 818 (1937).

R3: M. Reinganum, *Physik. Z.,* **12,** 1076 (1911).

R4: W. O. Reinhardt, *Proc. Soc. Exptl. Biol. Med.,* **50,** 81 (1942).

R4*a*: H. T. Richards and E. Hudspeth, *Phys. Rev.,* **58,** 382 (1940).

R5: H. T. Richards, *Phys. Rev.,* **59,** 796 (1941).

R6: H. T. Richards and L. Speck, *Phys. Rev.,* **71,** 141 (1947).

R7: M. Ritchie and J. A. Thom, *Trans. Faraday Soc.,* **42,** 427 (1946).

R8: E. Rona and W. Schmidt, *Wien. Ber.,* **137,** 103 (1928).

R9: E. Rona, *Am. Phil. Soc. Yearbook,* 1943, p. 136.

R10: E. Rona, *Am. Phil. Soc. Yearbook,* 1945, p. 142.

R11: R. R. Roy, *Nature,* **160,** 498 (1947).

R12: S. Rubin, W. A. Fowler, and C. C. Lauritsen, *Phys. Rev.,* **71,** 212 (1947).

R13: S. Rubin, *Phys. Rev.,* **72,** 1176 (1947).

R14: L. H. Rumbaugh and G. L. Locher, *Nat. Geog. Soc. Stratosphere Ser.,* **2,** 32 (1936).

R15: A. S. Russell, *An Introduction to the Chemistry of Radioactive Substances,* John Murray, London, 1922.

R16: W. J. Russell, *Proc. Roy. Soc. London,* **61,** 424 (1897); **63,** 102 (1898); **64,** 409 (1899); **78,** 385 (1906); **80,** 376 (1908).

R17: W. J. Russell, *Phot. J.,* **23,** 91–97 (1898).

R18: E. Rutherford and H. Geiger, *Phil. Mag.,* **20,** 691 (1910).

R19: E. Rutherford, *Proc. Roy. Soc. London,* **83A,** 561 (1910).

R20: E. Rutherford, J. Chadwick, and C. D. Ellis, *Radiations from Radioactive Substances,* Cambridge, England, 1930.

R21: F. Reines, *Bull. Am. Phys. Soc.,* **23,** No. 5, 15 (1948).

R22: S. Rosenblum and E. Cotton, *Compt. rend.,* **226,** 171 (1948).

S1: R. R. SAHNI, *Phil. Mag.*, **29**, 836 (1915).
S2: B. W. SAKMANN, J. T. BURWELL, and J. W. IRVINE, *J. Applied Phys.*, **15**, 459–473 (1944).
S3: E. SCHÄFLER, *Sitzber. Akad. Wiss. Wien,* Abt. 2*a*, **145**, 567–576 (1936).
S4: R. SCHIEDT, *Sitzber. Akad. Wiss. Wien,* Abt. 2*a*, **144**, 175–211 (1935).
S5: J. SCHINTLMEISTER, *Sitzber. Akad. Wiss. Wien,* Abt. 2*a*, **144**, 475 (1935).
S6: G. C. SCHMIDT, *Compt. rend.*, **126**, 1264 (1898).
S7: E. SCHOPPER, *Naturw.*, **25**, 557 (1937).
S8: E. SCHOPPER, *Photo. Ind.*, **36**, 845 (1938).
S9: E. SCHOPPER, *Veröffentl. wiss. Zentral-Labs. phot. Abt I. G. Farbinind. Akt.-Ges. AGFA,* **6**, 170–178 (1939).
S10: E. M. SCHOPPER and E. SCHOPPER, *Physik. Z.*, **40**, 22–26 (1939).
S11: W. C. SCHUMB, R. D. EVANS, and J. L. HASTINGS, *J. Am. Chem. Soc.*, **61**, 3451 (1939).
S12: G. M. SCHWAB and E. PIETSCH, *Z. physik. Chem.*, **2B**, 262 (1929).
S13: K. SCHWARZ, *Z. physik. Chem.*, **168A**, 241 (1934).
S14: G. H. SCOTT and N. L. HOERR, sections in *Medical Physics*, edited by OTTO GLASSER, The Year Book Publishers, Inc., Chicago, 1944, on histologic fixation, p. 466; and the microincineration method, p. 729.
S15: G. H. SCOTT and D. M. PACKER, *Anat. Rec.*, **74**, 17, 31 (1939).
S16: G. T. SEABORG, *Revs. Modern Phys.*, **16**, 1–32 (1944).
S17: G. T. SEABORG, *News Ed. Am. Chem. Soc.*, **23**, 2190 (1945); **25**, 358 (1947).
S17*a*: G. T. SEABORG and M. L. PERLMAN, *J. Am. Chem. Soc.*, **70**, 1571 (1948).
S18: W. SEITH and A. H. W. ATEN, *Z. physik. Chem.*, **10B**, 296 (1930).
S19: W. SEITH and A. KIEL, *Z. Metallkunde*, **25**, 104 (1933).
S20: W. SEITH and A. KIEL, *Z. Metallkunde*, **26**, 68 (1934).
S21: F. E. SENFTLE, *Trans. Can. Inst. Mining Met.*, **49**, 439–446 (1946).
S22: M. M. SHAPIRO, *Revs. Modern Phys.*, **13**, 58–71 (1941).
S23: M. M. SHAPIRO, *Phys. Rev.*, **61**, 115 (1942).
S23*a*: M. M. SHAPIRO and J. R. BARNES, *Bull. Am. Phys. Soc.*, **23**, No. 2, 11 (1948).
S24: S. E. SHEPPARD and E. P. WIGHTMAN, *J. Franklin Inst.*, **195**, 337 (1923).
S25: S. E. SHEPPARD, T. R. WILKINS, E. P. WIGHTMAN, and R. N. WOLFE, *J. Franklin Inst.*, **222**, 417–460 (1936).
S26: R. SHERR, *Rev. Sci. Instruments*, **18**, 767 (1947).
S27: N. SHIMOTORI and A. F. MORGAN, *J. Biol. Chem.*, **147**, 203 (1943).
S28: M. N. SHORT, "Microscopic Determination of the Ore Minerals," *U. S. Geol. Survey Bull.* 914, Washington, D. C., 1940.
S29: W. M. SHOUPP, *Iron Age*, **148**, 51 (1941); *Metal Progress*, **41**, 688 (1942).
S29*a*: C. G. SHULL, M. C. MARNEY, and E. O. WOLLAN, *Bull. Am. Phys. Soc.*, **23**, No. 2, 36 (1948); *Phys. Rev.*, **73**, 527 (1948).
S30: H. D. SMYTH, *Atomic Energy for Military Purposes,* Princeton Univ. Press, Princeton, New Jersey, 1945.
S31: F. SODDY, *The Chemistry of the Radioelements,* 2nd ed., Longmans, Green, London, 1914.

S32: F. Soddy, *The Interpretation of the Atom,* John Murray, London, 1932.

S33: H. S. Spence, *Sands, Clays and Minerals,* **2,** No. 3, 9 (1935).

S34: J. W. T. Spinks, *Proc. Conf. Nuclear Chem.,* Chemical Institute of Canada, Ottawa, 1947, pp. 134–151.

S35: A. V. St.George, A. O. Gettler, and R. H. Muller, *Arch. Path.,* **7,** 397 (1929).

S36: J. K. Stanley, *Nucleonics,* **1,** No. 2, 70 (1947).

S37: I. E. Starik, *Trans. Inst. Radium Leningrad,* **2,** 91 (1933).

S38: I. E. Starik, *Rep. 16th Sess. Intern. Geol. Congr., Washington, D. C.,* 1933, p. 217.

S39: M. M. Stephens, *Am. Mineral.,* **16,** 532–549 (1931).

S40: W. E. Stephens and M. N. Lewis, *Phys. Rev.,* **69,** 43 (1946).

S41: G. Stetter and H. Wambacher, *Physik. Z.,* **40,** 702 (1939).

S42: W. Stiles, *Trace Elements in Plants and Animals,* Cambridge, England, 1946.

S43: R. S. Stone, *Proc. Am. Phil. Soc.,* **90,** 11–19 (1946).

S44: W. W. Strong, *Phys. Rev.,* **29,** 170 (1909).

S45: B. E. Struckmeyer, *Am. J. Botany,* **30,** 477 (1943).

S46: T. Svedberg and H. Anderson, *Phot. J.,* **61,** 325 (1921).

S47: B. Szilard, *Le radium,* **6,** 233 (1909).

S48: G. Scharff-Goldhaber and S. K. Klaiber, *Phys. Rev.,* **70,** 229 (1946).

S49: E. N. Strait, C. G. Stergiopoulos, A. Sperdito, and W. W. Buechner, *Bull. Am. Phys. Soc.,* **23,** No. 3, 30 (1948).

S50: G. W. W. Stevens, *Nature,* **161,** 432 (1948).

S50*a*: G. W. W. Stevens, *Nature,* **162,** 526 (1948).

S51: R. Sagane, N. Yamamoto, and Y. Imai, *Inst. Phys. Chem. Research Tokyo,* **22,** 701 (1943).

S52: M. Schein and J. J. Lord, *Phys. Rev.,* **73,** 189 (1948).

S53: E. O. Salant, J. Hornbostel, and E. M. Dollman, *Phys. Rev.,* **74,** 694 (1948).

S54: J. Spence, J. Castle and J. H. Webb, *Phys. Rev.,* **74,** 704 (1948).

S55: M. H. Studier and E. K. Hyde, *Phys. Rev.,* **74,** 591 (1948).

S56: E. Smith and P. Gray, *Anat. Rec.,* **99** (supp.), 52 (1947).

S57: K. G. Scott, D. J. Axelrod, H. Fisher, J. F. Crowley, and J. G. Hamilton, *J. Biol. Chem.,* **176,** 283-293 (1948).

S58: K. G. Scott, D. H. Copp, D. J. Axelrod, and J. G. Hamilton, *J. Biol. Chem.,* **175,** 691–703 (1948).

S59: P. R. Stout and W. R. Meagher, *Science,* **108,** 471 (1948).

T1: S. Tamburino, *Phys. Rev.,* **69,** 35 (1946).

T2: G. Tammann and A. von Löwis, *Z. anorg. u. allgem. Chem.,* **205,** 145 (1932).

T3: G. Tammann, *Z. Elektrochem.,* **38,** 530 (1932).

T4: G. Tammann and G. Bandel, *Arch. Eisenhüttenw.,* **6,** 293 (1932–1933).

T5: G. Tammann and G. Bandel, *Z. Metallkunde,* **25,** 153, 207 (1933).

T6: H. J. Taylor, *Nature,* **136,** 719 (1935).

T7: H. J. Taylor, *Proc. Phys. Soc. London,* **47,** 873 (1935).

T8: H. J. TAYLOR and M. GOLDHABER, *Nature,* **135,** 341 (1935).
T9: H. J. TAYLOR, *Proc. Roy. Soc. London,* **150A,** 382 (1935).
T10: H. J. TAYLOR, *J. Univ. Bombay,* **4,** part 2, 70–73 (1935).
T11: H. J. TAYLOR and V. D. DABHOLKAR, *Proc. Phys. Soc. London,* **48,** 285–298 (1936).
T12: H. J. TAYLOR and V. D. DABHOLKAR, *Proc. Indian Acad. Sci.,* **3A,** 265–271 (1936).
T12*a*: R. H. THOMPSON and R. T. ELLICKSON, *Phys. Rev.,* **73,** 185 (1948).
T13: R. THORNTON and W. POWELL, *News Ed. Am. Chem. Soc.,* **25,** No. 30, 2144 (1947).
T14: C. TOBIAS and E. SEGRÉ, *Phys. Rev.,* **70,** 89 (1946).
T15: G. A. DE TREADWELL, V. A. LOW-BEER, H. L. FRIEDELL, and J. H. LAWRENCE, *Am. J. Med. Sci.,* **204,** 521 (1942).
T16: T. SAN TSIANG, R. CHASTEL, H. FARAGGI, and L. VIGNERON, *Compt. rend.,* **223,** 571 (1946).
T17: T. SAN TSIANG, HO ZAH WEI, L. VIGNERON, and R. CHASTEL, *Nature,* **159,** 773 (1947).
T18: T. SAN TSIANG, HO ZAH WEI, R. CHASTEL, and L. VIGNERON, *Phys. Rev.,* **71,** 382 (1947).
T19: T. SAN TSIANG and H. FARAGGI, *Compt. rend.,* **225,** 294 (1947).
T20: T. SAN TSIANG, HO ZAH WEI, and H. FARAGGI, *Compt. rend.,* **224,** 825 (1947).
T21: T. SAN TSIANG, *Phys. Rev.,* **72,** 1257 (1947).
T21*a*: T. SAN TSIANG, HO ZAH WEI, R. CHASTEL, and L. VIGNERON, *J. phys.,* **8,** No. 6 and 7, 1–26 (1947).
T22: S. T. TSIEN, M. BACHELET, and G. BOUISSIERES, *J. phys. radium,* **7,** 167 (1946).
T23: N. TSI-ZÉ and L. TA-YUAN, *J. Optical Soc. Am.,* **26,** 26–29 (1936).
T24: S. A. TYLER and J. J. MARAIS, *J. Sediment. Petrol.,* **11,** 145 (1941).
T25: A. TANNENBAUM, MDDC–1280 (MUC–RSS–563) reported October 1945.
T26: A. TANNENBAUM, H. SILVERSTONE, S. SCHWARTZ, and E. S. G. BARRON, AECD–1993D, declassified April 1948.
T27: F. L. TALBOTT, private communication.

U1: P. ULRICH and F. KOLBECK, *Centr. Mineral.* (1904), pp. 206–208.
U2: W. D. URRY, *Am. J. Sci.,* **239,** 191 (1941).
U3: W. D. URRY, J. SPIER, and L. E. CLUFF, *J. Lab. Clin. Med.,* **32,** No. 2, 147–154 (1947).

V1: P. J. VAN HEERDEN, *The Crystal Counter,* N. V. Noord-Hollandsche Uitgevers Maatschappij, Amsterdam, 1945.
V2: S. VEIL, *Compt. rend.,* **199,** 1044 (1934).
V3: V. I. VERNADSKY, *Geochemie in ausgewählten Kapiteln,* translated by E. KORDES, Akademische Verlagsgesellschaft, Leipzig, 1930.
V4: V. I. VERNADSKY, *Trav. lab. biogéochim. acad. sci. U.R.S.S.,* **5,** 517 (1939).
V5: G. VON BORN, *Centr. Mineral.* (1905), p. 58.

V6: A. VON GROSSE, *Science*, **80**, 512 (1934).
V7: A. VON GROSSE, *Repts. Comm. Meas. Geol. Time Natl. Research Council*, 1935, p. 45.
V8: A. VON GROSSE and J. C. SNYDER, *Science*, **105**, 240 (1947).
V9: A. VON GROSSE and W. LIBBY, *Science*, **106**, 88 (1947).
V10: G. VON HEVESY, *Biochem. J.*, **17**, 439 (1923).
V11: G. VON HEVESY and A. OBRUTSCHEVA, *Nature*, **115**, 674 (1925).
V12: G. VON HEVESY, M. PAHL, and R. HOSEMANN, *Z. Physik*, **83**, 43–54 (1933).
V13: G. VON HEVESY and H. LEVI, *Proc. Copenhagen Roy. Soc.*, **14**, 25 (1936).
V14: G. VON HEVESY and F. A. PANETH, *A Manual of Radioactivity*, 2nd ed., translated by R. W. LAWSON, Oxford Univ. Press, London, 1938.
V15: R. VON TRAUBENBERG, *Z. Physik*, **2**, 268 (1920).
V16: L. VIGNERON, *Compt. rend.*, **226**, 715 (1948).
V17: W. VAN DER GRINTEN, *Bull. Am. Phys. Soc.*, **23**, No. 3, 51 (1948).
V18: L. VAN MIDDLESWORTH, MDDC–1022 (BP–69), declassified June 6, 1947.

W1: B. J. WALKER, data quoted by von Hevesy.[V14]
W2: H. WAMBACHER, *Sitzber. Akad. Wiss. Wien*, Abt. 2*a*, **140**, 271 (1931).
W3: H. WAMBACHER, *Physik. Z.*, **39**, 883 (1938).
W4: H. WAMBACHER, *Z. tech. Physik*, **19**, 569–578 (1938).
W5: H. WAMBACHER, *Z. wiss. Phot.*, **38**, 38 (1939).
W5*a*: H. WAMBACHER, *Sitzber. Akad. Wiss. Wien*, Abt. 2*a*, **149**, 157–212 (1940).
W6: O. WERNER, *Z. physik. Chem.*, **156A**, 89–112 (1931).
W7: O. WERNER, *Mikrochemie*, **4**, 360 (1931).
W8: O. WERNER, *Z. Metallkunde*, **26**, 265–268 (1934).
W9: O. WERNER, *Naturw.*, **23**, 456–459 (1935).
W10: O. WERNER, *Z. Metallkunde*, **27**, 215–219 (1935).
W11: J. A. WHEELER, *Proc. Am. Phil. Soc.*, **90**, 40 (1946).
W12: E. T. WHERRY, *J. Franklin Inst.*, **165**, 57–78 (1908).
W13: R. WHIDDINGTON and J. E. TAYLOR, *Proc. Roy. Soc. London*, **136A**, 651 (1932).
W14: W. L. WHITEHEAD, *Econ. Geol.*, **12**, 697 (1917).
W15: A. WIDHALM, *Z. Physik*, **115**, 481 (1940).
W16: T. R. WILKINS and R. N. WOLFE, *J. Optical Soc. Am.*, **23**, 324–332 (1933).
W17: T. R. WILKINS and H. J. ST. HELENS, *Phys. Rev.*, **50**, 1099 (1936).
W18: T. R. WILKINS, *Phys. Rev.*, **49**, 639 (1936).
W19: T. R. WILKINS, *Phys. Rev.*, **49**, 403 (1936).
W20: T. R. WILKINS and H. J. ST. HELENS, *Phys. Rev.*, **49**, 649 (1936).
W21: T. R. WILKINS, *Natl. Geog. Soc. Stratosphere Ser.*, **2**, 37 (1936).
W22: T. R. WILKINS and A. J. DEMPSTER, *Phys. Rev.*, **54**, 315 (1938).
W23: T. R. WILKINS and H. J. ST. HELENS, *Phys. Rev.*, **54**, 783 (1938).
W24: T. R. WILKINS, *J. Applied Phys.*, **11**, 35 (1940).
W25: P. M. WOLF and H. J. BORN, *Strahlentherapie*, **70**, 342–348 (1941).

W26: E. O. Wollan, C. D. Moak, and R. B. Sawyer, *Phys. Rev.*, **72**, 447 (1947).
W27: D. E. Wooldridge, A. J. Ahearn, and J. A. Burton, *Phys. Rev.*, **71**, 913 (1947).
W28: R. Westöö, *Arkiv. Mat. Astron. Fysik.*, **34B**, No. 22, pp. 1–8 (1947).
W29: J. H. Webb, *Phys. Rev.*, **74**, 511-532 (1948).
W30: H. O. Whipple, C. S. Hornberger, J. G. Hoffman, and J. F. Nolan, *Am. J. Roentgenol.*, **60**, 175 (1948).

Y1: H. Yagoda, *Phil. Mag.*, (7), **13**, 1163–1171 (1932).
Y2: H. Yagoda, *J. Am. Chem. Soc.*, **57**, 2329 (1935).
Y3: H. Yagoda, *Ind. Eng. Chem. Anal. Ed.*, **9**, 79 (1937).
Y4: H. Yagoda, *Mikrochemie*, **24**, 117 (1938).
Y5: H. Yagoda, *Ind. Eng. Chem. Anal. Ed.*, **12**, 698 (1940).
Y6: H. Yagoda, *Ind. Eng. Chem. News Ed.*, **18**, No. 24, 1138 (1940).
Y7: H. Yagoda, *Ind. Eng. Chem. Anal. Ed.*, **15**, 135 (1943).
Y8: H. Yagoda, *J. Ind. Hyg. Toxicol.*, **26**, 224 (1944).
Y9: H. Yagoda, *Am. Mineral.*, **30**, 51 (1945).
Y10: H. Yagoda, *Am. Mineral.*, **31**, 87–124 (1946).
Y11: H. Yagoda, *Am. Mineral.*, **31**, 462 (1946).
Y12: H. Yagoda, *Econ. Geol.*, **41**, 813 (1946).
Y13: H. Yagoda and N. Kaplan, *Phys. Rev.*, **71**, 910 (1947).
Y14: H. Yagoda and N. Kaplan, *Phys. Rev.*, **72**, 356 (1947).
Y15: H. Yagoda, *Am. Mineral.*, **32**, 212 (1947).
Y16: H. Yagoda, *Phys. Rev.*, **73**, 263 (1948).
Y17: H. Yagoda, unpublished experiments.
Y18: H. Yagoda and N. Kaplan, unpublished experiments.
Y19: H. Yagoda and N. Kaplan, *Phys. Rev.*, **73**, 634 (1948).
Y20: H. Yagoda, *Nucleonics*, **2**, No. 5, part 1, 2–15 (1948).

Z1: A. Zhdanov, *J. phys. radium*, **6**, 233–241 (1935).
Z2: A. Zhdanov, *Proc. State Radium Inst. U.S.S.R.*, **3**, 7–36 (1937).
Z3: A. Zhdanov, *Nature*, **143**, 682 (1939).
Z4: A. Zhdanov and L. V. Myssovsky, *Compt. rend. acad. sci. U.R.S.S.*, **25**, 11 (1939).
Z5: A. Zhdanov, N. A. Perfilov, and M. Y. Deisenrod, *Phys. Rev.*, **65**, 202 (1944).
Z6: A. Zhdanov, *Compt. rend. acad. sci. U.R.S.S.*, **46**, 359 (1945).
Z7: B. R. Zimmerman and S. E. Maddigan, *Am. Inst. Mining Met. Engrs. Tech. Pub.* 1683, 1944, 26 pp.

APPENDIX 1

RANGE-ENERGY RELATIONS IN ILFORD NUCLEAR RESEARCH EMULSIONS *

Range, microns	Energy in Mev: Proton p	Deuteron d	Triton τ	Alpha Particle	Li^8 Fragment †
5	0.5	0.8	1.0	1.6	3
10	0.8	1.3	1.6	3.0	6
15	1.1	1.6	1.9	4.0	8
20	1.3	1.9	2.3	5.0	10
30	1.7	2.4	2.9	6.5	13
40	2.0	2.9	3.5	7.8	16
50	2.3	3.3	3.9	9.1	18
60	2.6	3.7	4.3	10.2	20
70	2.9	4.0	4.8	11.4	23
80	3.1	4.3	5.1	12.2	24
90	3.4	4.6	5.5	13.0	26
100	3.7	5.0	5.9	13.7	27
150	4.7	6.3	7.5	17.0	
200	5.5	7.4	8.8	20.0	
250	6.3	8.5	10.0	22.5	
300	7.0	9.3	11.1	24.6	
350	7.6	10.1	12.0	26.8	
400	8.2	11.0	13.0	29	
450	8.7	11.7	13.9	31	
500	9.3	12.4	14.8	33	
600	10.4	14.0	16.6	36	
700	11.4	15.3	18.2	39	
800	12.2	16.4	19.5	42	
900	13.0	17.5	20.8	44	
1000	13.9	18.6	22.1	47	
1200	15.4	20.6	24.6	51	
1400	16.9	22.6	26.9	55	
1600	18.1	24.3	28.8	60	
1800	19.4	26.0	30.9	64	
2000	20.7	27.8	33.0	68	
2500	23.6	31.6	37.6	76	
3000	26.2	35.2	41.8	84	
3500	28.8	38.5	45.8	90	
4000	30.8	41.3	49.0	100	
4500	33.0	44.3	52.6		
5000	35.3	47.4	56.3		

* Based on measurements by Lattes, Fowler, and Cüer [L17] and extrapolation from the relationships:

$$E_p = 0.262L^{0.575}$$
$$E_d = 0.352L^{0.575}$$
$$E_\tau = 0.418L^{0.575}$$

† Rough estimates based on the assumption that alpha particles and Li^8 fragments of equal velocity have approximately the same range.

APPENDIX 2

ATOMIC CONSTANTS AND CONVERSION FACTORS

Avogadro number	6.023×10^{23} atoms per mole
Electron mass	9.106×10^{-28} g
Proton to electron mass ratio	1836.57
Energy equivalent of 1 electron mass	0.5108 Mev
1 atomic mass unit is equivalent to	931.04 Mev

1 curie = 3.7×10^{10} disintegrating atoms per sec
1 rutherford = 10^{6} disintegrating atoms per sec
37 rutherfords = 1 millicurie
1 day = 8.64×10^{4} sec
1 year = 3.15×10^{7} sec

$$\text{Mev} \times \begin{cases} 1.07 \times 10^{-3} = \text{mass units} \\ 1.60 \times 10^{-6} = \text{ergs} \\ 3.83 \times 10^{-14} = \text{gram calories} \\ 4.45 \times 10^{-20} = \text{kilowatt-hours} \end{cases}$$

Author Index

Subject Index